The Role of Wnt-induced secreted proteins (WISPs) in Gastric Cancer

By

Jiafu Ji

Cardiff University-Peking University Collaborate Institute

Cardiff University School of Medicine

March 2015

Thesis submitted to Cardiff University for the degree of Doctor of Philosophy (PHD)

Cardiff University

The Role of Wnt-induced secreted proteins (WISPs) in Gastric Cancer

Student: Jiafu Ji

Student Number: 1221099

Supervisors: Professor Wen G. Jiang

and Professor Robert Mansel

Cardiff University-Peking University Collaborate Institute

Cardiff University School of Medicine

March 2015

DECLARATION

This work has not previously been accepted in substance for any degree and is not concurrently submitted in candidature for any degree.

Signed …… Date……03-31-2015……

STATEMENT 1
This thesis is being submitted in partial fulfilment of the requirements for the degree of PhD.

Signed …… Date ……03-31-2015……

STATEMENT 2
This thesis is the result of my own independent work/investigation, except where otherwise stated. Other sources are acknowledged by explicit references.

Signed …… Date ……03-31-2015……

STATEMENT 3
I hereby give consent for my thesis, if accepted, to be available for photocopying and for interlibrary loan, and for the title and summary to be made available to outside organisations.

Signed …… Date……03-31-2015……

DEDICATION

I would like to dedicate this work to my family. I would not be where I am today without them.

ACKNOWLEDGEMENTS

I would like to thank my supervisors Professor Wen G. Jiang and Professor Mansel RE for their guidance and support throughout my three years of study, from a part-time to a full-time PhD student. I enjoyed being a part of the Metastasis and Angiogenesis Research Group and Cardiff University-Peking University Cancer Institute and they were the perfect places to get my PhD.

I would especially like to thank Dr Shuqin Jia, Dr Jun Cai, Dr Lin Ye, Dr Yongning Jia and Dr Ke Ji for their friendship, help and support over the years. I am also very grateful to Mrs Fiona Ruge, Dr Andrew Sanders, Miss Sioned Owen, Miss Hoi Weeks, Dr Tracey Martin and Dr Jane Lane for their friendship and support over the years. Finally, I would like to dedicate this work to my family especially my wife and son. I would not be where I am today without them.

ABSTRACT

Introduction:

It has been recently shown that the WISP proteins (Wnt-inducted secreted proteins), a group of intra- and extra-cellular regulatory proteins, have been implicated in the initiation and progression of variety types of tumours including colorectal and breast cancer. However, the role of WISP proteins in gastric cancer (GC) cells and clinical implication in gastric cancer has not yet been fully elucidated.

Materials and methods:

The expression of the WISP transcript and proteins in a cohort of GC patients was analysed using real-time quantitative PCR and immunohistochemistry, respectively. The expression of a panel of recognised EMT (epithelial-mesenchymal transition) markers were quantified (Q-PCR) in paired tumour and normal gastric tissues. WISP-2 knockdown sublines using anti-WISP-2 ribozyme transgenes were created in GC cell lines AGS and HGC27. Using the cell models and proteins extracted from gastric tissue samples, protein microarray was used to search for potential protein partners and signalling pathways involved with WISP-2. Subsequently, the biological functions, namely, cell growth, adhesion, migration and invasion, were studied. Potential mechanisms related with EMT, extracellular matrix and MMP (Matrix metalloproteinases) and signalling pathways were investigated.

Results:

Expression of WISP-2 was frequently detected in GC tissues. Levels of WISP-2, not WISP-1 and WISP-3, was significantly correlated with early TNM staging and differentiation status. High levels of WISP-2 were associated with a favourable clinical outcome and survival of the patients. We also found that WISP-2 expression inversely correlated with Twist and Slug in the paired gastric samples. Knockdown of WISP-2 expression increased the rate of proliferation, migration and invasion of GC cells and influenced expression of EMT biomarkers including Twist, Slug and E-cadherin. Using an antibody based protein microarray, ERK, JNK as well as AKT proteins were found to be co-precipiated with WISP-2 protein from human gastric tissue proteins. Furthermore, WISP-2 knockdown gastric cell lines also demonstrated a change in the ERK and JNK phophorylation. Mechanistically, WISP-2 suppressed GC cell metastasis through reversing epithelial-mesenchymal transition and suppressing the expression and activity of MMP-9 and MMP-2 via JNK and ERK. Cell motility analysis indicated that WISP-2 knockdown contributed to GC cells' motility, an effect attenuated by PLC-γ and JNK small inhibitors.

Conclusions:

WISP-2 transcript and protein expressions are inversely linked to disease progression and linked to the survival of patients with gastric cancer. WISP-2 has a profound influence on the migration and adhesion of gastric cancer cells and is a powerful factor to reverse the EMT process in these cells. These effects of WISP-2 are via its involvement in the ERK and JNK pathways, which in turn modulate the MMP activities. Together, WISP-2 is an important regulator of the cellular function and an important factor in the progression of gastric cancer. It acts as a potential tumour suppressor in gastric cancer.

CONTENTS

LIST OF FIGURES

Chapter 1

Chapter 2

Chapter 3

Chapter 4

Chapter 5

Chapter 8

LIST OF TABLES

Chapter 1

Chapter 2

Chapter 3

Chapter 7

PUBLICATIONS

Full papers:

- **Ji J**, Jia S, Jia Y, Ji K, Hargest R, Jiang WG. WISP-2 in human gastric cancer and its potential metastatic suppressor role in gastric cancer cells mediated by JNK and PLC-γ pathways. *Br J Cancer*, July 2015, in press

- **Ji JF**, Jia S, Ji K, Jiang WG, Wnt1 inducible signalling pathway protein-2 (WISP-2/CCN5): Roles and regulation in human cancers (Review). *Oncol Rep*, 2014, 31: 533-539

- Jia S, Jia Y, Weeks HP, Ruge F, Feng X, Ma R, **Ji JF**, Ren J, Jiang WG. Down-regulation of WAVE2, WASP family verprolin-homologous protein 2, in gastric cancer indicates lymph node metastasis and cell migration. *Anticancer Res*. 2014, 34:2185-94

- Ji K, Ye L, Toms AM, Hargest R, Martin TA, Ruge F, **Ji JF**, Jiang WG. Signal-induce proliferation-associated gene 1 (SIPA1), a RapGTPase-activating protein is increased in colorectal cancer and has diverse effects on functions of colorectal cancer cells. *Cancer Genomics Proteomics*, 2012, 9:, 321-327

- Ye L, Ji K, **Ji JF**, Hargest R, Jiang WG. Application of Electric Cell-Substrate Impedance Sensing in evaluation of traditional medicine on the cellular functions of gastric and colorectal cancer cells. *Cancer Metastasis Biology Treatment.*, 2012, 17: 195-202

ABSTRACTS AND CONFERENCE PRESENTATIONS

- **Ji J,** Jia S, Ji K, Jiang WG. Correlation between WISP-2 and Epithelial to Mesenchymal Transition (EMT) in gastric cancer and its clinical application, Submitted. European Cancer congress 2015, Vienna, Austria.

- **Ji J,** Jia S, Ji K, Jiang WG. Identification of WISP-2 interacting proteins and potential signalling pathways associated with WISP-2. The 4th China-UK Cancer (CUKC) Conference, Cardiff, UK. *Anticancer Res*, 2015, in press

- **Ji J.** Strategies and controversies in the surgical treatment of gastric cancer, **Oral Presentation**, The 4th China-UK Cancer (CUKC) Conference, Cardiff, UK. *Anticancer Res*, 2015, in press

- **Ji J,** Jia S, Jiang WG. WISP-2 is an independent prognosis indicator of gastric cancer patients and regulates the biological function of gastric cancer cells via the JNK pathway, **Oral Presentation**, European Cancer Congress 2013, Amsterdam. *Eur J Cancer, 2013,* 45 (supplement-2), S572

- **Ji J,** Jia S, Jia Y, Jiang WG. The Prognostic value of a trio of the EMT (Tumour-Mesenchymal Transition) markers for patients with gastric cancer. Number: 2.643, European Cancer Congress 2013, Amsterdam. *Eur J Cancer, 2013,* 45 (supplement-2), S634

- Jia S, **Ji J**, Jiang WG. KIAA1199 knockdown attenuates cell growth of gastric cancer cells and its over-expression is associated with disease progression in patients with gastric cancer, Poster and Discussion Session Number: 2.458, European Cancer Congress 2013, Amsterdam. *Eur J Cancer, 2013,* 45 (supplement-2), S575

- Jia S, **Ji J**, Jiang WG. MAGIs, membrane-associated guanylate kinase with inverted structure protein, involved in the metastatic properties of gastric cancer cells, the clinical implications. Poster Number: 2.470, European Cancer Congress 2013, Amsterdam. *Eur J Cancer, 2013,* 45 (supplement-2), S579

- Jia S, **Ji J**, Jiang WG. Clinical significance and cell functions of Tubedown-100 (TBDN100) in gastric cancer. Poster Number: 2.471, European Cancer Congress 2013, Amsterdam. *Eur J Cancer, 2013,* 45 (supplement-2), S579

ABBREVIATIONS

AFP: Alpha-faetoprotein

AJCC: American systems for gastric cancer

API: Asian and Pacific Islander

APS: Ammonium persulphate

BSA: Bovine serum albumin

CEA: Carcino-embryonic antigen

CNPs: Copy number polymorphisms

CT: Computed tomography

CTGF: Connective tissue growth factor

CYR61: Cyteine-rich angiogenic protein 61

DAB: Diaminobenzidine

DEPC: Diethyl Pryoncarbonate

DMSO: Dimethylsulphoxide

DMEM: Dulbecco's Modified Eagle's medium

ECIS: Electric Cell-substrate Impedance Sensing

EGC: Early gastric cancer

EGJ: Oesophago-gastric junction

EMR: Endoscopic mucosal resection

EMT: Epithelial-mesenchymal transitions

ERBT: External-beam irradiation

ERK: Extracellular signal-regulated kinase

ESD: Endoscopic submucosal dissection

FAK: Focal adhesion kinase

FBS: Foetal bovine serum

FISH: Fluorescence *in situ* isationhybridisation

GAPDH: Glyceraldehyde 3-phosphate dehydrogenase

GC: Gastric Cancer

GISTs: Gastrointestinal stromal tumours

GnRH: Gonadotropin-Releasing Hormone

HCC: Hepatocellular carcinoma

HDGC: Hereditary Diffuse Gastric Cancer

hCG: Human chorionic gonadotrophic

HGF: Hepatocyte growth factor

IARC: International Agency for Research on Cancer

IGF: Insulin-like growth factor

IM: Intestinal metaplasis

IORT: Intra-operative radiotherapy

IP: Immunoprecipitation

LB: Liquid broth

MALT: Mucosa-associated lymphoid tissue

MAPK: Mitogen-activated protein kinase

MDCK: Madin-Darby canine kidney

MEK: MAPK/ERK kinase

MK2: MAPK-activated kinase 2; also known as MAPK2

MMP: Matrix metalloproteinase

NHW: Non-Hispanic White

NOV: Nephroblastoma overexpressed

PA: Pemicious anaemia

PCR: Polymerase chain reaction

QoL: Quality of life

RT-PCR: Reverse Transcription- Polymerase Chain Reaction

SDS-PAGE: Sodium Dodecyl Sulphate Polyacrylamide Gel Electrophoresis

SNPs: Single nucleotide polymorphisms

STN: Sialy1 Tn antigens

TBE: Tris-Boric-Acid-EDTA

TBS: Tris Buffered Saline

TGF: Transforming growth factor

TNM: Tumour, Node, Metastasis Classification

TP: Thymidine phosphorylase

TSP: Thrombospondin

UICC: International Union for Cancer control

WISP: Wnt-induced-secreted-protein

WNT1: Wingless-type MMTV integration site family, member 1

Chapter 1

Introduction

1.1 Gastric cancer

1.1.1 Introduction

Gastric cancer is one of the leading causes of cancer death all over the world and remains the second and fourth most common cancer in men and women respectively [1]. This is in spite of the fact that the incidence and mortality have decreased markedly over the last 50 years in most countries [2]. The incidence of gastric cancer varies in different areas of the world and among a variety of ethnic groups, especially high occurrence rate in Eastern Asian populations [3]. The lowest mortality rates include most countries of Northern Europe, in North America, and also in several Central American countries, namely Mexico, Cuba and Puerto Rico [4]. While the areas with persistently high incidence rates are observed in the Russian Federation and other countries of central and Eastern Asian (i.e. China, Japan and the Republic of Korea) and some countries of Latin America [5]. Globally, gastric cancer accounts for 1 million new cases and 738,000 deaths annually [5]. Despite advances in diagnosis and treatment, gastric cancer is usually, and unfortunately, detected after invasion of the muscularis propria [6]. The 5-year survival rate of gastric cancer is less than 30% in developed countries and around 20% in developing countries and the case: fatality ratio of gastric cancer is higher than that for most other commonly seen malignancies including colorectal, breast, and prostate cancers [6].

Most patients with gastric cancer underwent nonspecific symptoms in the early stages whilst anaemia, weight loss, and refusal of meat-based foods are mostly observed in advanced stages [7]. Furthermore, traditional treatment (i.e. surgery and chemotherapy) has limited value in advanced disease and there is a lack of molecular markers for targeted therapy [7].

Gastric cancer can be classified into intestinal and diffuse types based on epidemiological and clinico-pathological features [8]. The intestinal type of gastric cancer is thought to arise from a series of progressive changes of gastric epithelial cells, which their transformation is from normal mucosa to chronic atrophic gastritis [8], intestinal metaplasis (IM), dysplasia (DYS) and eventually cancer [9].

The aetiology of gastric cancer is multi-factorial and categorized as either dietary or non-dietary factors [4]. The major risk factors of dietary implicated in the development of gastric cancer include high content of nitrates, nitrosamine and high salt intake. Accumulating evidence has also clearly linked the role of *Helicobacter Pylori* (*H. Pylori*) infection to the pathogenesis of gastric cancer [5]. The oncogenesis of gastric cancer is a complex, multistep process including various genetic and epigenetic alterations of tumour suppressor genes, oncogenes, cell cycle regulators, signalling molecules and DNA repair genes [5].

A reasonable programme for gastric cancer prevention contains intake of a balanced diet (i.e. fruits and vegetables), improved sanitation and hygiene, screening and treatment of *H. Pylori* infection, and follow-up of precancerous lesions [10]. Diet is suggested as an important role in the aetiology of gastric cancer, which can offer scope for nutritional prevention [11]. Animal models have been extensively contributed in analyses of stepwise evolution of gastric carcinogenesis and detected dietary chemopreventative agents [11]. How to develop the multi-targeted preventive and therapeutic strategies for gastric cancer will be a major challenge in future.

1.1.2 Anatomy of the stomach

The stomach starts at the gastroesophageal (GE) junction and ends at the pylorus [12]. The stomach is covered with peritoneum of the lesser sac or omental bursa [13]. In general, the stomach is divided into four major anatomic sites, including the gastric cardia (the region around the superior opening of the stomach connected with the GE junction), the fundus, the body (central portion of the stomach), and the *Pyloric* canal (links to the duodenum) [12]. The pylorus is made up of two parts: the *Pyloric* antrum linking to the body of the stomach, and the *Pyloric* canal which proceeds to the duodenum (Figure 1.1) [14].

The pylorus connects with the duodenum of the small intestine through the *Pyloric* sphincter [14]. The *Pyloric* sphincter is a valve between the stomach and duodenum which guards against back flow of duodenal contents [14].

Peritoneum of the greater sac covers the anterior surface of the stomach and it adjoins left of the diaphragm and cranially. It is worth noting that there is either no, or variable, visceral peritoneal covering at the most proximal portion of the GE junction giving rise to the enhancive incidence of gastric cancer at the GE junction. Positive radial, which has a margin at this site, is in fact the most “true” positive margins, whilst many others in the stomach belong to free serosal margins only if the tumour is adherent to an adjacent structure.

The right segment of the anterior surface of stomach is adjacent to the left lobe of the liver and the anterior abdominal wall. The stomach is the junction of many visceral structures; from the direction of superior to inferior, it is adjacent to the spleen, left superarenal gland, upper kidney,

ventral part of the pancreas and transverse colon. The hepato-gastric ligament or lesser omentum is attached to the lesser curvature and includes the right gastric branch of the hepatic artery and the left gastric artery.

The stomach wall contains five layers: the mucosa, the submucosa, muscular layer, subserosa, and serosa. The muscularis layer consists of longitudinal layer, circular muscle layer, and inner oblique layer muscle in the outer to inner.

1.1.3 Epidemiology

The incidence rates of gastric cancer vary widely in different regions of the world (Table1.1 and 1.2 for males and females respectively). Global cancer statistics reported that the highest incidences of gastric cancer are observed in Japan, Southeast Asia and Eastern Europe, in which incidence rates reached 30 to 85 cases per 100,000 people.

1.1.3.1 Morbidity and mortality

Globally approximately 737,000 deaths are caused by gastric cancer each year (Figure 1.2), making it the third leading cause of cancer deaths in men and the fifth in women [15]. This is despite a global decrease in incidence and death rates over the last 50 years [16]. In general, the incidence rate in men is almost double that in women [16]. Survival is poor in most countries, although 5-year survival rates are as high as 50% in Japan, where screening for gastric cancer has been well developed [17].

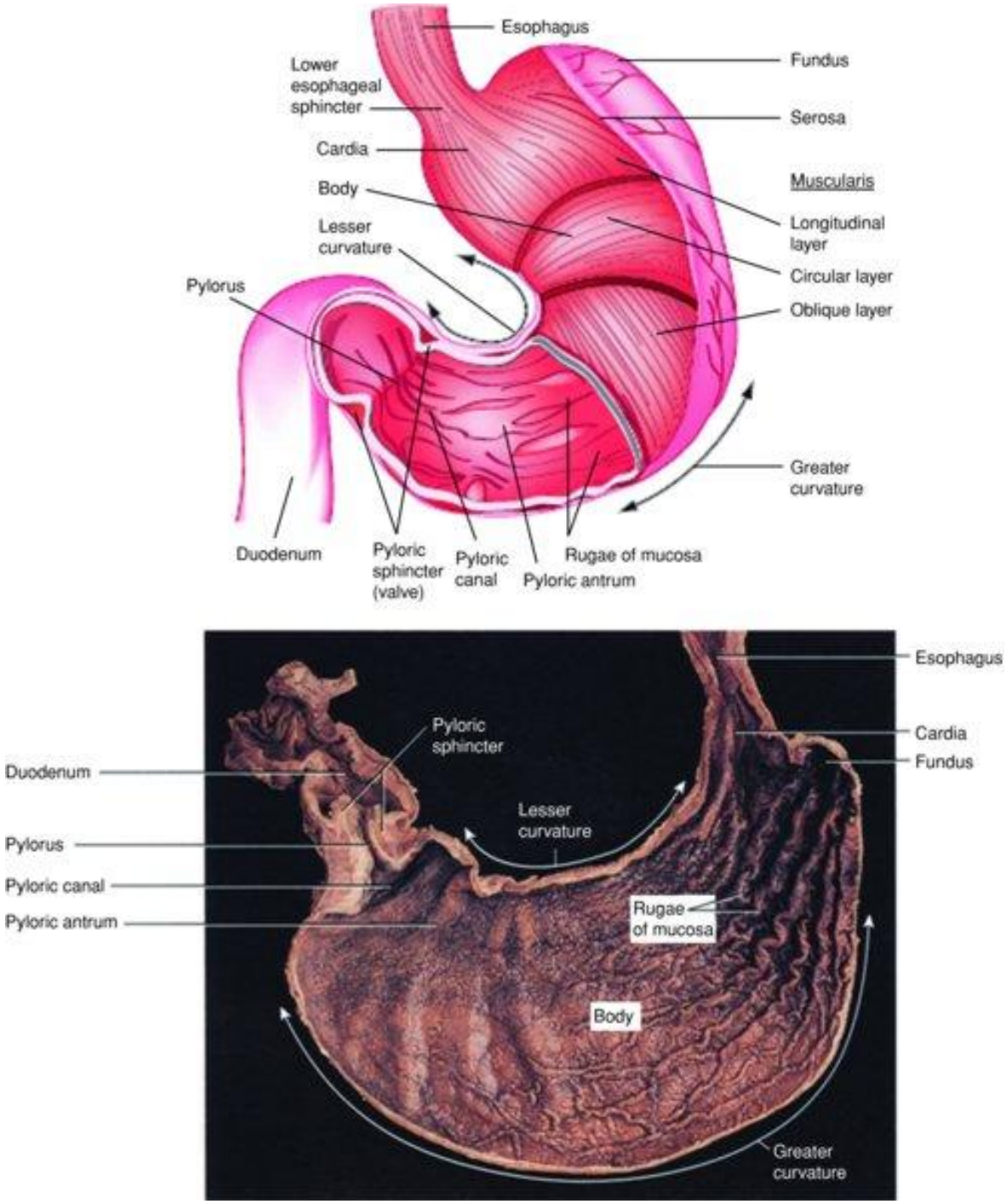

Figure 1.1 The anatomy of stomach.
Source: DeVita VT, Lawrence TS, Rosenberg SA: DeVita, Hellman, and Rosenberg's Cancer: Principles & Practice of Oncology, 9th Edition. Copyright © 2011 by LIPPINCOTT WILLIAMS & WILKINS, a WOLTERS KLUWER business.

Table 1.1 Stomach - Estimated incidence, all ages: male. Source: http://globocan.iarc.fr/

Stomach - Estimated incidence, all ages: male					
POPULATION	*Quality	Numbers	Crude Rate	ASR (W)	Cumulative risk
World		631293	17.7	**17.4**	2.01
More developed regions		175117	28.9	**15.6**	1.86
Less developed regions		456176	15.5	**18.1**	2.05
Very High Human Development		168036	29.5	**16.0**	1.90
High Human Development		84594	16.5	**16.1**	1.94
Medium Human Development		358122	19.7	**20.9**	2.34
Low Human Development		20414	3.1	**5.6**	0.67
WHO Africa region (AFRO)		10496	2.4	**4.7**	0.54
WHO Americas region (PAHO)		51704	11.0	**9.2**	1.09
WHO East Mediterranean region (EMRO)		14951	4.7	**7.2**	0.81
WHO Europe region (EURO)		97679	22.3	**14.0**	1.66
WHO South-East Asia region (SEARO)		60299	6.4	**8.0**	0.97
WHO Western Pacific region (WPRO)		396078	41.9	**33.4**	3.75
IARC membership (24 countries)		231832	17.6	**14.6**	1.72
Middle-East and Northern Africa (MENA)		13498	5.9	**8.3**	0.98
Africa		13216	2.5	**4.5**	0.52
Sub-Saharan Africa		9845	2.3	**4.5**	0.53
Eastern Africa		4357	2.5	**5.2**	0.61

Table 1.2 Stomach - Estimated incidence, all ages: Female. Source: http://globocan.iarc.fr/

Stomach - Estimated incidence, all ages: female					
POPULATION	*Quality	Numbers	Crude Rate	ASR (W)	Cumulative risk
World		320301	9.2	**7.5**	0.82
More developed regions		99392	15.5	**6.7**	0.75
Less developed regions		220909	7.7	**7.8**	0.85
Very High Human Development		88224	15.1	**6.7**	0.73
High Human Development		56419	10.6	**8.2**	0.97
Medium Human Development		160877	9.3	**8.5**	0.90
Low Human Development		14703	2.3	**3.7**	0.43
WHO Africa region (AFRO)		8614	2.0	**3.4**	0.40
WHO Americas region (PAHO)		33650	7.0	**5.0**	0.56
WHO East Mediterranean region (EMRO)		8503	2.8	**3.9**	0.45
WHO Europe region (EURO)		64167	13.8	**6.8**	0.79
WHO South-East Asia region (SEARO)		30259	3.3	**3.7**	0.42
WHO Western Pacific region (WPRO)		175061	19.5	**13.1**	1.39
IARC membership (24 countries)		123667	9.5	**6.3**	0.70
Middle-East and Northern Africa (MENA)		9365	4.3	**5.1**	0.60
Africa		10590	2.0	**3.2**	0.38
Sub-Saharan Africa		8257	1.9	**3.4**	0.40
Eastern Africa		3679	2.1	**3.9**	0.47

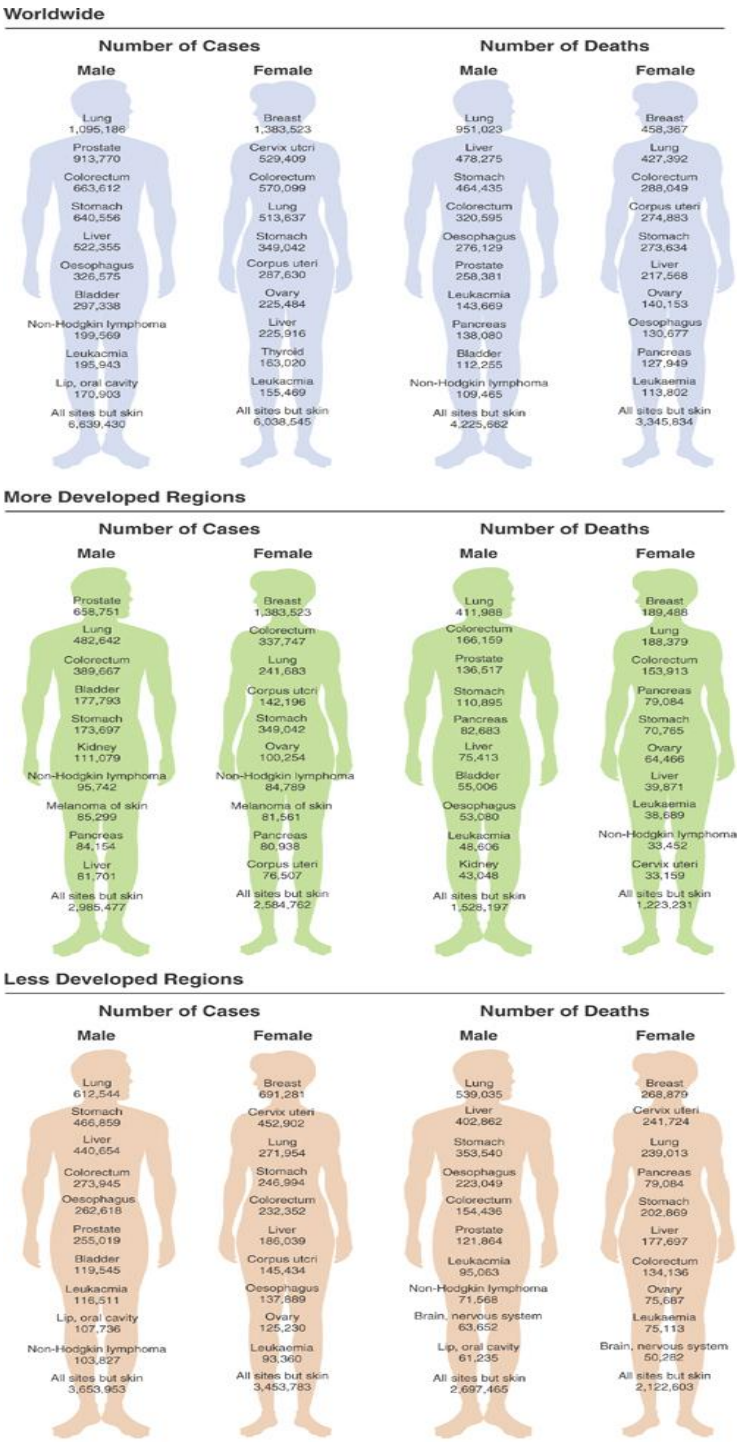

Figure 1.2 Number of cancer cases and deaths for the top ten cancer sites by sex, worldwide, and by level of economic development in 2008.
Source: DeVita VT, Lawrence TS, Rosenberg SA: DeVita, Hellman, and Rosenberg's Cancer: Principles & Practice of Oncology, 9th Edition. Copyright © 2011 by LIPPINCOTT WILLIAMS & WILKINS, a WOLTERS KLUWER business.

Gastric cancer shows the highest incidence rate in Eastern Asia and Central and Eastern Europe (Figure 1.3). The incidence rates (per 100,000) range from 2.4 cases in Gabon to 62.2 in Korea for men and from 1.3 in the Central African Republic to 25.9 in Guatemala. Factors which contribute to the geographic patterns contain variation in rifeness of chronic *Helicobacter Pylori* infection and dietary habits (e.g. high-salt diets, low in fresh vegetables and fruit) [18]. Both of these are considered to be the main factors which contribute to the geographic patterns [19]. *H. Pylori* infection makes up about around 61% of stomach cancer cases in developed countries and 64% in developing countries [20]. In addition, among Eastern European countries, the rifeness of *H. Pylori* infection is reportedly up to 80% in adults [21].

Mortality rates of gastric cancer have dropped more than 80% in most industrialised countries over the past 50 years [22]. Similar trends have been observed in a number of less developed countries, namely China, although the decline is smaller and the rates remains high in some regions [22]. Improved dietary habit (e.g. increase of fresh fruits and vegetables and decrease of salted and preserved foods) and a reduction in chronic *H. Pylori* infection, based on the development of good sanitation and antibiotics, are suggested to be the factors that have contributed to these distinct decreases in subsequent risk of gastric cancer [23].

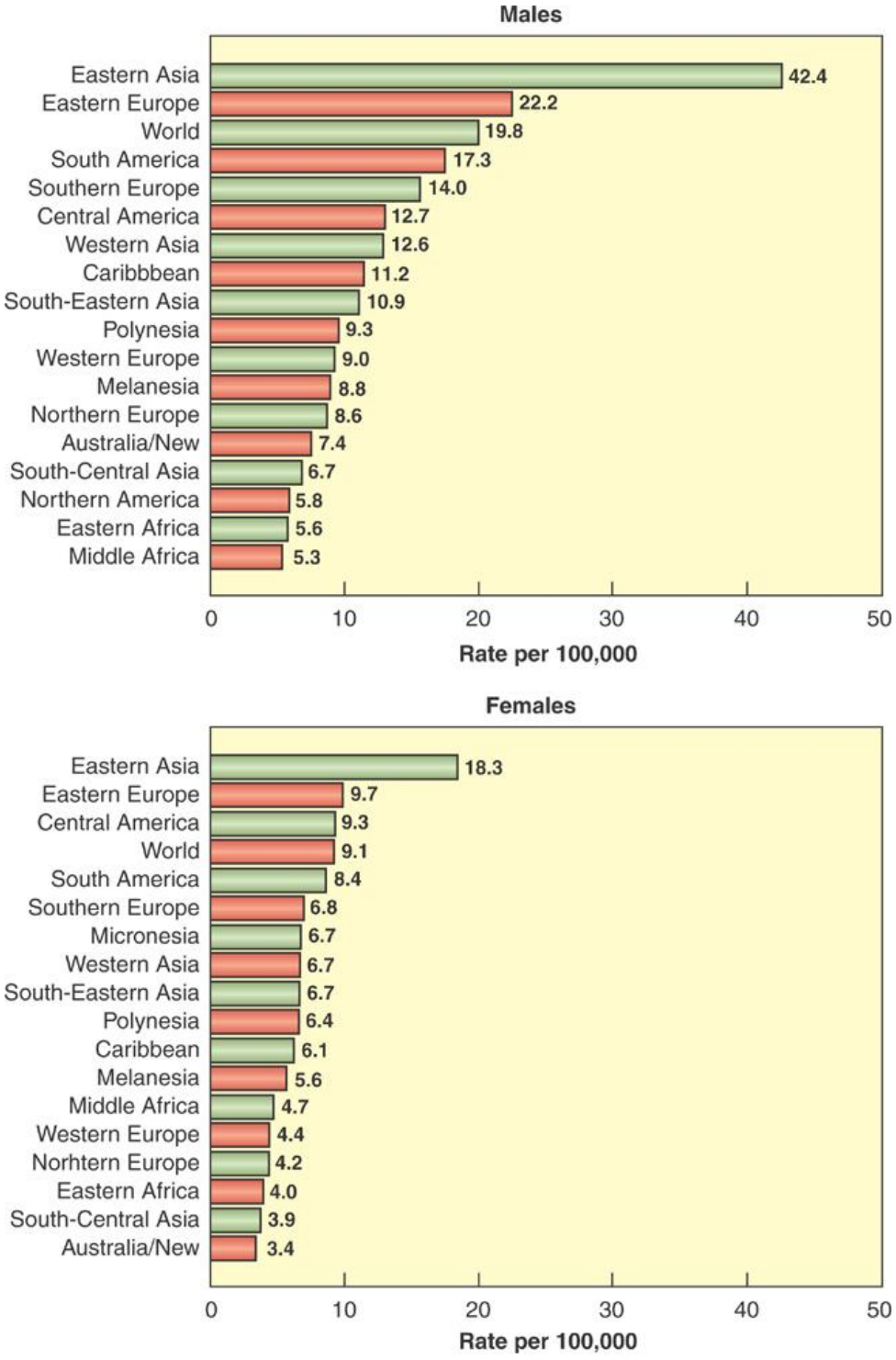

Figure 1.3 Incidence rates of Age-standardized Gastric cancer by World Health isationorganisation region and sex in 2008. Source: DeVita VT, Lawrence TS, Rosenberg SA: DeVita, Hellman, and Rosenberg's Cancer: Principles & Practice of Oncology, 9th Edition. Copyright © 2011 by LIPPINCOTT WILLIAMS & WILKINS, a WOLTERS KLUWER business.

1.1.3.2 Survival rate

Relative 5-year survival for all stages of gastric cancer is 27%. However, this improves to 59% when disease is localised [24]. The 5-year survival rate has improved over the last five decades by 11% [25].

1.1.3.3 Aetiology and risk factors

1.1.3.3.1 Aetiology

Development of gastric cancer can be induced by the interaction of both genetic and environmental factors in complex ways (Table 1.3) [26]. Based on the incidence of gastric cancer in the female and male populations and its close relationship with blood group A, the diffuse type of gastric cancer is considered to have a stronger genetic link compared to other cancers [27]. There is also a two- to three- fold increased risk among first-degree relatives in familial clustering caused by familial and hereditary factors [28]. Gastric cancer is known to have a high incidence in inherited syndromes (e.g. familial adenomatous polyposis, Gardner syndrome, hereditary nonpolyposis colon cancer and Peutz-Jeghers syndrome) [29]. Two molecular phenotypes are correlated with distinct genomic destabilisation pathways [29]. One reveals high-level microsatellite instability and the other displays intrachromosomal and chromosomal instability [29]. High levels of genetic abnormality have been detected in up to 59% gastric cancers in Western society [30]. Interestingly, phenotypic microsatellite instability-tumours have a positive correlation with the presence of *H. Pylori*- induced chronic gastritis alongside gastric cancer [31].

Interleukin-1β and *N*-acetyl cystine 1 genes have been reported to be consistently related with gastric cancer [29]. In addition, an Interleukin-1β polymorphism has been suggested to be involved in hypochlorhydria associated with *H. Pylori* infection [32]. Hence, host genetic factors are likely to be strongly linked to the development of gastric cancer in *H. Pylori* infected individuals [33]. The risk of noncardia gastric cancer may be conferred as more than a twofold increase by the polymorphisms of pro-inflammatory cytokine gene clusters, which include numerous additional interleukins and tumour necrosis factors [33].

Mutations in the *p53* gene resulting in the loss of heterozygosity is well described in gastric cancer, as with the majority of other tumours which also contain the loss of heterozygosity and one or more mutations [33]. The mechanisms of dysfunction and telomerase reactivation of the *p53* tumour suppressor are likely to trigger gastric cancer in conjunction with an *H. Pylori*-induced decrease in enhanced cellular proliferation combined with apoptosis [34]. The gastric metaplasia and dysplasia related with *p53* and the *p53* mutation appear to spring from the increase of mucosal free radical levels that conjugate *H. Pylori* infection [35].

Only 5% to 10% of all cases are the diffuse type of gastric cancer, which appears to depend on an autosomal dominant, incomplete penetrance pattern of inheritance [36]. *Helicobacter Pylori* infection, lifestyle, tobacco, alcohol and genetic susceptibility all belong to the aetiological factors of gastric cancer. Modified risk factors may explain approximate 60% of cancer deaths in China related to dietary factors, chronic *H. Pylori* infection and tobacco smoking, which could offer a basis for cancer prevention and control programs with the purpose of decreasing cancer risk in other countries [37, 38].

Table 1.3 Environment and genetic factors related with gastric adenocarcinoma.

Environmental	**Genetic**
*Helicobacter Pylori i*nfection	Familial tumour syndromes
Tobacco smoking	Familial adenomatous polyposis
Vitamin C deficiency	
Low dietary fruits/ vegetables	Gardner syndrome
High dietary	Hereditary nonpolyposis colon cancer
Salt	
Fat	Peutz- Jeghers syndrome
Nitrates	Blood group A
Polycyclic hydrocarbons	Genetic abnormalities
	Interleukin-1β
	N-acetyl cystine 1
	Adenomatous polyposis coli
	E-cadherin
	β-catenin
	Cyclin E
	Transforming growth factor-βIIR
	p 53
	BAX
	K- ras
	bcl-2
	c- met

Source: Principles and Practice of Surgical Oncology: Multidisciplinary Approach to Difficult Problems. Copyright © 2011 by LIPPINCOTT WILLIAMS & WILKINS, a WOLTERS KLUWER business.

1.1.3.3.1.1 Dietary factor

The decline in gastric cancer mortality rates is partly attributed to improved diet, including diet variety and food preservation. Particularly, a diet-rich in fruits and vegetables and diet-low in fat and salty foods may play a protective role. There is approximate 2-fold difference in the risk of gastric cancer between a diet high in fruits and vegetables and a diet-rich in salty foods and fats [4]. Vitamins participate in the progression of gastric carcinogenesis. Low dietary vitamin C may conduce to the progression of pre-cancerous lesions to gastric cancer. This is demonstrated in a Chinese high-risk population-Linqu county, a rural area of China with one of the world's highest rates of gastric cancer [39]. This finding is verified the results of previous studies of gastric cancer and pre-cancer lesions in Linqu [40] as well as reports in other countries [41]. In addition, others report that there are the similar concentration of vitamin C being detected in gastric juice between patients with metaplasia and patients with gastric cancer. This demonstrates that low concentration of vitamin C in gastric juice may have a role in the earliest stage of carcinogenesis [42]. It is already known that a high concentration of vitamin C induces apoptosis in tumour cells and recently, researchers have discovered that vitamin C increases the susceptibility of tumour cells to anti-Fas Abs and the expression of Fas (CD95) and MHC class I on tumour cells [43]. Studies in America indicated that the use of vitamin supplementation may not virtually reduce risk of gastric cancer mortality in North American populations in which the rates of gastric cancer are relatively low, while the influence of vitamin supplementation in areas of high rate of gastric cancer, cannot be ignored.

The relationship between the lack of intake of fresh vegetables and fruits resulted in a deficiency of vitamin C and gastric cancer, a condition known to be exacerbated by the reduction of *H. Pylori* of systemic bioavailability of the vitamin and *H. Pylori* infection [44]. In industrialised

countries, the decrease of gastric cancer is not only attributed to the declining prevalence of *H. Pylori* infection but also the availability of fresh produce through modern methods of refrigeration [45].

1.1.3.3.1.2 Tobacco

Cancer deaths related with smoking in males occupied approximate 9% of all global male cancer deaths [16]. Although not all epidemiologic studies of gastric cancer verified a direct relationship between cigarette smoking and gastric cancer, the majority of evidence demonstrates that the risk of gastric cancer is moderately increased among smokers [46, 47]. Tobacco smoking is the predominant cancer cause among men in China. A long term follow-up study by You *et al* indicated that cigarette smoking is a risk factor for development to dysplasia or gastric cancer [39].

1.1.3.3.1.3 Alcohol intake

Tong *et al.* reported that there were statistically significant dose-dependent effects of alcohol on gastric cancer ($p< 0.05$). It was associated with over 50% added risk of gastric cancer in the Chinese population [48].

1.1.3.3.1.4 H. *Pylori*

Helicobacter Pylori (*H. Pylori*) infection has been established as a major risk factor for gastric cancer [49]. IARC (International Agency for Research on Cancer) monograph classifies *H. Pylori* as a carcinogen to humans based on epidemiological evidence [50]. Although over 50% of the world population is infected with *H. Pylori*, less than 2% develop to gastric cancer [51]. Therefore, host genetic polymorphisms, lifestyle and even environmental and epigenetic factors

may also play a role in occurrence of *H. Pylori* [52]. The relationship between *H. Pylori* infection and gastric cancer stands for a typical model of a multistep process, characterised by atrophic gastritis, intestinal metaplasia and dysplasia, which belong to pre-neoplastic lesions with a high risk of progression [53].

In addition, *H. Pylori* also has an oncogenic role in the development of mucosa-associated lymphoid tissue (MALT) lymphoma, which occupies approximate 3% of all gastric cancers. Hyperplastic polyps are often detected in patients with atrophic gastric mucosa and *H. Pylori* -associated gastritis, while their malignant transformation is rare (<3% of cases). A number of trials showed the *H. Pylori* screening and eradication, particularly in high-risk populations, is an effective means of cancer prevention, however cost-effectiveness of screening is worth discussing in low risk areas [54].

In a Chinese follow-up study in Linqu county, You *et al* found that the infection rate of *H. Pylori* account for 65% among 3 to 12 years old children in Linqu County, which is much higher than among children of similar ages in another neighbouring county Cangshan (29%) [39]. This illustrated that acquisition of *H. Pylori* infection in early age plays an important role in the development of gastric cancer. The population infected *H. Pylori* at least occupied 70%, of which approximate 32.9% of these cases developed to dysplasia or gastric cancer in the 4.5-year period studied [39]. In conclusion, these findings suggests that eradication of *H. Pylori* in subjects with superficial gastritis, intestinal metaplasia or chronic atrophic gastritis possibly suppress disease development to dysplasia or gastric cancer [39].

1.1.3.3.1.5 Familial gastric cancer

The incidence rate of familial gastric cancer occupies approximately 10% of all patients with gastric cancer [36]. Epidemiological studies have demonstrated that the risk of gastric cancer in first-degree grows two-three fold in the normal population [55]. As yet, however, the underlying genetic causes remain mostly unclear for majority of the patients with familial gastric cancer. *CDH1*, which occupies 1-3% of gastric cancers, is suggested as the most important gastric cancer susceptibility gene [56]. Mutations of *CDH1* have been encountered in about one-third of strictly selected Hereditary Diffuse Gastric Cancer (HDGC) families [57, 58], but the genetic cause still remains unknown in at least two thirds of strictly selected HDGC families. Most of these families might carry mutations in other, which are identified as gastric cancer susceptibility genes. Moreover, familial intestinal type gastric cancer exhibiting an autosomal dominant inheritance pattern might also have genetic susceptibility genes. No gene has been related with this type of gastric cancer yet [28]. Application of novel gastric cancer susceptibility genes will be an important stage towards additional options for gastric cancer prevention and indeed therapies. Therefore, identification of new genetic gastric cancer predisposing factors is one of the important goals in the near future.

1.1.3.3.1.6 Other risk factors

Very early studies have demonstrated an excessive risk of gastric cancer associated with blood group type A [8, 59]. There is also a tendency for gastric cancer to show familial aggregation [60]. However, in a Chinese survey which aimed to examine the correlation between ABO blood types and gastric cancer, a history of gastric cancer in a parent or sibling and the presence of precancerous gastric lesions among the 3400 cases studied revealed that the increased probability of gastric cancer among subjects with blood type A were similar to magnitude (30%-

40%) for metaplasia (IM) and dysplasia (DYS) after adjusting for parental history of gastric cancer [61]. This suggests that type A is primarily correlated with transitions from gastritis to metaplasia with little additional influence on development to dysplasia. In contrast, parental history of gastric cancer, after adjusting for blood type, was associated mainly with dysplasia, indicating that blood type A and familial tendency may affect different stages of the carcinogenesis process but are not directly related with gastric cancer [62]. However, in another study, the risk of gastric cancer in non type-A groups was dramatically lower than that in blood group type A (O, B and AB) (odd ratio, OR1.34; 95% confidential interval, CI 1.25-1.44). Compared with blood group O, individuals with non type-O groups (A, B and AB) demonstrated an increased risk of gastric cancer (OR = 0.80; 95% CI 0.72-0.88). The proportion of *H. Pylori* infection in blood group type A individuals was significantly higher than that in non type-A blood groups (OR = 1.42; 95% CI 1.05-1.93). Along with the other published data and reference, it suggested that the risk of gastric cancer in the blood type A group was higher than that in the non type-A groups (OR = 1.11; 95% CI 1.07-1.15), and that blood type O individuals invariably displayed decreased risk of (OR = 0.91; 95% CI 0.89-0.94). the corollaries of these studies was that firstly a slightly increased risk of gastric cancer can be observed in individuals with blood group type A. Secondly, people with blood type A even more trend to be infected by H. *Pylori* than other ABO blood type individuals. Thirdly, a mildly decreased risk of gastric cancer was observed in blood type O individuals [63].

Pernicious anaemia (PA), also known as Biermer's disease, is suggested as an autoimmune disorder, which is distinguished by atrophic damage to the gastric body mucous membrane. Consequently, the damage is resulted in the loss of parietal cells, which normally secrete an intrinsic factor, a protein that stably combines with dietary vitamin B12 and supports its

transport through the terminal ileum mucosal wall [64]. Patients with PA can develop long-term complications including gastric cancer [65]. A systematic review between 1950 and 2011 showed a pooled gastric cancer incidence-rate in PA of 0.27% per business year, an estimated 7-fold relative risk of gastric cancer [2].

Table 1.4 Risk factors of gastric cancer

Risk factors	Specific exposures	Comments	Ref
Tobacco smoking	Ever smoked	A risk factor for progression to dysplasia or gastric cancer	[39]
Alcohol drinking	Ever drank	Association with over 50% risk of gastric cancer in the Chinese population	[48]
Infectious agents	Helicobacter *Pylori*	A carcinogen to humans based on epidemiological evidence	International Agency for Research on Cancer
Diet	Nitrite, high salt intake	The decrease of gastric cancer is attributed to the availability of fresh produce	[45]
Familial inheritance	Any types gastric cancer	The risk of GC in first-degree relatives is increased 2-3 fold	[55]
Other risk factor	*H. Pylori* infection or dysplasia	Gastric cancer risk in the blood A group was higher than that in the non-A groups	[63]

1.1.4 Early gastric cancer: diagnosis and treatment

Early diagnosis and treatment is suggested as an important strategy improving the prognosis of gastric cancer. The rapid advance in the diagnosis and management of early gastric cancer (EGC) has been witnessed over the past few decades: endoscopy has played an increasingly important character. Laparoscopic techniques have also been introduced for the treatment of

early gastric cancer treatment. Worldwide, however the ratio of early gastric cancer is gradually increasing, and this condition is rapidly developing into a hot topic of research.

1.1.4.1 Ambiguities in the diagnosis of early gastric cancer

1.1.4.1.1 Ambiguity of definition

Early gastric cancer is defined as a stomach lesion, which is restricted to the mucosa and/or submucosa regardless of whether its location within the stomach or level of lymph node metastasis on the basis of the Japanese Gastric Cancer Association [66]. The Japanese classification of early gastric cancer is an endoscope-based clinical diagnosis. Early gastric cancer is classified as type I (protruded), type II (superficial), type III (excavated), and the mixed type based on its morphological appearance through the analysis of endoscope. The type II lesions are further subdivided into IIa (elevated), IIb (superficial spread), and IIc (depressed) [67].

So far, the TMN system is also the most common staging system for gastric cancer, which is on the basis of post-operative pathology. However, early gastric cancer is not defined by the TNM system. Early gastric cancer of the Japanese “gastric cancer” classification is generally equivalent to a T1 gastric cancer scoring in the TNM system. The diagnosis, prognosis and treatment of early gastric cancer needs to be based on both clinical diagnosis and pathological staging [68].

1.1.4.1.2 Differences in diagnostic criteria in early gastric cancer

The criteria for the pathological diagnosis of early gastric cancer differs between China and Japan. The Vienna classification of gastrointestinal epithelial neoplasia is adopted in China; for instance, a gastric cancer is diagnosed only when the tumour has invaded deeper than the lamina propria mucosae. By comparison in Japan, gastric cancer is diagnosed on the basis of cellular or structural atypia rather than the degree of tumour invasion. Hence, several early gastric cancer cases are possibly either the atypical hyperplasia in Japan or high-grade adenoma/dysplasia in China. Therefore, we should pay particular attention to those citing literatures, which are authored by Japanese colleagues.

1.1.4.2 Accuracy of clinical staging

Treatment plans depend on tumour stage. So far we are incapable of accurately determining early gastric cancer. The infiltration of early gastric cancer [localized within the mucosa layer (T1a) or cancer which had already invaded the submucosa layer (T1b)] as well as lymph node metastatic status required accurate identification before the application of endoscopic treatment. Given the intervention that endoscopic diagnosis and intervention has provided further work into the classification of early gastric cancer is now required.

1.1.4.3 Various treatment options

The 5-year survival rate of patients with early gastric cancer exceed 90% through the treatment of standard radical surgery. However, the quality of life for patients is harmed ineluctably by radical surgery. Currently, how to minimize surgical intervention and improve quality of life

with regard to gastric cancer is becoming a topic of attention. Up until now endoscopic resection and modified radical surgery have been on the list of the standard treatments.

Endoscopic resection has become the standard treatment for early gastric cancer over recent decades. Endoscopic mucosal resection (EMR) is routine for differentiated mucosal cancer, when smaller than 2 cm, and without the presence of an ulcer(s). On the contrary, endoscopic submucosal dissection (ESD) enables the *en bloc* resection of the lesion, has wider resection potential and can be applied in patients with ulcer(s). Hence, ESD is better than EMR [69]. The clinical study of a multicenter prospective phase III trial demonstrated that laparoscopic procedures was superior to early gastric cancer surgery. As a viable and safe technique, laparoscopic short-term efficacy precedes open surgery [70].

1.1.4.4 Challenges associated with new techniques

Globally the rate of diagnosed early gastric cancer remains low. Both laparoscopy and endoscopy require high level of technology, and require a long period of time on training medical professionals. The Endoscopic or laparoscopic treatment is highly dependent on accurate clinical staging, with endoscopy being the required technique for clinical diagnosis of early gastric cancer. These new procedures could not be introduced without the support of experienced endoscopy experts. Investigations into the new techniques for early gastric cancer diagnosis should only be performed in large scale hospitals, in which several correlative clinical trials may be conducted. The application of these new techniques in the detection of early gastric cancer requires the close co-operation amongst medical specialists from the departments of endoscopy, pathology, and surgery [68].

1.1.5 Pathology and biology

Gastrointestinal stromal tumours (GISTs), lymphomas, or soft tissue sarcomas make up the majority of stomach malignancies in children, whose carcinomas are fewer than 5% [71-74]. In contrast, adenocarcinomas account for approximately 95% of stomach tumours of all other age groups. Less than 1% of all gastrointestinal malignancies are primary gastric adenocarcinoma in children [75]. Gastric adenocarcinomas are classified based on the degree of histological differentiation. More than half of all stomach neoplasms occur in the distal stomach [76, 77]; whilst nodal and omental involvement are possible to be encountered. Squamous cell carcinoma, carcinoid tumour, leiomyosarcoma, teratoma, and liposarcoma belong to other less frequently occurring gastric tumours [78-80].

Gastric carcinomas which spread include lymphaic and haematogenous metastasis, by direct extension, and through seeding of the peritoneal surfaces. These lesions may infiltrate the submucosa, extend directly, and involve the duodenum, oesophagus, colon, liver and even pancreas. Haematogenous (or systemic) metastases of gastric cancer frequently involve the lungs, liver, and skin [81].

1.1.5.1 Biology data

1.1.5.1.1Histogenesis of early gastric carcinoma

The digestive system is a long and tubular organ with multi-layered walls and a number of sphincters. The mucosa in the digestive system that causes adenocarcinomas is similar for stomach, small intestine, colon, and rectum after the upper digestive system passes the oesophagus [82]. The mucosa, which is covered by a simple layer of columnar epithelium, has

specific variation in villus size, which descends in size and cell kinetic turnover time from stomach to rectum [82].

The gastrointestinal canal includes the sections of the digestive tract from the stomach to the anus. It is housed within the abdominopelvic cavity that extends from the hemidiaphragm to the pelvic diaphragm. The abdominal cavity is lined by peritoneum, which is covered with a single layer of mesothelial cells. The peritoneal cavity is a complex structure containing fluid and protein secretions. The abdominal cavity is composed of numerous sacs and folds, in which fluids and peritoneal surface protective protein layers lubricate bowel surfaces. In general, the peritoneal cavity is a powerful system in fluid absorption. However, during cancer spread, peritoneal seeding in the cavity is a significant clinical concern.

A two-layer peritoneum connects the stomach with the lesser omentum (from the lesser curvature) and the greater omentum (from the greater curvature) respectively. A number of peritoneal folds consist of mesenteriums for the arteries, veins and gut. Peritoneal fossae and gutters determine initial pathways of tumour spread both for bowel cancer and ovarian cancer [83]. Figure 1.4 demonstrates overviews of the histological structural differences throughout gastrointestinal and the majority of digestive organ systems.

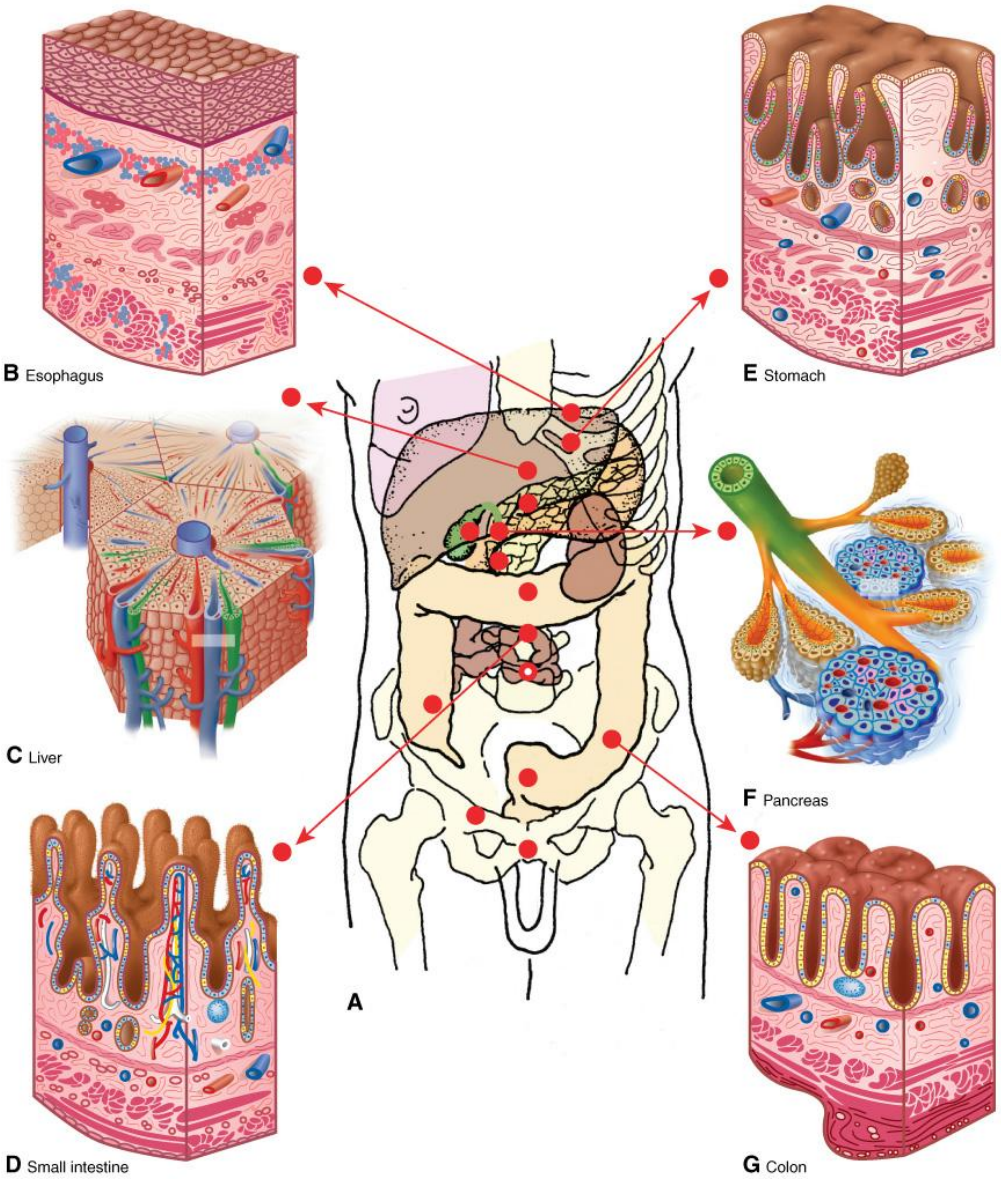

Figure 1.4 Overview of histogenesis of major digestive organ systems.
Source: TNM Staging Atlas with Oncoanatomy, Second Edition by Philip Rubin, John T. Hansen. Copyright © 2012 by LIPPINCOTT WILLIAMS & WILKINS, a WOLTERS KLUWER business.

1.1.5.2 Histopathology

The morphologic features of gastric tumours have been suggested as a standard reference in several staging schemes. For example, gastric cancer is divided into five types depending on macroscopic appearance in the Borrmann classification [84].

-Type I stands for polypoid or fungating cancers,

-Type II contains ulcerating lesions surrounded by elevated borders,

-Type III represents ulcerated lesions invading the gastric wall,

-Type IV are diffusely infiltrating tumours, and

-Type V gastric cancers are unclassifiable cancers [84].

Another histo-morphological staging system was proposed when gastric cancer could be divided into either a prognostically favourable expansive type or a poor prognosis infiltrating type [85]. Based on the analysis of numerous gastric cancer samples, infiltrative tumours were almost diffuse on gross appearance, whilst the expansive-type tumours were uniformly polypoid [86].

Broder's classification for gastric cancer classified tumours in the organizational structure, from 1 (well-differentiated) to 4 (anaplastic). Bearzi and Ranaldi have associate the degree of histological differentiation with the gross appearance of 41 primary gastric cancers endoscopically [87]. Approximately 90% of superficial tumours were well differentiated (Broder's grade 1), while more than 50% of ulcerated tumours were poorly differentiated or diffusely infiltrating (Broder's grades 3 and 4) [87].

The most commonly used classification of gastric cancer is by Laurén in 1965 [88]. According to the Lauren's scale, gastric cancers are divided into either intestinal or diffuse forms. On the

basis of tumour histology, two varieties of gastric adenocarcinomas are characterised. This classification scheme demonstrated distinctively different pathology, epidemiology, genetics, and etiologies of gastric cancer [88]. The intestinal form demonstrated a differentiated cancer with a tendency to form glands in the gastrointestinal tract, especially the colon type. In contrast, the diffuse form demonstrated little cell cohesion, which tended to incur extensive submucosal spread and early metastases [88]. The diffuse-type cancers are correlated with a worse outcome than the intestinal type, based on relationship analysis between the two forms and TNM stage. In addition, the molecular pathogenesis of the two distinct forms is also different [88]. The main carcinogenic event of the diffuse type is loss of E-cadherin expression (a protein product of the *CDH1* gene), which is a molecule involved in cell-to-cell adhesion and results in non-cohesive cell growth [89].

1.1.6 Staging

Proper staging of gastric cancer allows the clinician to choose the appropriate treatment modalities whilst viably evaluating and predicting outcomes of disease management, and uniformly documenting cancer cases worldwide. Although there are several classification systems for gastric cancer, globally the Cancer Staging Manual developed by the American Joint Committee on Cancer (AJCC) with support from the International Union for Cancer Control (UICC), the American Cancer Society, American College of Surgeons, American Society of Clinical Oncology, and International Union against Cancer, is the generally accepted classification system. The cancer-staging criteria have been continually refined since 1959, with the combined efforts of medical community, and multiple medical and oncology organisations. The latest edition (7th edition) of the AJCC Cancer Staging Manual was published in early 2010.

In the new edition, the AJCC and UICC used large datasets and emerging evidence to support changes in the cancer staging criteria in general, and they used data sets from Asia, Europe, and the United States on the gastric cancer staging system in particular.

1.1.6.1 Classification

Patients with gastric cancer, who require surgery, should be classified by both pathological staging (American Joint Committee on Cancer/International Union against Cancer [AJCC/UICC] or Japanese system) and classification of the completeness of resection (R classification). Collection of additional prognostic factors including tumour location, serum CEA CA 19.9, histopathologic grade and type is recommended by the AJCC [90].

1.1.6.1.1 AJCC/UICC Tumour, Node, Metastasis Staging

The AJCC/UICC TNM staging system for gastric cancer is described in table 1.5-continued. The stage-stratified survival rates of 10,601 AJCC/UICC of patients treated by surgical resection from SEER 1973–2005 public-use file diagnosed since 1991 to 2000 are shown in figure 1.5.

Tumours appearing at the oesophago-gastric junction (EGJ) including Siewert type I or arising in the stomach 5 cm or less from the EGJ and crossing into the EJG including Siewert types II and III are classified using the TNM system for oesophageal adenocarcinoma [90]. If gastric tumours do not cross the EGJ into the oesophagus, they should be staged as gastric cancer [90].

In the AJCC/UICC staging system, tumour (T) stage is defined by depth of tumour invasion into the stomach wall and extension into nearby organs (Figure 1.5). The correlation between T stage and survival is well determined (Figure 1.6). Nodal stage (N) is determined by the number of involved lymph nodes, which is suggested to evaluate outcome more precisely than the location of involved lymph nodes [91]. Tumours with one to two involved nodes are staged as pN1, involvement of three to six involved nodes is staged as pN2, whilst involvement of more than seven involved nodes is staged as pN3 (N3a has 7–15 nodes and N3b has ≥16 nodes) [92, 93].

Table 1.5 TNM Staging Classfication for Carcinoma of the Stomach (7th ed., 2010)

Primary Tumour (T)	
TX	Primary tumour cannot be assessed
T0	No evidence of primary tumour
Tis	Carcinoma in situ: intraepithelial tumour without invasion of the lamina propria
T1	Tumour invades lamina propria, muscularis mucosae or submucosa
T1a	Tumour invades lamina propria or muscularis mucosae
T1b	Tumour invades submucosa
T2	Tumour invades muscularis propria[1]
T3	Tumour penetrates subserosal connective tissue without invasion of visceral peritoneum or adjacent structures[2,3]
T4	Tumour invades serosa or adjacent structures[2,3]
T4a	Tumour invades serorosa
T4b	Tumour invades adjacent structures
Regional Lymph Nodes (N)	
NX	Regional lymph node(s) cannot be assessed
N0	No regional lymph node metastasis[4]
N1	Metastasis in 1-2 regional lymph nodes
N2	Metastasis in 3-6 regional lymph nodes
N3	Metastasis in seven or more regional lymph nodes
N3a	Metastasis in 7-15 regional lymph nodes
N3b	Metastasis in 16 or more regional lymph nodes
Distant Metastasis (M)	
M0	No distant metastasis
M1	Distant metastasis
Histologic Grade (G)	
GX	Grade cannot be assessed
G1	Well differentiated
G2	Moderately differentiated
G3	Poorly differentiated
G4	Undifferentiated

Table 1.5- continued. American Joint Committee on Cancer (AJCC) TNM Staging Classification for Carcinoma of the Stomach (7th ed., 2010)

Anatomic Stage/ Prognostic Groups			
Stage 0	Tis	N0	M0
Stage ⅠA	T1	N0	M0
Stage ⅠB	T2	N0	M0
	T1	N1	M0
Stage ⅡA	T3	N0	M0
	T2	N1	M0
	T1	N2	M0
Stage ⅡB	T4a	N0	M0
	T3	N1	M0
	T2	N2	M0
	T1	N3	M0
Stage ⅢA	T4a	N1	M0
	T3	N2	M0
	T2	N3	M0
Stage ⅢB	T4b	N0	M0
	T4b	N1	M0
	T4a	N2	M0
	T3	N3	M0
Stage ⅢC	T4b	N2	M0
	T4b	N3	M0
	T4a	N3	M0
Stage Ⅳ	Any T	Any N	M1

[1]A tumour may penetrate the muscularis propria with extension into the gastro-colic or gastro-hepatic ligaments, or into the greater or lesser omentum, without perforation of the visceral peritoneum covering these structures. In this case, the tumour is classified T3. If there is perforation of the visceral peritoneum covering the gastric ligaments or the omentum, the tumour should be classified T4.

[2]The adjacent structures of the stomach include the spleen, transverse colon, liver, diaphragm, pancreas, abdominal wall, adrenal gland, kidney, small intestine, and retroperitoneum.

[3]Intramural extension to the duodenum or oesophagus is classified by the depth of the greatest invasion in any of these sites, including the stomach.

[4]A designation of pN9 should be used if all examined lymph nodes are negative, regardless of the total number removed and examined.

Source: NCCN Guidelines Version 2.2013 Gastric Cancer. The original and primary source for this information is the AJCC Cancer Staging Manual, Seventh Edition (2010) published by Springer Science and Business Media LLC (SBM) www.springer.com.

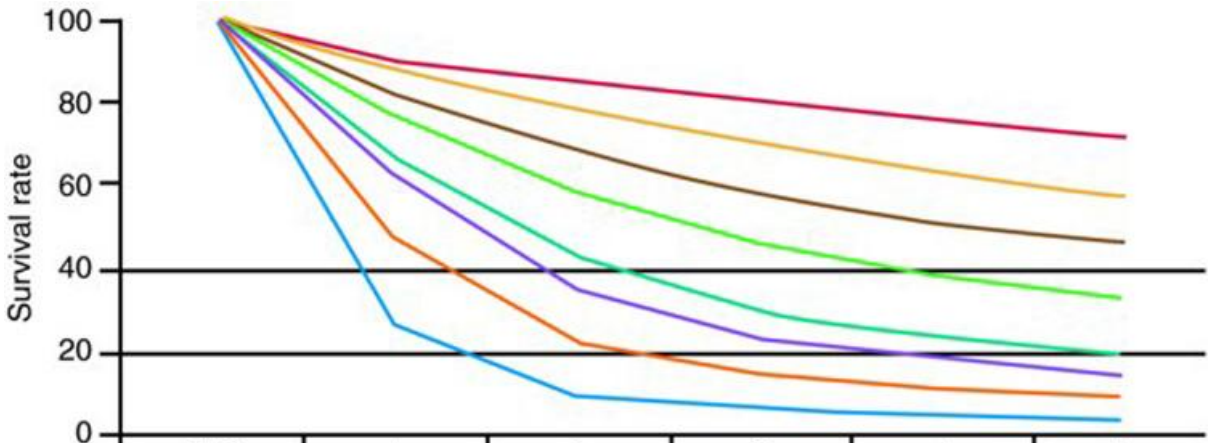

	At Dx	1	2	3	4	5
IA	100.0	90.2	84.4	79.8	74.8	70.8
IB	100.0	87.4	77.9	69.9	62.7	57.4
IIA	100.0	82.1	67.4	57.2	50.2	45.5
IIB	100.0	76.8	58.3	48.0	38.4	32.8
IIIA	100.0	66.5	42.4	29.9	23.5	19.8
IIIB	100.0	61.6	35.4	22.9	17.8	14.0
IIIC	100.0	47.4	21.8	14.2	11.0	9.2
IV	100.0	27.0	10.0	5.6	4.5	4.0

Figure 1.5 Disease-specific survival on Cancer stage grouping by American Joint Committee. Source: DeVita VT, Lawrence TS, Rosenberg SA: DeVita, Hellman, and Rosenberg's Cancer: Principles& Practice of Oncology, 9th Edition. Copyright © 2011 by Lippincott Williams& Wilkins, a Wolters Kluwer business.

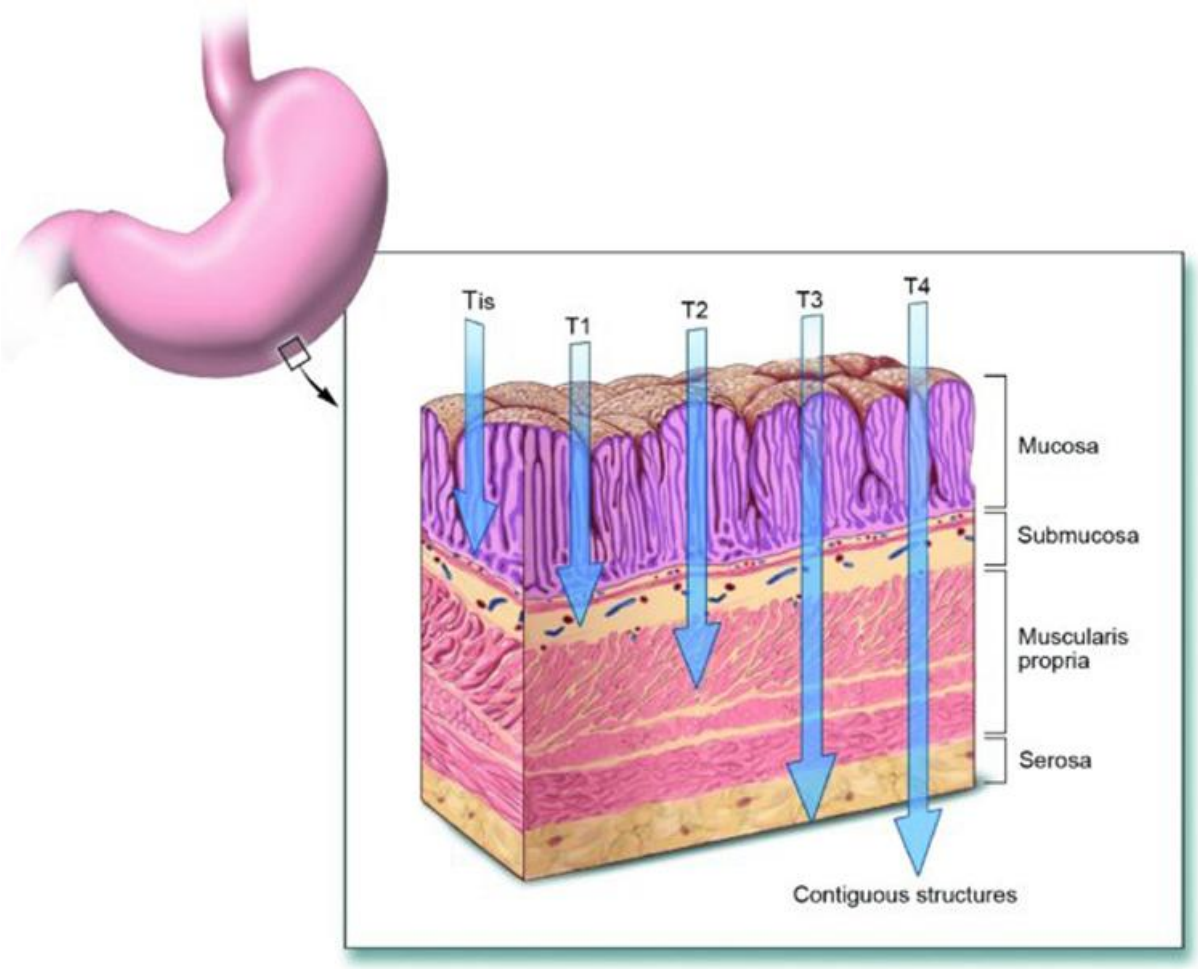

Figure 1.6 Cancer T stage defined by depth of penetration of the gastric wall by American Joint Committee on Cancer (AJCC). Source: DeVita VT, Lawrence TS, Rosenberg SA: DeVita, Hellman, and Rosenberg's Cancer: Principles& Practice of Oncology, 9th Edition. Copyright © 2011 by Lippincott Williams& Wilkins, a Wolters Kluwer business.

1.1.6.2 Japanese Staging System

The most latest Japanese classification for gastric cancer was published in 1998 [94]. The Japanese classification and staging system is more emphasized on the difference between surgical, pathologic and "final" staging (prefixes "c," "s," "p," and "f," respectively) compared with the AJCC/UICC staging system [94, 95]. For instance, a surgical patient with locally non-metastatic gastric tumour may be classified as sH0, sM0 or stage f-IIIB (H0 represents no hepatic metastases and the "f" prefix stands for final clinic-pathological stage). Furthermore, the Japanese classification system contains a classification system for early gastric cancer (Figure 1.7) [96].

In the Japanese classification system, primary tumour (T) stage is defined on the depth of invasion and extension to adjacent tissue, similarly to the AJCC staging system (Table 1.6). Whilst the assignment of lymph node (N) stage is more detailed than the AJCC staging based on rigorous pathological examination. Eighteen regions of lymph nodes are classified into four N categories (N0 to N3) depending on their correlation with the primary tumour and anatomical location. However, some lymph nodes, even peri-gastric nodes for specific tumour locations, can be considered as M1 disease. This is because their involvement shows a poor prognosis [97].

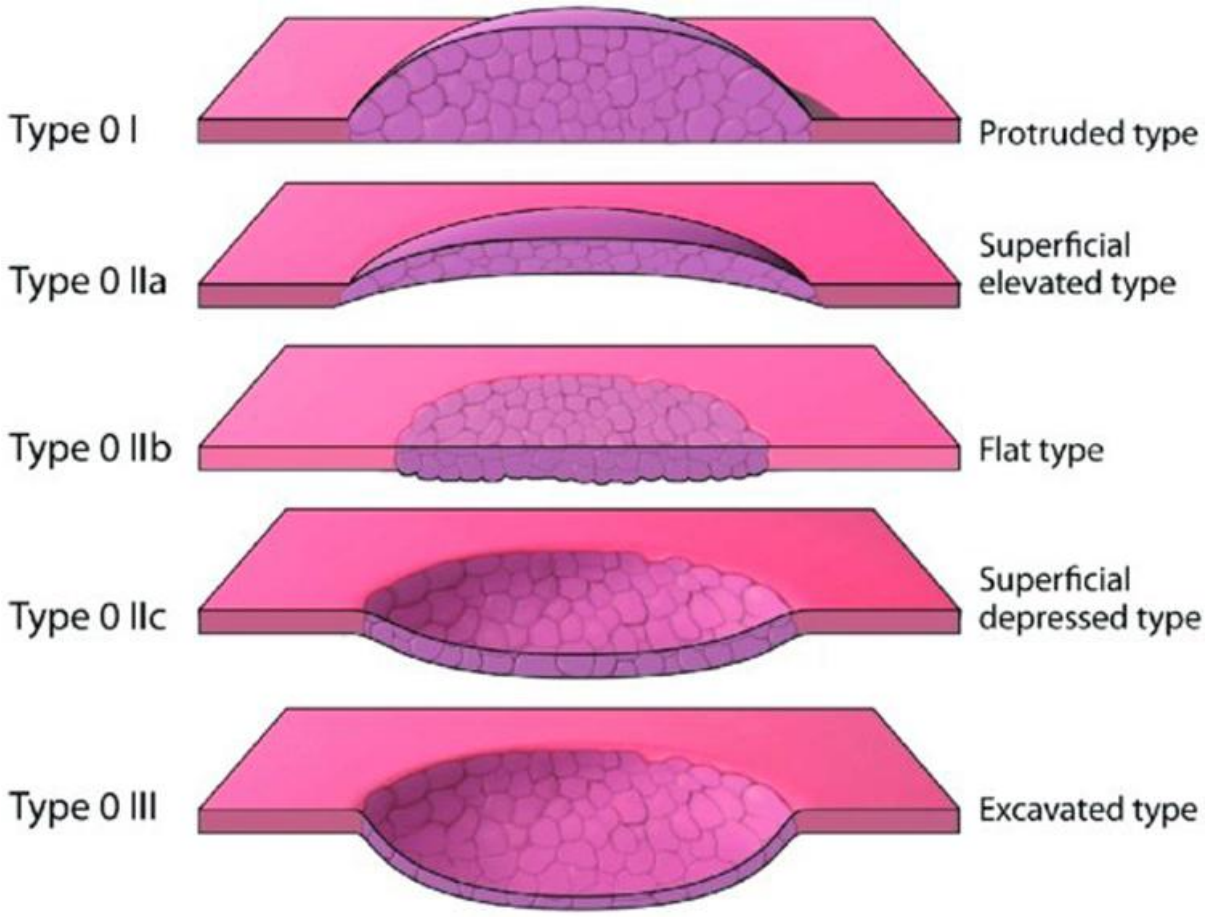

Figure 1.7 Japanese classification system for early stage gastric carcinoma. Source: DeVita VT, Lawrence TS, Rosenberg SA: DeVita, Hellman, and Rosenberg's Cancer: Principles& Practice of Oncology, 9th Edition. Copyright © 2011 by Lippincott Williams& Wilkins, a Wolters Kluwer business.

Table 1.6 Japanese Gastric Cancer Association Staging System for Gastric carcinoma.

Tumour stage					
T1	Tumour invasion of mucosa and/ or muscularis muscosa (M) or submucosa (SM)				
T2	Tumour invasion of muscularis propria (MP) or subserosa (SS)				
T3	Tumour penetration of serosal (SE)				
T4	Tumour invasion of adjacent structures (SI)				
TX	Unknown				
Nodal stage					
N0	No evidence of lymph node metastasis				
N1	Metastasis to group 1 lymph nodes, but no metastasis to groups 2 to 3lymph nodes				
N2	Metastasis to group 2 lymph nodes, but no metastasis to group 2 lymph nodes				
N3	Metastasis to group 3 lymph nodes				
NX	Unkown				
Hepatic metastasis stage					
H0	No liver metastasis				
H1	Liver metastasis				
HX	Unknown				
Peritoneal metastasis stage					
P0	No peritoneal metastasis				
P1	Peritoneal metastasis				
PX	Unkown				
Peritoneal cytology stage (CY)					
CY0	Benign/ indeterminate cells on peritoneal cytology				
CY1	Cancer cells on peritoneal cytology				
CYX	Peritoneal cytology was not performed				
Other distant metastasis (M)					
M0	No other distant metastases (although peritoneal, liver, or cytological metastases may be present))				
M1	Distant metastases other than the peritoneal, liver, or cytological metastases				
MX	Unknown				
Stage grouping					
	N0	N1	N2	N3	
T1	ⅠA	ⅠB	Ⅱ		
T2	ⅠB	Ⅱ	ⅢA		
T3	Ⅱ	ⅢA	ⅢB		Ⅳ
T4	ⅢA	ⅢB			
H1, P1, CY1, M1					

Table 1.6 to be continued on next page.....

Table 1.6 Table 1.6 continuing from previous page:

[a]Cytology beliwved to be "suspicious for malignancy" should be staged as CY0
Source: DeVita VT, Lawrence TS, Rosenberg SA: DeVita, Hellman, and Rosenberg's Cancer: Principles& Practice of Oncology, 9th Edition. Copyright © 2011 by Lippincott Williams& Wilkins, a Wolters Kluwer business.

1.1.7. Gastric cancer diagnosis strategy

1.1.7.1 Signs and Symptoms

Because non-specific symptoms can describe early gastric cancer, many patients are diagnosed in advanced stage disease. A combination of signs and symptoms e.g. weight loss, anorexia, fatigue, epigastric discomfort, pain, postprandial fullness, indigestion and vomiting may be detected in patients with gastric cancer. Whilst none of these can unequivocally manifest in gastric cancer, weight loss and abdominal pain are considered as the most common initial symptoms [98, 99]. In addition up to 17% of patients may be asymptomatic [100].

Dewys *et al.,* reported that in an investigation of 179 advanced gastric cancer patients more than 80% had a dramatic decrease in body weight (> 10%) prior to diagnosis [101]. In addition, Maconi *et al.,* found that patients with weight loss had a dramatically shorter survival than those without weight loss [99].

1.1.7.2 Screening

Successful screening programs for gastric cancer have been established in high-risk areas, such as Japan [102]. Numerous screening tests have been trialed in patients with gastric cancer in Japan, with a sensitivity and specificity of around 90% [103]. Serology for *H. Pylori*, which

double-contrast barium radiographs or upper endoscopy with risk stratification is one typical screening technique (OLGA staging system for gastric cancer risk) [104]. Phata *et al.,* reported a study with a 7.7 year follow-up period of 4,655 asymptomatic patients, in which, with a cohort average age of 50 years old, 2,341 (52%) were *H. Pylori*-positive with non-atrophic gastritis, 967 (21%) were *H. Pylori*-negative without atrophic gastritis, 1,316 (28%) were *H. Pylori*-positive with atrophic gastritis, and 31 (0.7%) had severe atrophic gastritis. [105].

1.1.7.3 Biomarkers

Serum markers are not applied for early cancer screening, but they are suitable for detection of recurrence and distant metastasis, prediction of patient survival and also postoperative monitor. The most frequently used serum tumour markers for clinical auxiliary diagnosis are CEA, CA19-9, and CA72-4. A systematic literature search before the end of November 2012 showed that these markers had remarkable association with tumour stage and survival time of the patients. Tumour marker monitoring may be useful for patients after surgery, as the positive conversion of tumour markers approximately recurs 2 months before the abnormal formation. Alpha-faetoprotein (AFP) is applicable to detect and predict liver metastases. Furthermore, CA125 and sialyl Tn antigens (STN) are used to detect peritoneal metastases. Although no prospective trial has yet completely assessed the clinical significance of these tumour markers, this literature search indicates that a combination of CEA, CA19-9, and CA72-4 is the most effective way for clinical staging before surgical therapy or chemotherapy. The increased level of monitoring tumour markers before surgery or chemotherapy is particularly useful for detection of recurrence or evaluation of treatment response [106].

In a large review in which 410 manuscripts were retrieved, and 7 manuscripts of high quality including 652 patients were of high quality in this meta-analysis, MG7-Ag is found to be a potential biomarker for the diagnosis of gastric cancer [107].

Systematic review and meta analysis suggests that circulating tumour cells (CTCs**)** detection alone cannot be recommended as a screening test for gastric cancer. However, it is possibly applied as a non-invasive method for making a prognosis of gastric cancer [108].

1.1.7.3.1 Analysis of Molecular Markers

Numerous reports demonstrate that analysis of various molecular markers is likely to be a guide to designing therapeutic agents and treatment regime, an effective way leading to personalised medicine [109]. For example, through the evaluation of microsatellite alterations and *p53* mutation status in biopsy material obtained from gastric cancer prior to any therapy, a high level of chromosomal instability would define a subset of patients who may benefit from cisplatin-based neo-adjuvant chemotherapy. In contrast, *p53* mutation status was not an effective marker for response prediction [110].

In addition, the gene expression of the enzyme thymidylate synthase (TS) in gastric cancer had a negative correlation with survival of patients required 5-FU-based chemotherapy [111]. Hence, those patients with express high expression of TS did not possibly benefit from irinotecan (CPT-11), while tumours expressing low TS levels maybe benefit from 5-FU-based chemotherapy [112]. The University of Southern California group reported that the relative

level of mRNA of the excision repair cross-complementing (*ERCC1*) gene had an adverse relationship with response and survival in an independent function to cisplatin efficacy [112].

In a study to investigate the expression of the *erbB-2* oncogene, which was expressed in more than 20% of gastric cancer and had a significant correlation with poor prognosis, Kasprzyk *et al.* indicated that a combination of two anti-*erbB-2*-specific antibodies had an inhibitory effect on the growth of human gastric cancer cells *in vitro*. This combinational antibody therapy also suppressed the growth of human gastric cancer cells growing as xenografts in athymic nude mice *in vivo* and was significant in the reduction of established tumours [113].

1.1.7.4 Diagnosis

The cure rate of gastric adenocarcinoma is high in patients who are diagnosed at an early stage however based on the aggressive biological nature of gastric cancer this rate declines with later diagnosed disease stages. The incidence of gastric cancer is low in most Western countries, so aggressive screening is not cost-effective [114] therefore alarm symptoms and signs (e.g. anorexia, early satiety, weight loss, fatigue, emesis or haematemesis, melena, anaemia, and a palpable abdominal mass) are considered as the key to early diagnosis of gastric cancer [115]. Dyspeptic pain unresponsive to standard anti-secretory therapy should also prompt for investigation into the possibility of early gastric cancer [116].

Flexible fibreoptic oesophago-gastro-duod-enoscopy is considered as first-line diagnostic procedure when a patient is suspected of having gastric cancer. Diagnostic accuracy for gastric

malignancy is approximately 95% based on multiple biopsies of any gastric mucosal abnormality, ulceration, or mass lesion [117]. Barium upper gastrointestinal radiological studies are no longer routinely performed for diagnostic purposes because early gastric cancer and sessile non-bulky tumours are easily missed through use of this technique and radiological discrimination between benign and malignant gastric ulcers is relatively poor. Because any mucosal abnormality identified on upper gastrointestinal series requires endoscopic biopsy for definitive diagnosis radiological diagnosis is inherently redundant or not cost-effective.

1.1.8 Tumour metastasis

The stomach, a distensible organ, is located in the left upper abdomen and is classically divided into four parts (cardia, fundus, body and pylorus). Gastric tumour metastasis includes four pathways:-

lymphatic metastasis

direct spread,

hematogenous metastasis and

peritoneal seeding.

Amongst these pathways lymphatic metastasis is the most common method of metastatic spread. Lymph node involvement is the most common route of metastasis in gastric cancer and is likely due to the extensive distribution of the lymphatic network within the stomach. Maruyama *et al.*, reported that the most common site of lymph node involvement was along the lesser and greater curvature (11%- 40%) [118]. Lymph node involvement around the cardia was common for proximal tumours (13%- 31%), but not for distal stomach tumours (<7%). In addition, infra-pyloric lymph node involvement was unusual for proximal tumours (3%), but common for

distant gastric cancers (49%). Other lymph node involvement was commonly detected along the left gastric artery (19%- 23%), hepatic artery (7%- 25%, most for distal tumours), and celiac axis (8%- 13%) [118-120].

After lymph node metastasis, peritoneal seeding is the second most common site for metastasis in gastric cancer [121]. Up to 20% of patients with gastric cancer have peritoneal deposits. Peritoneal metastasis can develop in almost 60% of T3 and T4 tumour cases [122]. Extensive studies into peritoneal seeding from gastric cancer conducted in Japan and Korea have shown that survival rates for patients with heated intra-peritoneal chemotherapy at the time of gastrectomy increased from 10% to 43% [123, 124].

1.1.9 Prognosis

1.1.9.1 Prognosis and factors

The survival rates are also influenced by the number of lymph nodes involved [125-128]. The finding of either in isolation lymph node involvement or complete wall penetration is usually not as predictive as the presence of both [126, 128, 129] (Table 1.7). A poor performance status, elevated alkaline phosphatase levels and ethnicity are also suggested as prognostic indicators [130]. Byfield *et al.,* reported that Asian and Pacific Islander (API) were more likely than non-Hispanic white (NHW) diagnosed at an early stage of gastric cancer, and foreign-born APIs rather than US-born APIs had more favourable survival outcome than NHWs [131]. Flow cytometry is also of prognostic significance. Aneuploidy is related to unfavourable tumour

location, primary tumour invasion and lymph node metastasis [132-134]. A poor prognosis has correlation with unfavourable DNA flow cytometry [132]. The gross pathological appearance of the primary tumour also provides important prognostic information, although there is uncertainty on whether this factor is independent of tumour stage. Patients with Borrmann type I and II tumours have relatively favourable 5-year survival rates, on the contrary, patients with type IV (linitis plastica) fare adversely [135-137].

Table 1.7 Survival rates compared with extent of initial disease for gastric cancer.

	5-year survival rate (%)	≥ 5-year survival rate (%)
Extent of disease	[138]	[129]
Negative lymph nodes		
Mucosa only	100	-
Beyond mucosa but within wall	61	-
Through wall	44	-
Positive lymph nodes		
Nodal extent	15	19
Regional only	-	-
Nonregional	-	-
Extent of primary		
Within wall	-	40
Through wall	-	12

1.1.9.2 Biological prognostic factors

Mutations in two genes, hMSH3 and hMLH1 on chromosomes 2 and 3 respectively, are reported to be implicated in cancer family syndromes and hereditary non-polyposis colorectal cancer, which is a disease related to a tendency for the development of gastric cancers [139]. Mutations in these genes generate genetic instability and have the potential to trigger further alterations in oncogenes.

Two proto-oncogenes, c-MET and k-sam, have association with scirrhous gastric carcinoma. c-MET encodes hepatocyte growth factor, which is a potent endogenous promoter of growth of gastric epithelial cells [140]. Overexpression of c-MET is associated with tumour metastasis [139, 141]. K-sam encodes a group of tyrosine kinase receptor family proteins [142]. There is a tendency for c-MET to be activated in men >50 years of age and k-sam to be amplified in women (<40 years of age) [142]. Genetic alterations, including p53 gene inactivation, CD44 expression, telomerase activation, dysfunction of hMSH3 and hMLH1, overexpression of proto-oncogenes (Erb-B2, Bcl-2, c-MET and k-sam) and oestrogenic receptor expression, are all associated with a poor prognosis [143].

1.2 Therapy

1.2.1 Overall therapeutic strategies for gastric cancer

To date there is sufficient evidence to support the use of adjuvant chemotherapy and radiotherapy either post-operatively or peri-operatively, especially when cancers are in their advanced stages, as commonly practiced in Europe, North America, and some parts of Asia.

Surgery alone is not any more the standard therapy for patients with resectable gastric cancer [144]. Randomised controlled trials and meta-analyses should contribute to explore the indications, dosage regimen, and opportunitiy of adjuvant therapy for gastric cancer.

1.2.2 Peri-operative adjunctive therapy

Over the past decade, there has been more extensive surgical treatment focus on gastric carcinoma, which progressively includes subtotal gastrectomy, total gastrectomy, radical gastrectomy with splenectomy, distal pancreatectomy and recently extended nodal dissections. More recently efforts in designing and testing multi-modality and peri-operative strategies with a vision to achieving the same favourable clinical outcome as seen in the treatment of other solid tumours, namely breast cancer. Some good examples include external-beam irradiation (ERBT), combined with chemotherapy, hypothermia, intraperitoneal chemotherapy, immunotherapy, intra-operative radiotherapy (IORT), anti-angiogenesis agents and oncogene function suppressors.

1.2.3 Surgery

For patients with early stage gastric cancer (T1/T2, N0, M0 tumours), laparoscopic gastric resection with lymphadenectomy has been suggested as the most commonly practised procedure [145]. Kitano reported short-term benefits following laparoscopic procedures included faster recovery, shorter hospital stay, and less pain whilst long-term benefits after the procedure included favourouable 5-year disease-free survival rates, for example 99.8% (Stage ⅠA), 98.7% (Stage ⅠB), and 85.7% (Stage Ⅱ) [146]. However, in a randomised controlled

clinical trial of subtotal gastrectomy by Cristiano *et al.*,, the rates of 5-year overall and disease-free survival did not show the significant difference for the two operative approaches [147].

In a recent randomised trial (164 patients in the two groups, with 82 patients each) which compared laparoscopic distal gastrectomy with open distal gastrectomy, patients who had undergone laparoscopic distal gastrectomy had an improved quality of life (QOL). This was seen through improved physical functions including appetite loss, sleep disturbance, anxiety, and body image, as well as intra-operative blood loss, reduced post-operative narcotic use and hospital stay [148].

1.2.4 Neo-adjuvant therapy

Auxiliary intraperitoneal chemotherapy

The clinical data regarding the integration of intraoperative radiation therapy (IORT) as a component of combined-modality treatment for resectable gastric cancer was recently summarised in detail. Three randomised prospective trials of IORT have been reported. In 1988, M. Abe from Kyoto University, Japan, reported a randomised trial in which more than 200 patients with stage I-IV stomach cancer (using the Japanese Surgical Staging System) were grouped into surgery alone versus surgery + IORT (28 to 35 Gy). A non–statistically significant trend toward improved 5-year overall survival was seen in stage II-IV patients. However, two smaller phase 3 studies did not show a survival benefit. At the National Cancer Institute, 40 stage III and IV (American Joint Committee on Cancer) patients were randomised to surgery + IORT (20 Gy) versus surgery + EBRT (50 Gy), whereas at the University of Freiburg (Freiburg, Germany), 115 patients were randomised to surgery versus surgery + IORT (28 Gy) [149, 150].

Data from other single-institution, nonrandomised studies suggest a benefit from IORT or IORT + EBRT compared with surgery alone [151]. The present standard of care for locally advanced (node positive and/or margin positive) gastric cancer includes post-operative chemo-radiation or peri-operative chemotherapy alone, based on recent phase 3 trial data [152, 153]. Thus, any future trial testing the integration of IORT in locally advanced gastric cancer must include these approaches.

1.2.5 Molecular-targeted therapy

Molecular-targeted therapy is defined as any inhibitor or monoclonal antibody which selectively suppresses a specific molecule, or molecular pathways, involved in the progression or metastasis of cancers [154]. Numerous biological anti-cancer agents mediating different pathways have been trialled over the past decade, examples including anti-angiogenesis agents, growth factor receptor inhibitors/antagonists, matrix metalloproteinase inhibitors and inhibitors to mammalian target of rapamycin (mTOR) [155, 156].

Based on the outcome of the Transtuzumab for gastric cancer (ToGA) trial, only trastuzumab, an anti-HER2 monoclonal antibody, has been approved for clinical use in combination with chemotherapy to treat HER2-positive advanced gastric and oesophago-gastric junction cancer [157]. Immunohistochemistry (IHC) and fluorescence *in situ* hybridisation (FISH) or dual colour silver- enhanced in situ hybridisation (DISH) is the main molecular diagnosis of HER2 status (Figure 1.8). DISH, which has the same accuracy (concordance rate reaches 97%) as FISH, can be observed under conventional light microscopy [158]. Because of the significant heterogeneity of HER2 status in gastric cancer, it has been recommended that the order of testing for HER2 should be IHC and then FISH/DISH [158].

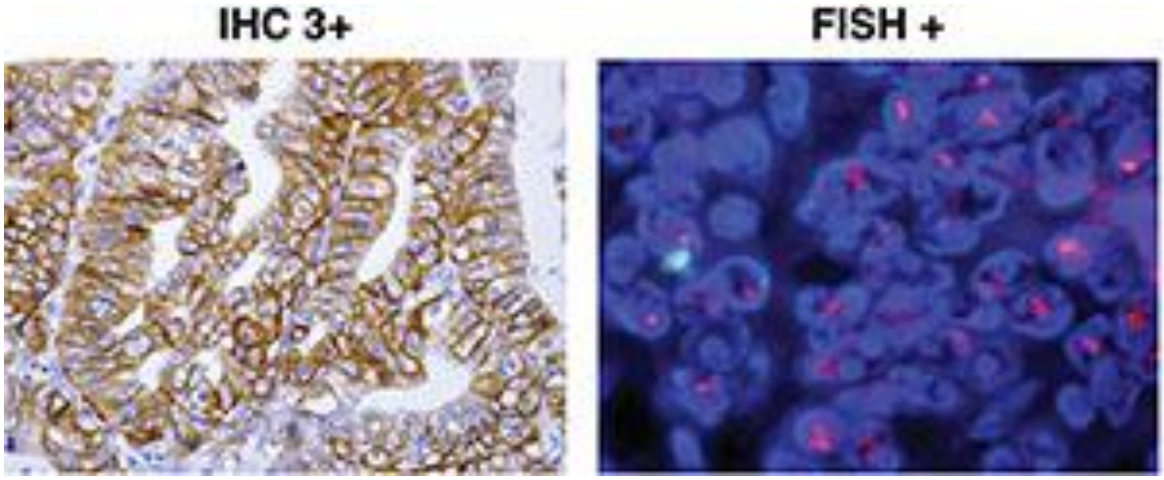

Figure 1.8 Evaluation of HER2 in gastro-oesophgeal junctional and gastric cancer.
Source: DeVita VT, Lawrence TS, Rosenberg SA: DeVita, Hellman, and Rosenberg's Cancer: Principles& Practice of Oncology, 9th Edition. Copyright © 2011 by Lippincott Williams& Wilkins, a Wolters Kluwer business.

1.3 EMT

1.3.1 Introduction

Epithelial–mesenchymal transitions (EMTs) was firstly perceived as a feature of embryonic development in mammal [159]. The formation of mesenchymal and non-epithelial cells loosely implanting in an extracellular matrix, from a primitive epithelium is an important characteristic of most metazoans [160]. During this transition, mesenchymal cells have a spindle-shaped morphology, which is applicable to migrate in an extracellular environment and move in areas involving in organ formation. Mesenchymal cells are also able to involve in the formation of epithelial organs through a reverse process of EMT, known as mesenchymal–epithelial transition [112].

In late 1960s, Elisabeth Hay reported a description of the formation of the chick primitive streak [161] - a structure that is in need of the transformation of epithelial to mesenchymal cells – while EMT was not acknowledged as an explicit process until 1982 by Elisabeth Hay and Garry Greenburg [162]. After that Michael Stocker and Michael Perryman showed that Madin–Darby canine kidney (MDCK) cells, a kind of epithelial cell line from mink kidney, were capable to transform into migratory fibroblasts from cultured fibroblasts through incubation with conditioned medium [163]. A factor participated in this conversion was specific scatter factor and was defined as hepatocyte growth factor (HGF) afterwards [164-166].

EMT was approved to be recognised as a potential mechanism of carcinoma process after a long time. The definition of carcinomas (tumours of epithelial origin) and sarcomas (tumours of mesenchymal origin) have been identified under numerous criterion by pathologists. These two separate entities are not thought to overlapping, unless in a very unusual tumour type namely sarcomatoid carcinoma [167-169]. However, various carcinoma cell lines expressed segmental or complete EMT. Furthermore, carcinomas can show a variety of phenotypes and malignant potential and most of their epithelial characteristics would be absent during progression. This phenomenon is considered in the classical tumour staging methods [160].

The mechanisms of EMT are now being illuminated, in the meantime, many parallels are being found among this process in embryo development, tissue culture and tumour. A number of signalling pathways have been disclosed that are common to the EMT development in progression of carcinoma. The definition of EMT, hence provides a new means of recognizing genes which are essential for the tumour progression towards undifferentiated and more

malignant states. Studying the cellular and developmental biology of the EMT process might provide insights into crucial mechanisms involved in tumour progression [160].

EMT has been intensively studied by cancer researchers in recent decades. It represents one of the major mechanisms by which tumour cells gain critical metastatic features including enhanced motility, invasiveness and resistance to apoptotic stimuli [170, 171]. While the EMT process has been well characterised in tumour cells in culture, there is accumulating evidence that EMT is involved in metastasis *in vivo* as well. Using an intravital imaging technique, Giampieri *et al.* showed that single breast cancer cells gained molility for hematogenous metastasis by activating EMT-promoting TGF-β–Smad2/3 signalling [172]. Indeed, EMT was also observed in metastasis from spontaneous tumour models in mice. The disseminated tumour cells in the lungs of MMTV-PyMT transgenic mice expressed a mesenchymal marker, FSP-1, suggesting a role for EMT in tumour metastasis [173]. Direct evidence of EMT was also found in Myc-initiated breast tumours [174] and K-Ras-mediated pancreatic tumours [175] by using a lineage-specific tracing strategy.

However, the simple EMT model does not explain the observation that metastatic lesions commonly resemble the epithelial phenotypes of the primary tumours. EMT in tumour cells appears to be transient – once a metastatic cell has invaded a new tissue, the mesenchymal features disappear. For instance, the disseminated MMTV-PyMT tumour cells shifted back to an Fsp-1-negative epithelial phenotype as metastatic lesions expanded [173]. Studies with patient cancer samples also showed that metastases in the liver, lung and brain expressed epithelial markers as highly as the primary breast tumours [176, 177]. Similarly, liver metastases from prostate cancer showed epithelial morphology in the majority of cases studied

[178] . These observations suggest that tumour cells may revert back to the epithelial phenotype during metastatic lesion growth through mesenchymal to epithelial transition (MET) [112]. MET, as the reverse process of EMT, has been characterised as an essential developmental process, especially in the organogenesis of the kidney. Despite observations in clinical studies, the evidence for MET in metastasis is very limited. By using an experimental metastasis model in mice, Gao *et al.,* found that tail vein injection of metastatic breast cancer cells (MDA-MB-231), which showed a mesenchymal phenotype with no detectable E-cadherin expression, resulted in E-cadherin (+) metastatic lesions in the lung, indicating MET may have occurred during metastasis formation [179]. Interestingly, recent studies have suggested that MET plays an active promoting role in metastasis along with EMT. For instance, the miR-200 family that enforces the epithelial phenotype by targeting ZEB1/2 [180] was surprisingly found to be pro-metastatic. Over-expression of miR-200s is associated with increased risk of metastasis in breast cancer and promotes metastatic colonisation in mouse models [181] . On the other hand, tumour cells that were trapped in the mesenchymal stage by constitutive activation of TGF-β/Smad2 signalling, failed to develop into metastatic lesions, although they were capable of disseminating into the secondary organs [172]. Taken together, current data suggests that both the EMT and MET processes are critical at different stages of tumour metastasis. Tumour cells need to exhibit EMT/MET plasticity to successfully establish metastatic lesions. The EMT/MET plasticity of these tumour cells may be regulated by both intrinsic and extrinsic factors. However, genomic analysis of primary tumours and distant metastases have found a high degree of similarity at several levels including total gene copy numbers, loss of heterozygosity and single nucleotide polymorphisms [182-184], indicating that intrinsic genomic alterations are not the driver of the EMT/MET cascade during metastasis formation (Figure 1.9). Instead, it is more likely that metastatic tumour cells exhibit their EMT/MET

plasticity to adapt to the changing microenvironments they encounter at either the primary or secondary site.

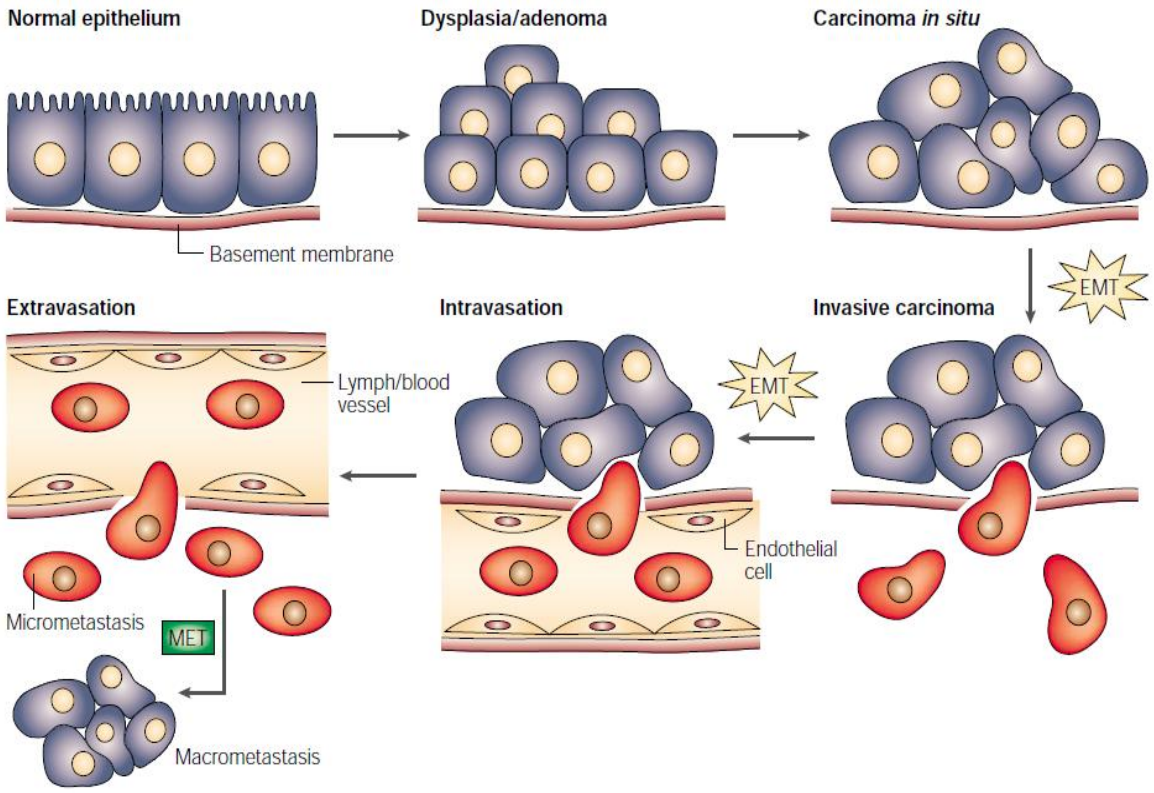

Figure 1.9 Sites of EMT and MET in the emergence and progression of carcinoma. Normal epithelial lined by a basement membrane can proliferate locally to give rise to an adenoma. Further transformation by epigenetic changes and genetic alterations leads to a carcinoma in situ, still outlined by an intact basement membrane. Further alterations can induce local dissemination of carcinoma cells, possibly through an epithelial-mesenchymal transition (EMT), and the basement membrane becomes fragmented. The cells can intravasate into lymph or blood vessels, allowing their passive transport to distant organs. At secondary sites, solitary carcinoma cells can extravasate and either remain solitary (micrometastasis) or they can form a new carcinoma through a mesenchymal-epithelial transition [112]. (Source: Epithelial mesenchymal transition in tumour progression, Nature reviews,2002,2,442-454)

1.3.2 EMT markers and transcriptional factors

1.3.2.1 EMT/MET biological markers

On the basis of the morphological, biological and biochemical changes of the cell during the EMT process, a considerable number of biomarkers have been reported and summarised recently as shown in Figure 1.10 (Zeisberg and Neilson 2010). The majority of markers are associated to the morphological and functional changes of cells during the EMT process and are grouped into three categories: the first category is related to cell surface (e.g. cadherins); the second one is related to cytoskeletal proteins (e.g. vimentin); the third one is related to extracellular proteins (e.g. fibronectin). Some of the key transcription regulators, namely Snail, Twist, LEF1, have also been suggested as valuable markers. Some markers are up-regulated during EMT, while the others are down-regulated (e.g. E-cadherin). More interestingly, some of the microRNA have also been considered to be useful markers for EMT, namely miR10B and miR21. The most valuable pair of these identified biomarkers is the switch between E-cadherin and N-cadherin. During the EMT transition, E-cadherin which belongs to the Class-1 cadherin family is reduced or even lost, conversely, N-cadherin expression which belongs to the Class-2 cadherin family is increased.

Acquired markers	Attenuated markers
Name	**Name**
Cell-surface proteins	
N-cadherin	E-cadherin
OB-cadherin	ZO-1
α5β1 integrin	
αVβ6 integrin	
Syndecan-1	
Cytoskeletal markers	
FSP1	Cytokeratin
α-SMA	
Vimentin	
β-Catenin	
ECM proteins	
α1(I) collagen	α1(IV) collagen
α1(III) collagen	Laminin 1
Fibronectin	
Laminin 5	
Transcription factors	
Snail1 (Snail)	
Snail2 (Slug)	
ZEB1	
CBF-A/KAP-1 complex	
Twist	
LEF-1	
Ets-1	
FOXC2	
Goosecoid	
MicroRNAs	
miR10b	Mir-200 family
miR-21	

Figure 1.10 EMT biomarkers. Adapted from Zeisberg and Neilson 2010.

1.3.2.2 E-cadherin

The E-cadherin gene at human chromosome 16q22.1 encodes E-cadherin. This gene is a classical cadherin belonging to the cadherin superfamily. Its encoded protein is a calcium dependent cell-cell adhesion glycoprotein, which is composed of five extracellular cadherin repeats, a highly conserved cytoplasmic tail and a transmembrane region. Mutations of this gene are associated with gastric, breast, colorectal, thyroid and ovarian cancer. Loss of function

is deemed to promote to cancer development by improving proliferation, invasion, and metastasis. Bacterial adhesion to mammalian cells is regulated by the ectodomain of the protein of E-cadherin and the cytoplasmic domain is essential for internalisation. Transcript variants have been identified which arise from mutations at consensus splice sites. Familial diffuse type gastric cancer occurs due to germ-line mutations of the E-cadherin gene. Down-regulation of E-cadherin function due to mutation, deletion, CpG hyper-methylation, and SNAIL1 - or SIP1-mediated transcriptional repression of the E-cadherin gene has also been shown to lead to EMT in gastric cancer [185].

A number of studies of the human E-cadherin promoter, primarily carried out by Cano *et al* [186-188] displayed regulatory elements located in the 5'-proximal sequence. Amongst them the E-pal element (including two E-boxes) which serves as a repressor can even exceed the influences of positive factors acting on the proximal promoter [186].

Cell adhesion mediated by Cadherin plays an important role in early embryonic development, where a lot of phenotypic changes arise through the EMT process. The acquisition of a fibroblastic phenotype is accompanied by the deletion of E-cadherin and allows cells to separate from epithelial tissue and migrate freely. This is a crucial event during gastrulation movements and the formation of neural crest, but has also been supposed to play a fundamental role during early stages of invasion and metastasis of cancer cells.

EMT participating in down-regulation of E-cadherin is suggested to play an essential role during early stages of invasion and metastasis of cancer cells, namely gastric cancer. Gastric carcinoma cells with fibroblastoid morphological changes demonstrate increased motility and

invasiveness based on decreased cell-cell adhesion, which is reminiscent of EMT during embryonic development.

Amplification of ERBB2, MET, FGFR2, PIK3CA, AKT1 genes, up-regulation of WNT2, WNT2B, WNT8B, and down-regulation of SFRP1 have been shown to lead to EMT in gastric cancer through GSK3β inhibition and following SNAIL-mediated CDH1 repression. Claudin (CLDN) and the PAR3/PAR6/aPKC complex at tight junctions are other key molecular targets of EMT. CLDN23 gene is down-regulated in intestinal type gastric cancer. Down-regulation of PAR3/PAR6/aPKC complex also leads to EMT. Single nucleotide polymorphisms (SNPs) and copy number polymorphisms (CNPs) of genes encoding EMT signalling molecules will be identified as novel risk factors of gastric cancer.

1.4 WISP family members

1.4.1 Introduction

WISP proteins [WNT1 (wingless-type MMTV integration site family, member 1)-inducible signalling pathway proteins)] are a subfamily of the CCN family [189]. WNT1 is a member of the family of cysteine-rich, glycosylated signalling proteins that mediate diverse developmental processes [190], such as the control of cell proliferation, adhesion, cell polarity, and the establishment of cell death pathways. Members of the CCN family were initially defined as secreted proteins whose complex was deregulated in transformed cells or induced by mitogenic growth factors or oncogenes. The first three members described – CYR61 (cysteine-rich 61; CCN1) [191], CTGF (connective tissue growth factor; CCN2) [192], and NOV

(nephroblastoma overexpressed; CCN3) [193] – provided the acronym for the CCN family. The three other family members WISP-1, WISP-2 and WISP-3 are designated CCN4, CCN5 and CCN6 [194]. Recent studies reported that CCN proteins are crucial regulators of embryonic development, and in adults they play essential roles in inflammation, injury repair, fibrotic diseases and cancer. The CCN proteins have a molecular structure with up to four distinct and highly conserved functional domains. They are specifically correlated with the ECM and are induced by growth factors (i.e. transforming growth factor (TGF)-β, cytokines like endothelin) and events that lead to cellular stress, namely hypoxia. They have also been thought to be over expressed in pathological conditions that influence connective tissue, namely scarring, fibrosis, and cancer. The CCN family as a whole seemingly promote adhesion, ECM production and migration as well as influencing cell cycle through the mediation of mitosis, growth arrest and apoptosis [194]. The diversity of cell functions affected is generally on the basis of the families capability to combine with and activate numerous of cell-surface integrins and intracellular signalling molecules, containing S100A4, Notch1, fibulin 1C and ion channels [195]. CCNs have also been shown to modulate the activity of different growth factors such as TGF-β. Cyr61 (CCN1) and Nov (CCN2) have been indicated as being pro-angiogenic [196] (Figure 1.11).

WISP-2 (rCop-1 /CCN5) was first identified as being down-regulated following transformation of rat embryo fibroblasts through inactivation of p53 and associated activation of H-ras [197]. Almost simultaneously, WISP-1 and WISP-2 were identified as an indirect response to WNT1 but not WNT4 induction in C57MG mouse mammary epithelial cells. After sequence alignment, human WISP-1, WISP-2 and WISP-3 were found homologous and cloned in 1998 [189]. These WISP proteins exhibited the modular structure of the CCN family, characterised by four

conserved cysteine-rich domains and believed to be homologous to the CTGF family of proteins of the CCN family. Another group analysed a human osteoblast cDNA library and identified an EST that contained an IGF binding domain, and based on sequence homology to the CCN family member CTGF, they named the presumed gene product CTGF-like protein or CTGF-L [198]. CTGF-L (CCN5), encoding a 250 amino acid (aa) single chain polypeptide of 26kDa protein which lacks the C-terminal domain implicated in dimerisation and heparin binding.

These early discoveries has laid the foundation for about 200 publications on WISP-1, WISP-2, WISP-3 and their role in cell signalling, proliferation, adhesion, invasion, wound healing, fibrosis, skeletal development, implantation, epithelial-mesenchymal-transition and angiogenesis, as well as in cancers.

New nomenclature 2003			*Mol Pathol.56(2):127-128*
1p22	CCN1	Cyr61	cystein rich
6q23	CCN2	Ctgf	connective tissue growth factor
8q24.1	CCN3	Nov	nephroblastoma overexpressed
8q24.2	CCN4	WISP-1	Wnt-induced secreted proteins
20q13.1	CCN5	WISP-2	Wnt-induced secreted proteins
6q21-22	CCN6	WISP-3	Wnt-induced secreted proteins

Figure 1.11 CCN nomenclature.

1.4.2 Chromosome location and structure of WISP family members

Clones encoding full-length human WISP-1 were disassociated by screening lung and fetal kidney cDNA libraries with the same probe at low stringency. The murine WISP-1 gene is located on chromosome 15 and the human WISP-1 gene is located on chromosome 8q24.1–q24.3. Both consist of five exons and four introns. The length of the murine and human cDNA is 1766bp and 2830bp, respectively, and predicted relative molecular mass of 40kDa. Murine and human WISP-1 proteins are composed of 38 conserved cysteine residues and four potential N-linked glycosylation sites [189].

Clones encoding full-length mouse and human WISP-2 were isolated by screening a C57MG/Wnt-1 or human fetal lung cDNA library with a probe, which is consistent with nucleotides 1463–1512. Human WISP-2 is located on chromosome 20q13.12 and comprise of 3 exons. The length of Full-length cDNA clones of human WISP-2 are 1293bps, and encode a protein of 250aa, with predicted proportional molecular masses of 26kDa [189]. The consistencies of mouse and human WISP-2 reach 73% at the aa level and are homologous to rat gene, rCop-1[197].

Full length cDNA encoding WISP-3 was cloned from human bone marrow and fetal kidney libraries [189]. A full-length human WISP-3 cDNA of 1,371bp was isolated corresponding to those ESTs that encode a 354aa sequence resulting in a protein with a predicted molecular mass of 39.3kDa. Human WISP-3 is located on chromosome 6q22–6q23, a locus which displays high rates of loss of heterozygosity in breast cancer [199, 200].

An alignment of the three human WISP proteins demonstrated that WISP-1 and WISP-3 are the most similar (42% consistencies), whilst WISP-2 has 37% consistencies with WISP-1 and 32% consistencies with WISP-3. WISP proteins exhibit the molecular architecture of CCN family members that are characterised by four conserved and discrete cysteine-rich domains that act both independently and in concert: The N-terminal domain, which includes the first twelve cysteine residues, contains a consensus sequence (GCGCCXXC) conserved in most insulin-like growth factor (IGF)- binding proteins (BP) (IGF-BP). This sequence is conserved in WISP-2 and it has been found that a truncated *nov* protein lacking the IGF-BP domain in chicken embryo fibroblasts was sufficient to induce their malignant transformation [193]. The von Willebrand factor type C module (VWC) covers the next ten cysteine residues, and is thought to participate in protein complex formation and oligomerisation [201]. A short variable region following closely to the VWC domain is highly susceptible to proteolytic degradation by matrix metalloproteases (MMPs) [202]. It has been shown that a wide variety of MMPs (1, 2, 3, 7, 9 ,13) target this central linker region and additional proteases such as elastase and plasmin could attack linkers that connect domains 1 and 2 or domains 3 and 4 [203]. The third domain, thrombospondin (TSP) domain is implicated in binding with sulphated glyco-conjugates and contains six cysteine residues and a conserved WSxCSxxCG motif first identified in TSP [204] and necessary for the regulation of endothelial cell proliferation and promotion of cell attachment [205, 206]. The C-terminal cysteine knot-like (CT) domain is present in all CCN family members described to date while WISP-2-encoded protein lacks this domain which is implicated in receptor binding and dimerisation [207]. These receptors include heparin [208] , matrix molecules, integrins and signalling molecules such as Notch 1 and LRP1 [209]. Because the CT domain is important for receptor binding, WISP-2 may bind its receptor

through other domains, like IGFBP domain [198]. Heparin-binding growth factor (HBGFs) from pig uterine luminal flushings were finally identified as highly truncated form of CTGF and showed that the N-terminal two-thirds of the CTGF primary translation product is not required for mitogenic activity or heparin binding, and for mitogenic activity of 10kDa truncated form of CTGF is heparin-dependent [208]. Other growth factors, such as platelet-derived growth factor, TGF-β, and nerve growth factor, which contain a cystine knot motif and exist as dimers. It leads to speculation that WISP-1 and WISP-3 may exist as dimers, whereas WISP-2 exists as a monomer [189]. This has also led some to hypothesise that WISP-2 might act as a dominant negative regulator of other CCN family members [210]. Furthermore, the existence of a putative signal sequence in front of the N-terminal IGF-BP domain and the absence of a transmembrane domain suggest that WISP proteins are secreted proteins (See Figure 1.12)

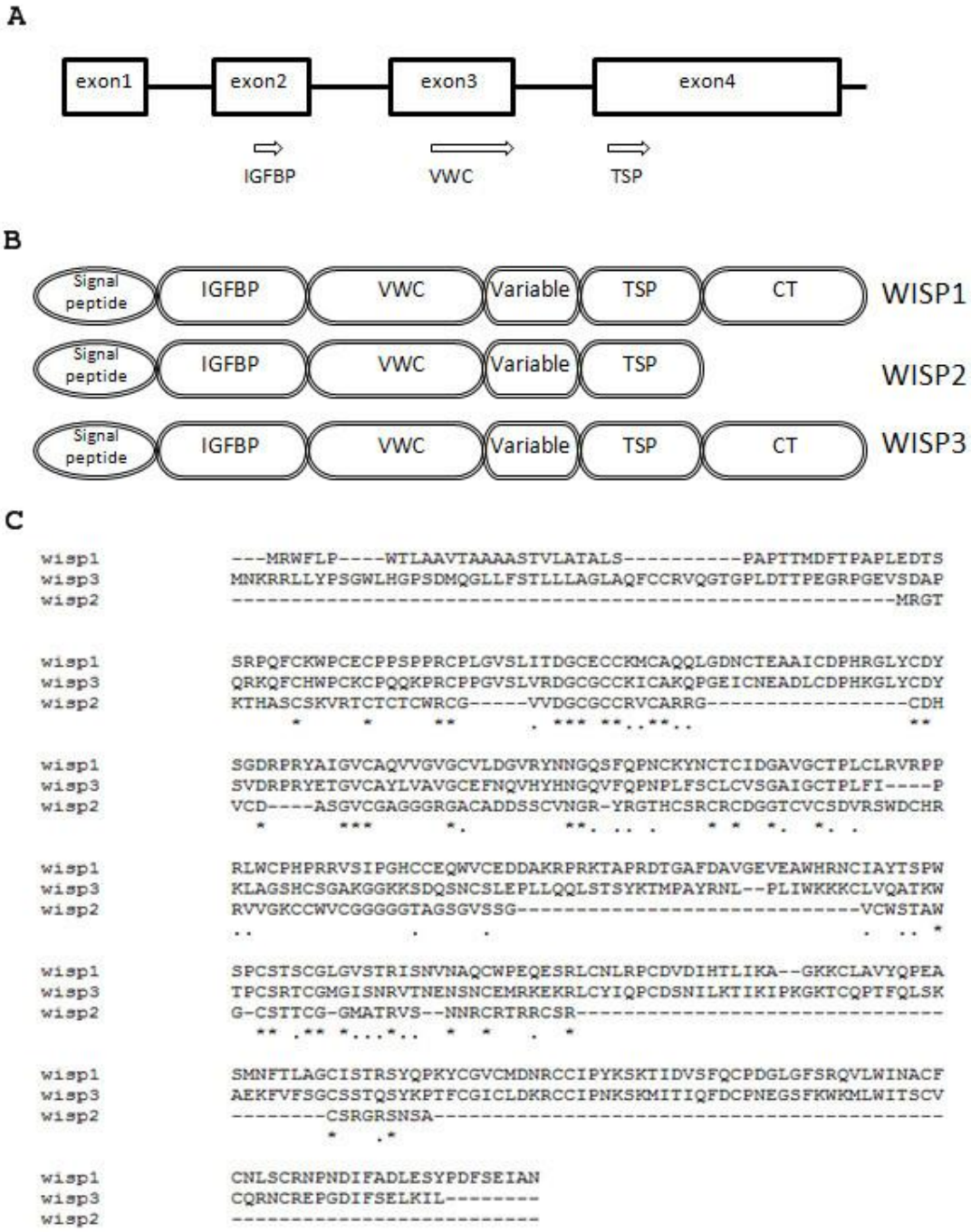

Figure 1.12 Structure of WISP proteins. (A), Exon-intron structure and domain location of WISP-2 gene. IGFBP: 37bp, VWC: 61bp, TSP: 44bp. (B), Schematic representation of the WISP proteins showing the domain structure. WISP-2 lacks the CT domain. (C), Sequence alignment of WISP proteins, identity=33.68%, with DNAman software).

1.4.3 WISP-1, WISP-2 and WISP-3 expression and clinical significance in human cancers

Following the identification of WISP proteins as Wnt1-inducible, a number of researchers focused on the roles and regulation for these three family molecules in human disorders, especially in cancers.

1.4.3.1 WISP-1, WISP-2 and WISP-3 expression detected jointly in cancer

Differential expression profiles and prognostic implications of WISP-1, WISP-2, and WISP-3 were detected in human colorectal cancer [211] and human breast cancer [212]. Davies *et al* found that WISPs may play essential, but reverse, roles in colorectal cancer with WISP-1 appearing to act as a factor promoting aggressiveness, WISP-2 as a tumour suppressor and WISP-3 having no explicitly beneficial or detrimental role. However, in breast cancer, they indicated that WISP-1 was thought to act as a tumour suppressor and WISP-2 as a factor that promotes aggressiveness; whereas WISP-3 has no precisely beneficial or detrimental role. The contrasting roles of WISP-1 and WISP-2 in colorectal and breast cancer implied that their roles may be tissue specific.

1.4.3.2 WISP-2 and cancer

Clinical studies have shown different expression profiles and roles in cancers for WISP-2. The inconsistency between the results in multiple cancer types has raised uncertainty concerning the role of WISP proteins in carcinogenesis. For example, induction of WISP-2 by IGF-1 or EGF is required for the mitogenic action in oestrogen-receptor-positive, non-invasive breast tumour cells [213-215], while it acts as a growth arrest specific (gas) gene in vascular smooth

muscle cells and prostate cancer cells [216]. In addition, it is most likely that WISP-2 plays a preventive role in the progression of pancreatic cancer as it participates in morphological alterations from mesenchymal to epithelial transition [112] of pancreatic adenocarcinoma cells [217] and breast cancer cells [218].

The first study in tumour cells was reported in 2000. WISP-2 was found to be markedly increased in 17 beta-oestradiol-treated MCF-7 human breast cancer cells compared with control cells and was directly regulated by the oestrogen receptor [219]. The induction of secreted WISP-2 protein by E2 in culture supernatant was dose-dependent at a certain range [220, 221] and thus was believed to be an oestrogen response gene. Soon afterwards, several intensive investigations relevant to WISP-2, oestrogen, breast and other cancers (cancer cells) have been carried out and, till now, the most studied and controversial was breast cancer.

Breast Cancer

More than 20 studies from several laboratories suggest that elevated WISP-2 has a particular relevance to human breast disease *in vitro* and *in vivo* [211, 217, 218, 221-223], and WISP-2 has been indicated as a useful indicator of breast cancer progression [223]. In these studies, WISP-2 mRNA and protein levels were found to be elevated in different human breast tumour-derived cell lines, such as MCF-7, ZR-75, T-47D and SKBR2 [222, 224], in node-positive breast tumours with metastatic potential and in breast tumours from patients with a poor prognosis [211], These studies also showed that WISP-2 was either undetectable or minimally detectable in normal breast epithelial cells. Similar reports from Banerjee *et al* showed that WISP-2 was upregulated in non-invasive MCF-7 cells by EGF, and was believed to be linked to poor prognosis in breast cancer [221], Silencing of the function of the *WISP-2* gene

minimized serum-induced breast tumour cell proliferation [213]. Banerjee *et al* found that WISP-2 expression in breast samples was biphasic; a marked increase was noted in non-invasive breast lesions but a significant decrease was found as cancers progressed from a non-invasive to an invasive type [218]. WISP-2 became almost undetectable in poorly differentiated cancers when compared with moderately or well-differentiated samples including testing with micro-dissected sections. This indicated a possible protective function of WISP-2 in non-invasive breast tumour cells. In contrast, the same group also reported that in hormone-related tumours, including breast cancer, the activation of WISP-2 expression by ooestrogen promoted cancer progression, and disruption of WISP-2 signalling by use of antisense oligomers in MCF-7 cells caused a significant reduction in tumour cell proliferation [221].

Pancreatic adenocarcinoma

Pancreatic adenocarcinoma exhibit greatly decreased levels of WISP-2 expression compared with adjacent normal pancreatic tissue and chronic pancreatitis, and the loss of WISP-2 mRNA was associated with overexpression of p53. Dhar *et al* revealed a strong correlation between the degree of differentiation and progression of pancreatic adenocarcinoma, decreased expression of the WISP-2 signalling protein indicated that the development of pancreatic adenocarcinoma was associated with the silencing of WISP-2 signalling [217]. It is suggested that WISP-2 may have a role in maintaining an epithelial-like phenotype in pancreatic adenocarcinoma cells thereby decreasing their invasive potential.

Colorectal cancer

Research has shown that WISP-2 is a potential tumour-suppressor in colorectal cancer. WISP-2 DNA was amplified in colon tumours, but its transcription was significantly reduced in the majority of tumours when compared with that in paired normal colonic mucosa [189]. The gene for human WISP-2 was localized to chromosome 20q13, in a region frequently amplified and associated with poor prognosis in node-negative breast cancer and colon cancers, suggesting the existence of 1 or more oncogenes at this locus [225, 226]. It is possible that the apparent amplification observed for WISP-2 may be caused by another gene in this amplicon [189]. In another cohort, comprised of 94 human colorectal tumours and 80 normal colorectal tissues, WISP-2 showed a significantly lower level of expression in colorectal cancer cells when compared with that in normal cells. Although no significant differences were found within the cancer group when indices of a more aggressive tumour were compared with the normal tissue, a significant reduction in expression was associated with Dukes' stage, poor differentiation, lower TNM stage and node-positive disease [212].

Hepatocarcinoma

Research found that the WISP-2 transcript was not expressed in the 4 hepatocellular carcinoma (HCC)-derived cell lines HepG2, HuH-6, HuH-7 and HA22T/VGH [227], however, overexpression of the hepatitis C viral core protein in Huh-7 cells caused up-regulation of Wnt-1 and WISP-2 and increased proliferation of these cells [228]. As 1 of the 13 genes activated by the Wnt/β-catenin signalling pathway, T-cell transcription factor 4J isoform in HCC cells, WISP-2 was also up-regulated in HCC tumours when compared with that in adjacent peri-tumour tissues [229].

Skin cancer

WISP-2 is one of the most abundantly expressed mRNAs of the CCN family members in normal human skin. Following exposure to UV irradiation, WISP-2 expression was found to be decreased by 50% at 24hrs and returned to a basal level at 48 hrs (37). [230].

Pituitary tumours

WISP-2 was found over-expressed in ACTH-secreting pituitary tumours compared with normal pituitaries, None- secretory (NS) pituitary tumours and GH-secreting tumours [231]. But there was no association between WISP-2 and gender, age at diagnosis, tumour size, altered visual field, remission of the disease, or tumour progression in any subtype of the pituitary tumours.

Gastric cancer

The expression of the 3 WISP molecules in a cohort of 316 cases of human gastric cancers and normal gastric tissues were analysed using q-PCR and IHC, respectively, and were correlated with the clinic-pathological features and outcome of the patients by our group. Knockdown of WISP-2 in human gastric cancer cell lines HGC27 and AGS was also carried out. The WISP family of proteins, in particular WISP-2, was a significant independent prognostic indicator for gastric cancer patients. WISP-2 knockdown resulted in significant changes in the growth rate and *in vitro* invasiveness, with little effect on the adhesive capability, when compared with its transfection controls. This was found to be linked to the MMP activities, mediated by the JNK pathway.

Table 1.8 Expression and roles of WISP-1, WISP-2 and WISP-3 in cancers compared with corresponding normal tissues.

	WISP-1			WISP-2			WISP-3		
	Expression	Role	Ref.	Expression	Role	Ref.	Expression	Role	Ref.
Colorectal cancer	↑	1) localisation 2) Stimulating aggressiveness 3) Diagnosis and prognosis marker	1)[189] 2)[212] 3)[232]	↓	Tumour suppressor	[212]	No difference	No definable beneficial or detrimental role	[212]
Breast cancer	↓	Tumour suppressor	[211]	↑	Stimulating aggressiveness; Indicator of breast cancer progression	[211, 223]	No difference	No definable beneficial or detrimental role	[211]
Gastric cancer							↑	A promising prognostic factor for gastric cancer	[233]
NSCLC	↑	1) Suppressing motility and invasion 2) Associated with tumour histology and age	1)[234] 2) [235]						

Table 1.8- continued Expression and roles of WISP-2 in cancers compared with corresponding normal tissues.

	WISP-2		
	Expression	Role	Ref.
Pancreatic adenocarcinoma	↓	Tumour suppressor	[217]
Hepatocarcinoma	No expression, up-regulation caused by overexpression of the hepatitis C viral core protein		[227]
Skin cancer	↓	Tumour suppressor	[230]
Pituitary tumours	Upregulation in ACT- secreting pituitary tumours		[231]

1.4.4 Signalling regulation of WISP proteins in cancers

1.4.4.1 WSP-1

WISP-1 was confirmed by many studies to be a Wnt-1 induced protein, but it was not clear whether it was a Wnt/β-catenin pathway regulated target gene [189]. The study of Xu *et al* not only suggested WISP-1 as a downstream target gene transcriptionally activated by Wnt-1 and β-catenin, but also demonstrated that Wnt/β-catenin pathway transcriptional factor TCF/LEF sites played only a peripheral role, whilst the CREB site played an essential role in regulating the observed β-catenin-dependent transcriptional activation of WISP-1 [236]. Furthermore, they indicated that WISP-1 maybe contribute to β-catenin-mediated tumourigenesis. WISP-1 was deemed to act in an autocrine fashion as its overexpression in normal fibroblasts induces morphological transformation, stimulates cell growth, strengthens saturation density, and induces tumour formation in a xenograft mouse model [236]. A summary of the signalling event is given in Figure 1.13.

1.4.4.2 WISP-2 and signalling

WISP-2 expression can be regulated by various factors. For example, WNT1 was found to regulate WISP-2 in the mouse mammary epithelial cell line C57MG [189]; Similarly, WNT signalling-activated aβ-catenin in synovial fibroblasts [237]. In cancer cells, much effort has focused on the roles of Wnt signalling, oestrogen signalling, serum and hormones [238].

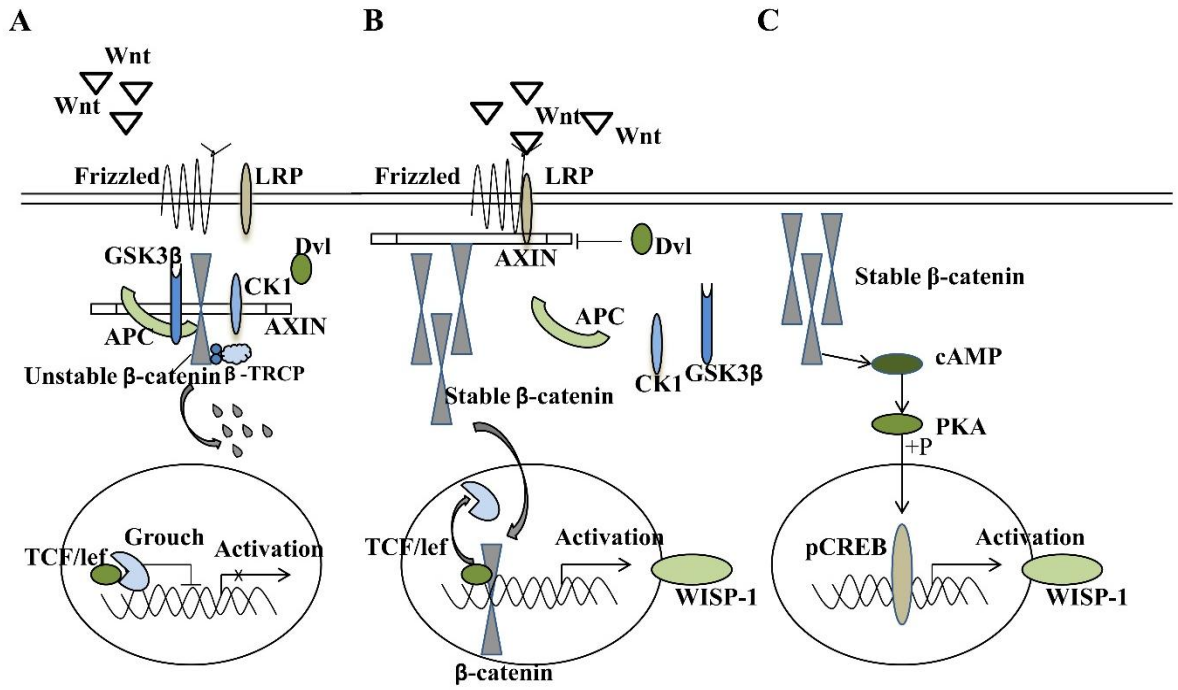

Figure 1.13 Potential WISP-1 signalling A: Wnt/β-catenin pathway. When there was no Wnt1 or β-catenin signal, transcription of Wnt/β-catenin pathway target genes was inactivated. B: Presence of Wnt1 induces the transcription of WISP-1 through canonical TCF/Lef transcription factor activation, while TCF/Lef sites played only a minor role. C: Accumulation of β-catenin in the cytoplasm might cause an increase in cAMP levels. Elevated levels of cAMP activate protein kinase A [58], which phosphorylates the CREB protein and induces transcription of downstream genes through the CREB-binding site.

Wnt signalling

The Wingless (Wg)/Wnt family of secreted signalling molecules and the downstream components of Wnt signal transduction are highly conserved among animal species. Canonical and non-canonical pathway transductions result in tissue-specific cell survival decisions during embryogenesis and regulates cell proliferation as well as proper alignment and bundling of actin filaments in adult tissues [228, 239]. Wnt-protein kinase A (PKA) and Wnt- protein kinase C(PKC) are both non-canonical Wnt signalling pathways [240]. Treatment with PKA [58] activators CT/IBMX induced WISP-2 mRNA expression in the MCF-7 human breast cancer cell line by a direct mechanism. Simultaneous treatment with PKC activators, 12-*O*-tetradecanoylphorbol-13-acetate (TPA) and oestrogen E2 completely prevented WISP-2 induction by E2 [241]. The Wnt/β-catenin signalling pathway regulates genes involved in cell proliferation, survival, migration and invasion through regulation by T-cell factor (TCF)-4 transcription factor proteins.

Oestrogen signalling

Several studies revealed that WISP-2 is oestrogen inducible in human breast cancer MCF-7 cells and is implicated in tumour cell proliferation [219-221]. Inadera *et al* found that WISP-2 induction was highly specific for hormones that interact with the oestrogen receptor in MCF-7 cells [220]. The oestrogen receptor α (ER-α) appears to be directly responsible for oestrogen induction of WISP-2 expression, as cultured human mammary epithelial cells that lack ER-α do not respond to oestrogen stimulation. However, stable transfection of ER-α into these cells rendered the ability of oestrogen to induce WISP-2 expression [221]. There is some evidence to suggest that oestrogen may also function to stabilise WISP-2 mRNA. Banerjee *et al* reported that WISP-2 was upregulated by progesterone (PR) through a PR-dependent mechanism in

MCF-7 cells, although the induction of PR was rapid and transient. When used in combination with oestradiol, PR acted as an antagonist to inhibit the expression of WISP-2, indicating a dual action of PR [221]. In addition, PLK1, a key regulator of cell division, was found to be overexpressed in many types of human cancers, mediating ER-regulated gene transcription by co-activating WISP-2 and suggesting a mechanism for the tumour-suppressive role of PLK1 in MCF7 cells as an interphase transcriptional regulator of WISP-2 [242].

Signalling pathway crosstalk within oestrogen/WISP-2 signalling has also been the subject of several investigations. Treatment of MCF-7 cells with TPA completely blocked oestrogen-induced WISP-2 mRNA transcription [241]. EGF has been shown to induce expression of WISP-2 mRNA in MCF-7 cells in a dose- and time-dependent manner and can act synergistically with oestrogen to raise WISP-2 expression levels, possibly through the PI3K and MAPK signalling pathways [213]. A similar study was carried out by the same group using IGF-1 and reported a similar result. IGF-1 induced WISP-2 mRNA expression in a dose- and time-dependent manner, and knockdown of WISP-2 abrogated the ability of IGF-1 to stimulate MCF-7 cell proliferation. The IGF-1 induction of CCN5 expression was blocked by a pure anti-oestrogen drug, but unlike EGF the signalling crosstalk appeared to function through PI3K/AKT signalling [214].

Other regulators: Serum, hormone and transcription factors

WISP-2 is serum-inducible during the process of mitogen-induced tumour cell proliferation [222]. WISP-2 was found to be overexpressed in ACTH-secreting pituitary tumours when compared with that in normal pituitaries, NS pituitary tumours and GH-secreting tumours [231], However, there were no differences in expression of genes in the canonical and non-canonical Wnt pathways between all studied subtypes of pituitary tumours and normal pituitaries. It has

been suggested that the elevated glucocorticoid levels observed in ACTH-secreting pituitary tumours activate WISP-2 transcription since WISP-2 has a glucocorticoid-responsive region in its promoter [243]. The same phenomenon was found in ER-negative breast cancer cells. MDA-MB-231 cells exposed to glucocorticoids underwent morphological alterations, decreased invasiveness and attenuated expression of mesenchymal markers. These results thus indicate that the induction of the WISP-2 gene promoter probably requires the agonist-activated glucocorticoid receptor. Taken together, these results indicate that glucocorticoid treatment of ER-negative breast cancer cells induces high levels of WISP-2 expression and is accompanied by a more differentiated and less invasive epithelial phenotype. These findings propose a novel therapeutic strategy for high-risk breast cancer patients [243]. In addition, Stiehl *et al* found that amphiregulin (AREG) and WISP-2 expression was strongly dependent on hypoxia inducible factor (HIF-2α and their promoters were particularly responsive to HIF-2α in breast cancer. A strong correlation among HIF-2α/AREG/WISP-2 protein levels in breast cancer samples provides evidence that the HIF-2α-specific transcriptional pathway could have an important role in maintaining a non-invasive phenotype [244], as it has been reported for tumours expressing WISP-2 before [218, 245].

WISP-2 in other pathophysiological processes

WISP-2 is also very important in many other patho-physiological processes except in cancer progression, including apoptosis, anti-proliferation and osteogenic differentiation. Retroviral overexpression of rCop-1 (WISP-2) was found to induce apoptosis in transformed rat fibroblasts, but was unable to affect normal fibroblasts [246]. Cop-1 mRNA is expressed at high levels in quiescent vascular smooth muscle cells (VSMC) and in heparin treated VSMC but at low levels in proliferating VSMC, indicating that COP-1 may play a role in the anti-

proliferative mechanism of action of heparin [246]. Other reports provided functional evidence that WISP-2 is a growth arrest-specific gene that is temporally and spatially expressed and can inhibit VSMC proliferation, motility, and invasiveness, however, adhesion and apoptosis are unaffected by WISP-2 in VSMC [216]. In addition,WISP-2 is relevant to the low osteogenic differentiation capacity of placenta mesenchymal stromal cells (pMSC) compared with mesenchymal stromal cells from bone marrow (bmMSC) [247]. Large-scale analysis of transcripts in non-familial, isolated (ACTH) -independent macronodular adrenal hyperplasia (AIMAH) confirmed clinical heterogeneity and revealed WISP-2 can be used as clinical indices of GIP-dependent AIMAH [248].

1.4.5 Mechanism

1.4.5.1 WISP-1

Wnt-induced-secreted-protein-1 (WISP-1 or CCN4) is a member of a family of cysteine-rich, glycosylated signalling proteins that play an important role in embryogenesis and organogenesis by modulating diverse developmental processes such as the control of cell proliferation, cell adhesion, cell polarity and the establishment of cell death pathways (Cadigan *et al* 1997, Dale 1998). WISP-1 is overexpressed in breast (Dong *et al* 2001), colorectal (Pennica *et al.,* 1998) and lung cancers (Soon *et al* 2003). Furthermore, overexpression of WISP-1 has been shown to inhibit the motility, invasiveness and metastasis of H460 lung cancer cells grown in culture (Soon *et al.,* 2003). In contrast, overexpression of WISP-1 has been reported to inhibit the growth and malignant transformation of NRK-49F fibroblast cells grown in culture (Igarashi 1993). Collectively, the results of these studies suggest that WISP-1 expression varies between, and within, various types of human solid malignancies and that overexpression of WISP-1 may suppress tumour progression, invasion and metastasis or

promote differentiation. However, previously there have been no published studies on the expression WISP-1 in prostate cancer.

Motility and invasion: Overexpression of WISP-1 inhibited invasion and motiliuty of lung cancer cells through suppression of Rac activation [234].

Effect of indomethacin on Bfl-1: The influence of WISP-1 and proliferating cell nuclear antigen on colon cancer cell line HCT116 cells [249]

1.4.5.2 WISP-2 with proliferation, motility, invasiveness, adhesion and EMT

In vitro and *in vivo* studies have indicated the potential roles of WISP-2 in regulating cell proliferation, motility, invasiveness, adhesion and EMT.

Proliferation

Overexpression of WISP-2 has been shown to inhibit serum-induced proliferation of highly invasive ER-negative breast cancer cell line MDA-MB-231 [245]. However, in the less invasive ER-positive MCF-7 cell line, the effect of WISP-2 is not consistent. Some have suggested an inhibitory role in serum-induced proliferation of MCF-7 cells (51). Others have suggested a promoting role in MCF-7 cell proliferation [245]. Moreover, the ability of PMA, EGF or IGF-1 alone to induce MCF-7 cell proliferation was blocked by WISP-2 knockdown [221] or had no effect [218]. Knockdown of WISP-2 in MCF-7 cells was found to eliminate the oestrogen-dependent growth requirement of these cells. More studies are needed to clarify the biochemical and biological basis of the contrasting role of WISP-2 in these cells.

Motility, invasiveness, and metastasis

Overexpression of WISP-2 was found to inhibit both motility and invasiveness in the highly aggressive breast carcinoma cell line, MDA-MB-231 [245]. The inhibitory effect of WISP-2 on motility was also observed in MCF-7 cells where knockdown of WISP-2 expression increased the IGF-1-induced motility of MCF-7 cells. WISP-2 knockdown in MCF-7 cells also induced expression of pro-motility enzymes such as MMP-2 and -9 [218, 245]. Induced mutant p53 overexpression in MCF-7 cells resulted in increased invasiveness which was inhibited by treatment with recombinant WISP-2 protein [250].

Adhesion

Little is known concerning the role of WISP-2 in cell adhesion. Kumar *et al* observed that 3 different osteoblastic cell lines, primary human osteoblasts, osteosarcoma MG63 cells, and rat osteoblast-like osteosarcoma Ros 17/2.8 cells, attached to immobilized CCN5 in a dose-dependent manner [198]. Recent data from our laboratory revealed that WISP-2 knockdown in gastric cancer cells resulted in little effect on the adhesive capability, compared with its transfection controls [251].

EMT: Epithelial-mesenchymal transition

Phenotypical alterations including EMT are a hallmark of the progression of cancer and provide a new basis for understanding the progression of cancer toward a more malignant state. Mesenchymal cells are also implicated in the formation of epithelial organs through mesenchymal-epithelial transition [112]. Cellular plasticity, the ability to undergo EMT and subsequently MET in the appropriate microenvironments are key features of a successful metastatic cell [252]. The process of EMT plays an important role during foetal, postnatal

development, invasion and metastases and is regulated by transcription factors such as Twist1, Snai1 and Slug, which inhibit E-cadherin expression [253].

Current evidence suggests that WISP-2 may suppress EMT in different cancers and that EMT in turn can suppress WISP-2 expression. Human pancreatic adenocarcinoma is associated with the silencing of WISP-2/CCN5 signalling. Functional analysis studies demonstrated that exposure of pancreatic cancer MIA-PaCa-2 cells to WISP-2 recombinant protein for 48hrs markedly altered the phenotype of these cells from a spindle shape (mesenchymal type) to a cobblestone-like shape (epithelial type) and also markedly reduced the expression of vimentin, a mesenchymal marker, in these cells, suggesting that WISP-2 may play a critical role in reversing EMT (or inducing MET) [217]. Although mitogen-induced up-regulation of WISP-2 participates in cell proliferation events of ER-positive breast cancer cells, the basal level of WISP-2 does not exert a mitogenic response in these cells [213-215], Instead, it protects cells from gaining invasive phenotypes. For example, silencing of WISP-2 in MCF-7 non-invasive carcinoma cells significantly enhanced motility and EMT, and it modulated the expression of several genes associated with invasive phenotypes of cancer cells [218, 245, 250, 254], while ectopic Snail expression suppressed WISP-2 transcripts and down-regulated WISP-2 gene promoter expression in transfected cells [254]. In WISP-2-knockout ER-α-positive breast cancer cells, IGF-1 and EGF lost their mitogenic effect [213, 214] but possibly gained aggressive phenotypes. Sabbah *et al* showed that WISP-2 silencing promoted EMT via activation of the TGF-β signalling cascade known to promote EMT in breast cancer [255]. Recently, Ferrand *et al* discovered that glucocorticoid treatment of ER-negative breast cancer cells induced high levels of WISP-2 expression and this was accompanied by marked changes in the cellular morphology. Cells were found to grow as groups of flattened cells consistent with a normal epithelial cell phenotype. This morphological change was correlated with a

reduction in cell motility and invasion, characteristic of a more differentiated and less invasive epithelial phenotype. Meanwhile, WISP-2 expression repressed cadherin 11, vimentin and ZEB1 expression [243].

1.4.5.3 WISP-3

In humans the Wnt-induced secreted protein 3 (WISP-3/CCN6) appears to be involved in skeletal growth and cartilage homeostasis and a relationship has been observed between functional mutations of CCN6 and progressive pseudo-rheumatoid dysplasia (Hurvitz *et al* 1999). There is also evidence to suggest that WISP-3/CCN6 acts as a tumour suppressor gene in breast cancer (Kleer *et al* 2004 and 2005). In contrast, in colorectal cancer, WISP-3 appears to function as an oncogene (Pennica 1998). However, the role of WISP-3 in prostate cancer has yet to be investigated.

1.4.6 A summary of WISP-2 in cancer

WISP-2 is a unique member of the CCN family that lacks the CT domain and exhibits different functions in multiple cellular processes. However, similar to the other CCN family members, WISP-2 is a protein with important roles in embryonic development, normal cell function and disease, particularly in cancers. The functions of WISP-2 in human cancers include effects on cell proliferation, adhesion, motility, invasiveness, metastasis and epithelial-mesenchymal transition (EMT); however these functions are dependent upon the cell and tissue type and the microenvironment. Several independent studies have shown the expression pattern of WISP-2 and a link with patient clinical course in breast cancer, pancreatic cancer, hepato-carcinoma, colorectal and gastric cancer. However, the results are inconsistent and somewhat conflicting

in certain tumour types. Further clinical research requires studies using larger clinical cohorts and scientific investigation into the cellular functions in more than 2 cell lines together, which would allow for more powerful statistical conclusions and further insight into the action of WISP-2. Studies to decipher the myth of its domain binding in relation to the differential response in different cell types to different stimuli would also be important. Together, WISP-2 is a potential regulator and a novel therapeutic target in cancer and warrants further investigation at the cellular and clinical levels.

1.5 Aims and objects

The aims of this study were:

1. To screen and identify the expression profiles of WISP family members, WISP-1, WISP-2 and WISP-3 on mRNA and protein levels in gastric cancer and normal gastric mucosa and carry out a clinical cohort study.

2. To investigate the expression of EMT markers and the association with WISP-1, WISP-2 and WISP-3 in paired gastric cancer tissues and normal gastric mucosa

3. To construct hammer-head ribozyme transgenes targeting human WISP-2 and establish WISP-2 knockdown cell lines for examining the influence of WISP-2 on the biological functions of cancer cells.

4. To understand how WISP-2 regulates growth, motility and invasiveness in gastric cancer, and to elucidate the potential pathways involved in the effect by WISP-2 using small inhibitors.

Chapter 2

Methodology

2.1 Materials

2.1.1 Cell lines

Two gastric cell lines, AGS and HGC27 [256] were acquired from the European Collection of Animal Cell Culture (ECACC, Salisbury, UK) and used in this study. Full details of these two cell lines are supplied in Table 2.1. Cells were maintained in DMEM-F12 medium supplemented with 10% foetal bovine serum (FBS) and antibiotics.

2.1.2 Collection of human gastric cancer and adjacent gastric tissues

Fresh tissue samples were collected immediately after surgery at Peking University Cancer Hospital and stored in liquid nitrogen and then transferred to a -80℃ freezer at Peking University Cancer bank until use. The collection took place between 2004 and 2007, with approval of the ethics committee of Peking University Cancer Hospital. All patients were informed and participated with written consent being obtained. All the specimens were verified by two consultant pathologists. Clinical and pathological information was collected and centrally stored in the Cancer Bank's database. Fellow up was carried out routinely in the clinics of Peking Cancer Hospital.

2.1.3 Primers

All the primers used in the current study were designed with the use of the Beacon Design Programme (Biosoft International, Palo Alto, California, USA) and were synthesised by either Invitrogen (Paisley, UK) or Sigma (Poole, Dorset, UK). Details of the primers used for conventional RT-PCR and Quantitative PCR (qPCR) are provided in Table 2.2. Details of the primers used for generating hammerhead ribozymes and testing orientation of inserts in ligation are found in Table 2.3.

2.1.4 Antibodies

2.1.4.1 Primary antibodies

Full details of primary antibodies used in this study are provided in Table 2.4.

2.1.4.2 Secondary antibodies

The secondary antibodies used for Western blotting were horseradish peroxidase (HRP) conjugated anti-goat IgG, goat anti-rabbit IgG, and rabbit anti-mouse IgG antibodies, all supplied by Sigma (Poole, Dorset, UK).

Table 2.1 Details of cell lines used in the current study.

Cell line	Origin	Cell moprphology	Tissue type	Features
AGS	derived from an adenocarcinoma of the stomach of a 54 year-old Caucasian female with no prior anti-cancer treatment	epithelial	adenocarcinoma	isolation date:1979
				growth:adherent
				organ:stomach
				Doubling time: 20 hours
HGC27	derived from an metastatic lymph node of a Japanese gastric cancer patient diagnosed histologically as undifferentiated carcinoma.	epithelial	lymph node of undifferentiated, mucinous adenocarcinoma	isolation date:1976
				growth:adherent
				organ:stomach
				Doubling time: 17 hours

Table 2.2 Primers for conventional RT-PCR and Q-PCR (Primers were designed using Beacon Design programme (Palo Alto, California, USA) and were synthesised by Invitrogen (Paisley, UK) and Sigma (Poole, Dorset, UK)).

Gene	**Primer name**	**Primer sequence (5'-3')**
WISP-1	WISP-1F	CAAGAGGCCACGCAAGAC
	WISP-1ZR	ACTGAACCTGACCGTACAGTAGGCTATGCAGTTCCTGT
WISP-2	WISP-2F	AGTGGGGCTGGAAGGTCT
	WISP-2ZR	ACTGAACCTGACCGTACACTCTTGGCAGAGGACGAC
WISP-3	WISP-3F	ACAAAACAAATGCCAGCTTAT
	WISP-3ZR	ACTGAACCTGACCGTACACATTGGTCACCCTGTTAGAT
CK19	CK19-F	CAGGTCCGAGGTTACTGAC
	CK19-ZR	ACTGAACCTGACCGTACACACTTTCTGCCAGTGTGTCTTC
GAPDH	GAPDHF8	GGCTGCTTTTAACTCTGGTA
	GAPDHR8	GACTGTGGTCATGAGTCCTT
GAPDH	GAPDHF2	CTGAGTACGTCGTGGAGTC
	GAPDHZR2	ACTGAACCTGACCGTACACAGAGATGATGACCCTTTTG
PDPL	PDPL-F	
	PDPL-ZR	
E-cadherin	E-cadherinF22	CAGGCGCCACACACATTTAT
	E-cadherinZR22	ACTGAACCTGACCGTACAGTTCTTCACGTGCTCAAAAT
N-cadherin	N-cadherinF22	CAACGACGGGTTAGTCAC
	N-cadherinZR22	ACTGAACCTGACCGTACAGCTAATGGCACTTGATTTTC
Snail	SnailF11	CGCTCTTTCCTCGTCAG
	SnailZR11	ACTGAACCTGACCGTACACTGCT
Slug	SlugF12	CGAACTGGACACACATACAG
	SlugZR12	ACTGAACCTGACCGTACAGGATCTCTGGTTGTGGTATG

Table 2.2 continued to Primers for conventional RT-PCR and Q-PCR.

Zeb1	Zeb1F1	CTTGTGATTTGTGTGACAAGA
	Zeb1ZR1	ACTGAACCTGACCGTACAATGCCTTTTTACAGATTCCA
Twist	TwistZF11	ACTGAACCTGACCGTACAACCCAGTCTCTGAACGAG
	TwistR11	GAGGACCTGGTAGAGGAAGT
Vimentin	VimentinF1	ATACCAAGACCTGCTCAATG
	VimentinZR1	ACTGAACCTGACCGTACAAGAGAAATCCTGCTCTCCTC
Zol	ZolF	TGGGTATGACACATGGTA
	ZolZR	ACTGAACCTGACCGTACAGGTGGTACTTGCTCGTAA
DDR2	DDR2F1	GTGTCAATACCATTTTGCAG
	DDR2ZR1	ACTGAACCTGACCGTACAAGGGCTTCAGAGTTGTTGTA
Fsp1	Fsp1F1	AGAACTAAAGGAGCTGCTGA
	Fsp1ZR1	ACTGAACCTGACCGTACACAGGACAGGAAGACACAGTA
MMP1	MMP1F1	GGATGCTCATTTTGATGAAG
	MMP1ZR	ACTGAACCTGACCGTACATAGAATGGGAGAGTCCAAGA
MMP-2	MMP-2F1	TTTGATGACGATGATGAGCTATG
	MMP-2R1	TGCAGCTCTCATATTTGTTG
MMP3	MMP3F2	TCATTTTGGCCATCTCTTCC
	MMP3R2	GTGCCCATATTGTGCCTTCT
MMP7	MMP7F3	CTACAGTGGGAACAGGCTCAG
	MMP7ZR	ACTGAACCTGACCGTACAATCTCCTTGAGTTTGGCTTC
MMP-9	MMP-9F1	AACTACGACCGGGACAAG
	MMP-9R1	ATTCACGTCGTCCTTATGC

Table 2.3 Primers used for generating hammerhead ribozymes and testing orientation of inserts in ligation.

Gene	Primer name	Primer sequence (5'-3')
WISP-2 Ribozyme 1	WISP-2 Rib1F	CTGCAGGAGGCAGAGGAGGGACTGATGAGTCCGTGAGGA
	WISP-2 Rib1R	ACTAGTACCCACCTCCTGGCCTTTTCGTCCTCACGGACT
WISP-2 Ribozyme 2	WISP-2 Rib2F	CTGCACTCCTCGCAGCGGCAGCGCRGATGAGTCCGTGAGGA
	WISP-2 Rib2R	ACTAGTTCCAGCCCCACTGCAGCATTTCGTCCTCACGGACT
pEF/His TOPO TA plasmid vector	T7F	TAATACGACTCACTATAGGG
	BGHR	TAGAAGGCAGTCGAGG
Ribozyme clone verification	RbBMR	TTCGTCCTCACGGACTCATCAG
	RbTPF	CTGATGAGTCCGTGAGGACGAA

Table 2.4 Primary and secondary antibodies used in the present study.

Antibody name	Molecular weight (kDa)	Supplier	Product code
Rabbit anti-WISP-2 (for WB)	26	SANTA CRUZ Biotechnology	SC-25443
Mouse anti-GAPDH(for WB)	36	SANTA CRUZ Biotechnology	SC-47724
Rabbit anti-WISP-1 (for IHC)	--	Abcam	AP6255a
Rabbit anti-WISP-2 (for IHC)	--	Abcam	AP6256a
Rabbit anti-WISP-3 (for IHC)	--	Abcam	AP6257a
Rabbit anti-JNK	44/48	SANTA CRUZ Biotechnology	SC-571
Mouse anti-p-JNK	44/48	SANTA CRUZ Biotechnology	SC-6254
Rabbit anti-ERK1/2	42/44	SANTA CRUZ Biotechnology	SC-93
Mouse anti-p-ERK1/2	42/44	SANTA CRUZ Biotechnology	SC-136521
Rabbit anti-mouse(whole molecule) IgG peroxidase conjugate	Dependent on primary	Sigma-Aldrich	A-9044
Goat anti-rabbit (whole molecule) IgG peroxidase conjugate	Dependent on primary	Sigma-Aldrich	A-9169
Rabbit anti-goat (whole molecule) IgG peroxidase conjugate	Dependent on primary	Sigma-Aldrich	A-5420

2.2 Standard reagents and solutions

2.2.1 Solutions for use in cell culture

0.05M EDTA

One gram of KCl (Fisons Scientific Equipment, Loughborough, UK), 5.72g Na_2HPO_4 (BDH Chemical Ltd., Poole, England, UK), 1g KH_2PO_4 (BDH Chemical Ltd., Poole, England, UK), 40g NaCl (Sigma-Aldrich, Inc., Poole, Dorset, England, UK) and 1.4g EDTA (Duchefa Biochemie, Haarlem, The Netherlands) were dissolved in 5L distilled water, adjusted pH value to 7.4, autoclaved, and stored until use.

Trypsin (25mg/ml)

Five hundred milligrams of trypsin were dissolved in 0.05M EDTA and then filtered through a 0.2μm minisart filter (Sartorius, Epsom, UK). This solution was aliquoted and stored at -20^{0}C until further use. When trypsin was required for cell culture work, 250μl of the trypsin stock was diluted in 10ml 0.05M EDTA and used to detach the cells.

Balanced Saline Solution (BSS)

Seventy-nine point five grams of NaCl, 2.1g KH_2PO_4, 2.2g KCl and 1.1g of Na_2PO_4 were dissolved in 10L of distilled water, and the pH value was adjusted to 7.2 using NaOH (Sigma-Aldrich, Inc., Poole, Dorset, England, UK).

100X Antibiotics

Five grams of streptomycin, 3.3g penicillin and 12.5mg amphotericin B in DMSO were dissolved in 0.5L of BSS and filtered. 5ml of the antibiotics was then added to a 500ml bottle of DMEM medium.

2.2.2 Solutions for use in molecular biology

Tris-Boric-Acid-EDTA (TBE)

TBE solution (5X) (1.1M Tris; 900mM Borate; 25mM EDTA; pH 8.3) was made by dissolving 540g Tris-HCl (Melford Laboratories Ltd, Suffolk, UK), 275g Boric acid (Melford Laboratories Ltd, Suffolk, UK) and 46.5g of EDTA in 10L of distilled water. The pH was adjusted to 8.3 using NaOH and then stored at room temperature. It was diluted in distilled water to 1X TBE for preparing agarose gels and DNA electrophoresis.

DEPC water

Two hundred and fifty millilitres of Diethyl Pryoncarbonate (DEPC) (Sigma-Aldrich, Inc., Poole, Dorset, England, UK) was added to 4.75ml of distilled water and then autoclaved .

Loading buffer (used for DNA electrophoresis)

Twenty-five milligrams of bromophenol blue (Sigma-Aldrich, Inc., Poole, Dorset, England, UK) and 4g sucrose (Fisons Scientific Equipment, Loughborough, UK) were dissolved in 10ml of distilled water and stored at 4 ℃.

Sybgreen staining

Five microliter of Sybgreen stain was added to 100 ml of distilled water and used to stain agarose gels for half to one hour on a horizontal shaker.

2.2.3 Solutions for gene cloning

LB agar

LB agar was prepared by dissolving 10g tryptone (Duchefa Biochemie, Haarlem, Netherlands), 5g yeast extract (Duchefa Biochemie, Haarlem, Netherlands), 15g agar, and 10g NaCl, in 1L of distilled water then adjusting the pH to 7.0 and autoclaving the solution. The solution was melted, antibiotics added and the solution poured into $10cm_2$ Petri dishes (Bibby Sterilin LTd., Staffs, UK). These dishes of agar were left to cool and harden, inverted and stored at 4^0C before use.

LB broth

Ten grams tryptone, 10g NaCl and 5g yeast extract were dissolved in 1L of distilled water. The pH of the solution was adjusted to 7.0 and then autoclaved. After cooling down, antibiotics were added and the solution stored at 4 ℃ until use.

2.2.4 Solutions for Western blot

Lysis Buffer

This was made up by dissolving NaCl 150mM (8.76g), Tris 50mM (6.05g), Sodium azide 0.02% (200mg), Sodium deoxycholate 0.5% (5g), Triton X-100 1.5% (15ml), Aprotinin 1μg/ml (1mg), Na_3VO_4 5mM (919.5mg), Leupeptin 1μg/ml (1mg) in 1 litre of distilled water. The solution was then stored at 4 ℃ for further use.

10% Ammonium Persulphate (APS)

One gram APS was dissolved in 10ml distilled water and then stored at 4^{oC} for further use.

Tris Buffered Saline (TBS)

10X TBS (0.5M Tris, 1.38 M NaCl, pH 7.4) was prepared by dissolving 24.228g of Tris and 80.06g of NaCl (Melford Laboratories Ltd., Suffolk, UK) in 1L of distilled water to provide a stock solution. The pH was adjusted to 7.4 using HCl and stored at room temperature.

Running buffer (10X) (for SDS-PAGE)

Ten times running buffer (0.25M Tris, 1.92M glycine, 1% SDS, pH8.3) was prepared by dissolving 303g Tris, 1.44kg of glycine (Melford Laboratories Ltd., Suffolk, UK) and 100g SDS (Melford Laboratories Ltd., Suffolk, UK) in 10L distilled water. Prior to use this solution was diluted to 1X running buffer with distilled water.

Transfer buffer

Fifteen point five grams of Tris and 72g glycine were dissolved in 4L distilled water. 1L of methanol (Fisher Scientific, Leicestershire, UK) was added to make a final volume of 5L.

Blocking milk

Two gram of skimmed milk was added into 1000 ml of TBS with 0.1% Tween 20. The solution was mixed fully on a roller mixer (Stuart, Wolf-Laboratories, York, UK).

Ponceau S stain

Supplied by Sigma.

Luminata fotre western HRP substrate

Supplied by Millipore.

2.2.5 Solutions for use in immunocytochemical staining

Secondary antibody

Supplied by DAKO.

Diaminobenzidine [42] chromagen

Two drops (approximately 50µl) of wash buffer, 4 drops of DAB (Vector Laboratories, Inc., Burlingame, USA) and 2 drops of H_2O_2 were added to 5ml of distilled water and mixed well before use.

2.2.6 Solutions for use in gelatine zymography

Wash buffer

This was made up by 2.5% Triton X-100 and 0.02% NaN_3.

Incubation buffer

This was made up by 50mM Tris-HCl, 5mM CaCl2 and 0.02% NaN3. The pH was adjusted to 8.0 and stored at room temperature.

Destain buffer

This was made up by 100ml Acetic acid and 250ml Ethanol in 1 litre of distilled water.

2.3 Cell culture, maintenance, and storage

2.3.1 Preparation of growth media and cell maintenance

• Dulbecco's Modified Eagle's medium (DMEM/ Ham's F-12 with L-Glutamine; Sigma-Aldrich, Inc., Poole, Dorset, England, UK), pH 7.3 containing 2mM L-glutamine and 4.5mM $NaHCO_3$, supplemented with 10% heat inactivated Foetal Bovine Serum (Sigma-Aldrich, Inc., Poole, Dorset, England, UK) and antibiotics, was used to routinely culture the cells.

• Cell lines transfected with the pEF6/His plasmid or constructed plasmid vectors were subjected to a selection period of 2 weeks using 5-7.5μg/ml blasticidin (Melford laboratories ltd, Suffolk, UK), the resultant transfectants were then cultured in medium supplemented with 0.5μg/ml blasticidin for maintenance purposes. The transfectants were then verified and used for subsequent studies.

• All the cell lines were cultured in 25cm^2 and 75cm^2 culture flasks (Greiner Bio-One Ltd, Gloucestershire, UK) with a loosed cap in an incubator at 37 ℃, 95% humidity, and 5% CO_2.

• Cell confluence was visually measured with a light microscope and the percentage of cells covering the surface of the tissue culture flasks was estimated. If needed for experimental work, the cells were left to grow until they reached sub-confluency (2-3 days). All handling of cells was carried out using a Class II Laminar Flow Cabinet with autoclaved and sterile equipment (manufacturor). Cells were routinely sub-cultured when they had reached a confluency of 80-90% as explained in section 2.3.2.

2.3.2 Trypsinisation (detachment) of adherent cells and cell counting

Once the cells had reached a confluency of approximately 80-90%, the medium was aspirated and the cells briefly rinsed with sterile EDTA BSS buffer in order to remove any remaining serum which would have an inhibitory effect on the action of trypsin.

• Adherent cells were then detached from the tissue culture flask using 1-2ml of Trypsin/ EDTA (0.01% trypsin and 0.05% EDTA in BSS buffer) and incubating the cells at 37^0C for approximately 5 minutes.

• Once detached, the cell suspension was then collected into 30ml universal containers (Greiner Bio-One Ltd, Gloucestershire, UK) and centrifuged at 1,780rpm for 8 minutes in order to collect the cell pellet.

• The supernatant was removed and the cell pellet resuspended in an appropriate amount of medium. Cells were either counted for immediate use in experiments, or transferred into fresh tissue culture flasks for re-culturing.

• Cells were counted with a Neubauer haemocytometer counting chamber (Mod-Fuchs Rosenthal, Hawksley, UK) using a light microscope at a magnification of 10 x 10 (Reichert, Austria). A haemocytometer allows for the calculation of the number of cells in a predetermined volume of fluid in order to obtain the quantity of cells per millilitre, and an accurate estimation of cell density for use in *in vitro* and *in vivo* cell function assays.

• The haemocytometer chamber is divided into 9 squares with dimensions of 1mm x 1mm x 0.2mm. For consistency of cell density, five of these 9 squared areas were counted. This allowed for determination of cell number by using the following equation:

Cell number/ml= (number of cells in five of nine squares ÷ 10) x (1×10^4).

2.3.3 Storing cells in liquid nitrogen and cell resuscitation

Cell stocks of low passage number that needed to be stored were done so in liquid nitrogen.

• Cells were trypsinised as described in section 2.3.2 and resuspended in medium with 10% Dimethylsulphoxide (DMSO; Fisons, UK) at a cell density of $1x10^6$cells/ml.

• This cell suspension was then divided into 1ml aliquots and transferred into pre-labelled 1ml CRYO.STM tubes (Greiner Bio-One, Germany) and the tubes were wrapped in protective tissue paper, stored overnight at -80 ℃, and then transferred to liquid nitrogen tanks for long term storage.

• In order to resuscitate the cells, they were removed from liquid nitrogen and left to rapidly thaw before being transferred into a universal container containing 5ml pre-warmed medium and incubated for 10 minutes at 37 ℃.

• This was followed by centrifugation at 1,600 rpm for 5 minutes to remove any excess DMSO, before resuspending the cells in 5ml medium. The cell suspension was then transferred into a fresh $25cm^2$ tissue culture flask and kept in an incubator.

2.4 Methods for RNA detection

2.4.1.1 Total RNA isolation

• The protocol followed for RNA isolation was using the Tri Reagent kit (Sigma-Aldrich, Inc., Poole, Dorset, England, UK).

• For cells: cells were grown in a monolayer of 85-90% confluency before the medium was aspirated and replaced with TRI reagent (1ml per 5-10 x 10^5 cells), in order to induce cell lysis.

•For tissues: tissues were taken out from -80 ℃ refrigerator and put into liquid nitrogen immediately and homogenized with a liquid nitrogen-precooled ceramic mortar and pestle.

• The homogenate was transferred into a 1.5ml eppendorf tubes, and incubated at 4°C for 5 minutes.

• This was followed by the addition of 0.2ml (per 1ml of TRI reagent) chloroform (Sigma-Aldrich, Inc., Poole, Dorset, England, UK), 15 seconds of shaking, and incubation at 4 ℃ for 5 minutes.

• The resulting homogenate was centrifuged at 12,000rpm for 15 minutes at 4°C (Boeco, Wolf laboratories, York, UK). Under these acidic conditions, the homogenate separated into three phases; a lower pink organic phase containing protein, an inter phase containing DNA, and an upper aqueous phase containing RNA.

• The aqueous phase should constitute around 40-50% of the total volume, and was carefully transferred into a fresh 1.5ml eppendorf tube, then an equal volume of isopropanol was added (Sigma-Aldrich, Inc., Poole, Dorset, England, UK) and incubated for 10 minutes at 4 ℃. After centrifuging the samples at 12,000rpm for 10 minutes at 4 ℃, the RNA precipitated as a white pellet on the bottom of the eppendorf tube.

• The supernatant was discarded, and the RNA pellet was washed twice with 75% ethanol (Fisher Scientific, Leicestershire, UK) in DEPC water. Each wash was carried out by adding 1ml 75% ethanol, vortexing and centrifuging the samples at 7,500rpm for 5 minutes at 4 ℃.

• After the final wash, the RNA pellet was briefly dried at 55°C for 5-10 minutes, in a Techne Hybridiser HB-1D drying oven (Wolf laboratories, York, UK), to remove any remaining traces of ethanol.

• The final step was to dissolve the RNA pellet in 50-100µl (dependent on pellet size) of DEPC water. DEPC was used as it is a histidine specific alkylating agent and inhibits the effect of RNAases, which require histidine active sites to carry out their function.

2.4.2 RNA Quantification

• Once RNA isolation was completed, the concentration and purity of the resulting RNA was measured with the use of a UV1101 Biotech Photometer (WPA, Cambridge, UK). This spectrophotometer had been previously set to detect single strand RNA (μg/μl) at a dilution of 1:10, measuring the difference of absorbance between the RNA sample and DEPC water at a wavelength of 260nm.

• By using a ratio of A260nm/A280nm, an estimation of the purity of the RNA was determined. Pure RNA reaching an optical density of 2.0, and RNA contaminated with ethanol or protein, reaching optical density values less than 1.5.

• The samples were measured using Starna glass cuvettes (Optiglass limited, Essex, UK). The RNA samples were used immediately for reverse transcription (RT) or placed at -80 ℃ for long term storage.

2.4.3 Reverse Transcription--- from RNA to cDNA

Reverse transcription (RT) is a simple and sensitive technique for mRNA analysis and acts as an enhanced and more rapid alternative to the more conventional methods of RNA examination.

• In this study, RT was carried out by converting 0.5μg/μl of RNA into complementary DNA (cDNA) using the iScript™ cDNA Synthesis Kit (Bio-Rad Laboratories, California, USA). The protocol carried out is outlined below:

• Each reaction was set up in thin-walled 200μl PCR tubes (ABgene, Surrey, UK) as follows:

Component	*Volume per reaction*
5X iScript Reaction Mix	4µl
iScript Reverse Transcriptase	1µl
Nuclease-free water	xµl
RNA template (0.5µg/µl)	xµl
Total Volume	20µl

• The complete reaction was mixed and then incubated in a T-Cy Thermocycler (Creacon Technologies Ltd, The Netherlands) at the following temperatures:

5 minutes at 25 ℃

30 minutes at 42 ℃

5 minutes at 85 ℃

• Once the process was completed, the cDNA was diluted at the ratio of 1:4 or 1:8 with PCR water, and either used immediately as a template for conventional PCR, or stored at -20 ℃ for further use.

2.4.4 Polymerase Chain Reaction (PCR)

The Polymerase Chain Reaction (PCR) was initially devised in 1983 by Karey Mullis as a method for detecting and amplifying a specific target sequence of nucleic acids.

• In this study, a particular gene of interest was amplified by PCR using the GreenTaq™ ReadyMix PCR Reaction mix (Sigma-Aldrich, Inc., Poole, Dorset, England, UK). The reactions were set up in PCR tubes in aliquots of 16µl as follows:

Component	**Volume**
cDNA template	2µl
Forward primer	1µl(working concentration of 1 µM)
Reverse primer	1µl(working concentration of 1 µM)
2X green Taq^{TM}ReadyMix	8µl
PCR H_2O	4µl

A negative control containing PCR water instead of the template (cDNA) was run alongside the test samples to ensure there was no contamination.

• The PCR reactions were then briefly mixed before being placed in a 2720 Thermo Cycler (Applied Biosystems) set to the following conditions;

Initial denaturation: 94 ℃ for 5-10 minutes

Followed by 28-36 cycles of:

Denaturation: 94 ℃ for 30 seconds

Annealing: gene/primer specific temperature (55 ℃) for 30 seconds

Extension: 72 ℃ for 40 seconds

And finally:

Final extension: 72 ℃ for 7-10 minutes

The cycling conditions were dependent on different sets of primers and the size of the PCR products.

• The products were stained with Sybrgreen and visualised using an agarose gel electrophoresis system (section 2.4.5). In order to demonstrate a representative and reliable expression pattern, each RT-PCR was repeated at least three times.

2.4.5 Agarose gel electrophoresis and DNA visualisation

Agarose gel electrophoresis is the simplest and the most common method of DNA separation and analysis. It works by using an electrical current to separate the amplified DNA according to charge and size. Depending on the product size, the samples were either run on a 0.8% agarose gel (used for large DNA fragments 1-10kb) or a 2% gel (used for smaller fragments less than 1kb).

• The agarose gels were prepared by adding the required amount of agarose (Melford Chemicals, Suffolk, UK) to 400ml of (1x) TBE solution before being heated to completely dissolve the agarose. An appropriate amount of this solution was then poured into electrophoresis cassettes (Scie-Plas Ltd., Cambridge, UK) containing well forming combs, before the gel was left to set at room temperature for 30-40 minutes.

• Once the gel was set, (1X) TBE buffer was poured over the gel until it reached to a level of 5mm above the gel surface. The comb was removed, and approximately 5µl of 1Kb DNA ladder (Cat No. M106R; GenScript USA Inc.), or 8-10µl of each PCR reaction, was loaded into the well by placing the gel loading tip just over the well and dispensing the product into it.

• A power pack (Gibco BRL, Life Technologies Inc.) was then used to run the samples electrophoretically through the gel at a constant voltage of around 100V for approximately 30-50 minutes until the samples had migrated to as far as required for that particular product size.

• The DNA was then visualised by the addition of Sybrgreen which acts as a DNA intercalator and fluoresces once intercalated, thereby absorbing invisible UV light and transmitting the energy into visible orange light. The gel was placed in Sybrgreen stain diluted in the ddH_2O and left for 15 minutes with constant agitation to ensure even staining, before being visualised under UV light using a VisiDoc-It imaging system (UVP).

• Images were captured with the use of an UV camera imaging system (UVP), and printed with a SONY thermo printer (SONY UK, London, UK) or saved as a TIFF file. If insufficient staining was found, the gel was returned to the Sybrgreen stain for additional staining or destaining in water to remove any background staining if required.

2.4.6 Quantitative RT-PCR (Q-PCR)

Unlike conventional RT-PCR, which only allows for semi-quantification, Q-PCR is a method of detecting extremely small amounts of cDNA template within a sample while also determining an accurate and reliable value of the template copy number in each sample. This method works due to the use of a sequence specific DNA based fluorescent reporter probe which only quantifies the levels of DNA containing the probe sequence, thereby greatly increasing specificity.

This current study used the Ampliflour™ Uniprimer™ Universal system (Intergen company®, New York, USA) to quantify transcript copy number. The ampliflour probe consists of a 3' region specific to the Z-sequence (ACTGAACCTGACCGTACA) present on the target specific primers and a 5' hairpin structure labelled with a flourophore (FAM). When in this

hairpin structure, the flourophore is linked to an acceptor moiety (DABSYL) which acts to quench the fluorescence emitted by the flourophore, preventing any signal from being detected.

During PCR, the probe becomes incorporated and acts as a template for DNA polymerisation in which DNA polymerase uses its 5'-3' exonuclease activity to degrade and unfold the hairpin structure, thereby disrupting the energy transfer between flourophore and quencher, allowing sufficient fluorescence to be emitted and hence detected. The fluorescent signal emitted during each PCR cycle can then be directly correlated to the amount of DNA that has been amplified.

• Each reaction to be amplified was set up as follows:

Component	***Volume per reaction***
Forward primer	0.3µl (10pmol/µl)
Reverse Z primer	0.3µl (1pmol/µl)
Ampliflour probe	0.3µl (10pmol/µl)
2X iQTM Supermix	5µl
cDNA and PCR H_2O	4µl

• Each sample was then loaded into a 96 well plate (BioRad laboratories, Hemel Hampstead, UK), alongside standards (ranging from copy numbers of 10^1-10^8), covered with optically clear Microseal® (Biorad laboratories, California, USA) and this was placed in an iCyclerIQ thermal cycler (Figure-2.1) and detection software (BioRad laboratories, Hemel Hampstead, UK) at the following conditions:

Initial denaturation: 94 ℃ for 5 minutes

Followed by 80-90 cycles of:

Denaturation: 94 ℃ for 10 seconds

Annealing: 55 ℃ for 35 seconds

Extension: 72 ℃ for 20 seconds

• The fluorescent signal is detected at the annealing stage by a camera where its geometric increase directly correlates with the exponential increase of product. This is then used to determine a threshold cycle (TC) for each reaction and the transcript copy number depends on when fluorescence detection reaches a specific threshold.

• The degree of fluorescence emitted by a range of standards with a known transcript copy number was used to compare the amount emitted by each sample, allowing for the transcript copy number in each sample to be accurately calculated.

• Furthermore, the transcript copy number of each sample was normalised against the detection of GAPDH copy numbers. The procedure was repeated at least three times, and representative date is demonstrated as expressional trends.

Figure 2.1 ICycler-IQ thermocycler used for quantitative Q-PCR.

2.5 Methods for protein detection

2.5.1 Protein extraction and preparation of cell lysates

• Once cells reached an adequate confluency, the cell monolayer was scraped off in BSS using a cell scraper. The cell suspension was then transferred into a universal tube.

• This was followed by centrifugation at 1,780rpm for 8 minutes before the supernatant was poured off, and the cell pellet was lysed in 200-300µl of lysis buffer (depending on total cell number, approximately 100µl/10^6 cells), before being transferred into a 1.5ml eppendorf tube and placed for an hour at room temperature on a Labinco rotating wheel (Wolf laboratories, York, UK) to allow for cell lysis.

• The resulting suspension was then centrifuged at 13,000rpm for 15 minutes so any unwanted cell debris formed a pellet. The supernatant was transferred to a fresh eppendorf tube and the pellet discarded.

• The protein samples were then either quantified for SDS-PAGE as explained below, or stored at -20 ℃ until further use.

2.5.2 Protein quantification and preparation of samples for SDS-PAGE

In order to standardise the protein sample concentration for western blotting, the amount of protein in each sample was quantified following the protocol outlined in the Bio-Rad DC Protein Assay kit (Bio-Rad laboratories, Hemel Hampstead, UK).

• In a 96 well plate, 50mg/ml of bovine serum albumin (BSA) standard (Sigma, Dorset, UK) was serially diluted from 10mg/ml to 0.005mg/ml in lysis buffer and used to set up a standard curve of protein concentration.

• Five microlitres of either protein sample or standard was added into each well, before adding 25µl of 'working reagent A' (prepared by adding 20µl of reagent S per millilitre of reagent A), followed by 200µl of reagent B to each well.

• After samples were mixed, the plate was left at room temperature for 30-45 minutes to allow the colorimetric reaction to take place. Once this was complete, the absorbance of each sample was measured at 620nm using the ELx800 plate reading spectrophotometer (Bio-Tek, Wolf laboratories, York, UK).

• A standard curve and an equation to calculate protein concentration based on absorbance were established using the scatter line chart in Microsoft Excel. Protein concentration of each sample

was determined using the corresponding absorbance and the equation of the standard curve. The samples were then diluted in an appropriate amount of lysis buffer in order to normalise them to the required final concentration of 1.0-2.0mg/ml.

• This was then further diluted with 2x Lamelli sample buffer concentrate (Sigma-aldrich, St Louis, USA) in a ratio of 1:1 before the samples were denatured by boiling at 100 ℃ for 5-10 minutes and either loaded onto a SDS-PAGE gel or stored at -20 ℃ until further use.

2.5.3 Preparing immunoprecipitates

Immunoprecipitation (IP) can be used for analysing intracellular phosphorylation that occurs in downstream signalling cascades. The process involves adding a specific antibody targeting a protein of interest within a cell lysate. This is then mixed with sepharose or agarose bonded staphylococcal protein A, protein G, or both, in order to collect the resulting protein-antibody complexes. These complexes are then centrifuged to precipitate the protein-IgG-protein A/G beads. After being denatured at 100 ℃ for 10 minutes, the samples were separated on an SDS-PAGE gel, and evaluated using immunoprobing. The process was carried out as follows:

• Antibody targeted against a protein of interest was added to the cell lysate samples before being incubated at 4 ℃ for 1 hour on a Labinco rotating wheel.

• Following incubation, 20µl of conjugated A/G protein agarose beads (Santa Cruz Biotechnology, supplied by Insight Biotechnologies Inc, Surrey, England, UK) were added to each sample and placed back on the wheel for another hour to allow for the antibody-protein complexes to bind to the beads.

• Centrifugation at 8,000rpm for 5 minutes was carried out to remove any unbound protein or excess antibodies present in the supernatant. The protein pellet was subsequently washed twice

with 300µl of lysis buffer before being resuspended in 40-60µl of 1x sample buffer and boiled for 10 minutes. The resulting samples were then run on SDS-PAGE gels as explained below.

2.5.4 Sodium Dodecyl Sulphate Polyacrylamide Gel Electrophoresis (SDS-PAGE)

• The system used to carry out SDS-PAGE in this study was the Omni PAGE VS10 vertical electrophoresis system. Resolving gels of a required percentage (depending on protein size) were prepared in 15ml aliquots, in a universal container, (enough for 2 gels) by adding all the constituents at the amounts indicated in Table 2.5:

• The resulting mixture was then poured in between two glass plates held in place by a loading cassette, until at a level 1.5cm below the top edge of the plate, to prevent gel oxidation the top of the resolving gel was covered with a 0.1% SDS solution.

• The gels were then left to polymerise at room temperature for approximately 30 minutes, or until fully set. The excess SDS solution was then poured off before adding a sufficient amount of stacking gel in its place, prepared as Table 2.6:

Table 2.5 Ingredients for resolving gel.

Component	**8% Resolving gel (proteins size over 100kDa)**	**10% Resolving gel (proteins size below 100kDa)**
Distilled water	6.9ml	5.9ml
30% acrylamide mix (Sigma-Aldrich, St Louis, USA)	4.0ml	5.0ml
1.5M Tris (pH 8.8)	3.8ml	3.8ml
10% SDS	0.15ml	0.15ml
10% Ammonium persulphate	0.15ml	0.15ml
TEMED (Sigma-Aldrich, St Louis, USA)	0.009ml	0.006ml

Table 2.6 Ingredients for stacking gel.

Component	**Stacking gel**
Distilled water	3.4ml
30% acrylamide mix (Sigma-Aldrich, St Louis, USA)	0.83ml
1.0M Tris (pH 6.8)	0.63ml
10% SDS	0.05ml
10% Ammonium persulphate	0.05ml
TEMED (Sigma-Aldrich, St Louis, USA)	0.005ml

• After the addition of the stacking gel, a well forming Teflon comb was inserted before allowing the gel to polymerise at room temperature for around 20 minutes.

• Once set, the loading cassette was transferred into an electrophoresis tank and covered with 1X running buffer before the well comb was removed, and by use of a 50µl syringe (Hamilton), 10µl of Broad range markers were loaded (Santa Cruz Biotechnology, supplied by Insight Biotechnologies Inc, Surrey, England, UK), followed by 10-15µl of the required protein samples.

• The gels were then run at 100-120V, 50mA, and 50W for a length of time appropriate for the size of the protein of interest, in order to separate the proteins according to charge and molecular weight.

2.5.5 Western blotting: transferring proteins from gel to nitrocellulose membrane

• Once SDS-PAGE was completed, the protein samples were transferred onto a nitrocellulose membrane by western blotting. The electrophoresis equipment was disassembled and the gel removed from the two glass plates before discarding the stacking gel. The resolving gel was then placed on an SD10 Semi Dry Maxi System blotting unit (Semi DRY, Wolf Laboratories, York, UK) on top of 3 pieces of 1X transfer buffer pre-soaked filter paper (Whatman International Ltd., Maidstone, UK), and 1 sheet of Hybond nitrocellulose membrane (Amersham Biosciences UK Ltd., Bucks, UK).

• An additional 3 sheets of pre-soaked filter paper were placed on top of the gel to form a sandwich arrangement in order from anode to cathode: filter papers- membrane- gel- filter papers, as shown in Figure 2.3. Electroblotting was then carried out at 15V, 500mA, and 8W for 20-60 minutes (depending on protein size.

2.5.6 Protein staining

2.5.6.1 Staining membranes in Ponceau S

Ponceau S is a reversible and re-usable protein stain that does not interfere with any subsequent immuno-probing. Its main use is to confirm a successful transfer of proteins from the polyacrylamide gel onto the nitrocellulose membrane, but can also be used to aid in membrane sectioning for multiple immune-probing. The protocol was carried out as follows:

• After the transfer was completed and before probing began, the membrane was immersed in Ponceau S solution for a few minutes at room temperature.

• The solution was then washed off with distilled water until the bands become visible. If required, the membrane was then cut into several sections using a sharp and sterile scalpel.

• Once the staining was completely washed off the membrane was placed in 0.2% milk solution.

2.5.6.2 Coomasie blue staining of polyacrylamide gels

Coomasie blue is used to stain polyacrylamide gels following SDS-PAGE or transfer. This allows for visualisation of protein bands if no immuno-probing is required or observation of transfer efficiency and can be used as a way of semi-quantifying the volume of the protein bands. The protocol was carried out as follows:

• The gel was immersed in Coomassie blue stain solution for approximately 30 minutes before being repeatedly washed in destaining solution until the background staining disappeared, and the protein appeared as blue bands. The gel was then photographed or analysed.

2.5.7 Protein detection using specific immuno-probing

• Once staining was completed, the blocking and immuno-probing were carried out with a WBAVDBASE-SNAP i.d. protein detection system (Merck Millipore, USA, Figure 2.2). The blotted membrane was placed in the centre of a pre-wet blot holder and flattened gently with a roller to remove any air bubbles. A spacer was then added on top of the membrane and rolled again before the holder was securely closed and placed within the system. Blocking solution (10-30ml dependent on holder size) was added and a vacuum applied.

• Approximately 1-3ml (dependent on holder size) of primary antibody diluted 1:500 in 5ml of 0.2% milk in TBS with 0.1% Tween 20 solution was then added and left to incubate for 15 minutes at room temperature.

• After the probing with primary antibody, any remaining unbound antibody was then removed by applying the vacuum and the holder was washed 3 times with TBS with 0.1% Tween 20.

• The membranes were further incubated with 5ml of 1:5000 HRP conjugated secondary antibody diluted in 0.2% milk for 15minutes.

• This was followed by 3 washes with TBS with 0.1% Tween 20 using the vacuum in order to wash off any unbound secondary antibody.

• The membrane was then removed and chemiluminescent detection carried out.

2.5.8 Chemiluminescent protein detection

Chemiluminescent protein detection was carried out using the chemiluminescence detection kit (Luminata, Millipore), which consists of a highly sensitive chemiluminescent substrate that

detects the horseradish peroxidise (HRP) used during the western blot procedure. The protocol was carried out as follows:

• One millilitre of reagent was added onto the membrane and incubated for 5 minutes at room temperature in the dark with constant agitation.

• Excessive solution on the membrane was then drained off using a pasteur pipette and the membrane was transferred into a plastic tray. The chemiluminescent signal was detected using an UVITech Imager (UVITech Inc., Cambridge, UK) which contains both an illuminator and a camera linked to a computer (Figure 2.3).

Figure 2.2 Overview of the SNAP i.d.® 2.0 Protein Detection System.

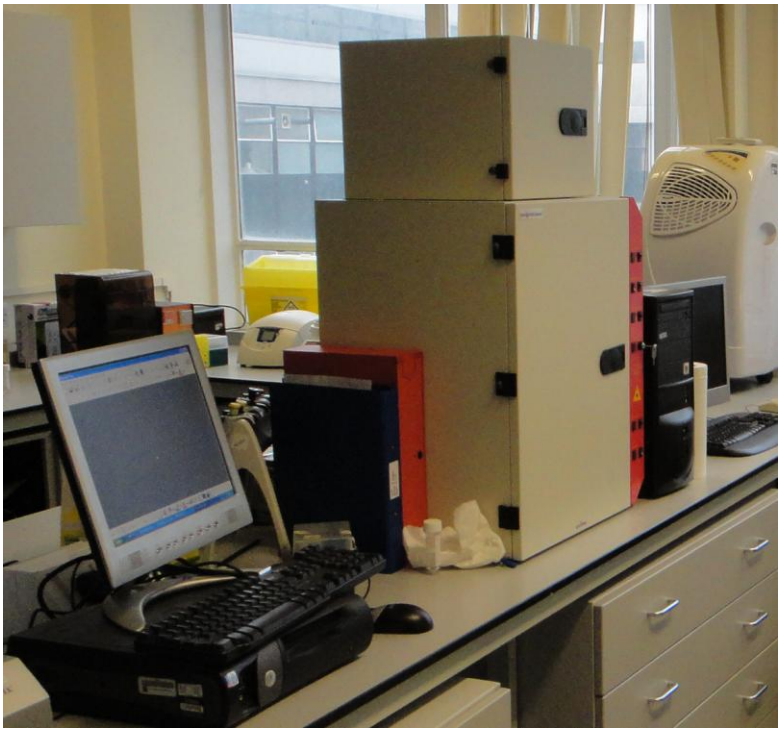

Figure 2.3 Imager used in the Western blot study.

• Each membrane was subjected to varying exposure times until the protein bands were sufficiently visible. These images were then captured and further analysed with the UVI band software package (UVITEC, Cambridge, UK), which allows for protein band quantification.

• In this study, glyceraldehyde 3-phosphate dehydrogenase (GAPDH) was used as a loading control and ran alongside any other proteins to be detected, so as to allow for additional normalisation of the samples and to compensate for any other negligible inaccuracies which may have occurred during the process. The GAPDH is used due to its highly abundant and conserved nature within eukaryotic cells, and is one of the most widely employed and accepted internal controls in determining mRNA and protein expression.

• In order to verify the results, each western blot was carried out three times and the protein bands quantified and standardised separately.

2.5.9 Immunohistochemical staining

•Briefly, 4~5μm sections from formalin-fixed, paraffin-embedded tissues were mounted on poly-L-lysine-coated glass slides and placed into an incubator of 62 ℃ for 2 hours.

•The sections were de-waxed in xylene and rehydrated through alcohol to distilled water. Endogenous peroxidase activity was blocked with 3% hydrogen peroxide for 15 min at room temperature.

•After pressure cooking the sections in 10 mmol/l EDTA (pH 8.0) for 3 minutes, the sections were incubated at room temperature with mouse monoclonal anti-WISP-1,WISP-2 and WISP-3 antibodies (1:50, 1:100 and 1:50 dilution respectively) for 3 hrs. Slides were given 3 x 5 minute washes with PBS.

•This was followed by incubation of HRP-conjugated secondary antibody for 1h. Slides were given 3 x 5 minute washes with PBS.

•Development of slides was performed using peroxidase substrate (diaminobenzidine tetrahydrochloride) solution, followed by counterstaining with hematoxylin for approximately 1 minute. After three washes with distilled water, slides were dehydrated for 5 minutes in each of 50% ethanol, 70% ethanol, 90% ethanol, 100% ethanol, 50% ethanol/ 50% xylene, 100% xylene. Slides were then mounted with DPX and left to dry in an incubator.

• Normal breast epithelia were used as positive controls. Normal gastric mucosa stained with PBS as primary antibody was used as negative controls. Slides were analysed independently by two observers using light microscopy. Photographs were recorded on an Olympus CKX41 microscope (Figure 2.4).

Figure 2.4 Microscope used in the imaging of the current study.

2.5.10 Gelatine zymography

•$3x10^6$ cells were counted and seeded in a tissue culture flask and incubated overnight.

• Following incubation, samples were washed once with 1x BSS followed by a wash with serum-free DMEM and then either incubated in serum-free DMEM control or treated medium for 4 hours.

• After 6 hours, the conditioned medium was collected and samples were prepared in non-reducing sample buffer.

• Protein samples were separated using SDS-PAGE on gels containing 1% gelatine (Sigma-Aldrich Inc, USA).

• After SDS-PAGE, gels were renatured for 1 hour at room temperature in wash buffer and then incubated at 37 ℃ in incubation buffer for 36 hours.

• Following incubation, the gels were stained with coomassie blue for 1 hour and washed in destain buffer for another 1 hour. The brightness of clear bands where MMP-2 and MMP-9 were located and gelatine was degraded.

2.6 Genetic manipulation of gene expression

2.6.1 Knocking down gene expression using ribozyme transgenes

In order to knockdown the expression of WISP-2, hammerhead ribozyme transgenes which specifically target and cleave the WISP-2 mRNA transcript were employed (Figure 2.6). The hammerhead ribozyme was first described by Forster and Symons in 1987 as a self-cleaving

region in the RNA genome of various plant viroids and virusoids. The hammerhead motif was subsequently integrated into short synthetic oligonucleotides, transforming it into a turnover catalyst capable of cleaving various RNA targets [257, 258] .

Hammerhead motifs contain a conserved secondary structure that consists of three helical stems (I, II, and III) enclosing a junction known as the catalytic core, typified by various invariant nucleotides. The best codons demonstrated to be suitable for cleavage are AUC, GUC and UUC. In order to generate a ribozyme transgene specific to WISP-2, primers were designed using Zuker's RNA mFold programme [259] according to the secondary structure of the gene (Figure 2.6). Subsequently, an appropriate GUC ribozyme target site was chosen according to the secondary structure of WISP-2 mRNA and the ribozyme created to specifically bind the sequence adjacent to this GUC codon. This made it possible for the hammerhead catalytic region of the ribozyme to bind to and specifically cleave the GUC sequence within the target mRNA transcript.

Following ribozyme design, the sequences were ordered from Invitrogen as sense/antisense strands (as shown in Table 2.3) and the transgenes were then synthesised using touchdown PCR using the following conditions:

Initial denaturation: 94 ℃ for 5 minutes

Followed by 8 cycles of each annealing temperature (total of 48 cycles):

Denaturation: 94 ℃ for 10 seconds

Various annealing steps: 70 ℃ for 15 seconds, 65 ℃ for 15 seconds,

60 ℃ for 15 seconds, 57 ℃ for 15 seconds, 54 ℃ for 15 seconds and 50 ℃ for 15 seconds.

Extension: 72 ℃ for 20 seconds

Final extension: 72 ℃ for 7 minutes

• Subsequently, the transgenes were run on a 2% agarose gel in order to verify their presence as well as size before being cloned into the pEF6/His plasmid in the TOPO cloning reaction.

2.6.2 TOPO TA gene cloning and generation of stable transfectants

The TOPO TA expression system provides a highly efficient and simple one step cloning approach without the requirement of ligases, specific PCR primers, or any post PCR procedures. The process involves the direct insertion of Taq polymerase amplified PCR products into a plasmid vector suited for high level and constitutive expression in mammalian host cell lines, following transfection.

The current study used the pEF6/V5-His-TOPO plasmid vector (Invitrogen Inc., Paisley, UK).,which allows linearisation with a single 3' Thymidine (T) overhang for TA cloning, and a covalently bound Topoisomerase (Figure 2.5). Due to its template independent terminal transferase activity, Taq polymerase catalyses the addition of a single deoxyadenosine (A) to the ends of PCR products, which allows for efficient ligation of the PCR product into the plasmid vector due its 3' T overhang mentioned above**.**

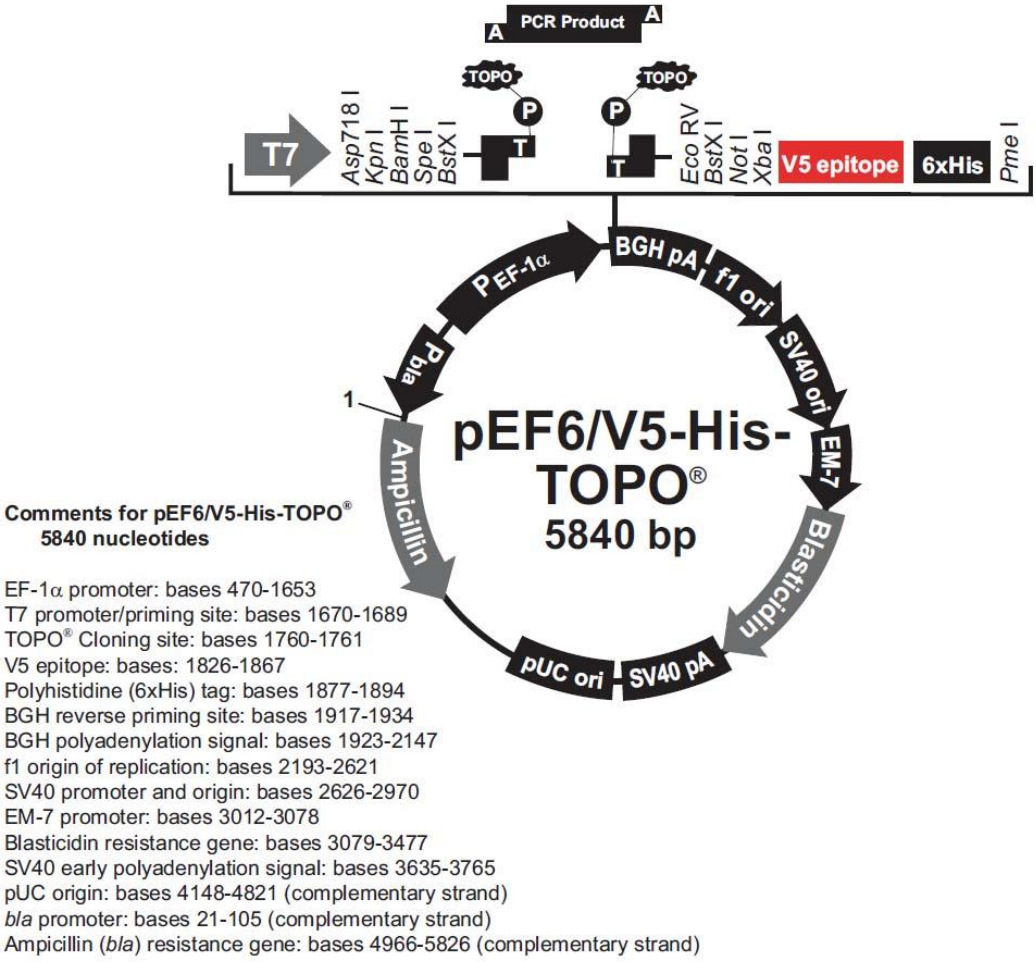

(From http://tools.lifetechnologies.com/content/sfs/manuals/pef6v5histopo_man.pdf)

Figure 2.5 Schematic of pEF6/V5 His TOPO expression plasmid.

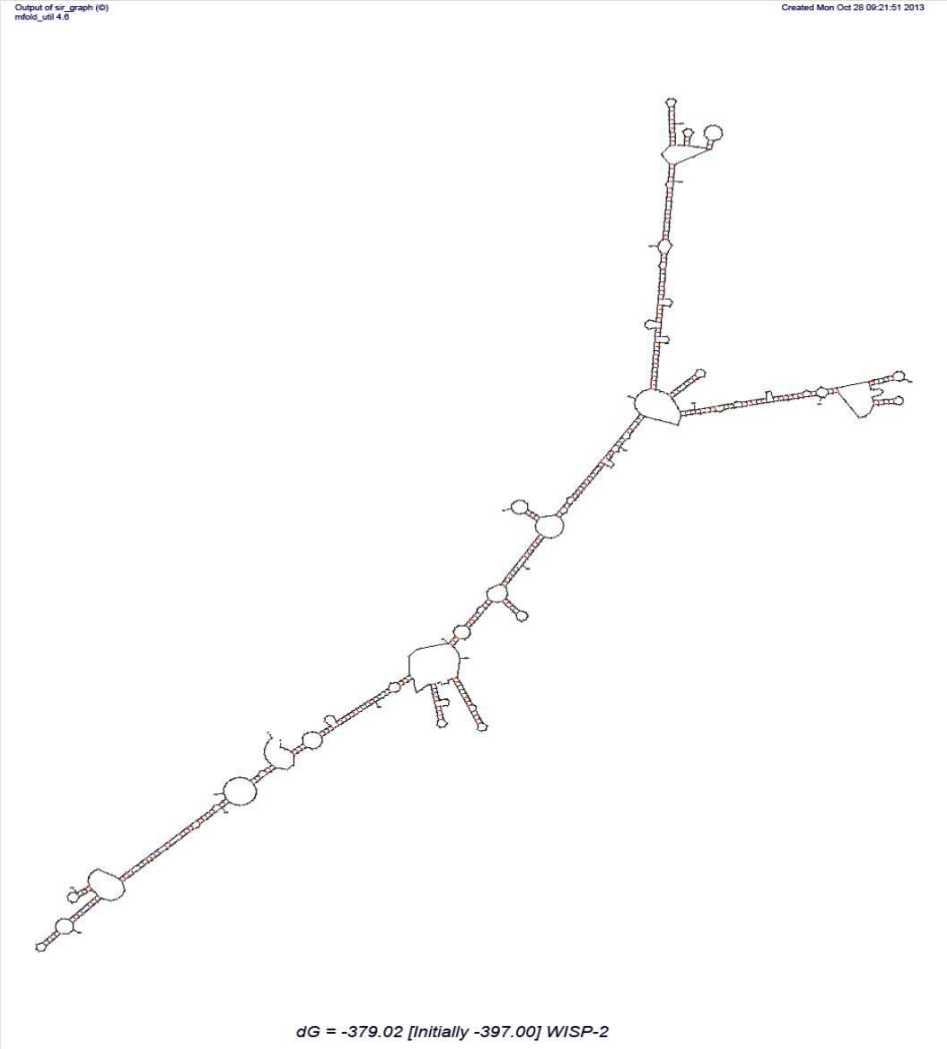

Figure 2.6 The predicted secondary structure of human WISP-2 mRNA.

2.6.3 TOPO cloning reaction

• The following reagents were placed in a pre-labelled eppendorf tube and mixed gently before being incubated for 5 minutes at room temperature.

4ul of PCR product

1ul salt solution

1ul TOPO vector

2.6.4 Transformation of chemically competent E. coli

• A 6µl cloning reaction was set up (section 2.6.3) and mixed in a vial with chemically competent One Shot™ TOP10 *E.coli* (Invitrogen Inc., Paisley, UK) before being incubated on ice for 30 minutes.

• To transform the *E.*coli bacteria the mixture was heat-shocked at 42 ℃ for 30 seconds in a water bath, and immediately placed back onto ice for 2 minutes.

• SOC medium (250µl warmed to room temperature) was then added to the cell suspension and left to shake horizontally at 200rpm on an orbital shaker (Bibby Stuart Scientific, UK) at 37 ℃ for an hour.

• Following this incubation period, the *E.coli* mixture was spread onto pre-warmed selective LB-agar plates (with 100µg/ml ampicillin) at high and low seeding densities, before being incubated at 37 ℃ overnight.

• As the pEF6 plasmid contains antibiotic resistance genes to both ampicillin and blasticidin, only the cells that contain the plasmid are capable of growing on the agar. This is a way of selecting only the colonies positive for the plasmid containing a gene of interest. However, to confirm that the gene sequence has been inserted in the correct orientation, the colonies need to be further tested (explained in section 2.6.5) (Figure 2.7)

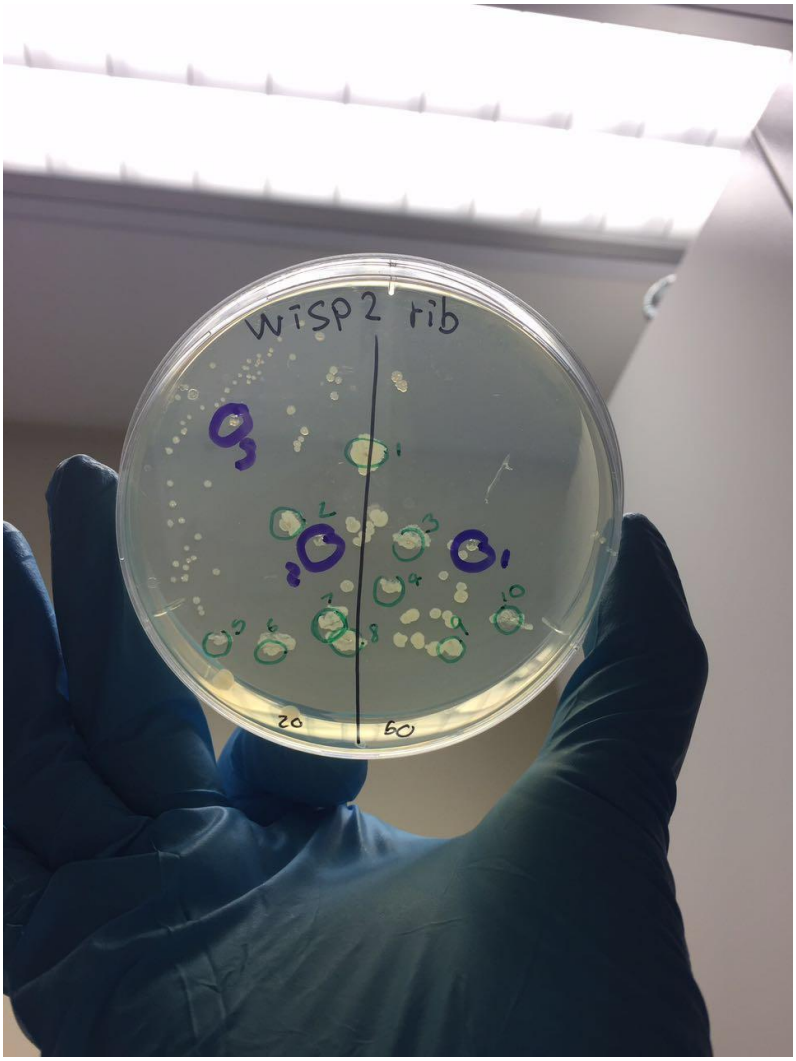

Figure 2.7 E.coli colonies from the cloning.

2.6.5 Colony selection and analysis

• In order to confirm that the correct product would be produced, the colonies were analysed to verify that the gene sequence had been ligated into the vector in the correct orientation.

• Two PCR reactions were performed to analyse each of 10 isolated colonies. The first reaction used a forward primer T7F and a reverse primer specific for the plasmid vector (RbTOPF) for incorrect insertion. The second reaction contained T7F and a reverse primer RbBMR. If a product was seen in the second reaction, it indicated the insert was ligated in the right orientation. If a band was seen for both reactions then the colonies contained a mixture of plasmids with both correctly and incorrectly inserted sequences.

• Individual colonies were examined by lightly touching a labelled colony with a pipette tip, and mixing it into each PCR reaction before specific amplification of the desired sequence. The thermal cycler was set to the following conditions:

Initial denaturation: 94 ℃ for 10 minutes

Followed by 35 cycles of:

Denaturation: 94 ℃ for 30 seconds

Annealing: 56 ℃ for 40 seconds

Extension: 72 ℃ for 1.5 minutes

And finally: Final extension: 72 ℃ for 7 minutes

2.6.6 Plasmid DNA purification and amplification

• Following colony analysis, colonies exhibiting the correct orientation were picked from the plate and inoculated in 10ml of LB broth with 100µg/ml ampicillin and then incubated at 37ºC over night with constant agitation.

• The amplified *E.coli* were then pelleted by centrifugation at 4 ℃ for 15 minutes at 6,000rpm, and then used for plasmid extraction. This was carried out using the Sigma GenElute Plasmid MiniPrep Kit (Sigma-Aldrich, USA) according to the provided protocol, outlined below.

• The bacterial pellet was resuspended in 200µl of resuspension fluid (containing RNase A) before being mixed thoroughly and transferred into the provided 2ml collection tubes.

• This was followed by the addition of 200µl lysis solution and gentle mixed by inverting the tubes 5-6 times. The resulting mixture was left at room temperature for 5 minutes before adding 350µl of neutralisation solution.

• The tubes were inverted several times, and centrifuged at 12,000rpm for 10 minutes. The resulting supernatant was then transferred into a fresh collection tube containing a Mini Spin Column, which bound the plasmid DNA after centrifugation at 12,000rpm for 1 minute.

• The flow through was discarded before the column was washed with 700µl of wash solution (containing ethanol) and centrifuged at 12,000rpm for 1 minute. The flow through was discarded once more, before the column was dried by another centrifugation at 12,000rpm for one minute.

• The column was then transferred into a fresh collection tube for elution. This was carried out by adding 100µl of elution solution and centrifuging at 12,000rpm for 1 minute. The resulting flow through containing the purified plasmid was collected, and around 4µl was run on a 0.8%

agarose gel using electrophoresis in order to confirm the presence and purification of the plasmid.

2.6.7 Transfection of mammalian cells using electroporation

• Following plasmid extraction, the empty plasmid, and the plasmid containing the ribozyme transgene was used to transfect both AGS and HGC27 gastric cancer cell lines.

• The method of transfection used in this study was electroporation using an Easyjet electroporator (Easyjet, Flowgene, Surrey, UK).

• Once the cells had reached confluency they were detached from their tissue culture flasks, counted, and approximately $1x10^6$ cells were resuspended in 1ml of normal medium.

• One millilitre of the cell suspension was then added into an electroporation cuvette (Eurgenetech, Southampton, UK), and following the addition of 5-10µl of plasmid, left at room temperature for 5-10 minutes.

• The cuvette was placed into the electroporator and subjected to an electrical pulse of 290-310V before immediately being transferred into a fresh tissue culture flask containing normal medium.

2.6.8 Establishment of a stable expression mammalian cell line

• Following transfection, in order to obtain a stable cell line carrying the constructed vector, the electroporated and cultured cells needed to be selected.

• As previously mentioned, the pEF plasmid contains a resistance gene against blasticidin and this is used as a selection of mammalian cells. Therefore, the cells were cultured in selection medium containing 5-7.5μg/ml blasticidin for around 1-2 weeks which only allowed the cells containing the plasmid to survive.

• After selection, the cells were transferred into maintenance medium containing 0.5μg/ml blasticidin. In order to verify the knockdown of the gene of interest, the cells were analysed using RT-PCR and western blotting.

• Once the cells had been verified to stably express the desired molecule, they were subjected to various *in vitro* assays in order to test the effect of altering the expression of that molecule on the biological properties of the cells. These assays are outlined in section 2.7 Figure 2.12 summarises the experimental steps in this chapter.

2.7 *In vitro* cell function assays

2.7.1 *In vitro* cell growth assay

• The protocol by Jiang *et al.* was followed [260]. Two hundred microlitres of medium containing 3,000 cells was seeded into three 96 well plates and if required, cells were treated with a protein of interest in serum free media.

• These plates were then left to incubate at 37°C, with 5% CO_2, for a period of 24 hours, 72 hours and 120 hours respectively.

• After the incubation, the cells were fixed with 4% formalin for 10-20 minutes, before being subsequently stained with 0.5% crystal violet for 10 minutes. The dye was washed off with water, and the plates left to dry.

• The dye was then solubilised using 200µl acetic acid, and cell growth was assessed by measuring the absorbance at 540nm using a spectrophotometer (BIO-TEK, Elx800, UK) (Figure 2.8). The growth rate was calculated as a percentage, using the absorbance taken at 24 hours as a baseline.

Figure 2.8 Multiple plate reader.

2.7.2 *In vitro* adhesion assay

• Wells in a 96 well plate were coated with 100µl of serum free medium with 5µg (stock concentration 0.05µg /µl) Matrigel (BD Matrigel™ Matrix, Matrigel™ Basement Membrane Matrix, Biosciences). The Matrigel was then left to dry for 2 hours at 55^{o}C.

• To rehydrate the Matrigel, 200µl of sterile water was added to each well and left for 45 minutes at room temperature.

• The medium was aspirated and 20,000 cells diluted in 200µl media, were seeded into each well and left to adhere to the Matrigel over a 40minute culture at 37 ℃, with 5% CO_2.

• After the incubation, the wells were washed with BSS to remove any non-adherent cells. The adherent cells were fixed with 4% formalin for 10-20 minutes, and then stained with 0.5% crystal violet for 10 minutes. Following substantial washes, the plates were left to dry before counting the adherent cells and taking photos under a microscope. Due to the fluid dynamics within the small sized wells of a 96 well plate, Matrigel sets unevenly, causing cell aggregation around the edges of the well. Therefore, in order to avoid these areas, only the cells which had adhered to the central area of the well were counted.

2.7.3 *In vitro* invasion assay

• Transwell inserts containing 8µm pores(FALCON®, pore size 8.0µm, 24 well format, Greiner Bio-One, Germany) were placed into wells of a 24 well plate (NUNC™, Greiner Bio-One, Germany), using sterile forceps in order to prevent contamination.

• Each insert was subsequently coated with 100µl serum free medium containing 50µg Matrigel, and left to dry for 2 hours at 55 ℃.

• The Matrigel was then rehydrated with 100µl sterile water for an hour at room temperature.

• The water was discarded, and 20,000 cells in 200µl medium were seeded into each insert. Six hundred microliters of medium was then added to the lower chamber of each well (outside the inserts) and the cells were incubated for a maximum of 96 hours, with 5% CO_2 at 37 ℃.

• After 72 hours incubation, the invasive cells migrated through the Matrigel, and the porous membrane to the other side of the insert. The Matrigel layer and the non-invasive cells were then removed from inside the insert using tissue paper. If this step is not carried out, the Matrigel would also be stained with crystal violet, making it difficult to distinguish between the background and invading cells.

• The invasive cells were then fixed with 4% formalin for 10-20 minutes, and then stained with 0.5% crystal violet for 10 minutes. The crystal violet was washed off, the plates left to dry, and the stained cells photographed and counted under a microscope.

2.7.4 *In vitro* motility assay

• The protocol by Jiang *et al*. was followed [261]. Seven hundred microlitres of medium containing 200,000-300,000 cells were seeded into a 24 well plate and cells were treated with the protein of interest in serum free medium if required.

• These plates were then left to incubate at 37°C, with 5% CO_2, for a period of 24 hours to allow cells to form a confluent monolayer. The cells were then wounded and photographs taken using EVOS system (Life Technologies Ltd, Paisley, UK) at 0.25, 1, 2, and 3 hours after wounding. Migration distances were measured using Image J software (National Institutes of Health, USA).

Figure 2.9 EVOS system used in cell migration study.

2.7.5 Electric Cell-substrate Inpedence Sensing (ECIS)

• Electric Cell-substrate Impedance Sensing (ECIS) is a novel method used as an alternative to the conventional function assays mentioned above (Figure 2.10). It works using an array of 96 wells, each containing two gold electrodes. These measure the current and voltage across this electrode, calculating the impedance and resistance. From the impedance changes, effects on cell attachment and motility can be examined [262]. Using 96W1E+ arrays (ECIS™ cultureware, Applied Biophysics, Inc., NY, USA), each well was stabilised at room temperature for around 20 minutes using 200µl electrode stabilising solution (ECIS™, Applied Biophysics, Inc., NY, USA) (Figure 2.11).

• The solution was then aspirated and replaced with 200µl DMEM F12 media containing Hepes buffer (Lonza, Verviers, Belgium) and left until needed.

• The medium was aspirated, and 40,000 cells diluted in 200µl DMEM were seeded into each well, and treated with a protein of interest if required.

• The array was then placed into an ECIS™ CO_2 incubator (RS biotech 9600, R galaxy R+) s connected to the ECIS™ Model 9600 Controller (Applied Biophysics, Inc., NY, USA). The software was set up so that resistance to the current flow was measured at 4000Hz. Cell adhesiveness was assessed within the first 40 minutes and electric wounding was set at the 14^{th} hour when the resistance reached a platform and migration data could be obtained over 6 hours. Data was normalised using resistance from the first time point.

This instrument provides researchers with automated, non-invasive mechanism capable of monitoring cell behaviour in real-time without the use of labels. The ECIS® Zθ measures the complex impedance spectrum (Z, R, C) of adherent cells growing on gold electrodes.

Each of the 96 wells in a standard plate configuration contains two circular 350 µm diameter active electrodes on a transparent PET substrate. As with other 1E arrays, a major use of this array is for the ECIS wound-healing assays where the small size of the electrodes assures the high current pulse will result in complete cell killing. Only a small population of cells is monitored on the small electrodes resulting in a fluctuating impedance signal due to the random like movement of the cells (micromotion).

Figure 2.10 The ECIS® Zθ (theta) instrument.

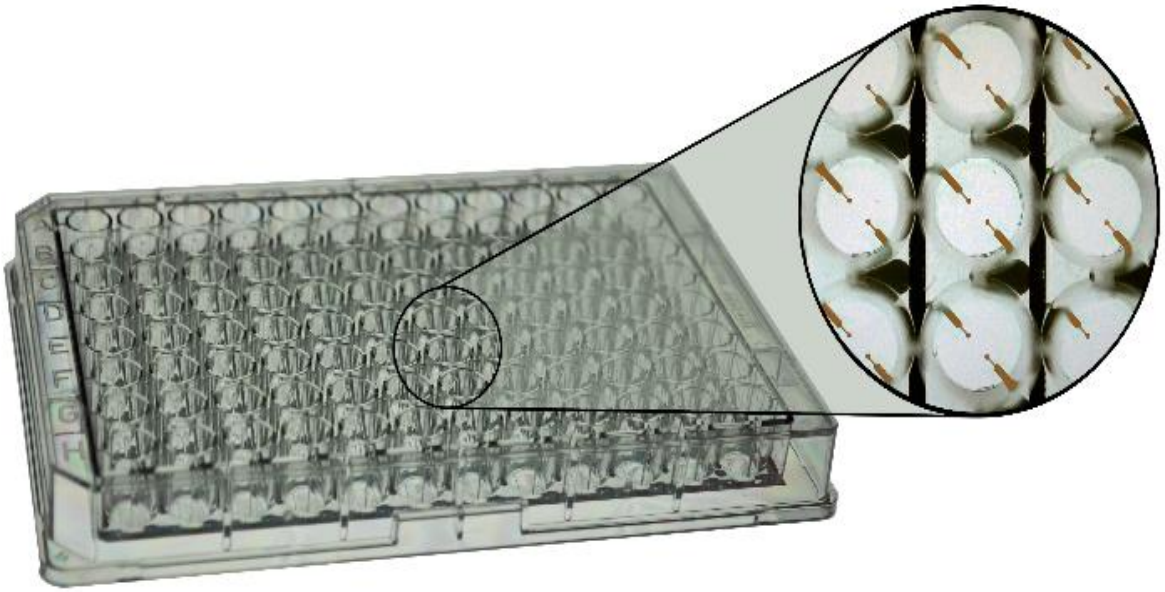

Figure 2.11 ECIS 96W1E+ PET plate.

(From official website http://www.biophysics.com/cultureware.php#link1)

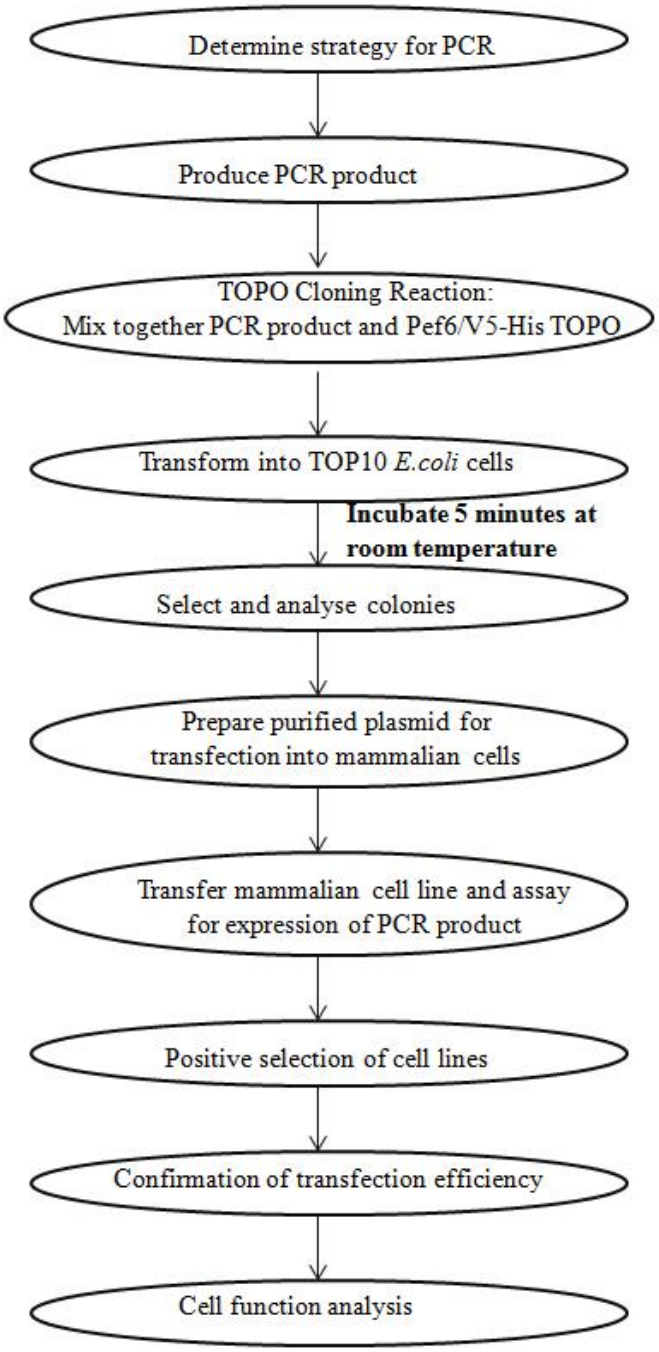

Figure 2.12 Flow chart outlining the experimental steps necessary to clone, express PCR product and follow test.

2.8. Protein arrays for detecting proteins interacting with WISP-2

2.8.1 Tissue and sample preparation

Fresh tissues were obtained immediately after surgery. One piece of normal gastric mucosa (10cm away from the tumour margin) and one piece of tumour tissue was obtained from the same patients. This was carried out under the ethics approval from Peking University Research Ethics Committee.

Tissues were immediately placed in a universal tube, filled with ice cold protein extraction buffer with a mixture of protease inhibitors (BD Biosciences, San Jose, USA). The tissues were then subject to homogenisation using a handheld homogenizer. The homogenates were dispensed into 1.5ml eppendorf tubes and subsequently spun at 12,000g for 10 minutes. Supernatants were carefully collected and placed in new tubes and stored at -20^{o}C until use.

2.8.1.1 Immunoprecipitation

Protein preparations were first subject to protein quantitation, using a colorimetric protein quantitation Kit (Chapter 2.5.2). The concentrations were subsequently standardised at 2mg/ml. Small amounts of the proteins were set aside as a total protein preparation for verification purpose.

Equal volumes of protein from each sample were placed into universal tubes. Equal amounts of Anti-WISP-2 antibodies were added to each protein sample. The tubes were then placed onto a spinning wheel, which was placed into the cold room (4^{o}C) at 100rpm. After 24 hours,

protein A/G conjugates were added to the mixture, which again was placed in the cold room at 100rpm for 4 hours.

The protein-antibody-agarose mixture was dispensed into eppendorf tubes which were microfuged at 4^{o}C, 5,000g for 10 minutes. After carefully discarding the supernatants, three washings were carried out, by adding the same lysis buffer to the immunoprecipitates followed by centrifugation.

After removal of the washing solutions, an extraction buffer (Chapter 2.5.2) was added to the immunoprecipitate and then subject to boiling at 100^{o}C for 5 minutes. After cooling down, the mixture was spun at 12,000g for 10 minutes. The supernatant, which contains the proteins precipitated by the antibody was then carefully collected and stored at -20^{o}C, ready for protein array analysis.

2.8.1.2 Antibody microarrays

We chose an antibody based protein array, namely KAM850, which has 854 capture antibodies spotted on to each array slides (Kinexus Bioinformatics Ltd, Vancouver, Canada). Each array slide has two array spots (Figure 2.13).

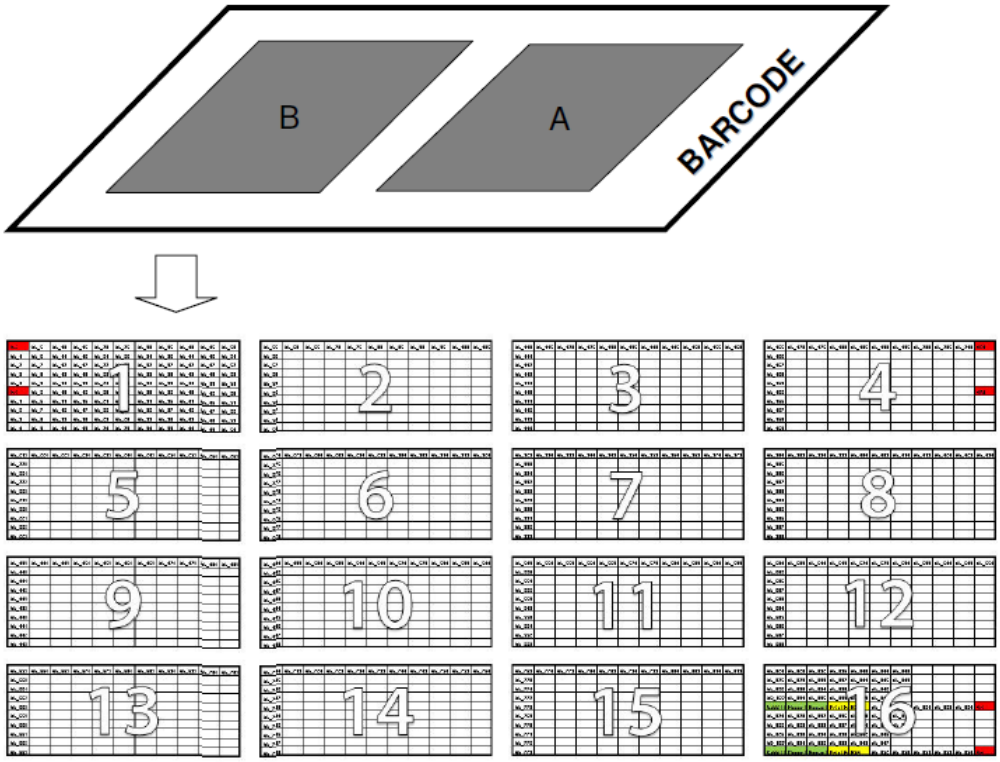

Figure 2.13 Antibody layout on the KAM850 protein microarray.

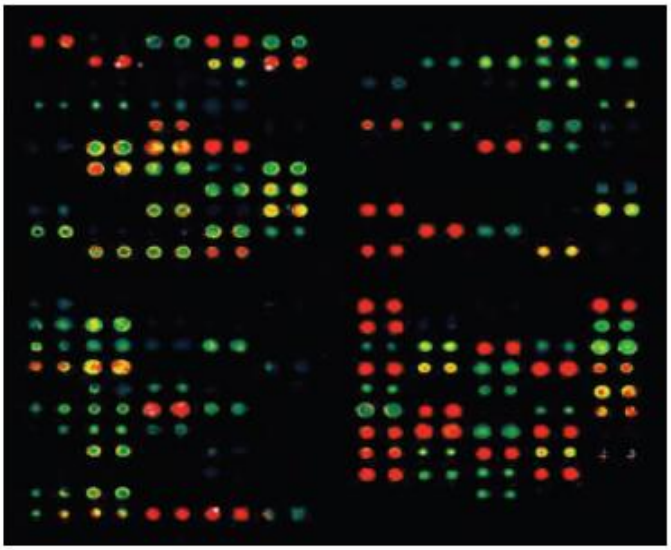

Figure 2.14 An example of close up examination of the antibody array. Image obtained from Kinexus Bioinformatics Ltd.

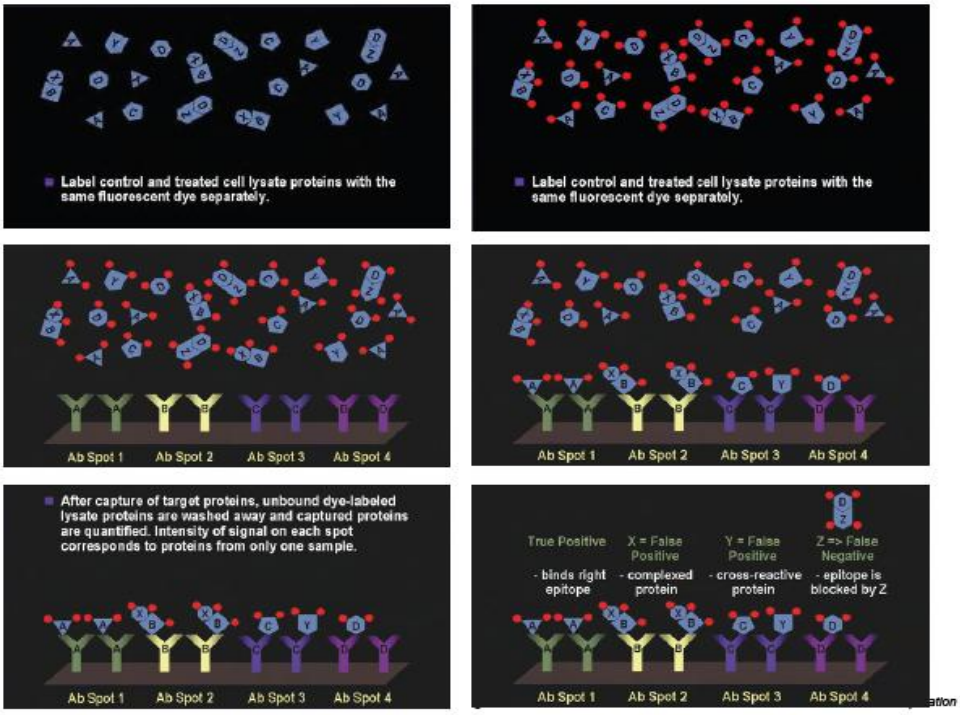

Figure 2.15 An illustration to demonstrate the procedure of KAM850 protein microarrays.Image obtained from Kinexus Bioinformatics Ltd.

Content	Total	Non-redundant	Redundant
Number of pan-specific antibodies: 517	60.5%		
Number of phospho-specific antibodies: 337	39.5%		
Number of protein kinase antibodies - pan-specific	309	189	120
Number of protein kinase antibodies - phosphosite-specific	157	128	29
Number of protein phosphatase antibodies - pan-specific	38	31	7
Number of protein phosphatase antibodies - phosphosite-specific	6	4	2
Number of stress antibodies - pan-specific	37	22	15
Number of stress antibodies - phosphosite-specific	9	6	3
Number of transcription antibodies - pan-specific	24	20	4
Number of transcription antibodies - phosphosite-specific	51	44	7
Number of other antibodies - pan-specific	109	100	9
Number of other antibodies - phosphosite-specific	114	105	9
Total Number of Antibodies	**854**	**649**	**205**

Figure 2.16 The antibodies used in the KAM850 antibody protein microarrays Image obtained from Kinexus Bioinformatics Ltd.

2.8.1.3 Key parameters in the protein microarray analyses

The following are the key parameters collected and used for the data analyses:

Globally Normalized Signal Intensity - Background corrected intensity values are globally normalized. The Globally Normalized Signal Intensity is calculated by summing the intensities of all the net signal median values for a sample.

Flag - An indication of the quality of the spot, based on its morphology and background. The flagging codes used in the reports are as follows:

0: acceptable spots;

1: spots manually flagged for reasons and may not be very reliable;

3: poor spots defined by various parameters;

%CFC - The percentage change of the treated sample in Normalized Intensity from the specified control.

Calculation = (Globally Normalized Treated – Globally Normalized Control) /Globally Normalized Control)*100

% Error Range - A parameter to show how tightly the "Globally Normalized Net Signal Intensity" varies for adjacent duplicate spots of the same protein in the sample compared to each other.

Calculation = ABS (Globally Normalized Spot 1- Globally Normalized Spot 2) /Globally Normalized Spot 2*100

Log2 (Intensity Corrected) - Spot intensity corrected for background is log transformed with the base of 2.

Calculation = LOG (Average Net Signal Median, 2)

Z Scores - Z score transformation corrects data internally within a single sample.

Z Score Difference - The difference between the observed protein Z scores in samples in comparison.

Z Ratios - Divide the Z Score Differences by the SD of all the differences for the comparision.

2.8.1.4 Antibody array analysis of WISP-2 interacting proteins

The immunoprecipitates from normal and tumour tissues of the same patient were applied to the same slide, to reduce the inter-assay variance.

The proteins samples were labelled, applied to the microarray, and images subsequently scanned using a Perkin-Elmer ScanArray Reader laser array scanner, according to manufacturer's instructions.

Analysis was carried out using the *ImaGene 9.0* from BioDiscovery (El Segundo, CA).

Here, our analysis had focused on the Globally Normalized Signal Intensity, %CFC and the Z-scores.

2.8.2 Protein array based analyses for screening potential signalling events associated with WISP-2 in gastric cancer cell lines

Here, we determined the potential signalling pathways that are influenced by WISP-2 in gastric cancer cells. We used the WISP-2 knock down cell model and compared the knockdown cells and control cells.

2.8.2.1 Cell and sample preparation

AGS/pEF6 (control transfected cells) and AGS/WISP-2KD (WISP-2 knockdown cells) at 90% confluence each in two T75 tissue culture flasks were washed with BSS buffer, then placed with a fresh batch of DMEM supplemented with 5% FCS. After 5 hours, cells were removed from the flasks with a cell scraper. The cells were pelletted using a centrifuge at 2,500rpm for 5 minutes.

Lysis buffer was added to the cell pellets and placed on a spinning wheel for 1 hour at 4^{o}C. The lysates were then spun at 12,000g for 10 minutes at 4^{o}C. The supernatant were carefully collected and insolubles discarded.

2.8.2.2 Protein concentration

Based on absorbance the protein concentration in the cell lysates was quantified using the scatter line chart of Microsoft Excel and then adjusted to 2mg/ml. The samples were stored at -20^{o}C until use.

2.8.2.3 KAM850 protein microarray analysis

We used an antibody based protein array (KAM850, Kinexus Bioinformatics Ltd, Vancouver, Canada), which has 854 capture antibodies spotted on to each array slide, and applied the samples, pairwise, on the sample array slides, for the sake of reducing the inter-assay variance and ease of comparative analysis.

In this case, we were focused on comparing the difference between the two comparable cell types, by emphasising the Z-difference and Z-ratio.

2.9 Clinical cohort study

2.9.1 Gastric cancer

A total of 502 stomach tissues samples were collected and used in the present study. The cohort included 320 gastric cancer tissues and 182 background normal gastric tissues (Table 2.7). All the specimens were verified by pathologists and a routine follow-up period of at least 60 months was carried out after surgery. Ethics approval was obtained from the Peking University Cancer Hospital Ethics Committee (Ethics approval reference number: 2006021) and consents were obtained from all the patients.

2.10 Statistical analysis

Statistical analysis was performed using SPSS18 (SPSS Inc., Chicago, USA). IHC data was cross-tabulated and a Chi-square test performed. Survival analysis was evaluated using life tables constructed from survival data with Kaplan-Meier plots and analysed using log-rank

statistics. Overall survival was measured from date of initial surgery to date of death, counting death from any cause as the end point, or the last date of information as the end point if no event was documented. The association of the expression of genes was analysed using Spearman Rank Order Correlation analysis. Other data sets were analysed using Student's t-test for normally distributed data and Mann-Whitney U-test for non-normally distributed data. P-value$<$0.05 was considered statistically significant.

Table 2.7 Sample numbers of cohort study.

Clinical/pathological features	Sample numbers
Tissue sample	
Normal	182
Tumour	320
Gender	
Male	230
Female	90
Tumour Depth	
T1	15
T2	26
T3	41
T4	230
Lymph node	
Negative	69
Positive	245
Metastasis	
M0	278
M1	41
TNM staging	
TNM1	24
TNM2	59
TNM3	219
TNM4	9
Differentiation	
High	1
High-Medium	6
Medium	60
Medium-low	81
Low	137
Clinical outcome	
Alive	133
Died	184
Disease free	118
Metastasis	15
Died of GC	184

Chapter 3

WISPs expression in gastric tissues and gastric cancer cell lines

3.1 Introduction

Cancer development is a multistep process, during which the cell acquires new phenotypic traits (overriding growth controls, induction of angiogenesis, evasion from host anti-tumour responses, extravasation and growth at metastatic sites etc.) as a result of successive genetic alterations. The main threat and the reason for most cancer deaths are not the primary tumours, but secondary tumours, the metastasis [263]. Tumours are heterogeneous populations composed of different cells types: stem cells with the capacity for self-renewal and more differentiated cells lacking such ability. The overall growth behaviour of a developing primary tumour is largely determined by the combined cell-cell interactions. The dominating influence of migration on tumour growth leads to unexpected dependencies of tumour growth on proliferation capacity and cell death [264]. During metastasis, cells from primary neoplasias follow a number of seemingly separate but highly related steps in order to acquire properties necessary for successful metastasis, namely, EMT, migration and invasion, anoikis resistance, extravasation and organ colonisation.

WISP proteins are a subfamily of the CCN family [189]. The CCN family of proteins is a crucial group of signalling molecules found in eukaryotic organisms, whose nomenclature is due to the first three members of the family: Cyr61 (Cysteine rich protein 61), CTGF (Connective tissue growth factor) and NOV (Nephroblastoma overexpressed gene) [206], which are now designated CCN1, CCN2 and CCN3, and three other family members WISP-1, WISP-2 and WISP-3 are designated CCN4, CCN5 and CCN6 [194]. It has been shown that WISP proteins were up-regulated in Wnt-1 transformed cells [189].

WISPs are secreted matricellular proteins, which are a subset of the ECM modulating cellular responses, such as cell growth, differentiation, invasion, migration and survival [265]. WISP-1 expression has been found in several cell types and it is implicated in cellular and tissue

homeostasis by a variety of autocrine and paracrine effects, thereby representing a highly attractive therapeutic target for medical applications. Elevated WISP-1 expression has recently been reported in several cancers, including hepatocellular carcinoma [266], colon adenocarcinoma [212, 232], lung carcinoma [234, 235] and breast cancer [211, 267]. But the functions WISP-1 plays in cancer development and progression are controversial. WISP-2 is structurally similar to other members of the CCN family, except for the carboxyl-terminal (CT) domain, which is absent in this protein [194, 238]. WISP-2 is relevant to tumourigenesis and malignant transformation, especially in breast cancer [211, 222], colorectal cancer [212] and heptocarcinoma [227]. But its function varies depending on cell types and the microenvironment. The striking difference in structure with other two family members may contribute to its difference in functions and WISP-2 might act as a dominant negative regulator of other CCN family members, although to date there is little evidence to support this hypothesis. Of the WISPs, WISP-3 is probably the least-studied, a secreted protein that modulates the insulin-like growth factor-1 (IGF-1) signalling pathway. This matricellular protein was found to have inhibitory functions on tumour growth, proliferation and invasion in inflammatory breast cancer and aggressive non-inflammatory breast cancer [268].

Clinical studies showed different expression profiles and roles of WISPs in cancers. The inconsistency between the results in multiple cancers has raised uncertainty concerning the role of WISPs in carcinogenesis and metastasis. It is now increasingly apparent that the relative abundance of individual WISPs members, which often have contradictory activities, has a profound effect on tumour progression. It is also suggested that the relative abundance of WISP-1, WISP-2 and WISP-3 may be a novel therapeutic approach to highly invasive cancers. These observations attracted us to explore the expression status at mRNA and protein levels of

WISP family members in gastric cancer samples and their adjacent normal tissues and different gastric cancer cell lines.

3.2 Materials and methods

3.2.1 Gastric cancer tissues

Gastric cancer tissues were collected immediately after surgery and stored in liquid nitrogen and then transferred into -80 ℃ freezer until further use, with approval of the Peking University Cancer Hospital Research Ethics Committee. All patients were informed and participated with written consent. All the specimens were verified by a consultant pathologist.

3.2.2 Antibodies and primers

Polyclonal rabbit anti-WISP-1, WISP-2 and WISP-3 antibodies were obtained from Abcam Company listed in Table 2.4. All the primers used were synthesised and provided by Sigma (Paisley, UK). Primer sequences are shown in Tables 2.2 and 2.3.

3.2.3 Cell lines

AGS and HGC27 cells were routinely cultured in DMEM-F12 medium as described in section 2.3. AGS is derived from an adenocarcinoma of the stomach of a 54 year-old Caucasian female with no prior anti-cancer treatment. HGC27 is derived from a lymph node of a Japanese patient with undifferentiated mucinous gastric adenocarcinoma.

3.2.4 RNA isolation, cDNA synthesis, and RT-PCR

RNA was isolated from cells using Tri Reagent (Sigma-Aldrich, Inc., Poole, Dorset, England, UK), and converted into cDNA by reverse transcription using the iScript™ cDNA Synthesis Kit (Bio-Rad Laboratories, California, USA), as described in section 2.4. RT-PCR was carried out at the following conditions; 94˚C for 5 minutes, followed by 26 to 30 cycles of 94˚C for 30 seconds, 56˚C for 30 seconds, and 72˚C for 1 minute and a final extension of 7 minutes at 72˚C. The products were run on a 2% agarose gel and visualised using Sybrgreen under UV light using a VisiDoc-It imaging system (UVP).

3.2.5 Immunochemical staining of WISP-1, WISP-2 and WISP-3

Immunochemical staining of WISP-1, WISP-2 and WISP-3 in gastric cancer cells and tissues were carried out using specific primary antibody for the protein, followed by secondary antibody. For the detailed procedure refer to Section 2.5.9.

3.2.6 Statistical analysis

Statistical analysis was performed using SPSS18 (SPSS Inc., Chicago, USA). IHC data was cross-tabulated and a Chi-square test performed. Survival analysis was evaluated using life tables constructed from survival data with Kaplan-Meier plots and analysed using log-rank statistics. Overall survival was measured from date of initial surgery to date of death, counting death from any cause as the end point, or the last date of information as the end point if no event was documented. The association of the expression of genes was analysed using Spearman Rank Order Correlation analysis. Mann-Whitney U-test for non-normally distributed data was used for Q-RT-PCR data. P-value$<$0.05 was considered statistically significant.

3.3 Results

3.3.1 RNA extraction of gastric tissues

Using Tri-reagent, tissue RNA was extracted from samples stored in the tissue bank of Peking University Cancer Bank. Figure 3.1 showed representative images from 502 cases of RNA.

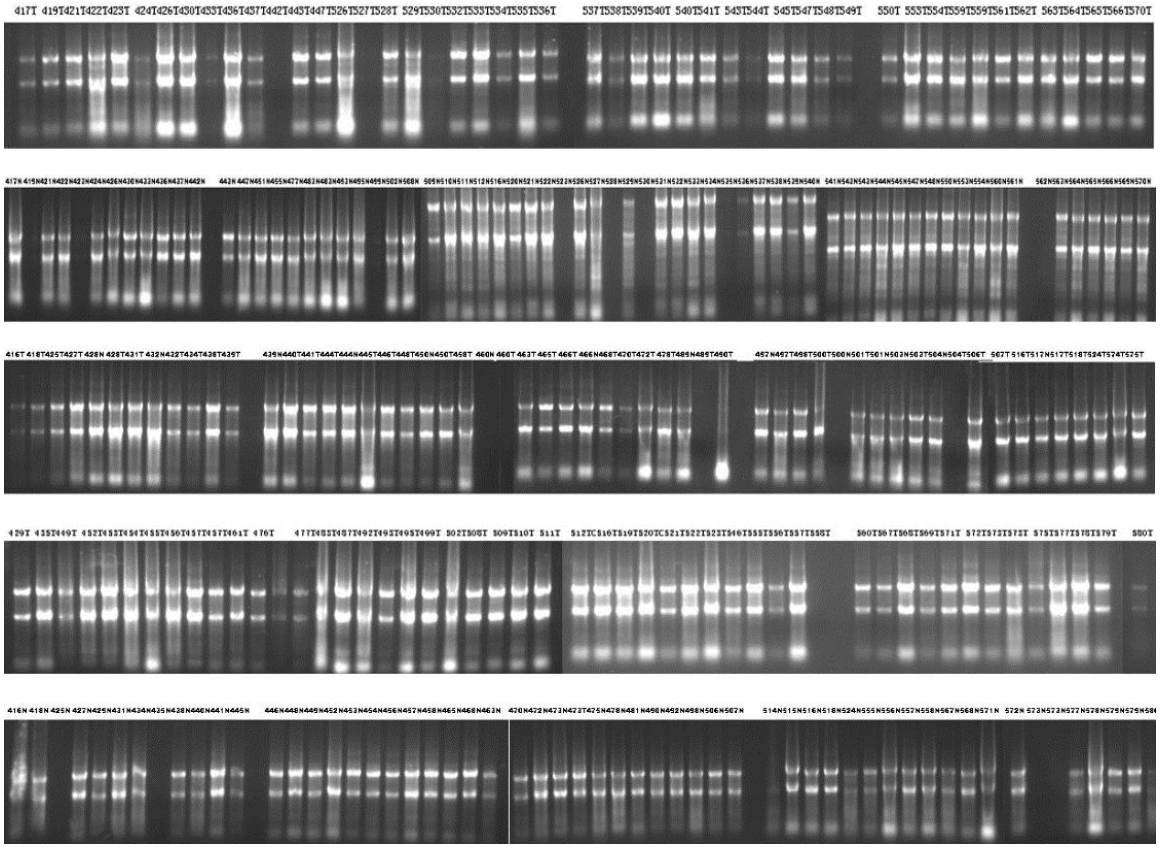

Figure 3.1 Representative images of RNA samples

3.3.2 Gastric tissues screening for WISPs expression

Analysed by Q-RT-PCR, WISP-2 transcripts showed a higher level in tumours than in normal tissues (P=0.0028) but WISP-1 and WISP-3 showed no significant difference between normal tissues and tumours (P=0.0642 and P=0.9076, respectively). Figure 3.2 showed the bar graph

of the expression of WISP-1 and WISP-2 in tumours and normal tissues. For WISP-3, the median values in both groups were very low, thus it was not possible to display the data in a bar graph. Instead, the result is given in Table 3.3

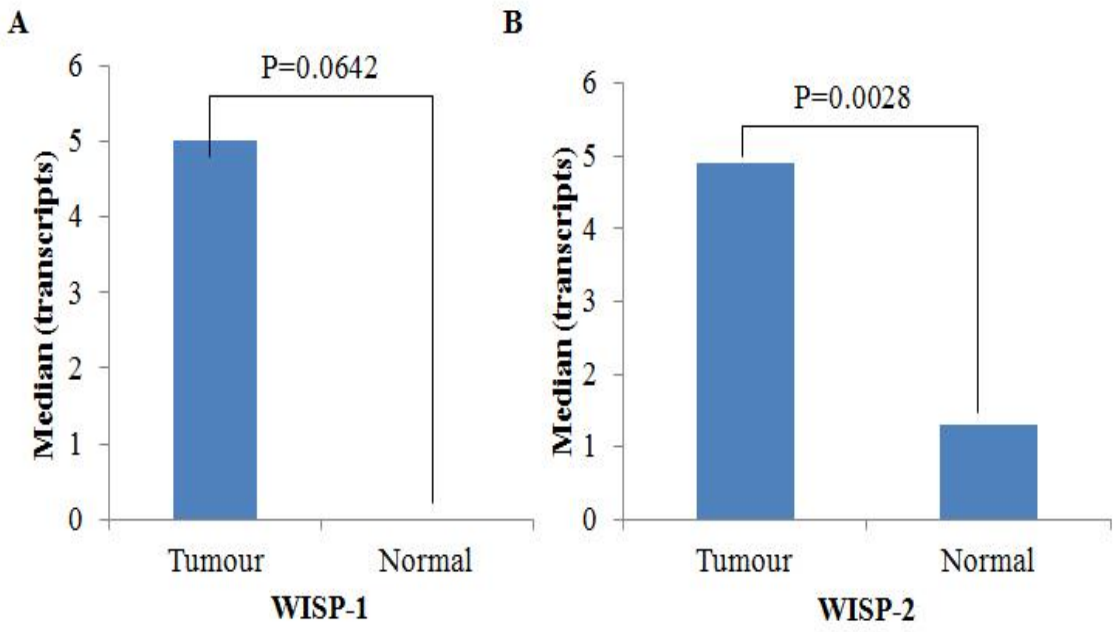

Figure 3.2 Expression of WISPs in gastric tissues (Median). A: WISP-1 expression in gastric cancer and normal gastric tissues. It was seen that there was a big difference between tumours and normal tissues, although it was not significant (P=0.0642). B: there was significant difference of WISP-2 expression in gastric cancer and normal gastric tissues (P=0.0028).

However, levels of the WISP-1 were highly expressed in tumours without distant metastasis at diagnosis compared to those with metastatic diseases (P=0.0168). Levels of the WISP-2 transcript were found significantly higher in TNM1 and TNM2 stage tumours (P =0.0249) than in TNM3 and TNM4 stages and also higher in T1 and T2 than in T3 and T4 (P=0.1817); higher in node negative than in node positive tumours (P=0.128); higher in tumours without distant metastasis than those with (P=0.39), and much higher in the patients alive than in those who died before the follow-up end time (P=0.1698) although without statistical significance (See

Table 3.1, 3.2 and 3.3). Table 3.1, 3.2 and 3.3 showed the association of WISP-1, WISP-2 and WISP-3 mRNA expression with clinic-pathological parameters in gastric cancer patients.

Table 3.1 Association of WISP-1 mRNA expression with clinic-pathological parameters in gastric cancer patients.

Clinicolpathological Parameters	WISP-1			
	Cases	**N$^{\alpha}$**	**Median (Q1,Q3)**	***P***
Tissue sample				
Normal	158	31	5(0,243)	0.0642
Tumour	260	64	0(0,135)	
Gender				
Male	185	46	0(0,126)	0.12
Female	75	18	3(0,501)	
Infiltration depth				
T1+T2	40	2	2(0,611)	0.3487
T3+T4	213	61	0(0,130)	
Lymph node status				
N0	55	16	0(0,468)	0.716
N1+2+3	201	46	0(0,126)	
M-staging				
M0	227	55	1(0,269)	0.0168*
M1	33	8	0(0,11)	
TNM staging				
TNM1+2	70	15	1(0,759)	
TNM3+4	183	47	0(0,110)	0.3029
Differentiation				
High	0	1		
High-Medium	5	1	0(0,1232)	
Medium	52	10	0(0,230)	0.592$^{\Delta}$
Medium-Low	61	21	1(0,737)	0.3264$^{\Delta}$
Low	112	26	1(0,82)	0.5091$^{\Delta}$
Clinical outcome				
Alive	106	28	1(0,440)	
Died	152	35	0(0,71)	0.227
Disease Free	94	25	0(0,440)	
Metastasis	12	3	1(0.873)	0.8341$^{\#}$
Died of GC	152	35	0(0,71)	0.2529$^{\#}$

Notes : Cases: the total number of cases; N$^{\alpha}$: missing cases; median is the middle on from lowest value to highest value of WISP-1 mRNA expression; *:P<0.05, $^{\Delta}$: Compared with "High-medium", $^{\#}$: Compared with "Disease Free "

Table 3.2 Association of WISP-2 mRNA expression with clinic-pathological parameters in gastric cancer patients.

Clinicolpathological Parameters	WISP-2			
	Cases	**N$^{\alpha}$**	**Median (Q1,Q3)**	***P***
Tissue sample				
Normal	182	7	1.3(0.1,58.9)	
Tumour	320	4	4.9(0,28)	0.0028**
Gender				
Male	230	1	4.9(0.1,55)	
Female	90	3	5.1(0.2,69.6)	0.8387
Infiltration depth				
T1+T2	41	1	15.9(1.1,116.9)	
T3+T4	271	3	4.6(0.1,58.9)	0.1817
Lymph node status				
N0	69	2	14.8(0.4,83.4)	
N1+2+3	133	1	4(0.1,55)	0.128
M-staging				
M0	278	4	5.4(0.2,63.1)	
M1	41	0	4(0,45)	0.39
TNM staging				
TNM1+2	83	2	15.9(1.4,77.7)	
TNM3+4	228	2	3.2(0.1,50.5)	0.0249*
Differentiation				
High	1	0		
High-Medium	6	0	0.9(0.2,52.9)	
Medium	60	2	5.3(0.1,76.4)	0.7464$^{\Delta}$
Medium-Low	81	1	15.9(0.2,49.6)	0.5028$^{\Delta}$
Low	137	1	5.2(0.2,78.4)	0.5525$^{\Delta}$
Clinical outcome				
Alive	133	1	9.1(0.2,92.4)	
Died	184	3	3.8(0.1,41.7)	0.1698
Disease Free	118	1	10.5(0.2,95.5)	
Metastasis	15	0	1.9(0.1,31.6)	0.4747$^{\#}$
Died of GC	184	3	3.8(0.1,41.7)	0.1236$^{\#}$

Notes : Cases: the total number of cases; N$^{\alpha}$: missing cases; median is the middle on from lowest value to highest value of WISP-2 mRNA expression; *:P<0.05, $^{\Delta}$: Compared with "High-medium", $^{\#}$: Compared with "Disease Free "

Table 3.3 Association of WISP-3 mRNA expression with clinic-pathological parameters in gastric cancer patients.

Clinicolpathological Parameters	WISP-3			
	Cases	**N$^{\alpha}$**	**Median (Q1,Q3)**	***P***
Tissue sample				
Normal	155	34	0(0,499)	
Tumour	227	97	0(0,257)	0.9076
Gender				
Male	159	72	0(0,327)	
Female	68	25	0(0,2241)	0.7591
Infiltration depth				
T1+T2	32	10	1(0,7706)	0.1337
T3+T4	191	83	0(0,281)	
Lymph node status				
N0	51	20	0(0,537)	
N1+2+3	173	74	0(0,363)	0.5634
M-staging				
M0	192	84	0(0,651)	
M1	29	12	0(0,0)	0.103
TNM staging				
TNM1+2	62	23	1(0,9690)	
TNM3+4	161	69	0(0,79)	0.136
Differentiation				
High	1	0		
High-Medium	4	2	0(0,37978)	
Medium	40	22	0(0,407)	0.7907$^{\Delta}$
Medium-Low	59	23	0(0,4211)	0.9663$^{\Delta}$
Low	100	38	0(0,427)	0.8724$^{\Delta}$
Clinical outcome				
Alive	93	41	0(0,1074)	0.2984
Died	132	55	0(0,231)	
Disease Free	82	37	0(0,1985)	
Metastasis	11	4	0(0,5)	0.8724$^{\#}$
Died of GC	132	55	0(0,231)	0.2548$^{\#}$

Notes : Cases: the total number of cases; N$^{\alpha}$: missing cases; median is the middle on from lowest value to highest value of WISP-3 mRNA expression; *:P<0.05, $^{\Delta}$: Compared with "High-medium", $^{\#}$: Compared with "Disease Free "

3.3.3 Immunohistochemistry staining analysis of WISPs on pathological slides

Table 3.4~3.6 showed expression levels of WISP-1, WISP-2 and WISP-3 in gastric cancer tissues and normal gastric mucosas using IHC staining and Chi-square test to analyse the staining intensity.

IHC staining of WISP-1, WISP-2 and WISP-3 in corresponding gastric cancer pathological slides showed a much stronger staining intensity of WISP-2 in tumour tissues than in normal background, whereas, no statistically difference in WISP-1 and WISP-3 expression was seen in Figure 3.3 and 3.7. Expression of WISP-2 was found in a relatively higher level in well and medium differentiated tumours than in poor differentiated tumours (P=0.024). Survival analysis using Kaplan-Meier plot showed patients with a high expression of level of WISP-2 had higher overall survival compared with patients with a low expression of level of WISP-2 (Figure 3.6A). In regards to disease free survival, a poor survival rate was observed in the group with low expression levels of WISP-2 compared with the high expression levels (Figure 3.6B). However, the data of WISP-1 and WISP-3 did not demonstrated statistical significance respectively in figure 3.4 and 3.8 (P> 0.05).

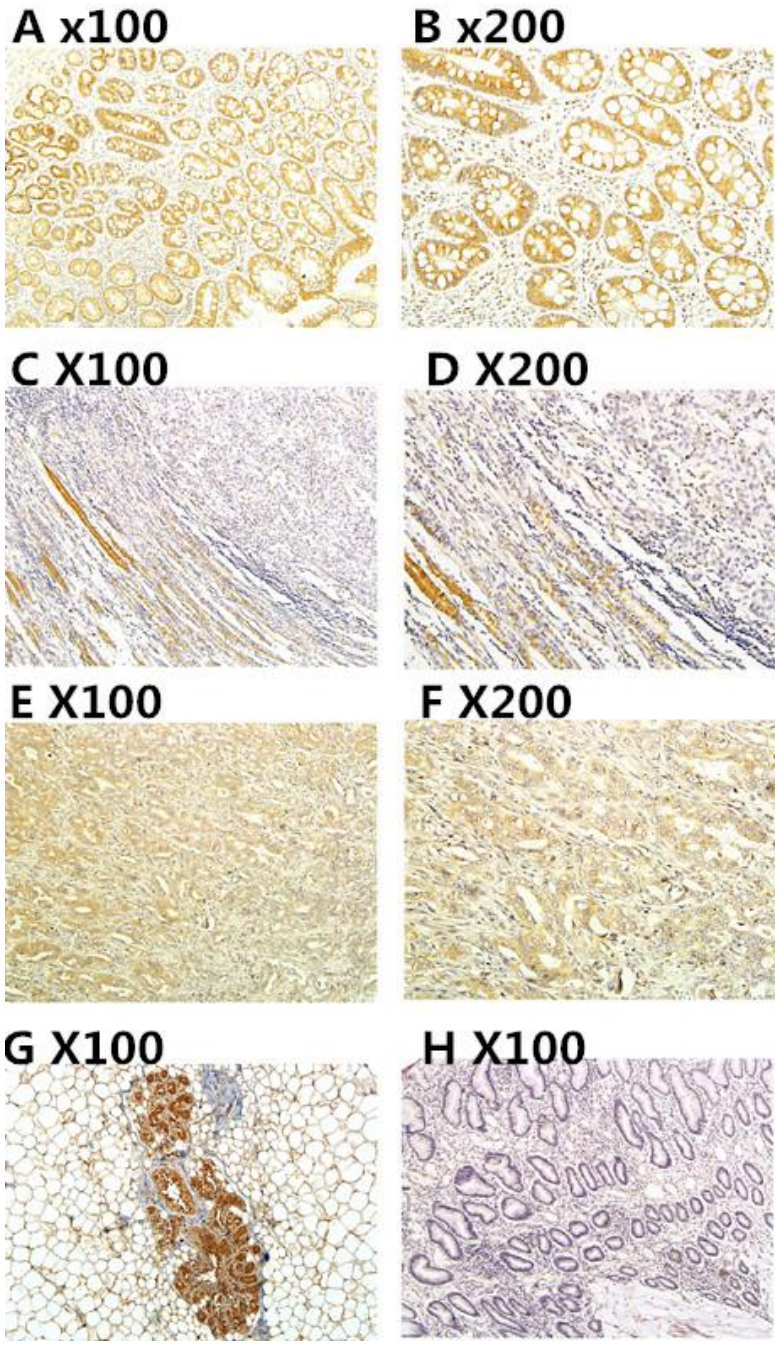

Figure 3.3 Protein expression of WISP-1 in gastric cancer and normal gastric mucosa. Figure A and B, representative images of WISP-1 staining in normal gastric mucosa (A and B represent the same image of 100×and 200×, respectively). Figure C and D, representative images of WISP-1 staining in diffuse gastric cancer and adenocarcinoma (Figure E and F). Figure G: positive control in breast epithelium, and H: negative control using PBS as primary antibody in normal gastric mucosa.

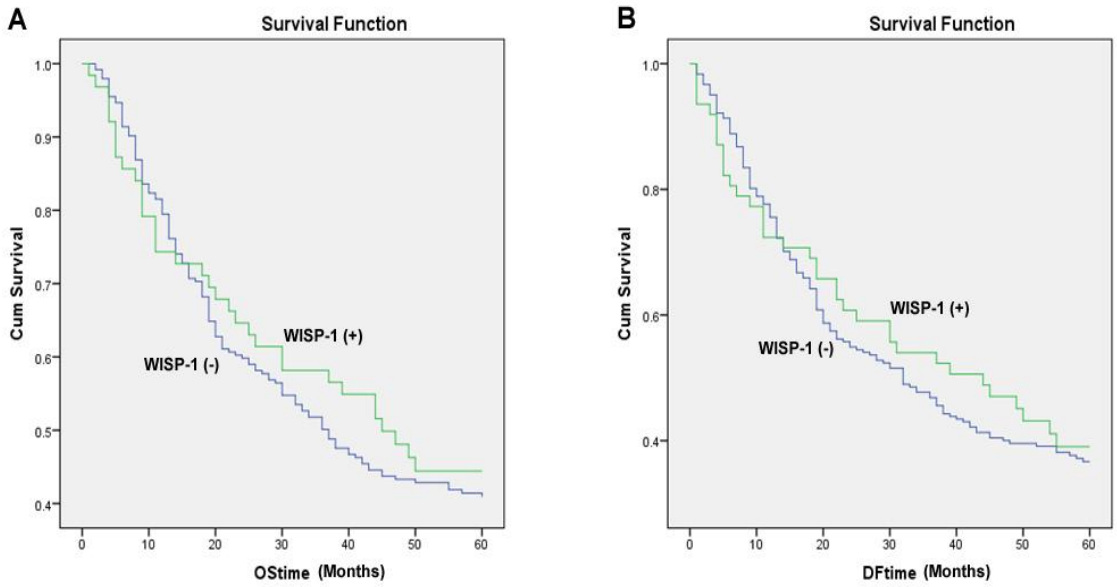

Figure 3.4 Survival analysis of WISP-1 expression in gastric cancer with Kaplain-Meier plots and analysed using log-rank statistics. A. The Kaplan-Meier survival model of correlation between WISP-1 protein levels and overall survival [(+) group: n= 120; (-) group: n=85, P= 0.573]. B. The Kaplan-Meier survival model of correlation between WISP-1 protein levels and disease-free survival. (+) represents for the high level of expression of WISP-1; (-) stands for the low level of expression of WISP-1 [(+) group: n= 136; (-) group: n=95, P= 0.628].

Table 3.4 Association of WISP-1 protein expression with clinico-pathological parameters in gastric cancer patients.

Variables	WISP-1 expression			
	Cases	**WISP-1- (*n*=123)**	**WISP-1+ (*n*=114)**	***P***
Gender				
Male	172	89	83	0.938
Female	65	34	31	
Age (y)				
<=60	114	60	54	0.686
>60	122	61	61	
Depth of Wall Invasion				
T1+T2	35	20	15	0.437
T3+T4	190	95	95	
Differentiation				
Well &Moderated	40	16	24	0.097
Poorly	146	80	66	
Lymph Node Metastasis				
negative	46	26	20	0.373
positive	173	85	88	
Liver metastasis				
M0	185	94	91	0.808
M1	35	17	18	
Vascular Invasion				
V(-)	126	69	57	0.348
V(+)	109	53	56	
TNM stages				
I+II	72	39	33	0.441
III+IV	144	70	74	

Notes: Cases: the total number of cases; *:P< 0.05.

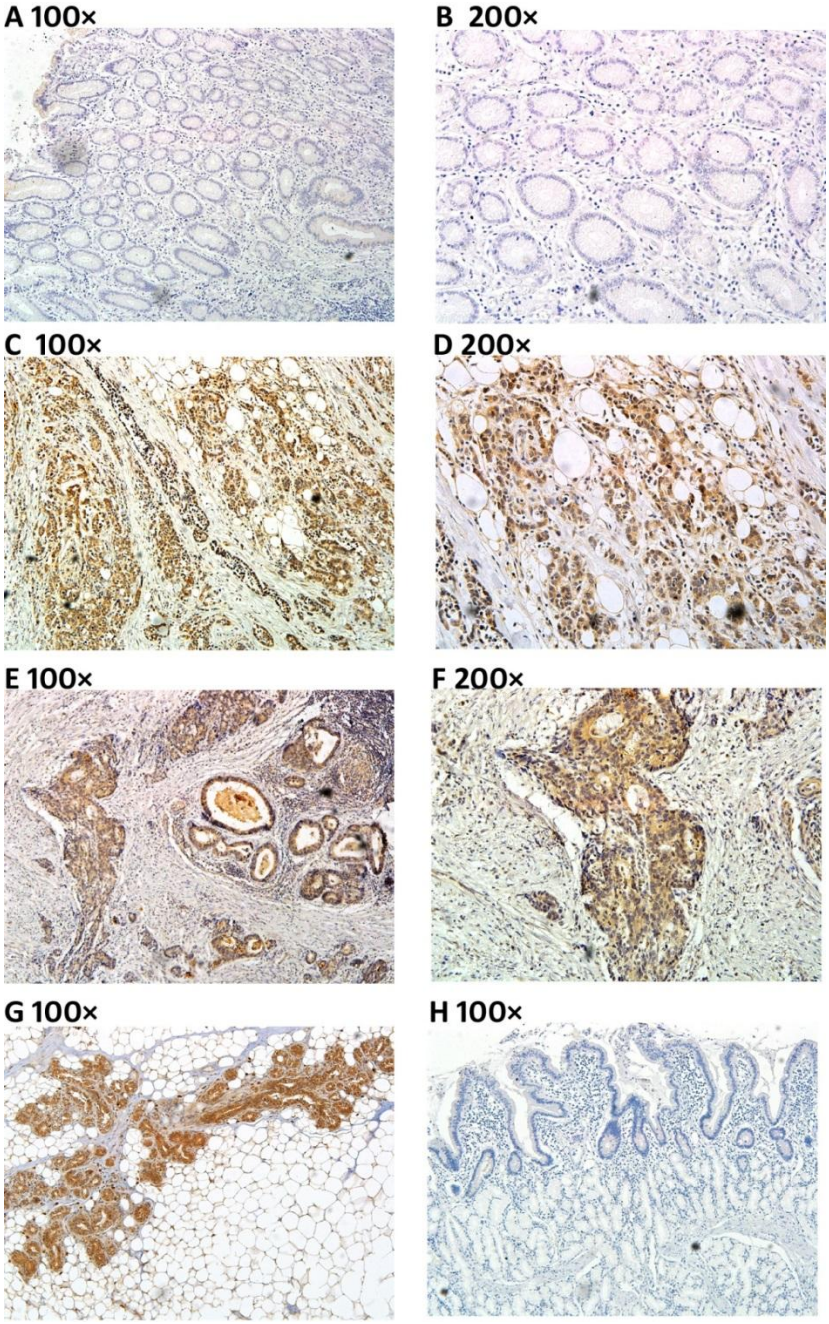

Figure 3.5 Expression of WISP-2 in gastric cancer and normal gastric mucosa.
In gastric cancer, WISP-2 protein was immunoreactive in the cytoplasm of malignant cells. The intensity of WISP-2 immunoreactivity was remarkably higher in primary gastric carcinoma when compared with matched normal mucosa. Figure A and B, representative images of WISP-2 staining in normal gastric mucosa showed absent or weak cytoplasmic reactivity (A and B represent the same image of 100 ×and 200 ×, respectively). Figure C and D, representative images of WISP-2 staining in diffuse gastric cancer and adenocarcinoma (Figure E and F). Figure G: positive control in breast epithelium, and H: negative control using PBS as primary antibody in normal gastric mucosa.

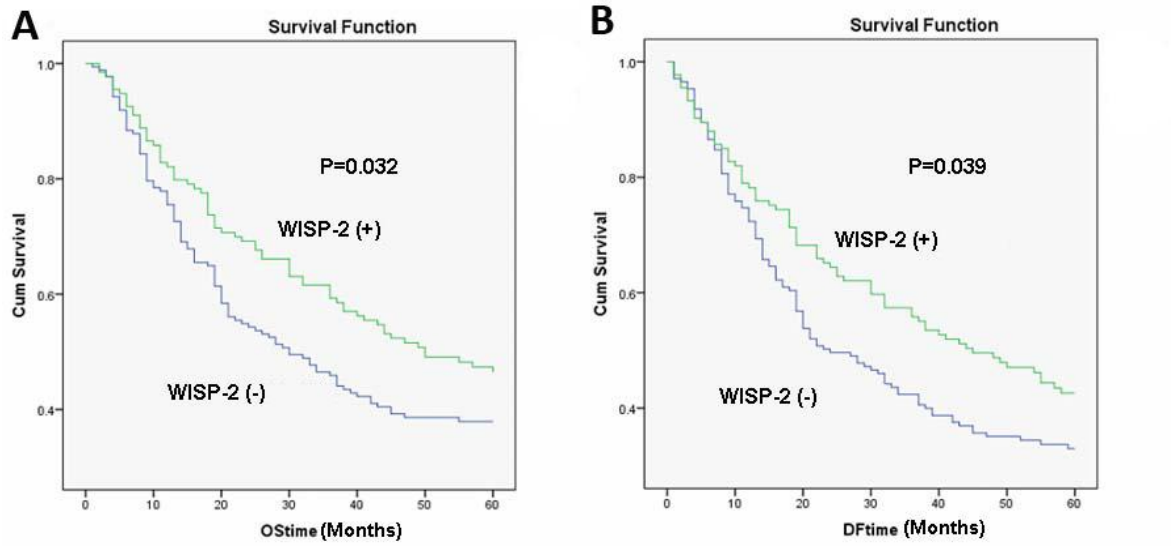

Figure 3.6 Survival analysis of WISP-2 expression in gastric cancer with Kaplain-Meier plots and analysed using log-rank statistics. A. The Kaplan-Meier survival model of correlation between WISP-2 protein levels and overall survival [(+) group: n= 127; (-) group: n=120, P= 0.032]. B. The Kaplan-Meier survival model of correlation between WISP-2 protein levels and disease-free survival. (+) represents for the high level of expression of WISP-2; (-) stands for the low level of expression of WISP-2 [(+) group: n= 89; (-) group: n=105, P=0.039].

Table 3.5 Association of WISP-2 protein expression with clinic-pathological parameters in gastric cancer patients.

Variables	Cases	WISP-2 expression		*P*
		WISP-2- (*n*=128)	WISP-2+ (*n*=101)	
Gender				
Male	161	87	74	
Female	68	41	27	0.384
Age (y)				
<=60	114	67	47	
>60	113	59	54	0.32
Depth of Wall Invasion				
T1+T2	35	20	15	
T3+T4	182	102	80	0.904
Differentiation				
Well &Moderated	37	14	23	
Poorly	140	82	58	0.024*
Lymph Node Metastasis				
negative	47	30	17	
positive	164	88	76	0.216
Liver metastasis				
M0	179	97	82	
M1	33	22	11	0.184
Vascular Invasion				
V(-)	121	75	46	
V(+)	106	53	53	0.069
TNM stages				
I+II	72	43	29	
III+IV	137	74	63	0.43

Notes: Cases: the total number of cases;*:P< 0.05.

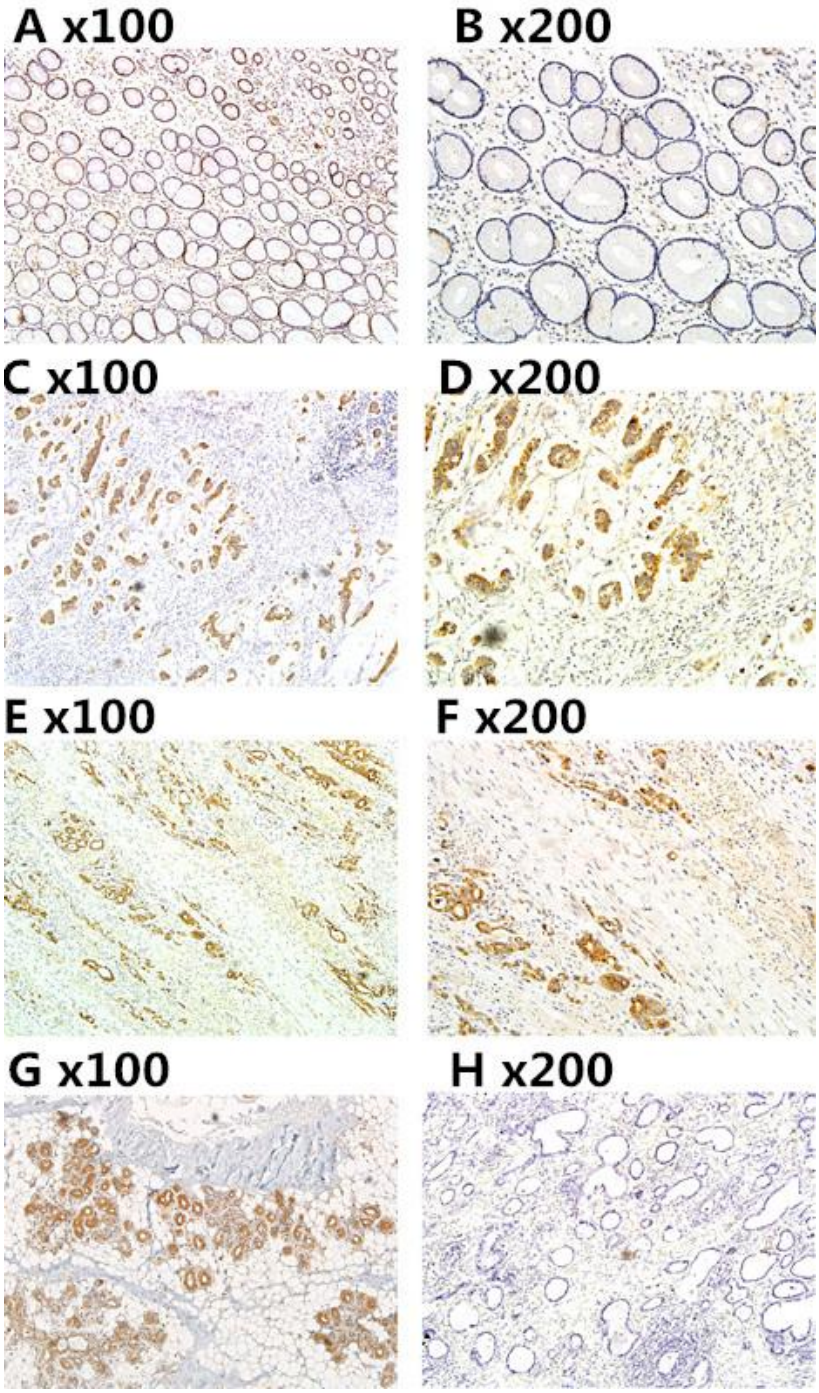

Figure 3.7 Expression of WISP-3 in gastric cancer and normal gastric mucosa. Figure A and B, representative images of WISP-3 staining in normal gastric mucosa (A and B represent the same image of 100 ×and 200 ×, respectively). Figure C and D, representative images of WISP-3 staining in diffuse gastric cancer and adenocarcinoma (Figure E and F). Figure G: positive control in breast epithelium, and H: negative control using PBS as primary antibody in normal gastric mucosa.

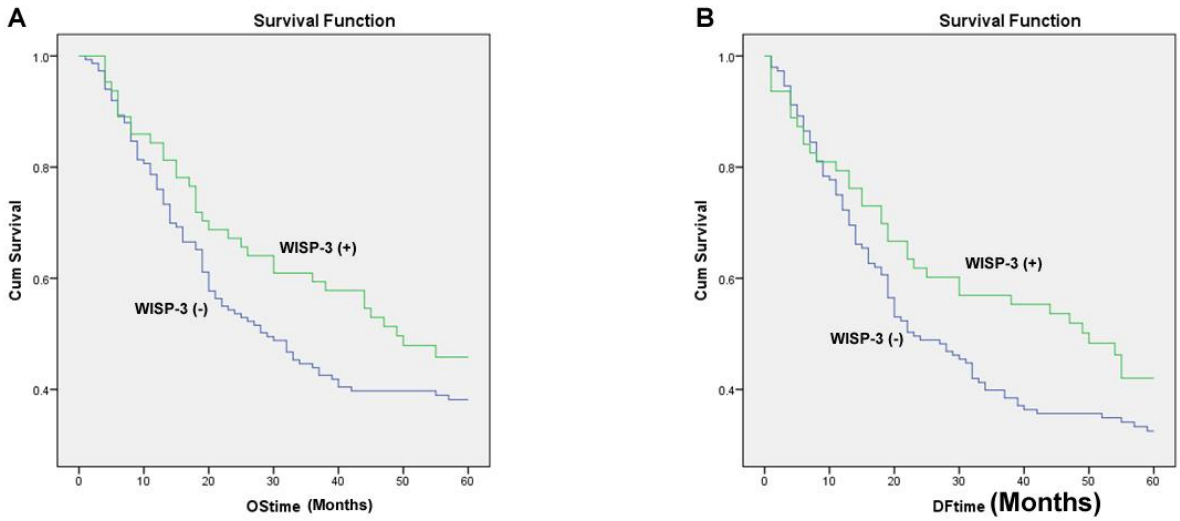

Figure 3.8 Survival analysis of WISP-3 expression in gastric cancer with Kaplain-Meier plots and analysed using log-rank statistics. A. The Kaplan-Meier survival model of correlation between WISP-3 protein levels and overall survival [(+) group: n= 87; (-) group: n=103, P= 0.491]. B. The Kaplan-Meier survival model of correlation between WISP-3 protein levels and disease-free survival. (+) represents for the high level of expression of WISP-3; (-) stands for the low level of expression of WISP-3 [(+) group: n= 94; (-) group: n=81, P= 0.527].

Table 3.6 Association of WISP-3 protein expression with clinicopathological parameters in gastric cancer patients.

Variables	Cases	WISP-3 expression		*P*
		WISP-3- (*n*=56)	WISP-3+ (*n*=185)	
Gender				
Male	174	39	135	
Female	67	17	50	0.626
Age (y)				
<=60	117	31	86	
>60	123	24	99	0.198
Depth of Wall Invasion				
T1+T2	38	7	31	
T3+T4	192	45	147	0.499
Differentiation				
Well &Moderated	41	8	33	
Poorly	147	35	112	0.562
Lymph Node Metastasis				
negative	45	31	14	
positive	121	65	56	0.307
Liver metastasis				
M0	190	41	149	
M1	36	10	26	0.415
Vascular Invasion				
V(-)	126	31	95	
V(+)	113	25	88	0.651
TNM stages				
I+II	78	17	61	
III+IV	146	34	112	0.8

Notes: Cases: the total number of cases; *:P<0.05.

3.3.4 WISP-2 expression in gastric cancer cells

Due to the high expression of WISP-2 in gastric cancer tissues both in mRNA and protein levels, we planned to regulate genetic expression and investigate the subsequent events. The first step was to select cell lines for further targeting. The expression of WISP-2 was examined in AGS and HGC27 cell lines, and both showed a strong expression using PCR for 30 cycles (See Figure 3.9).

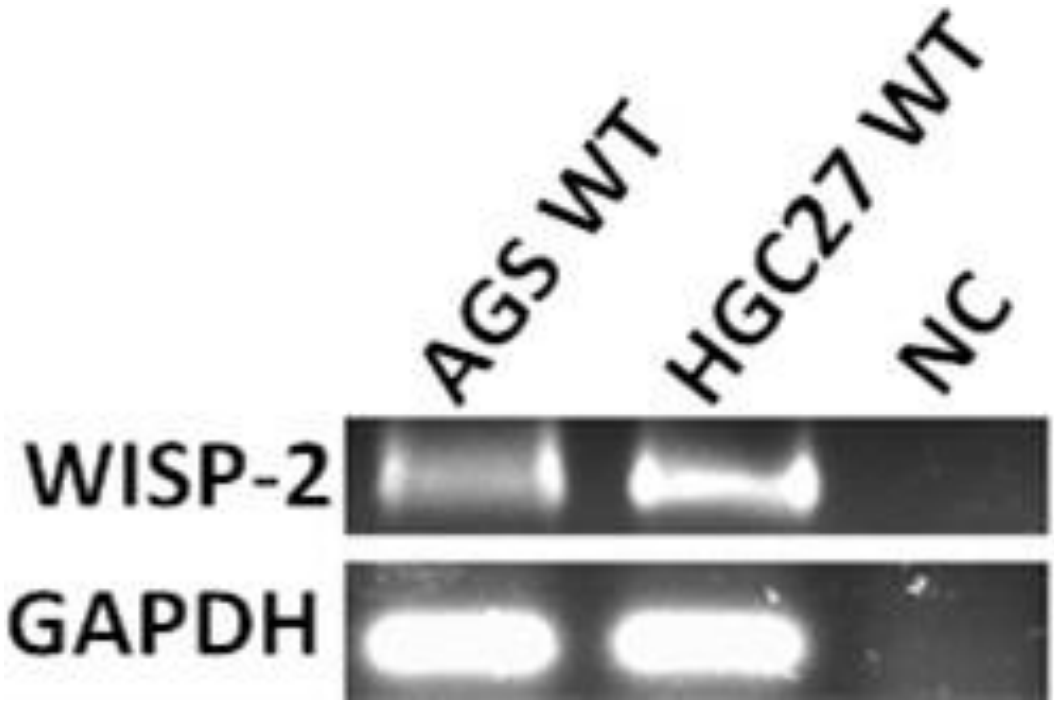

Figure 3.9 Cell lines screening for WISP-2 mRNA expression. Two gastric cancer cell lines were screened for mRNA expression of WISP-2 using conventional RT-PCR techniques. Both showed high levels of WISP-2 transcripts after 30 cycles of PCR reaction. GAPDH was used as an internal control. AGS WT: AGS wild type cell; HGC27 WT: HGC27 wild type cell; NC: negative control.

3.4 Discussion

Q-PCR analysis showed that there was a significant difference in WISP-2 expression between normal gastric tissue and tumours, however this pattern was not one seen with WISP-1 or WISP-3 expression. Using Kaplan-Merier plot and log rank test, WISP-2 was found to be positively related with overall survival and disease free survival of gastric cancer patients. Expression of WISP proteins were analysed using immunohistochemical method for whichall three proteins were found to be located in the cytoplasmic region. Representative images showed that WISP-2 protein staining in normal gastric tissues was largely negative. In a clear contrast and supporting the Q-PCR data, the staining in gastric tumour tissues was highly positive and cytoplasmic. In addition, higher levels of WISP-2 staining was seen in well and medium differentiated tumours than in poor differentiated tumours (P=0.024). Semi-quantitative analysis has shown that also in line with Q-PCR findings, no differences were seen with WISP-1 and WISP-3.

WISP family members have been shown to play multiple roles in a number of patho-physiological processes, including cell proliferation, adhesion, invasiveness, wound healing, ECM regulation, and EMT. Previous studies have shown that WISP family members were de-regulated and related with cancer metastasis in plenty of clinical cohort studies [221, 222, 238, 269]. From the publised studies of our group, WISP-1 appeared to act as a factor stimulating aggressiveness and WISP-2 as a tumour suppressor in colorectal cancer , while in breast cancer, the role of WISP-1 and WISP-2 were the other way around. WISP-3 has no determined role in both colorectal and breast cancers [211, 212]. Of the most studied molecules, WISP-2 exhibits divergent roles in a tissue-specific manner and is constitutively expressed in less aggressive human breast cancer cells (i.e. MCF-7 and ZR-75-1), whereas its expression is

minimally detected in moderately aggressive breast cancer cell lines (i.e. SKBR-3), and it is undetected in the highly aggressive breast cancer cell line (i.e. MDA-MB-231) [213, 215]. This screening process also helped determine which molecules and cell lines should be used for the reminder of this study. As previously mentioned, WISP-2 exhibited divergent roles in a tissue-specific manner , we should clarify by which manner WISP-2 exerts its cell functions on gastric cancer cells. The two gastric cell lines, which have different race origin, have similar mRNA expression levels and therefore we chose both for transfection with WISP-2 ribozyme transgenes in order to determine the consequences of WISP-2 knockdown on *in vitro* cellular functions. The findings of the functional based studies are presented in the next chapter.

Chapter 4

Knockdown of WISP-2 and the effect on the functions of gastric cancer cells

4.1 Introduction

WISP-2 is a secreted matricellular protein, which is a subset of the ECM modulating cellular responses. Matricellular proteins have been classified as a family of non-structural matrix proteins capable of modulating a variety of biological processes within the ECM. These proteins are expressed dynamically and their cellular functions are highly dependent upon cues from the local environment. The most important functional changes may be in cell growth, adhesion, invasion and migration. Some genes have important roles on these processes. *In vitro* and *in vivo* studies indicated potential roles for WISP-2 in regulating cell proliferation, motility, invasiveness and adhesion. Overexpression of WISP-2 has been shown to inhibit serum-induced proliferation of the highly invasive, oestrogen receptor negative breast cancer cell line, MDA-MB-231 [245]. However, in the poorly invasive oestrogen receptor positive MCF-7 cell line, the effect of WISP-2 is not consistent. Some have suggested an inhibitory role in serum-induced proliferation of MCF-7 cells [245]. Others have suggested a promoting role in MCF-7 cell proliferation [221] or no effect [218]. Moreover, the ability of PMA, EGF or IGF-1 alone to induce MCF-7 cell proliferation was blocked by WISP-2 knockdown [213, 215, 217], and knockdown of WISP-2 in MCF-7 cells was found to eliminate the oestrogen dependent growth requirement of these cells. Overexpression of WISP-2 inhibited both motility and invasiveness in highly aggressive breast carcinoma cell line, MDA-MB-231 [245]. The inhibitory effect of WISP-2 on motility was also observed in MCF-7 cells where knockdown of WISP-2 expression increased the IGF-1-induced motility of MCF-7 cells. WISP-2 knockdown in MCF-7 cells also induced expression of pro-motility enzymes such as MMP-2 and MMP-9 [218, 245]. Mutant p53 overexpression induced MCF-7 exhibiting increased invasiveness expression was inhibited by treatment with recombinant WISP-2 protein [250]. Little is known about the role WISP-2 plays in cell adhesion. Kumar *et al.*, observed that three different osteoblastic cell lines:- primary human osteoblasts, osteosarcoma MG63, and rat osteoblast-like osteosarcoma

Ros 17/2.8- attached to immobilized CCN5 in a dose dependent manner [198]. More studies are needed to find out if it is the differences in the cell types tested or the different assays accounts for the conflicting role reported of WISP-2 in cancers.

In this chapter, WISP-2 was knocked down in AGS and HGC27 cells using a ribozyme transgene and the effect on cellular functions was subsequently investigated.

4.2 Materials and methods

4.2.1 Cell lines

AGS and HGC27 gastric cancer cell lines were used in this chapter, including empty plasmid control and transfected sublines. Cells were continuously maintained in normal DMEM media with 10% FBS and antibiotics. For ribozymes selection, cells were maintained in normal media supplemented with 5～7.5 μg/ml blasticidin (5μg/ml for HGC27 and 7.5μg/ml for AGS selection). The stable transfected cells were maintained in normal media supplemented with 0.5 μg/ml blasticidin.

4.2.2 Generation of WISP-2 ribozyme transgenes

Hammerhead ribozymes targeting WISP-2 were designed using Zuker's mRNA Fold programme [259], based on the predicted secondary structure of WISP-2 mRNA. Primers containing restriction sites were then generated (Table 2.3). The ribozymes were then synthesised using a touch-down PCR procedure with the following conditions: 94˚C for 5 minutes, followed by 8 cycles at each annealing temperature (total of 48 cycles): 94˚C for 10 seconds, 70˚C, 65˚C, 60˚C, 57˚C, 55˚C, and 50˚C for 15 seconds, 72˚C for 20 seconds and a

final extension of 7 minutes at 72˚C. Subsequently, the transgenes were run on a 2% agarose gel in order to verify their presence as well as size, before being cloned into a pEF6/V5-His-TOPO plasmid vector.

4.2.3 TOPO TA cloning of WISP-2 fragments or transgenes into pEF6/V5-His-TOPO plasmid vector

Following verification, the WISP-2 transgenes were cloned into a pEF6/V5-His-TOPO plasmid (Invitrogen Inc., Paisley, UK), followed by transformation of constructed plasmid into *E.Coli*. The correct constructs were then amplified and purified using the Sigma GenElute Plasmid MiniPrep Kit (Sigma-Aldrich, USA). We also used a plasmid in which the ribozyme transgene was inserted in the wrong direction (namely sense direction) and a control. Multiple clones were combined and grown as a new population of sublines. RT-PCR and Q-RT-PCR and Western blotting were used to verify the efficiency of knock down in the new sublines.

4.2.4 Gastric cancer cell transfection and generation of stable transfectants

Following plasmid verification using DNA electrophoresis, the plasmids were transfected into target cells using electroporation at 290V. The transfectants were then selected with 5μg/ml blasticidin for a period of two to three weeks. Empty plasmid vectors were also used to transfect the same cells as a control for the following experiments. After the selection, the cells were verified for WISP-2 knockdown using RT-PCR, Q-PCR, and western blotting. Full details of the cloning process have been given in section 2.7.

4.2.5 RNA isolation, cDNA synthesis, RT-PCR, and Q-RT-PCR

RNA was isolated from the cells using the Tri Reagent kit (Sigma-Aldrich, Inc., Poole, Dorset, England, UK) and converted into cDNA by reverse transcription using the iScript™ cDNA Synthesis Kit (Bio-Rad Laboratories, California, USA), as described in section 2.4. RT-PCR was carried out with the following conditions: 94 ˚C for 5 minutes, followed by 28 to 35 cycles of 94 ˚C for 30 seconds, 55 ˚C for 30 seconds, and 72 ˚C for 30 seconds, and a final extension of 7 minutes at 72 ˚C. The products were run on an agarose gel and visualised using sybrgreen. Q-RT-PCR was performed following the conditions: 94˚C for 5 minutes, followed by 90 cycles of 94˚C for 10 seconds, 55˚C for 15 seconds, and 72˚C for 20 seconds.

4.2.6 Protein extraction, SDS-PAGE, and Western blot analysis

Protein was extracted and then quantified using the DC Protein Assay kit (BIO-RAD, USA). After SDS-PAGE, proteins were transferred onto nitrocellulose membranes which were then blocked and probed with specific primary (anti-WISP-2 1:200) and the corresponding peroxidise-conjugated secondary antibodies (1:1000). All of the antibodies used in this study are listed in Table 2.4. The protein bands were eventually visualised using the chemiluminescence detection kit (Luminata, Millipore).

4.2.7 *In vitro* cell growth assay

Cells were seeded into three 96 well plates, and incubated for 1, 3 and 5 days respectively, as described in section 2.7.1. Following incubation, the cells were fixed with 4% formalin and stained with crystal violet before the absorbance was measured.

4.2.8 *In vitro* cell Matrigel adhesion assay

The cells were seeded into a 96 well plate coated with Matrigel as described in section 2.7.2. The cells were left to adhere for a period of 40 minutes, and then fixed and stained with crystal violet. Photos were taken using a microscope with camera.

4.2.9 *In vitro* cell motility assay

The protocol followed is described by Jiang [270]. Cells are seeded into a 24-well plate and cells were treated with a protein of interest in serum free media if required. These plates were then left to incubate at 37˚C, with 5% CO2, for a period of 24 hours to allow cells to form a confluent monolayer then the cells were wounded with a sterile tip and photos were taken using EVOS system at 0.25, 1, 2, 3 and 4 hours after wounding. Migration distances were measured using Image J software (National Institutes of Health, USA).

4.2.10 *In vitro* cell Matrigel invasion assay

The cells were seeded into transwell inserts with 8μm pores coated with 50μg Matrigel in a 24-well plate and were incubated for a period of 3 days. Following incubation, the cells which had migrated through the Matrigel to the other side of the insert were fixed in 4% formalin, stained with crystal violet and counted.

4.2.11 The effects of different small inhibitors on the cell motility

Using 96W1E+ array, cell adhesion and wounding assay were also conducted with ECIS instrument. Cells were seeded into each ECIS plate well as described in section 2.7.5, and treated with a protein of interest. In this study, we treated the cells respectively with different concentrations of PLC-γ inhibitor U73122, FAK inhibitor PF573228, JNK inhibitor SP100625

and N-WASP inhibitor Wiskostatin, respectively. Inhibitors were first dissolved in DMSO to 1mM and then diluted with serum free medium to different concentrations (0.4μM, 0.75μM, 1μM, 1.5μM, 3μM). For the control group, identical volume of serum free medium was added into wells. Cell adhesiveness was assessed within the first 40 minutes and electric wound was set at the 14th hour when the resistance reached maximum levels and migration data could be gathered for a further continuous 6 hours.

4.2.12 Electric Cell-Substrate Impedance Sensing

ECIS (Electric Cell-Substrate Impedance Sensing) is a novel method used as an alternative to the conventional function assays. It works with an array of 96 wells, each containing a gold electrode. These measure the current and voltage across this electrode, calculating the impedance and resistance. From the impedance changes, effects on cell attachment and motility can be examined [262]. Using 96W1E+ array, cell adhesion and wounding assay were also conducted with ECIS instrument. 40,000 cells diluted in 200μl DMEM were seeded into each ECIS plate well, and treated with a protein of interest.

4.3 Results

4.3.1 Generation of a WISP-2 ribozyme transgene

In order to knockdown the expression of WISP-2 in gastric cancer cells, two ribozyme transgenes targeting WISP-2 were generated based on the secondary structure of human WISP-2 mRNA (Figure 2.6) and cloned into a pEF6/His plasmid vector. It depicts the series of PCR reactions carried out to construct a plasmid containing a WISP-2 ribozyme transgene in Chapter

3. Based on the secondary structure of WISP-2, an appropriate targeting site for the ribozyme was first ascertained.

This was followed by ribozyme synthesis through touchdown PCR, and cloning into a pEF6/His plasmid. In order to verify correct orientation of the ribozyme transgenes, primers RbTPF and RbBMR were paired with T7F, respectively. These primers were specific to the ribozyme transgenes. If the transgene is correctly orientated, a PCR product of around 140bp (T7F promoter starts 90bp before insert and ribozyme sequence is around 50bp) should arise for the T7F+RbBMR reaction. However, if it is incorrectly orientated, a product of a similar size should appear for the T7F+RbTPF reaction. Following colony analysis, all those found to be positive for the transgenes underwent further amplification and finally, plasmid extraction. Ribozyme 1 colony 5 and ribozyme 2 colony 3 were shown to have the highest levels of correctly orientated ribozyme transgene. The plasmids were then verified using DNA electrophoresis, in order to demonstrate successful isolation of correctly sized plasmids (Figure 4.1).

4.3.2 Verification of WISP-2 knockdown in AGS and HGC27 cells

To examine the function of WISP-2 on gastric cancer cells, we established WISP-2 knockdown cell lines (AGS WISP-2kd and HGC27 WISP-2kd) and control cell lines (AGS pEF and HGC27 pEF) from two gastric cancer cell lines. Q-PCR, RT-PCR and western blotting were carried out to ensure that the knockdown of WISP-2 was successful at both mRNA and protein levels in AGS and HGC27 cells (Figure 4.2-4.7). Figure 4.2 and 4.3 shows the WISP-2 mRNA transcript numbers of three repeats which were normalised against corresponding internal control (GAPDH) using quantitative real time PCR. WISP-2 expression was decreased in WISP-2 knockdown cells compared with empty plasmid pEF controls in AGS and HGC27 cell

lines. Figure 4.4 and 4.5 showed knockdown of WISP-2 in mRNA level using RT-PCR. Figure 4.6 and 4.7 showed WISP-2 protein bands using western blotting. WISP-2 expression was decreased in WISP-2 knockdown cells compared with pEF control.

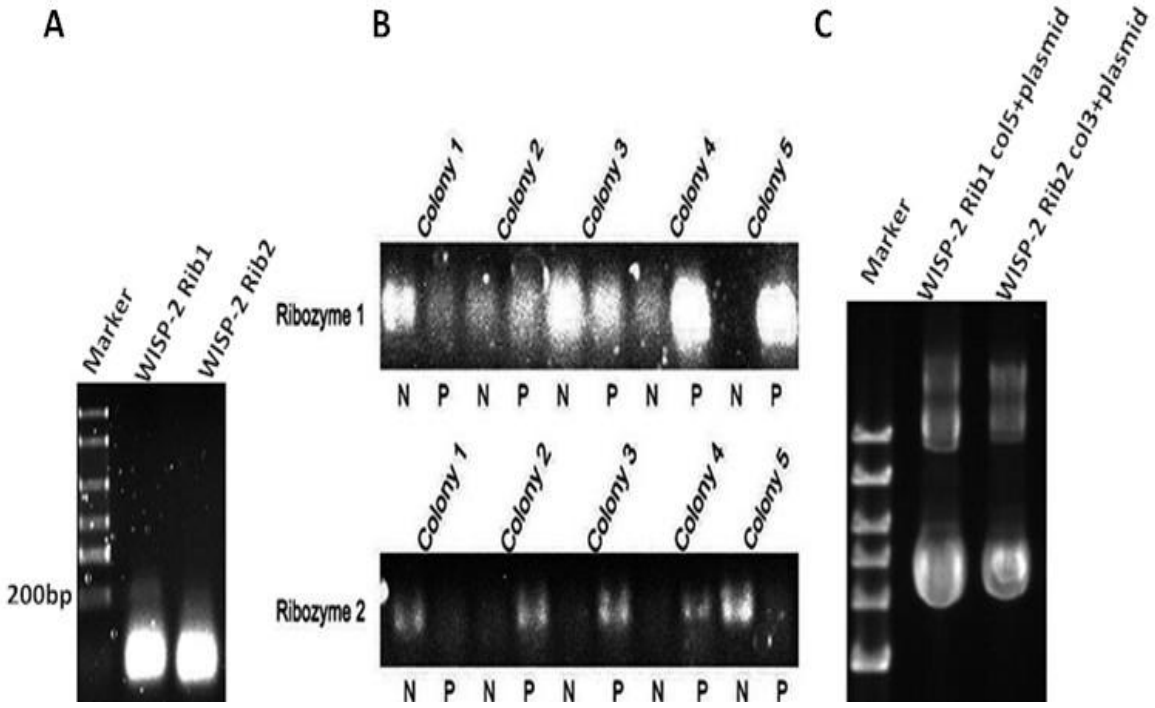

Figure 4.1 Ribozyme transgene synthesis. A. The ribozymes were generated using touchdown PCR and run on a 2% agarose gel. B. After transformation into *E.coli* cells, the colonies were analysed using PCR in order to verify correct orientation of the transgene. P stands for correct orientation (T7F promoter starts 90bp before insert and ribozyme sequence is around 50bp) arised from the T7F+ RbBMR reaction, and N stands for incorrect orientation of a similar size which arised from the T7F+RbTPF reaction. C. The plasmids were extracted from the correct colonies and verified with DNA electrophoresis.

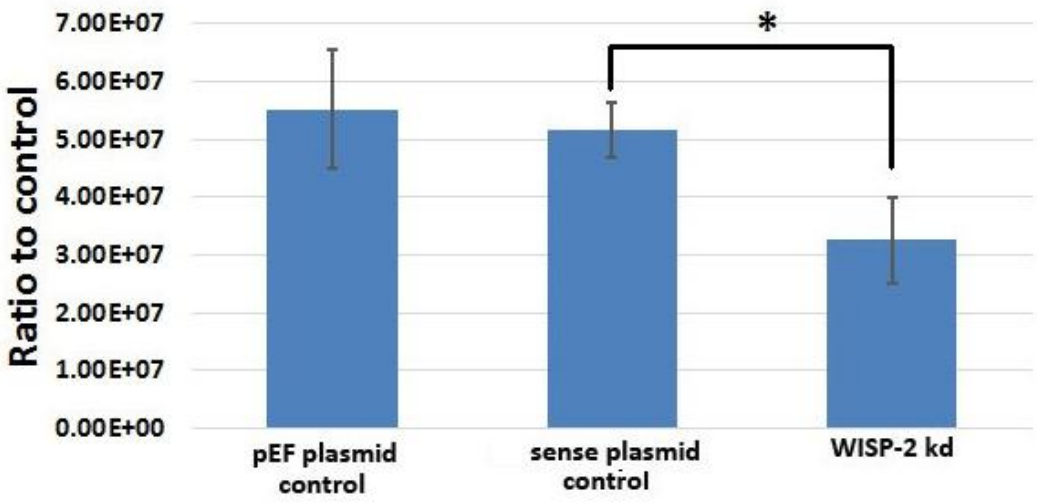

Figure 4.2 Verification of knockdown (kd) of WISP-2 in AGS cells. Quantitative real time PCR showing WISP-2 mRNA volume of three repeats which was normalised against corresponding internal control (GAPDH). WISP-2 expression was decreased in AGS WISP-2 kd compared with corresponding pEF plasmid control cells and anti-sense plasmid control cells (*: $P< 0.05$).

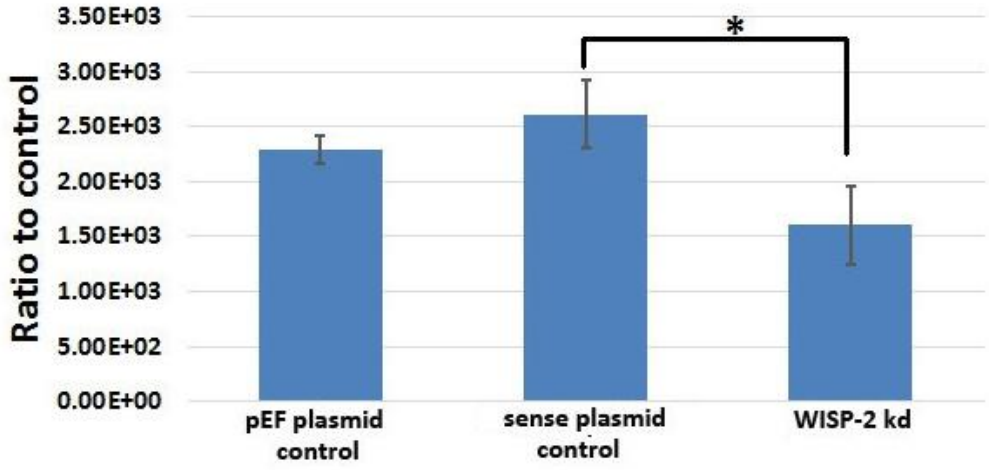

Figure 4.3 Verification of knockdown (kd) of WISP-2 in HGC27 cells. Quantitative real time PCR showing WISP-2 mRNA volume of three repeats which was normalised against corresponding internal control (GAPDH). WISP-2 expression was decreased in HGC27 WISP-2 kd compared with corresponding pEF plasmid control cells and anti-sense plasmid control cells. Asterisk represented $P< 0.005$.

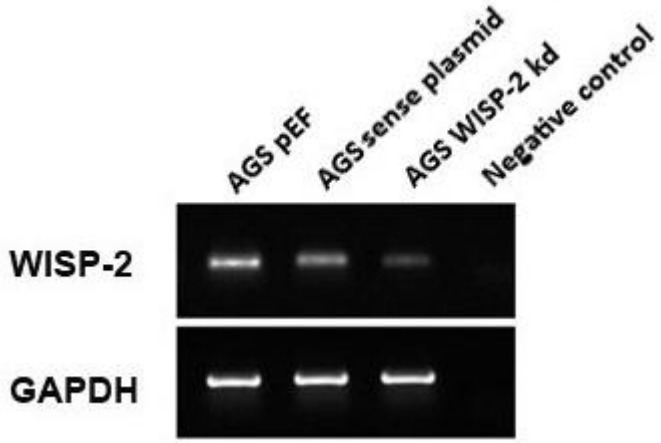

Figure 4.4 Verification of knockdown (kd) of WISP-2 in AGS cells. RT-PCR displayed reduced level of WISP-2 mRNA in AGS WISP-2 kd cells compared with control cells (AGS pEF and AGS sense plasmid cells).

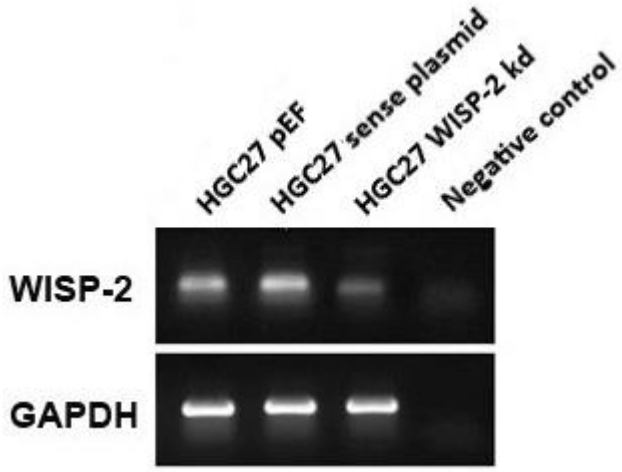

Figure 4.5 Verification of knockdown (kd) of WISP-2 in HGC27 cells. RT-PCR displayed reduced level of WISP-2 mRNA in HGC27 WISP-2 kd cells compared with control cells (HGC27 pEF and HGC27 sense plasmid cells).

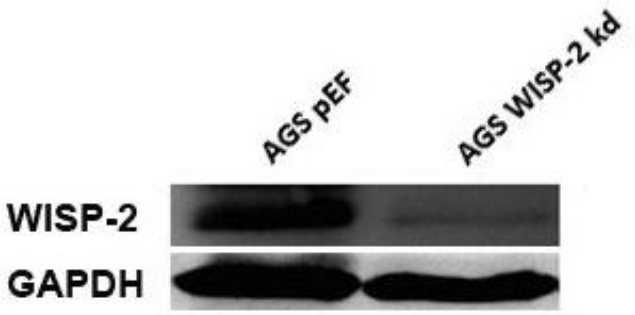

Figure 4.6 Confirmation of WISP-2 knockdown in AGS cells. WISP-2 protein bands volume was normalised against corresponding internal control (GAPDH). The expression of WISP-2 showed a significant decrease in AGS WISP-2 kd cells compared with AGS pEF cells.

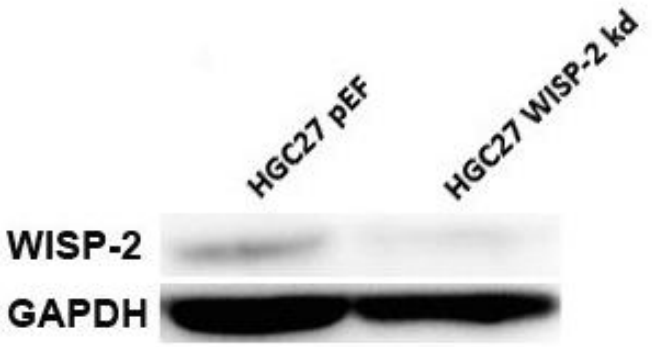

Figure 4.7 Confirmation of WISP-2 knockdown in HGC27 cells. WISP-2 protein bands volume was normalised against corresponding internal control (GAPDH). The expression of WISP-2 showed a significant decrease in HGC27 WISP-2 kd cells compared with HGC27 pEF cells

4.3.3 Effect of WISP-2 knockdown on the growth of gastric cancer cells

The cell lines displaying knockdown of WISP-2 were used in an *in vitro* cell growth assay along with the empty plasmid controls. There was a significant increase in the growth of the AGS WISP-2kd cells (Figure 4.8). The growth rate increased significantly in the $AGS^{WISP\text{-}2kd}$ cells (23.961 ± 4.11, $p<0.001$) compared with the control AGS pEF (13.199 ± 5.63). There was also a significant increase in the growth seen in the $HGC27^{WISP\text{-}2kd}$ cells (Figure 4.9). The growth rate increased significantly in the HGC27WISP-2-kd cells (27.635 ± 2.51, $p<0.001$) compared with the control $HGC27^{pEF}$ (15.939 ± 4.95).

4.3.4 Effect of WISP-2 knockdown on in vitro cell-matrix adhesion

The AGS and HGC27 cells were further analysed for their adhesive capacity using an *in vitro* Matrigel adhesion assay and ECIS assay. The cells with WISP-2 knockdown displayed no significant difference in adhesive capability compared with its controls in both AGS and HGC27 cells (Figures 4.10 and 11 respectively). Similarly, there was no significant difference in adhesion between WISP-2 knockdown cells and pEF cells in both AGS and HGC27 cells through the analysis of ECIS assay (Figure 4.12).

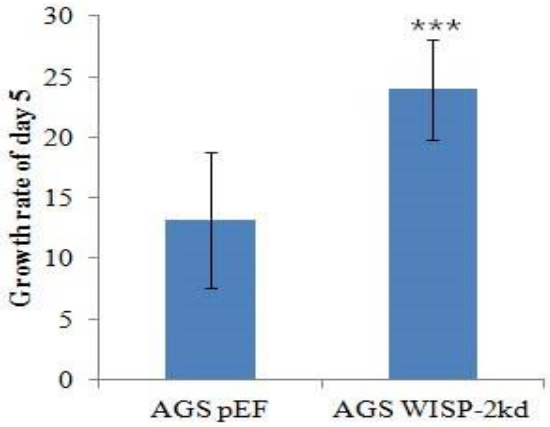

AGS pEF (mean±SD) n=6	AGS WISP-2kd (mean±SD) n=6
13.199±5.63	23.961±4.11

Figure 4.8 Knockdown of WISP-2 has a significant increase in the growth of the AGS WISP-2 knockdown cells. After 5 days' incubation, there was a significant increase in the AGS WISP-2kd cells (23.961±4.11) compared with the control AGS pEF cells (13.199+5.63) ($p<0.001$). Data shown is representative of at least 6 independent repeats. Error bars represent standard deviation. The data of day 1 time point was used as a baseline to normalise the data.

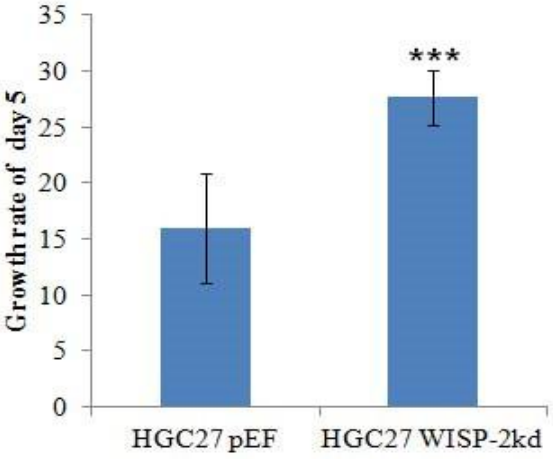

HGC27 pEF (mean±SD) n=6	HGC27 WISP-2kd (mean±SD) n=6
15.939±4.95	27.635±2.51

Figure 4.9 Knockdown of WISP-2 has a significant increase in the growth of the HGC27 WISP-2 knockdown cells. After 5 days' incubation, there was a significant increase in the HGC27 WISP-2kd cells (27.635±2.51) compared with the control HGC27 pEF cells (15.939±4.95) ($p<0.001$). Data shown is representative of at least 6 independent repeats. Error bars represent standard deviation. The data of day 1 time point was used as a baseline to normalise the data.

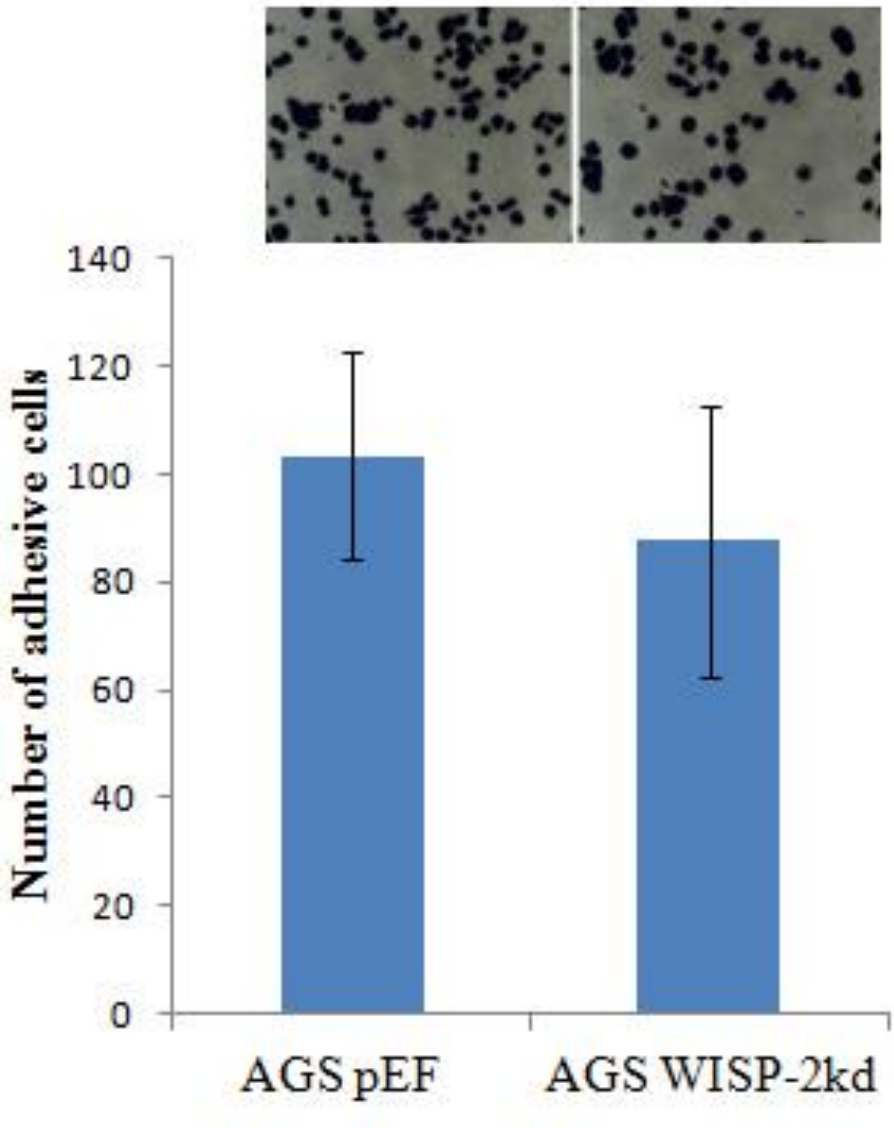

Figure 4.10 Representative images of adhered AGS cells. There was no significant effect in cell adhesion of AGS WISP-2kd cells compared with the control AGS^{pEF} (P> 0.05).

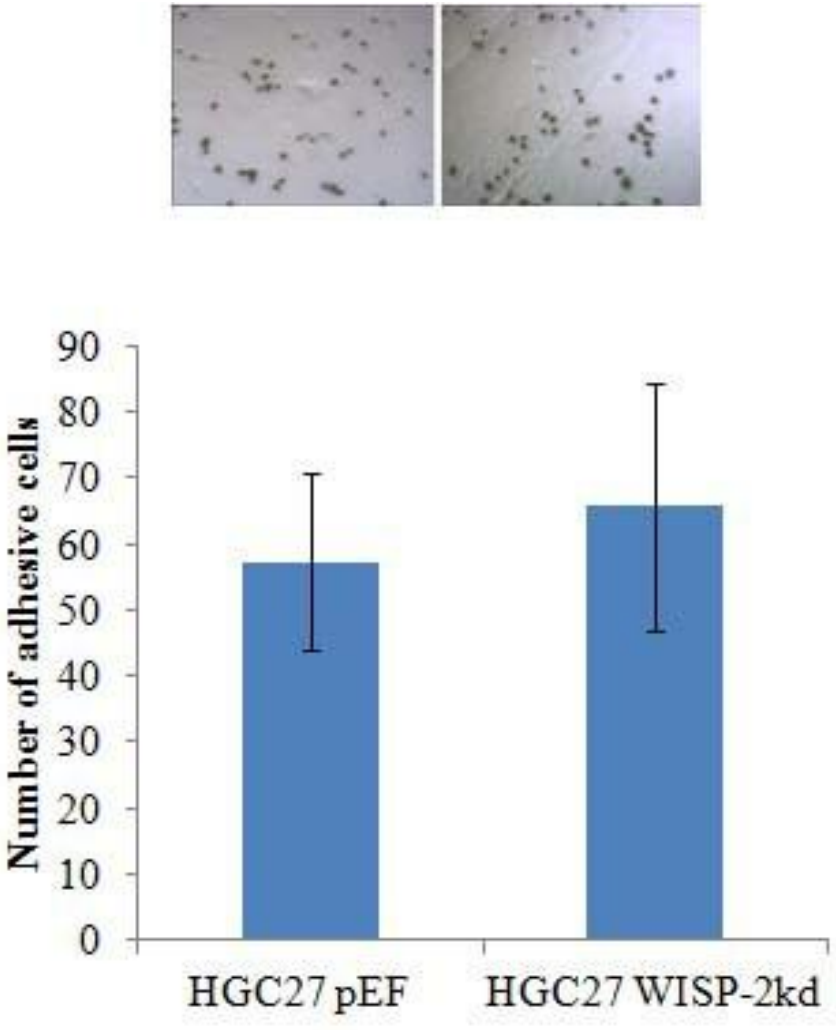

Figure 4.11 Representative images of adhered HGC27 cells. It demonstrated that there was not significant effect in cell adhesion with $HGC27^{WISP\text{-}2kd}$ cells compared with the control $HGC27^{pEF}$ ($p > 0.05$).

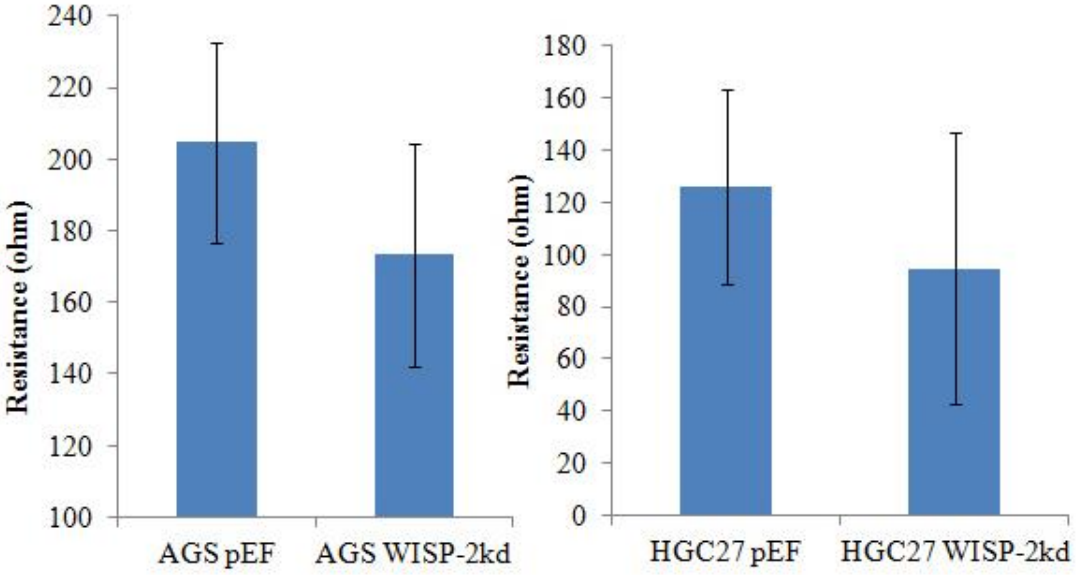

Figure 4.12 The effect of WISP-2 on cell adhesion of AGC and HGC27 cell lines through the analysis of ECIS assay. ECIS results also showed that there were no significant differences in adhesiveness in the first 45 minutes of knock down groups compared to the respective pEF controls in AGS and HGC27 cells (P> 0.05 respectively).

4.3.5 Effect of knockdown of WISP-2 in the cell motility

The cells were further analysed for their motility using scratch or wounding assay. The cells with knockdown of WISP-2 displayed a significant increase in motility compared with control cells. Figure 4.13 and 4.14 respectively show that there was a significant increase in cell motility of WISP-2 knockdown cells compared with pEF cells in both AGS and HCG27 cell lines ($p<0.05$).

4.3.6 Effect on invasion of AGS cells by WISP-2 knockdown

WISP-2 knockdown cells displayed a significant increase of invasion compared with the controls in both AGS and HGC27 cell lines. The number of invaded cells was 207.36 ±19.71 after WISP-2 knockdown compared with that of the control (133.58 ±18.8) in AGS cell lines (Figure 4.17). The number of invaded cells of HGC27 WISP-2 kd was 153.66 ±10.01 compared with that of HGC27 pEF cells (88.66 ±27.43) (Figure 4.18).

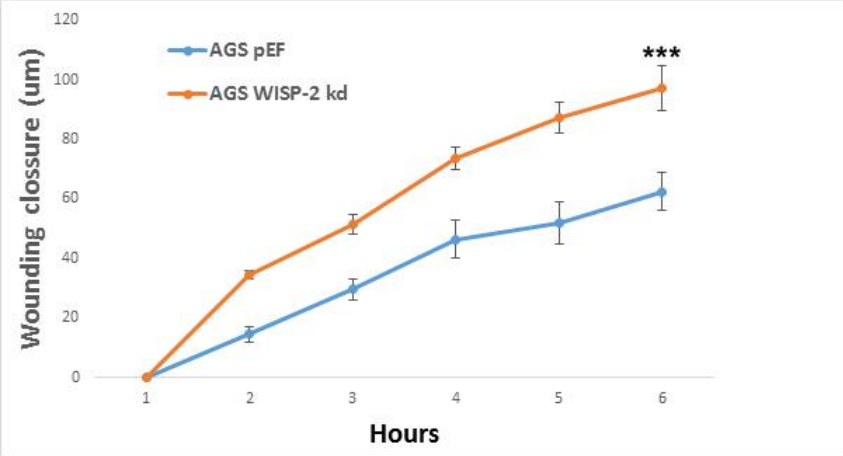

AGS pEF (mean ±SD) N=3	AGS WISP-2 kd (mean ±SD) N=3
62.5±7. 09	97.14±10. 11

Figure 4.13 Knockdown of WISP-2 had a discernible effect on the migration of AGS cells. After 1 hour the significant difference in cell motility of AGS WISP-2 knockdown was visualized compared with the control AGS pEF. Data shown is representative of 3 repeats of experiment. Error bars represent standard deviation. *** stand for $p < 0.001$, analysed by T-test (AGS WISP-2 kd vs AGS pEF : $p = 0.00063$).

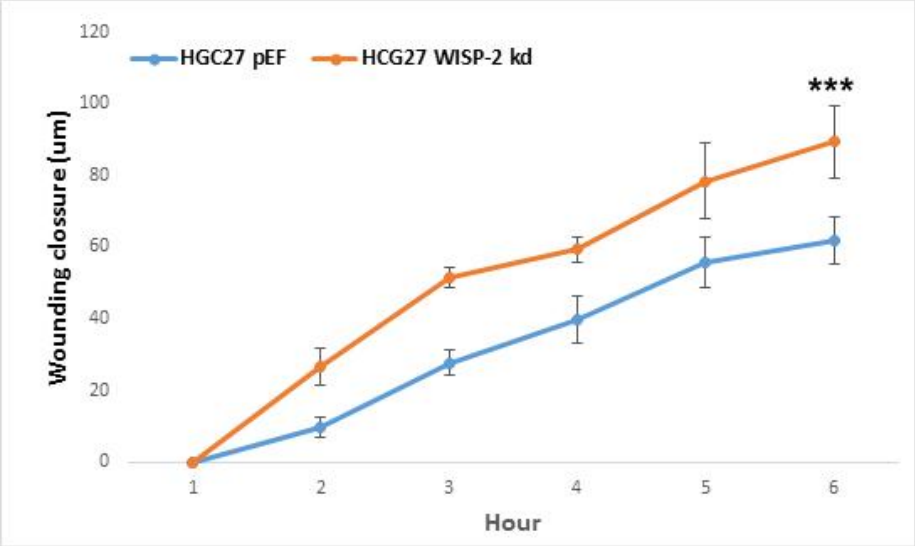

HGC27 pEF (mean ±SD) N=3	HGC27 WISP-2 kd (mean ±SD) N=3
61.7±6. 51	89.3±10. 62

Figure 4.14 Knockdown of WISP-2 had a marked influence on the migration of HGC27 cells. There was a consistent difference in cell motility of WISP-2 knockdown cells compared with pEF cells since 1st hour. Data shown is representative of 3 repeats of experiment. Error bars represent standard deviation. Three asterisks stand for $p < 0.001$ analysed by T-test (HGC27 WISP-2 kd vs HCG27 pEF : $p = 0.00089$).

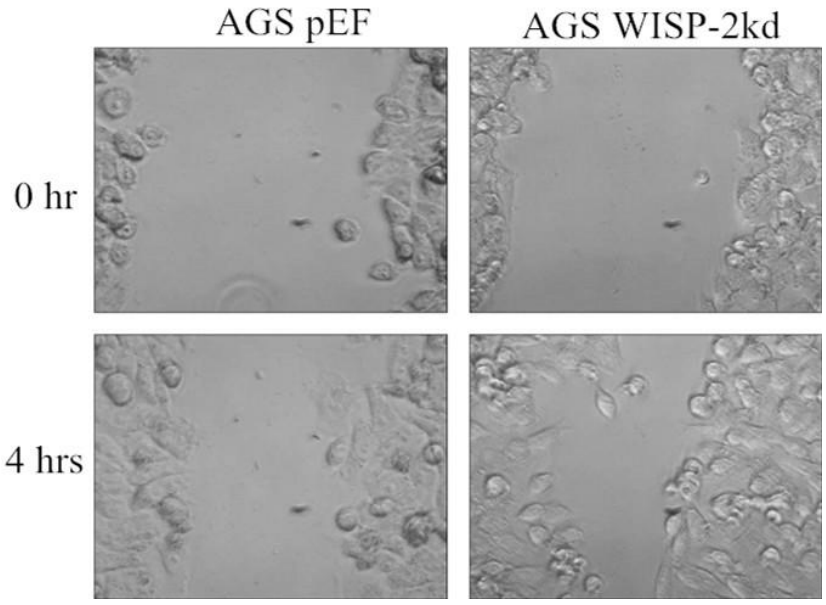

Figure 4.15 Four representative images of cell migration of AGS pEF and WISP-2 kd cells at 0 hour and 4th hour photoed by EVOS system.

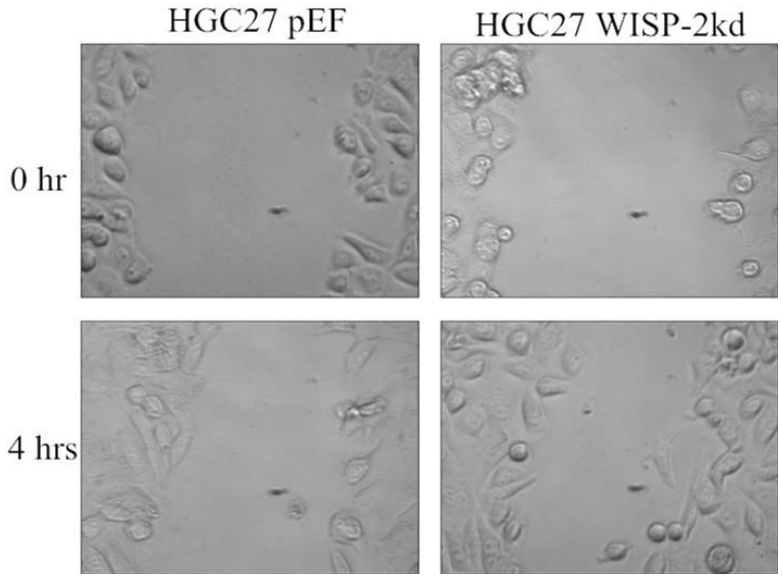

Figure 4.16 Four representative images of cell migration of HGC27 pEF and WISP-2 kd cells at 0 hour and 4th hour photoed by EVOS system.

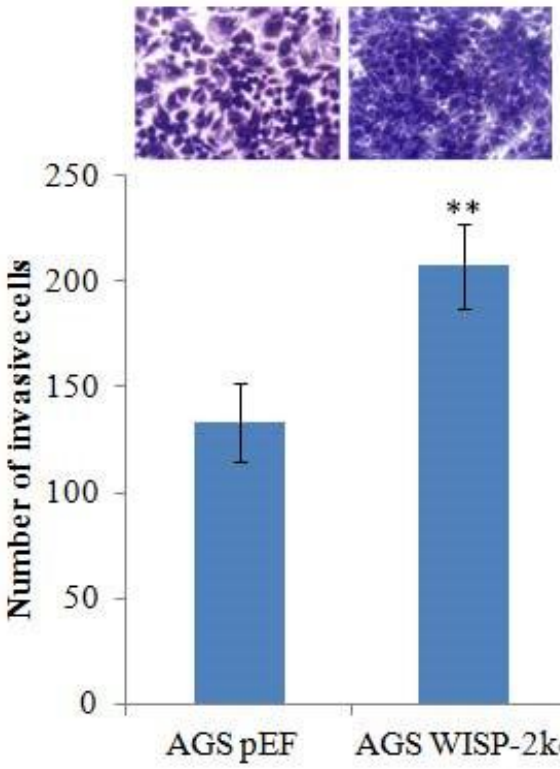

AGS pEF (mean±SD) n=3	AGS WISP-2kd (mean±SD) n=3
133.58±18.8	207.36±19.71

Figure 4.17 WISP-2 knockdown has an increased effect on the invasiveness of AGS cells after 3 days incubation of the cells on an artificial Matrigel basement membrane. Two representative images of cells following staining are shown in the top. Data shown is representative of 3 repeats of experiment. Error bars represent standard deviation. Two asterisks stand for $P< 0.01$.

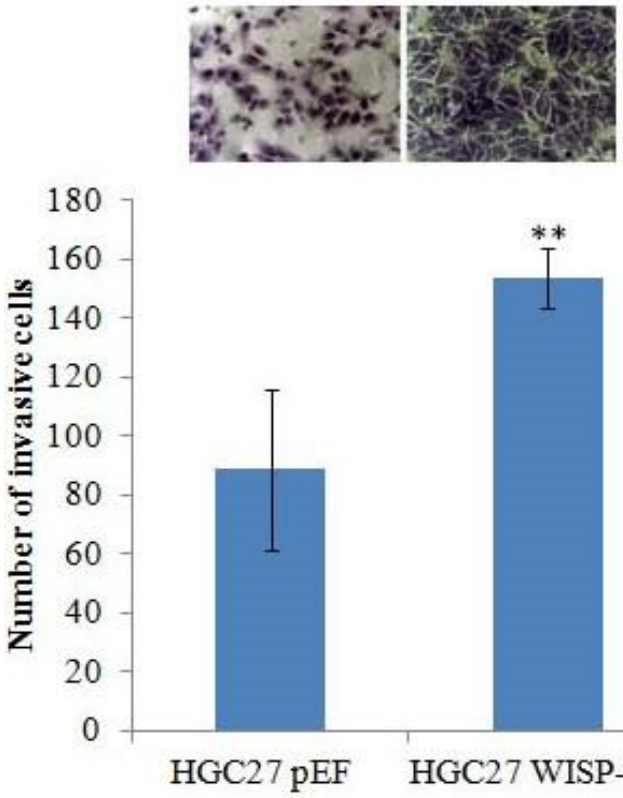

HGC27 pEF (mean±SD) n=3	HGC27 WISP-2kd (mean±SD) n=3
88.66±27.43	153.66±10.01

Figure 4.18 Knockdown of WISP-2 has a significant increase in the invasiveness of HGC27 cells. WISP-2 knockdown has an increased effect on the invasiveness of HGC27 cells after 3 days incubation of the cells on an artificial Matrigel basement membrane. Two representative images of cells following staining are shown in the top. Data shown is representative of 3 repeats of experiment. Error bars represent standard deviation. Two asterisks stand for $P< 0.01$.

4.4 Discussion

Metastasis involves the spread of cancer cells from the primary tumour to surrounding tissues and to distant organs and is the primary cause of cancer morbidity and mortality. In order to complete the metastatic cascade, cancer cells must detach from the primary tumour, intrude into the circulatory and lymphatic systems, evade immune attack, extravasate at distant capillary beds, and invade and proliferate in distant organs. However, the influence and function of WISP-2 in the metastatic cascade of some cancers, including gastric cancer, is not clear. For this purpose, we used transfected AGS and HGC27 cells with WISP-2 knockdown and empty plasmid (pEF) to deduce the influence of WISP-2 on the function of gastric cancer cells (AGS and HGC27). Through the comparison between the control group and the knockdown groups, we wanted to verify if WISP-2 may transform the function of gastric cancer cells. The *in vitro* function assays included growth, adhesion, invasion and migration assays, we repeated each assays more than three times to avoid artificial errors and ensure stability and accuracy of the results. The general trend of all repeats manifested consistency.

Targeting of WISP-2 resulted in significant increases in gastric cell proliferation, migration and invasion *in vitro* all of which are functions necessary for successful tumour progression and metastatic spread. Interestingly there was no statistically significant effect on cell-matrix adhesion after successful targeting of WISP-2 expression. These results suggest that WISP-2 may act in a tumour suppressive role in gastric cancer.

Chapter 5

Identification of WISP-2-Interacting Proteins and Potential Signalling Pathways Associated with WISP-2

5.1. Introduction

Results presented in the previous chapters have suggested an important role for WISP-2 in the clinical course, disease progression and the survival of patients with gastric cancer. *In vitro* experimental results have further demonstrated that manipulating the expression of WISP-2 has a direct impact on the cellular functions of gastric cancer cells, including that of invasiveness, migration and to some degree the growth of the cells. Collectively, this data argues an important and critical role for WISP-2 in gastric cancer cells and in shaping the clinical course of the patients with the cancer type.

WISP-2 is an intracellular protein that can be regulated by external factors such as glucocoricoids and IGF-1 [243, 271], though the function of the WISP-2 protein is not clear. We have hypothesised that the cellular protein plays important roles by interacting with other cellular and signalling proteins, by which it regulates the complex signalling and functions of the cells.

Although previous studies have preliminarily indicated that the WISP-2 protein may be involved in events including acting as a transcription repressor for EMT related molecules in breast cancer cells [243, 272, 273]. It has been shown that WISP-2 may form a protein complex with the peroxisome proliferator-activated receptor γ (PPARγ) transcriptional activator zinc finger protein 423 (Zfp423) in adipocytes [274]. It has also been shown that exogenous WISP-2 is able to activate the AKT1 pathway, by inducing the phosphorylation of AKT1 [275].

Thus, the interacting proteins and potential pathways associated with WISP-2 are less well known. To address this, we took an approach using an established protein array. We chose an antibody based protein array by aiming to: 1: Determine the proteins that are

associated/interacted with WISP-2, by way of precipitating WISP-2 protein and analysing the proteins co-precipitated with WISP-2; 2: To determine the changes of protein phosphorylation of certain key signalling pathways. Combining this with the results of Chapter 4, we tried to detect the effect of WISP-2 on cell motility of HGC27 cells through the signalling pathways which may be interested after the analysis of protein array.

5.2 Materials and Methods

5.2.1 Protein arrays for searching for interacting proteins with WISP-2

i. Tissue and sample preparation

Two pairs of fresh human stomach tissues (Pair 1 and pair 2) were obtained immediately after surgery. One piece of normal stomach tissue (N) (10cm away from the tumour margin) and one piece of matched tumour tissues (T) were obtained from the same patient. Of the normal tissues, we collected the mucosal tissues after stripping the tissues with a scalpel. The remaining tissues, primarily muscular and serosa were discarded. Tumour tissues were obtained by section a small portion of the tumour under direct visualisation.

Both normal and tumour tissues, approximately 1-2 grams from each tissue were immediately placed in a universal tube, which was pre-filled with an aliquot of ice cold protein extraction buffer which also contained a mixture of protease inhibitors **(**BD Biosciences, San Jose, USA**)** **(**1ml). The tissue containing tubes were placed on ice and then subject to homogenisation using a handheld homogeniser, at 150 rpm, for 30 seconds. The homogenates were dispensed into 1.5ml EEppendrof vials and subsequently spun at 12,000g for 10 minutes. Supernatants were

carefully collected and placed in new tubes and stored at -20℃ until use. The insolubles were discarded.

ii. Immunoprecipitation of WISP-2 interacting proteins

Protein preparations were first subject to protein quantitation, using a colorimetric protein quantitation kit. The concentrations were subsequently adjusted to 2mg/ml, using the same protein extraction buffer. A small amount of the proteins were set aside as a total protein preparation for verification purposes by subsequent Western blotting analysis.

Using a WISP-2 specific antibody that is suitable for immunoprecipitation, namely a mouse monoclonal antibody to WISP-2 (SC-514070, Santa Cruz Biotechnologies Inc.,), 2 mg of total protein from each sample was added to 1.5ml (contained 300μg) of anti-WISP-2 IgG in a small universal tube. After careful mixing, the tubes were then placed onto a blood wheel. The blood wheel was placed into a cold room (4℃) with the speed set at 100rpm.

Twenty four hours after the antibody-antigen reaction, the tubes were taken out and each tube (now containing 2mg of total protein and 300 μg anti-WISP-2 antibody) was added to 2ml protein A/G agarose conjugates (SC-2003). The agarose was pre-loaded with a mixture of Protein-A and Protein G. The tubes were placed back onto the blood wheel and were again placed in cold room to be spun at 100rpm for 4 hours.

After four hours, the protein-antibody-agarose mixture was dispenses into 1.5ml Eppendrof vials. The vials were spun at 5,000g, 4^{o}C, for 10 minutes in a refrigerated microfuge. After carefully discarding the supernatants (which contained proteins not precipitated by the anti-WISP-2 antibody), the remaining pellets now would have the agarose-Protein A/G and the WISP-2/anti-WISP-2 complex and of course proteins interacted with WISP-2. Each pellet was washed three times by using the same protein extraction buffer.

After removal of the washing solutions, the agarose protein complex from each sample was combined to one Eppendrof vial, to which 0.5ml of an extraction buffer was added. This was then boiled at 100 ℃ for 5 minutes, to allow proteins (antibody, WISP-2 protein, and proteins co-precipitated with WISP-2) to be dissociated from the agarose beads. After cooling down, the mixture was spun at 12,000g for 10 minutes. The supernatant, which contains the proteins (WISP-2 and WISP-2 interacting proteins) precipitated by the antibody and then was carefully collected, stored at -20 ℃, ready for protein array analysis.

5.2.2 Protein preparation from gastric cancer cell line, AGS, for screening potential signalling events associated with WISP-2

i. Cell and sample preparation.

AGS/pEF6 (control transfected cells) and AGS/WISP-2KD (WISP-2 knockdown cells) were that prepared in the previous experiments (Chapter 4 and Chapter 5). In AGS/WISP-2KD cells, WISP-2 expression was markedly reduced/ lost by way of the anti-WISP-2 transgene. The AGS/pEF6 cells, transfected with a pEF6 plasmid as a control, had regular level of WISP-2.

Both cells (two T75 tissue culture flasks for each) were grown to 90% confluence. The flasks were washed with BSS buffer, and then placed with a fresh batch of DMEM supplemented with 5% FCS. After 5 hours, cells were removed from the flasks with a rubber policeman. The cells were pelleted using a centrifuge at 2,500rpm for 5 minutes.

Cell pellets were added with a lysis buffer (0.6ml) and then subsequently placed on a blood wheel for 1 hour at 4℃. The lysates were then spun at 12,000g for 10 minutes at 4℃. The supernatant were carefully collected and discarded.

ii. Protein concentration.

The protein concentration in the cell lysates were quantified and then adjusted to 3.5 mg/ml final concentration. The samples were stored at -20℃ until use.

5.2.3 Antibody microarrays

We chose an antibody based protein array, namely KAM850, which have more than 850 capture antibodies spotted on to each array slides (Kinexus Bioinformatics Ltd, Vancouver, Canada). Each array slide has two array spotted.

5.2.4 Key parameter in the protein microarray analyses

The following are the key parameters collected and used for the data analyses:

Globally Normalised Signal Intensity - Background corrected intensity values are globally normalised. The Globally Normalised Signal Intensity is calculated by summing the intensities of all the net signal median values for a sample.

Flag - An indication of the quality of the spot, based on its morphology and background. The flagging codes used in the reports are as follows:

0: acceptable spots;

1: spots manually flagged for reasons and may not be very reliable;

3: poor spots defined by various parameters;

%CFC - The percentage change of the treated sample in Normalised Intensity from the specified control.

Calculation = (Globally Normalised Treated – Globally Normalised Control)/Globally Normalised Control)*100

% Error Range - A parameter to show how tightly the "Globally Normalised Net Signal Intensity" for adjacent duplicate spots of the same protein in the sample compare to each other.

Calculation = ABS (Globally Normalised Spot 1- Globally Normalised Spot 2)/Globally Normalised Spot 2*100

Log2 (Intensity Corrected) - Spot intensity corrected for background is log transformed with the base of 2.

Calculation = LOG (Average Net Signal Median,2)

Z Scores - Z score transformation corrects data internally within a single sample.

Z Score Difference - The difference between the observed protein Z scores in samples in comparison.

Z Ratios - Divide the Z Score differences by the SD of all the differences for the comparison.

5.2.5 Antibody array analysis of WISP-2 interacting proteins

The immuno-precipitates from normal and tumour tissues of the same patient were applied to the same slide, to reduce the inter-assay variance.

The proteins samples were labelled, applied to the microarray, and image subsequently scanned using Perkin-Elmer ScanArray Reader laser array scanner, according to manufacturer's instructions. Analysis was carried out using the *ImaGene 9.0* from BioDiscovery (El Segundo, CA). Here, our analyses had focused on the Globally Normalised Signal Intensity, %CFC and the Z-scores.

iii. KAM850 protein microarray analysis.

We used KAM850 protein microarray and applied the samples, pairwise, on the sample array slides, for the sake of reducing the inter-assay variance and ease of comparative analyses.

In this case, we were focused on comparing the difference between the two comparable cell types, by emphasising the Z-difference and Z-ratio.

5.2.6 Cell lines

AGS and HGC27 gastric cancer cell lines were used in this chapter, including empty plasmid control and transfected sublines. Cells were continuously maintained in normal DMEM media with 10% FBS and antibiotics. For ribozymes selection, cells were maintained in normal media supplemented with 5～7.5μg/ml blasticidin (5μg/ml for HGC27 and 7.5μg/ml for AGS selection). The stable transfected cells were maintained in normal media supplemented with 0.5μg/ml blasticidin.

5.2.7 The effects of different small inhibitors on the cell motility

Using 96W1E+ array, cell adhesion and wounding assay were also conducted with ECIS instrument. Cells were seeded into each ECIS plate well as described in Chapter 2 and treated with a protein of interest. In this study, we treated the cells respectively with different concentrations of FAK inhibitor PF573228, JNK inhibitor SP100625 and N-WASP inhibitor Wiskostatin, respectively. For the control group, identical volume of serum free medium was added into wells. Cell adhesiveness was assessed within the first 40 minutes and electric wound was set at the 14^{th} hour when the resistance reached maximum levels and migration data could be gathered in the continuous 6 hours.

5.2.8 Electric Cell-Substrate Impedance Sensing

ECIS (Electric Cell-Substrate Impedance Sensing) is a novel method used as an alternative to the conventional function assays. It works with an array of 96 wells, each containing a gold electrode. These measure the current and voltage across this electrode, calculating the impedance and resistance. From the impedance changes, effects on cell attachment and motility

can be examined [262]. Using 96W1E+ array, cell adhesion and wounding assay were also conducted with ECIS instrument. 40,000 cells diluted in 200µl DMEM were seeded into each ECIS plate well, and treated with a protein of interest.

5.3 Results

5.3.1 Proteins interacted with WISP-2 in normal gastric tissues

We first verified the presence of WISP-2 protein in the protein samples prepared from gastric tissues, by way of Western blotting. As shown in Figure 5.1, both normal and tumour tissues expressed WISP-2 proteins which echoes well with what was observed from the immuno-histochemical analysis (Chapter 3).

Our antibody microarray tests revealed that all the protein preparations and the reactions were successful, with all the sample reaction Flagged as '0'.

KAM850 antibody array had detected a number of proteins that have been co-precipitated by the anti-WISP-2 antibody (Figure 5.2). Given the nature of the study, namely searching for proteins that interacted with WISP-2 in a given tissue, we focused our analyses by using:

i. Globally Normalised Signal Intensity, which is the signalling with background corrected intensity values are globally normalised. The Globally Normalised Signal Intensity is calculated by summing the intensities of all the net signal median values for a sample.

ii. Log2 (Intensity Corrected). This was the Spot intensity corrected for background is log transformed with the base of 2.

Calculation = LOG (Average Net Signal Median 2)

iii.Z Scores. The Z score transformation corrects data internally within a single sample. The background corrected spot intensity values for individual proteins are expressed as a unit of standard deviation (SD) from the normalised mean of zero. Since the transformation is done before sample-to-sample comparison, it is therefore comparison-independent, and would allow evaluation of the degree of proteins pooled out by the anti-WISP-2 antibody.

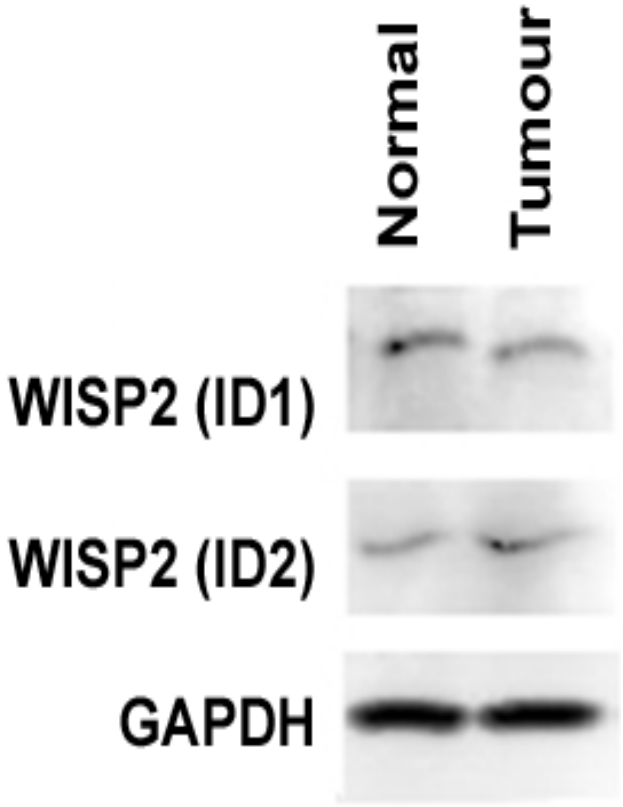

Figure 5.1 The protein expression of WISP-2 in two pairs of stomach tissues from two patients with gastric cancer (one piece of normal tissue and matched tumour tissue). GAPDH was used as house keeping control.

Figure 5.2 Images of the antibody microarray for normal (Left: 1A and 2A) and tumour (Right: 1B and 2B) from patients (ID1 and ID2).

5.3.1.1 ERK Proteins interacted with WISP-2 in normal gastric mucosa

From the cell function changes as presented in Chapter-4, we have focused on the ERK family protein kinases that are widely involved in the functions seen after WISP-2 modification. We aimed at first looking at the ERK proteins precipitated by WISP-2 in the tissues. Here, we chose the globally normalised signal, the Log2 transformed signal and the Z-score, all the parameters indicate the level of the protein precipitated and are independent of the sample comparison.

WISP-2 interacted with ERK1. As shown in Figure 5.3, high levels of ERK1 protein was precipitated from antibodies recognised in the total WISP-2 protein (namely the pan-antibody). WISP-2 also interacted with the phosphorylated WISP-2 whether the phophorylation was on serine-74, threonine-207 or tyrosine-204.

WISP-2 interacted with ERK5. As shown in Figure-5.4, WISP-2 also interacted strongly with ERK5 total proteins, although the three antibodies delivered varying degree of interaction. It is very interesting to observe that WISP-2 strongly interacted with ERK5 which had strongly phosphorylated on tyrosine-221.

Interaction between WISP-2, ERK2 and ERK3. WISP-2 was also detected to interact with ERK2 (Figure-5.5). On this antibody array, there was no antibody to detect phosphorylated ERK2, thus the data only provides support that these two proteins are associated with each other. The similar pattern was observed with ERK3 (Figure 5.6).

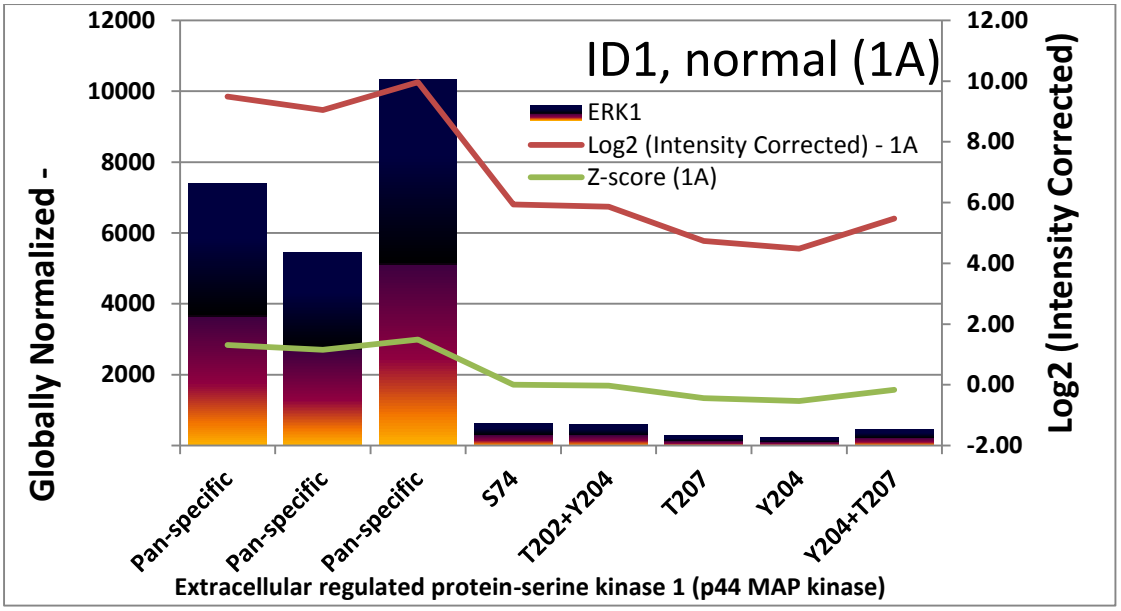

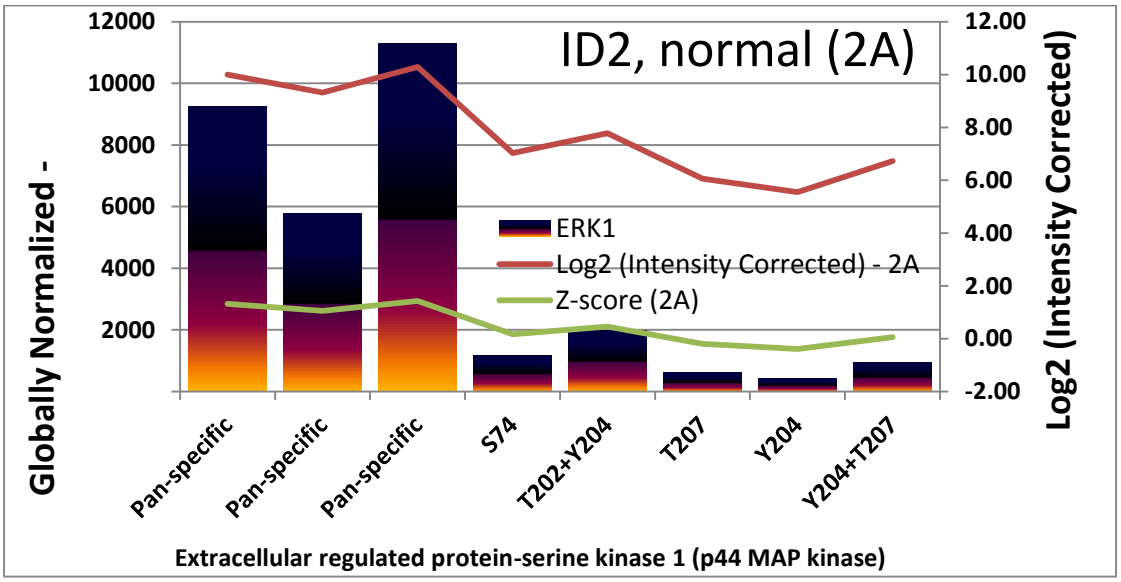

Figure 5.3 ERK1 protein interacted with WISP-2 in normal stomach mucosa. Pan-specific antibodies recognised the total ERK1 protein (phosphorylated and non-phosphorylated). The vertical bars shows the levels of the ERK1 protein precipiated by anti-WISP-2 antibody after normalisation. The red line shows the levels of the signal in Log2 transformation and the green line shows the transformation that corrects data internally within a single sample. Top: first sample (1A); Bottom: the second sample (2A).

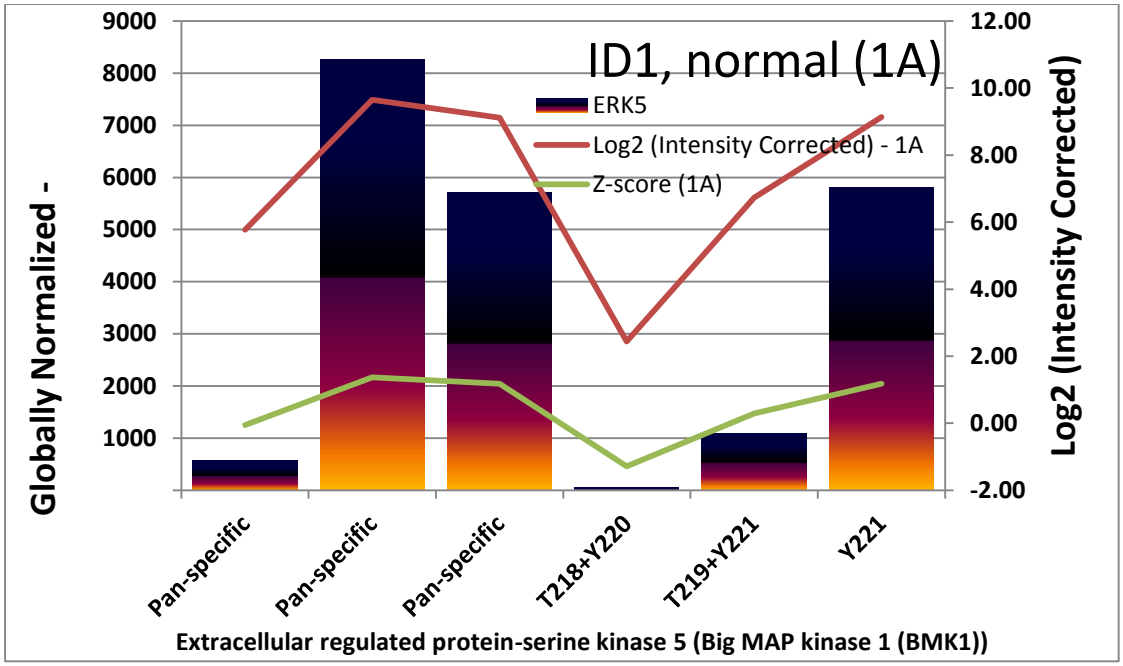

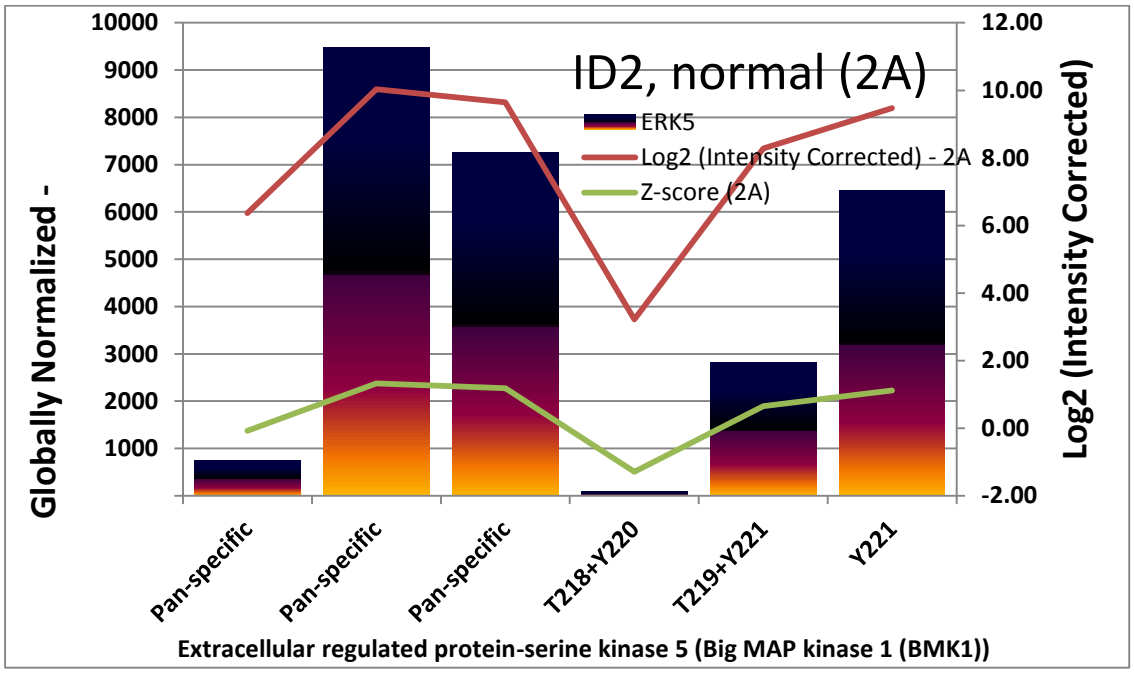

Figure 5.4 ERK5 protein interacted with WISP-2 in normal stomach mucosa. The layout is similar to Figure-5.2, except that the detected proteins are ERK5.

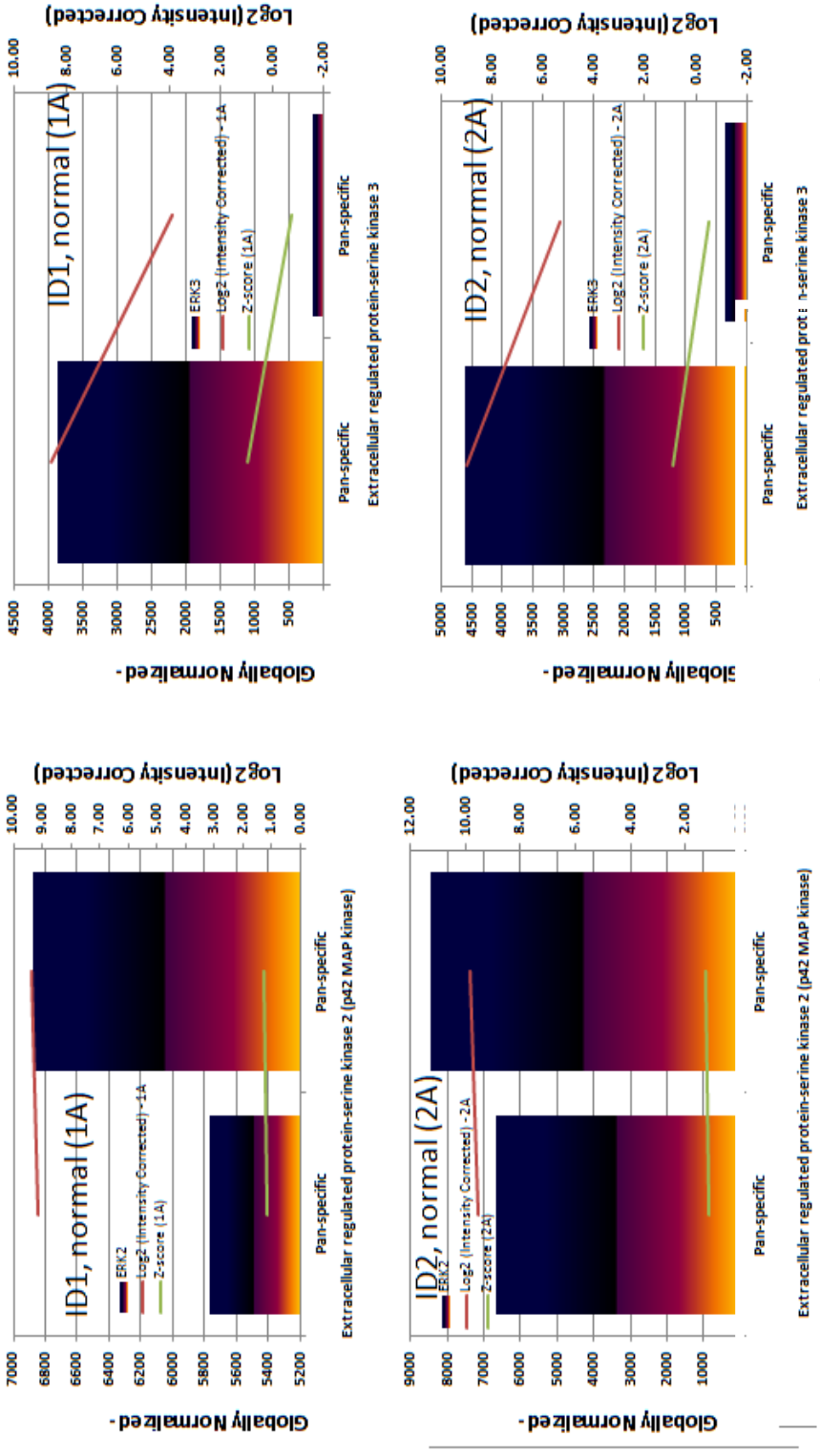

Figure 5.5 Interaction between WISP-2 and ERK2 (left) and ERK3 (right) in normal stomach tissues.

5.3.1.2 Interaction between JNK protein kinases and WISP-2 in normal gastric mucosa

Three panels of antibodies were available to capture the JNK proteins. Shown in Figure-5.6 are the panel of antibody that recognised a common domain of JNK1/2/3. It was clear that one set antibody has shown a strong signal that JNK1/2/3 proteins were co-precipitated by WISP-2. It is also interesting to note that the antibody recognising T183/Y185 sites on JNK1/2/3 also recognised the presence of phosphorylated JNK1/2/3 from the WISP-2 precipitate.

A respective panel of antibodies to pan-JNK2 (Figure 5.7) and pan-JNK3 (Figure 5.8) proteins had identified the presence of JNK2 and JNK3 proteins in the precipitates of WISP-2 from the normal tissues. Captured antibodies to phosphorylated JNK2 and JNK3 proteins are otherwise not available on the KAM850 microarray.

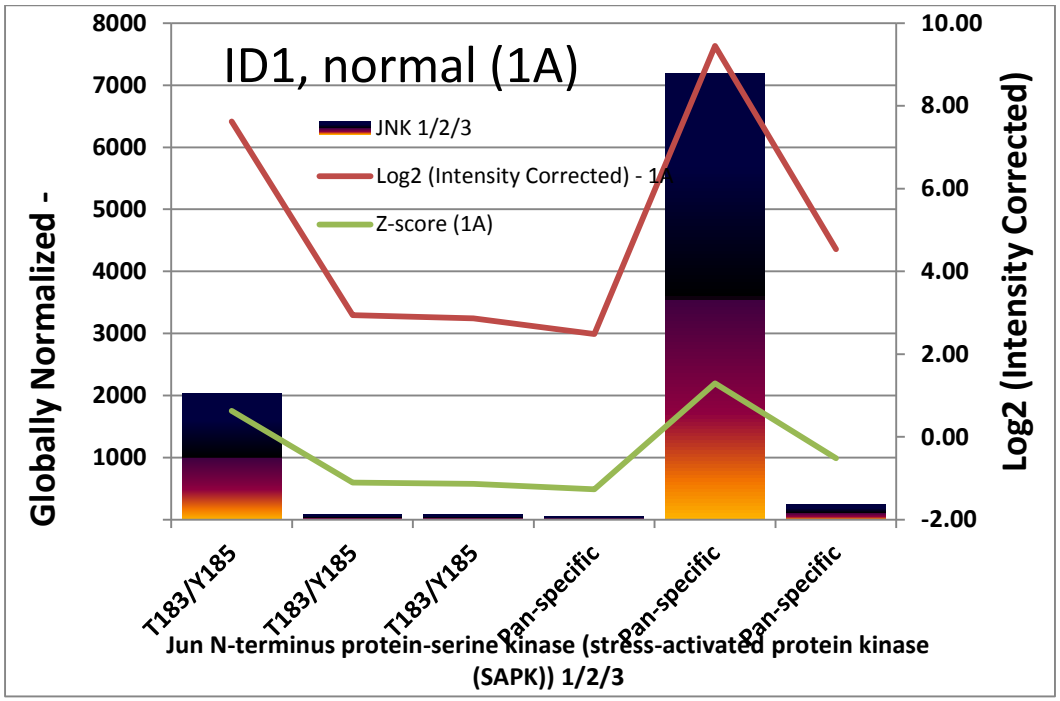

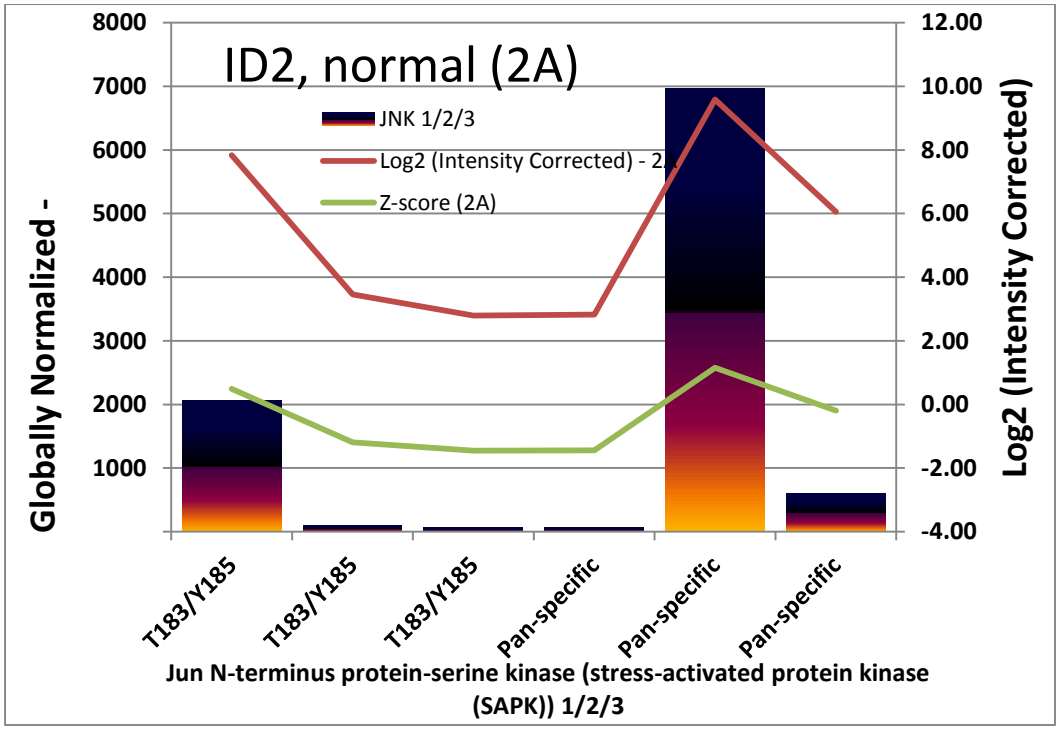

Figure 5.6 Interaction between WISP-2 and the JNK proteins in normal stomach mucosal tissues.

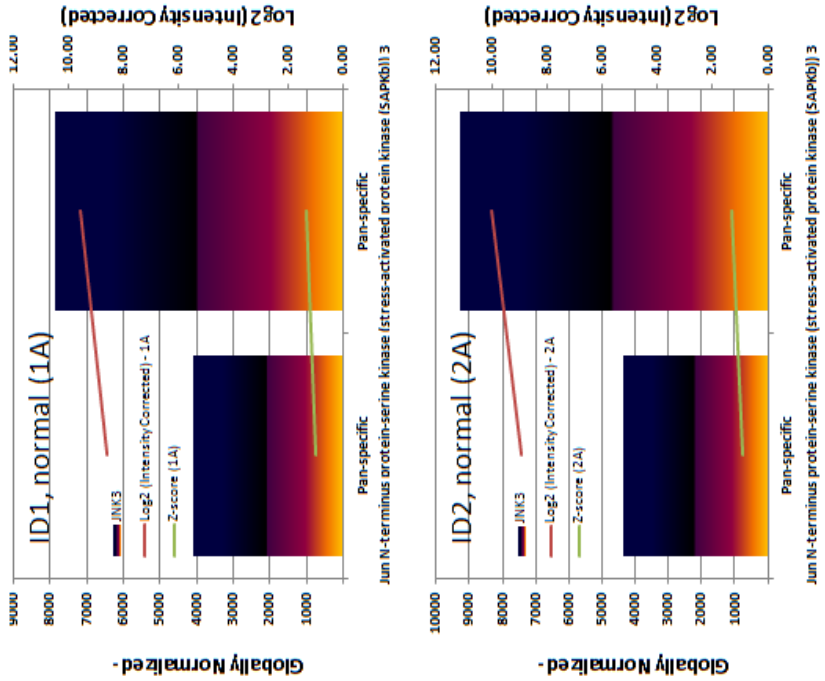

Figure 5.8 Interaction between WISP-2 and the JNK3 proteins in normal stomach mucosal tissues.

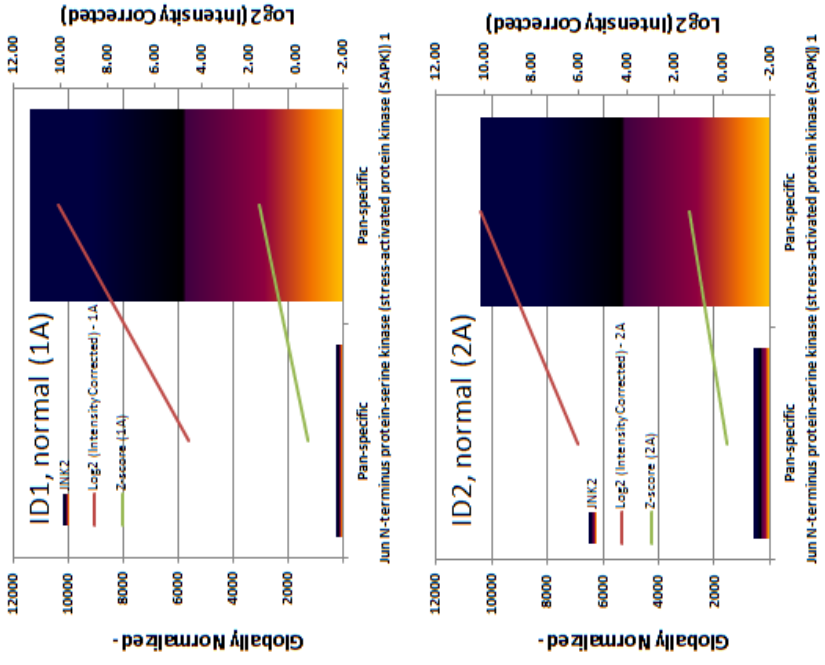

Figure 5.7 Interaction between WISP-2 and the JNK2 proteins in normal stomach mucosal tissues.

5.3.2 Proteins interacted with WISP-2 in gastric cancer tissues

In a similar matter to the analyses on normal stomach mucosa, the interaction between WISP-2 and co-precipitated proteins were analysed on the gastric cancer tissues.

5.3.2.1 ERK Proteins interacted with WISP-2 in gastric cancer tissues

WISP-2 strongly interacted with ERK1 in gastric cancer tissues (Figure 5.9), in a similar fashion to that observed in normal mucosal tissues (Figure 5.3). Again, antibodies recognising Y204 showed that WISP-2 appears to co-precipitated well with the ERK1 protein phosphorylated on this tyrosine site.

ERK5 also strongly co-precipitated with WISP-2 (Figure-5.10) and that antibodies recognising Y204 displayed a particularly strongly signal, indicating that WISP-2 may interact with tyrosine phosphorylated ERK5 proteins.

A strong interaction was also observed between WISP-2 and ERK2 and ERK3 proteins (Figure 5.11 and 5.12).

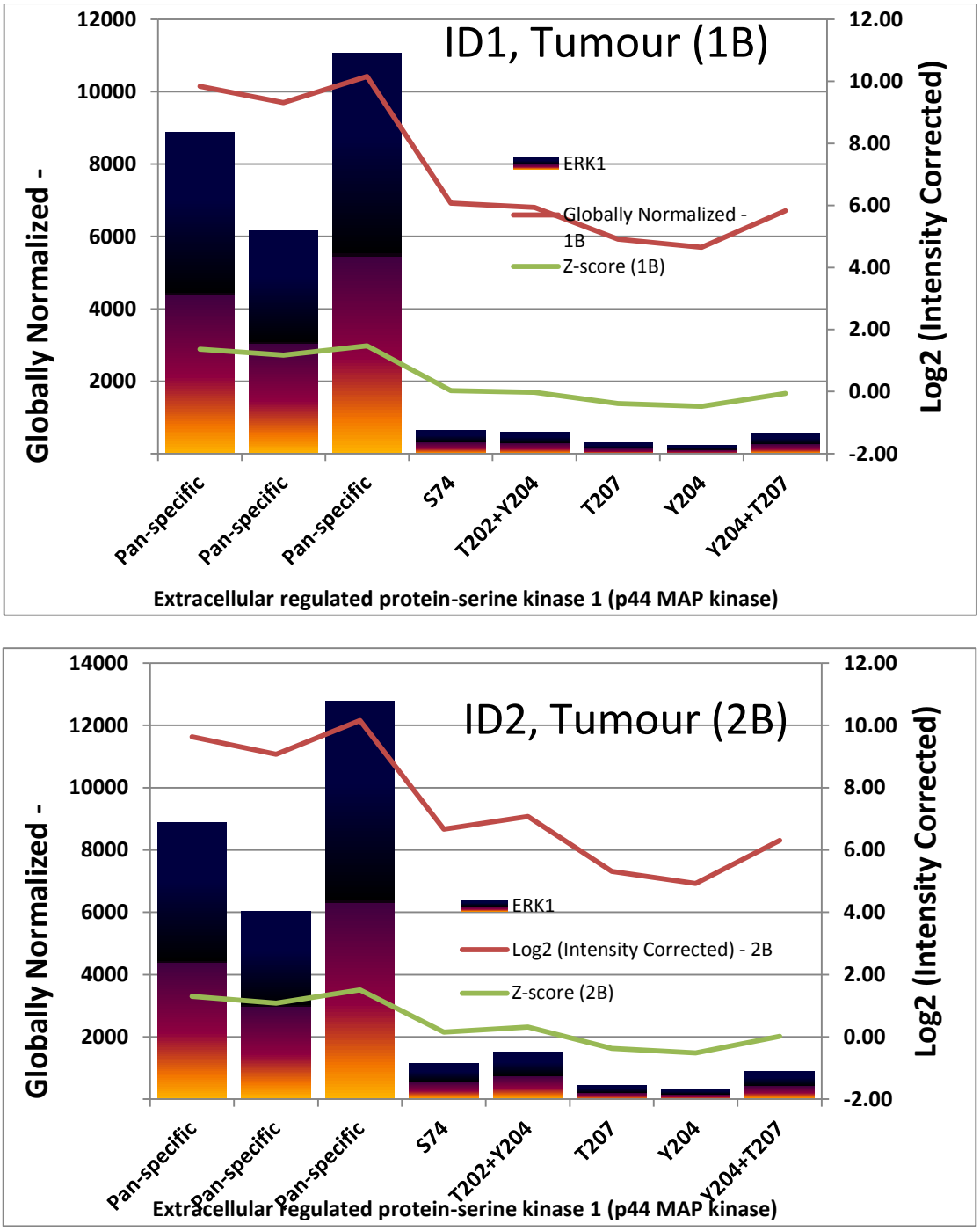

Figure 5.9 Interaction between WISP-2 and the ERK1 protein in gastric cancer tissues. Results from phospho-specific antibodies and pan-specific antibodies recognised the total ERK1 protein (phosphorylated and non-phosphorylated) were plotted. The vertical bars show the levels of the ERK1 protein precipitated by anti-WISP-2 antibody after normalisation. The red line shows the levels of the signal in Log2 transformation and the green line shows the transformation that corrects data internally within a single sample. Top: first sample (BA); Bottom: the second sample (2B).

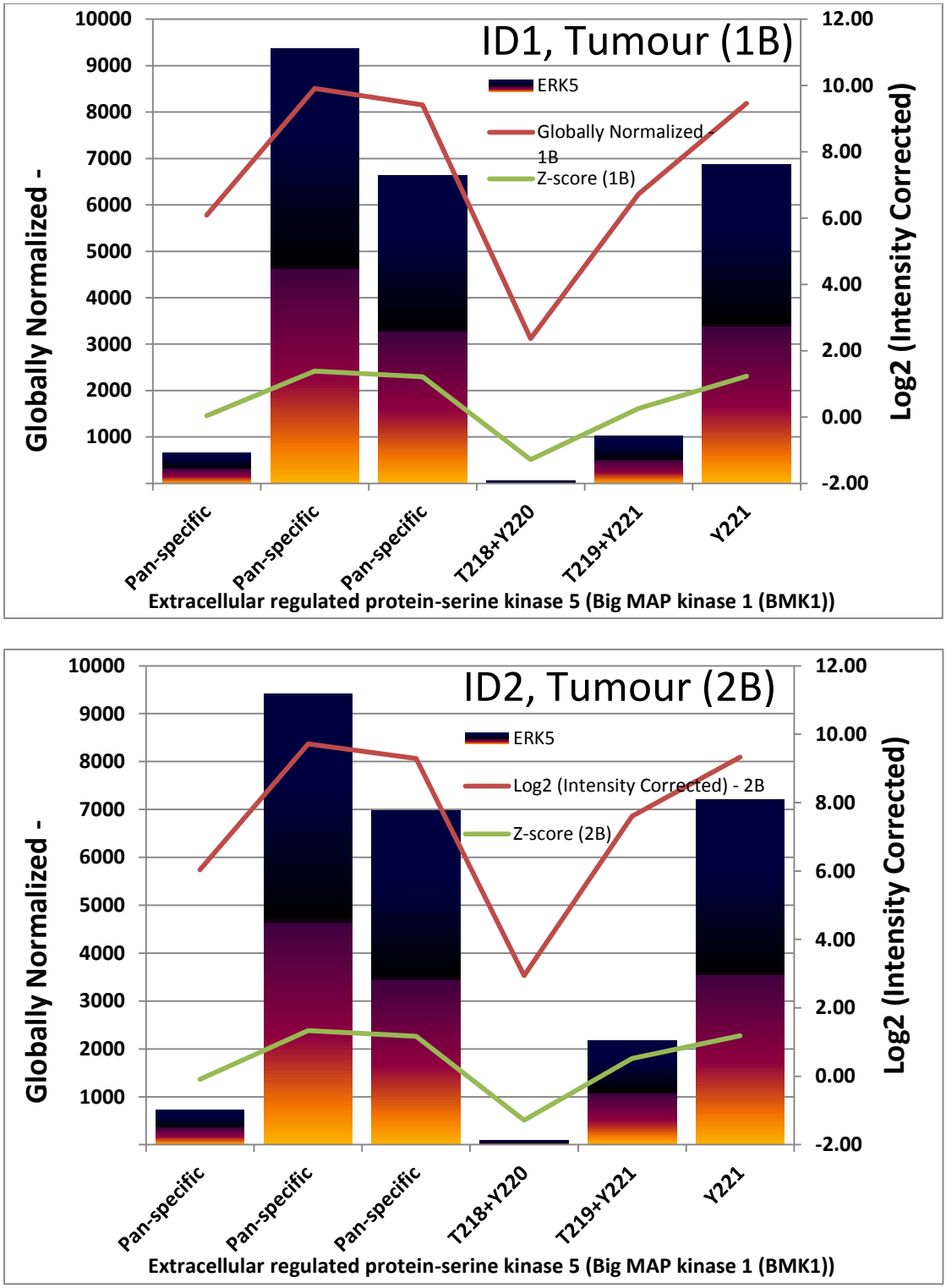

Figure 5.10 Interaction between WISP-2 and the ERK5 protein in gastric cancer tissues.

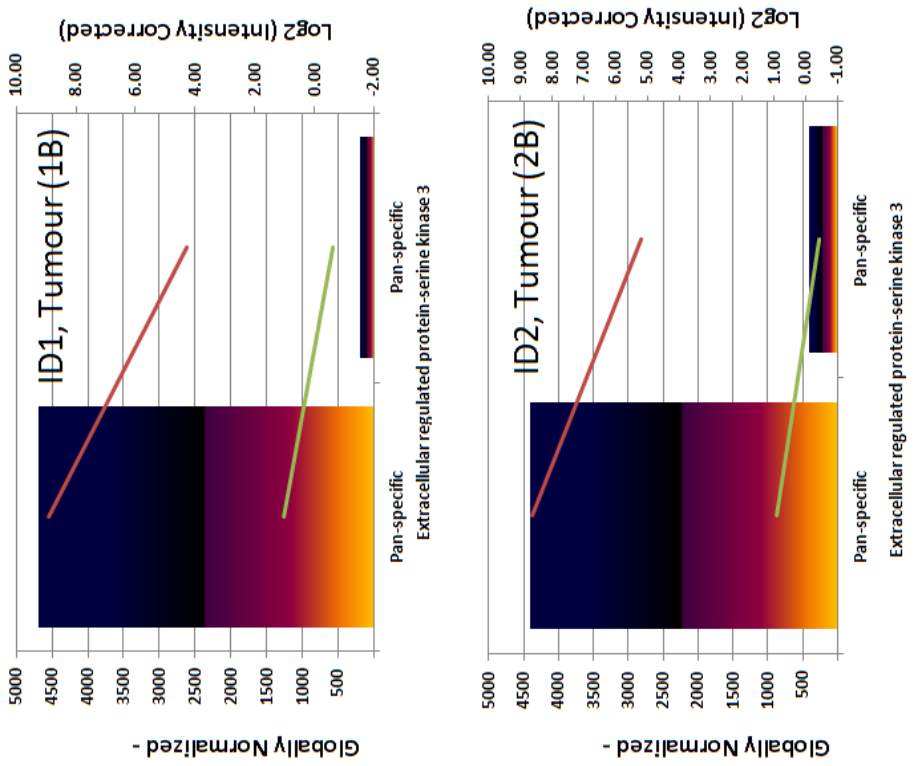

Figure 5.12 Interaction between WISP-2 and the ERK3 protein in gastric cancer tissues. The vertical bars show the levels of the ERK3 protein precipiated by anti-WISP-2 antibody after normalisation. The red line shows the levels of the signal in Log2 transformation and the green line shows the transformation that corrects data internally within a single sample.

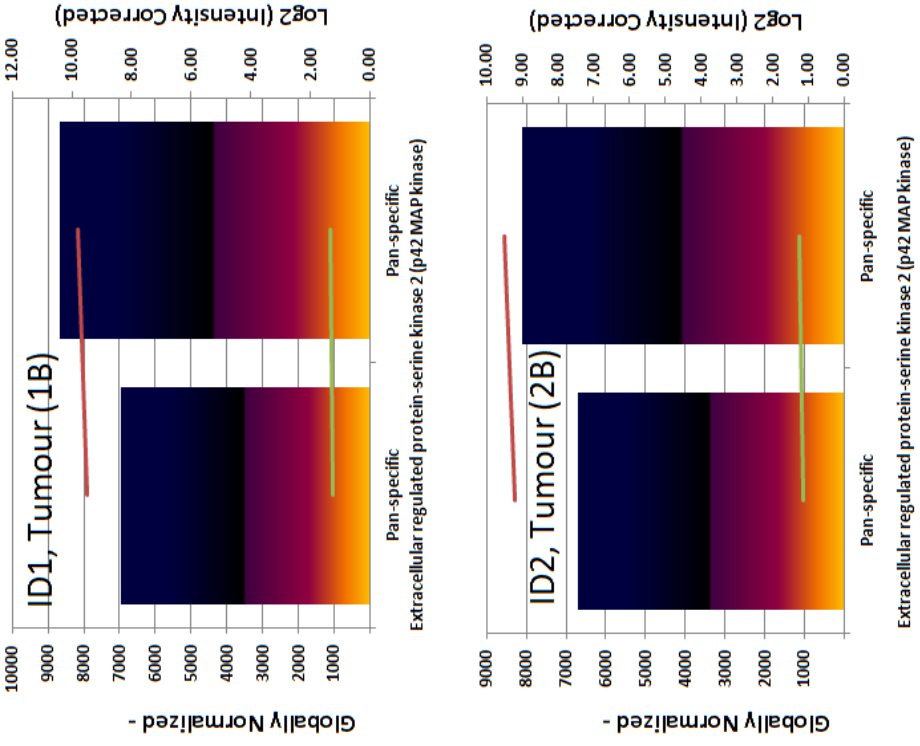

Figure 5.11 Interaction between WISP-2 and the ERK2 protein in gastric cancer tissues. The vertical bars show the levels of the ERK2 protein precipiated by anti-WISP-2 antibody after normalisation. The red line shows the levels of the signal in Log2 transformation and the green line shows the transformation that corrects data internally within a single sample.

5.3.2.2 JNK Proteins interacted with WISP-2 in gastric cancer tissues

Antibodies recognising the pan-JNK-1, -2 and -3 proteins have displayed a strong signal in the WISP-2 protein precipitate from gastric cancer tissues (Figure 5.13). Again, it was shown that WISP-2 protein interacted with the JNK proteins that had been phosphorylated on T183/Y185 sites.

Likewise, WISP-2 interacted strongly with the JNK2 and JNK3 proteins (Figure 5.14 and 5.15). Information on the phosphorylation status of JNK2 and JNK3 proteins are not available on the protein microarray.

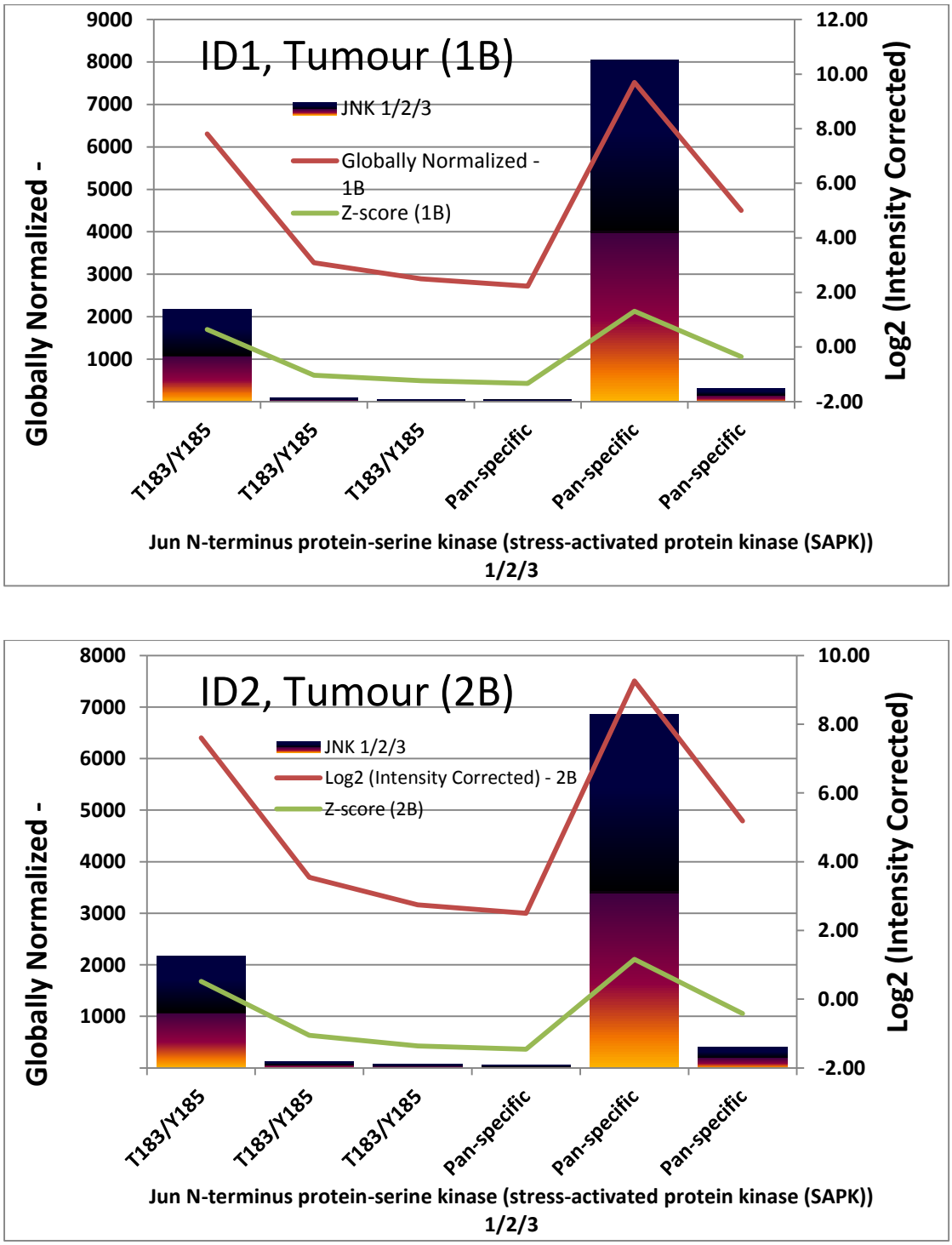

Figure 5.13 Interaction between WISP-2 and the JNK-1/2/3 proteins in gastric cancer tissues. The layout of the graph is similar to that of Figure-5.9.

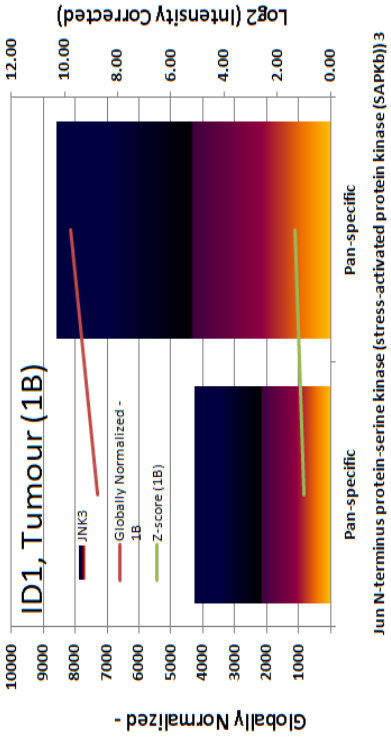

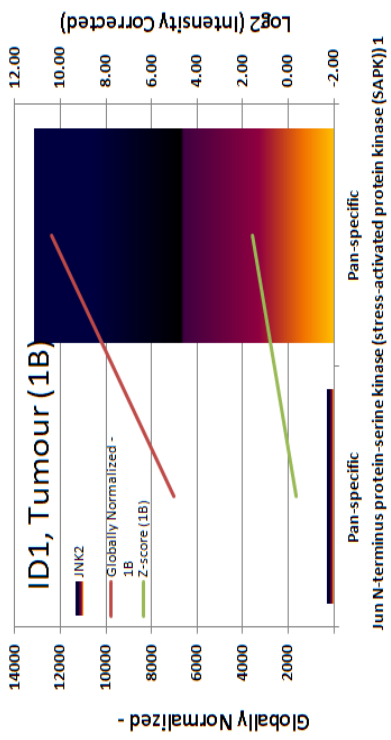

Figure 5.14 Interaction between WISP-2 and the JNK-2 proteins in gastric cancer tissues.

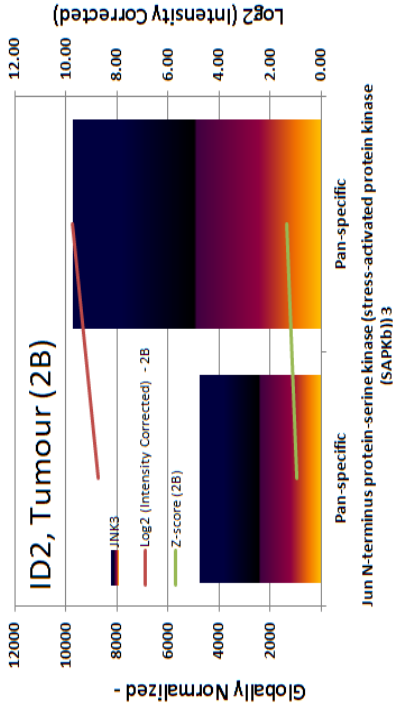

Figure 5.15 Interaction between WISP-2 and the JNK-3 proteins in gastric cancer tissues. by anti-WISP-2 antibody after normalisation. The red line shows the levels of the signal in Log2 transformation and the green line shows the transformation that corrects data internally within a single sample.

5.3.3 The difference between normal and tumour tissues in WISP-2 interacting proteins

In order to have a preliminary estimation of the difference in WISP-2 interacting proteins between normal and tumour tissues, we have used the Z-Score Difference, Z-Ratio between the same pair of normal tissues and the tumour tissues from the same patients. These two parameters reflected the difference in the paired samples.

Figure 5.17 has shown that WISP-2 in tumour tissues strongly interacted with ERK5 which was phosphorylated at the Y221 site, but showed reduced interaction with T219 phosphorylated ERK5, when compared with that in normal tissues. In contrast, the pattern of differences between the interaction of WISP-2, ERK1 (Figure 5.16), ERK2 and ERK3 (Figure 5.18 and Figure 5.19) in tumour and normal tissues are not consistent.

When comparing the difference in JNK1 interaction with WISP-2 proteins, it is indicated that tumour tissues had a more profound interaction pattern when T183/Y185 phosphorylated antibody was used (Figure 5.20). A similar pattern was seen with ERK3 (Figure 5.22), although the pattern with ERK2 was not consistent (Figure 5.21).

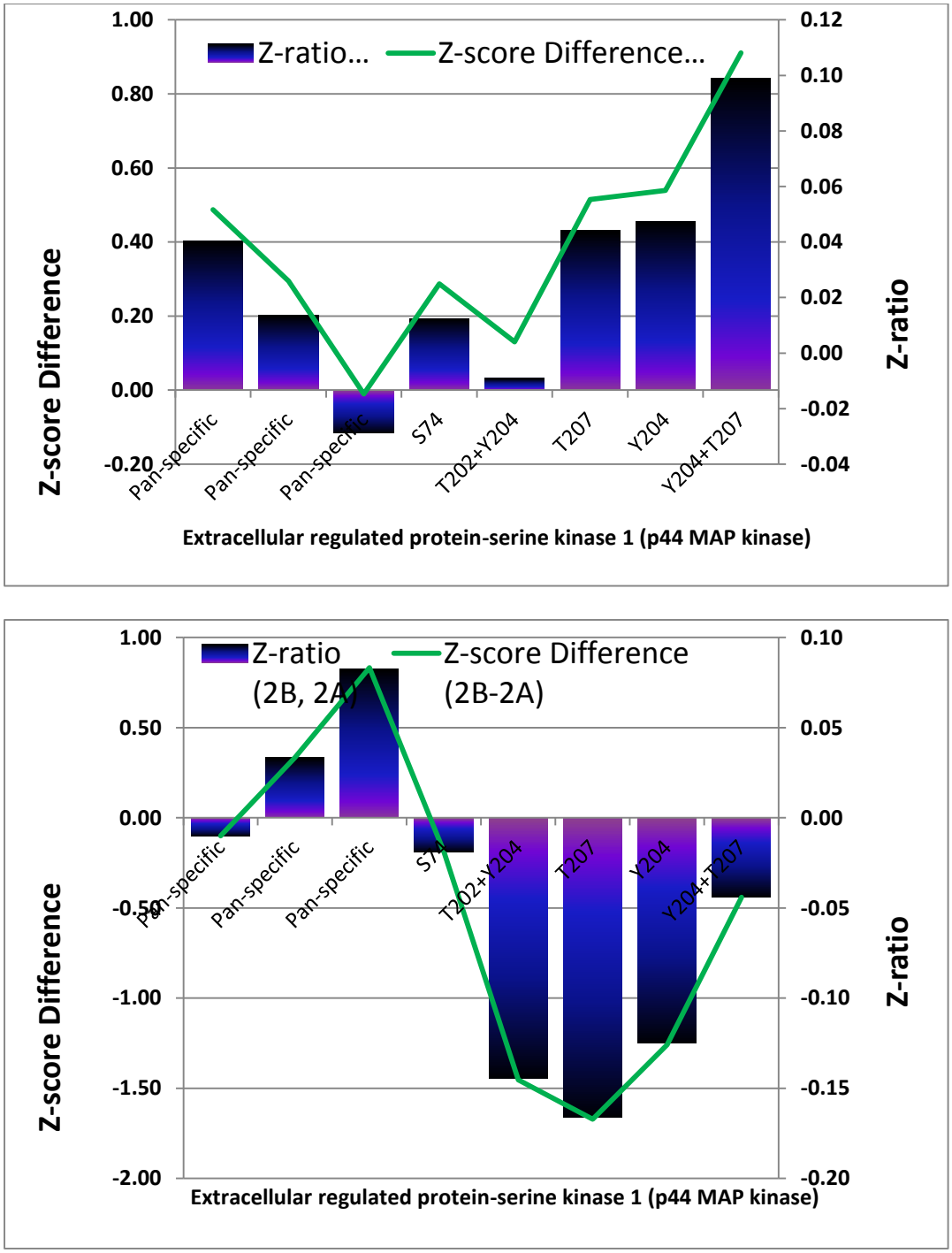

Figure 5.16 WISP-2 and ERK1 interaction in gastric tissues. The difference between cancer and normal tissues. Vertical bars are the Z-Ratio and greens are the Z-Score Difference between normal and tumour tissues. Top: patient ID1; Bottom: patient ID2.

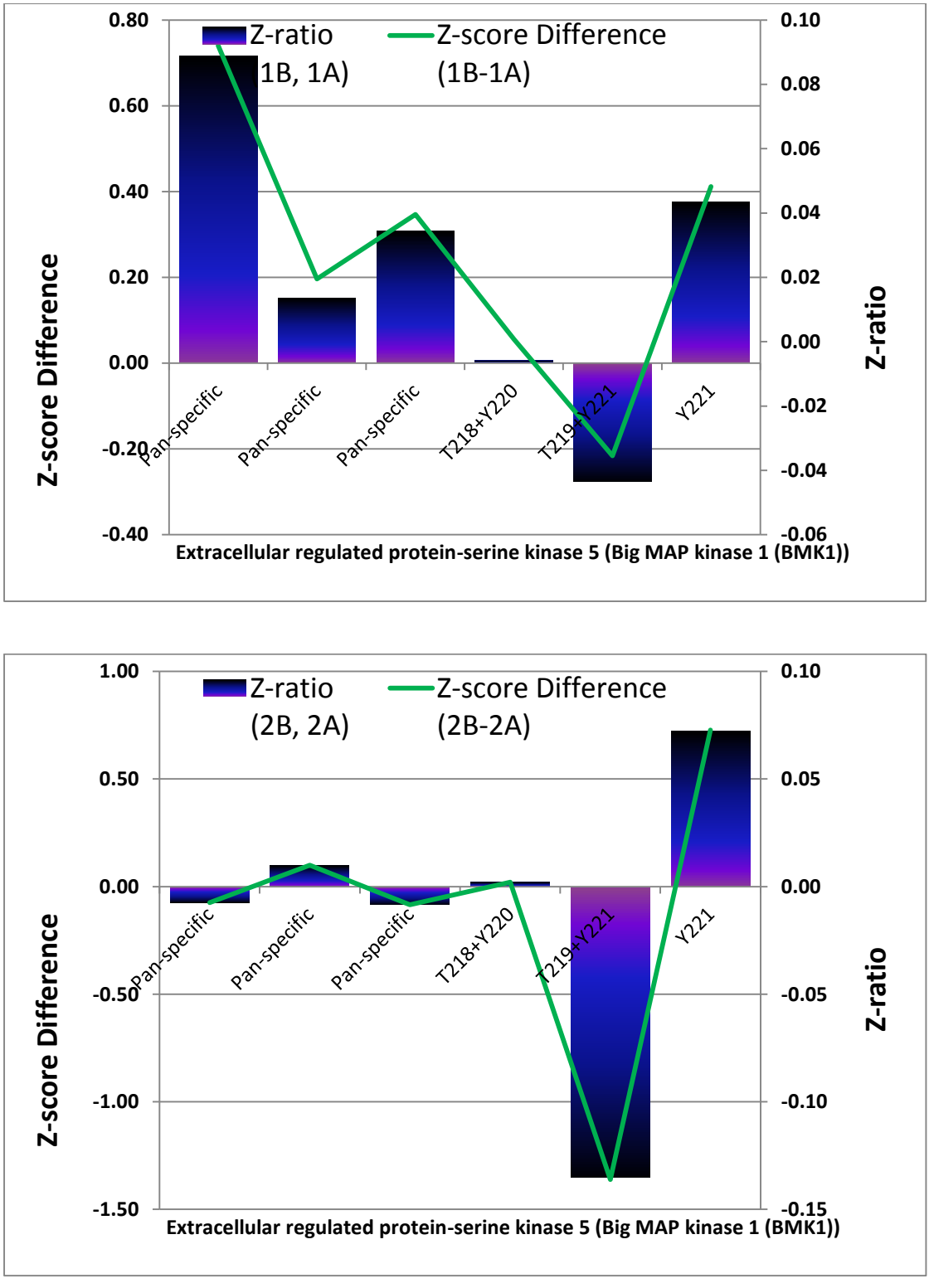

Figure 5.17 WISP-2 and ERK5 interaction in gastric tissues. The difference between cancer and normal tissues. Vertical bars are the Z-Ratio and greens are the Z-Score Difference between normal and tumour tissues. Top: patient ID1; Bottom: patient ID2.

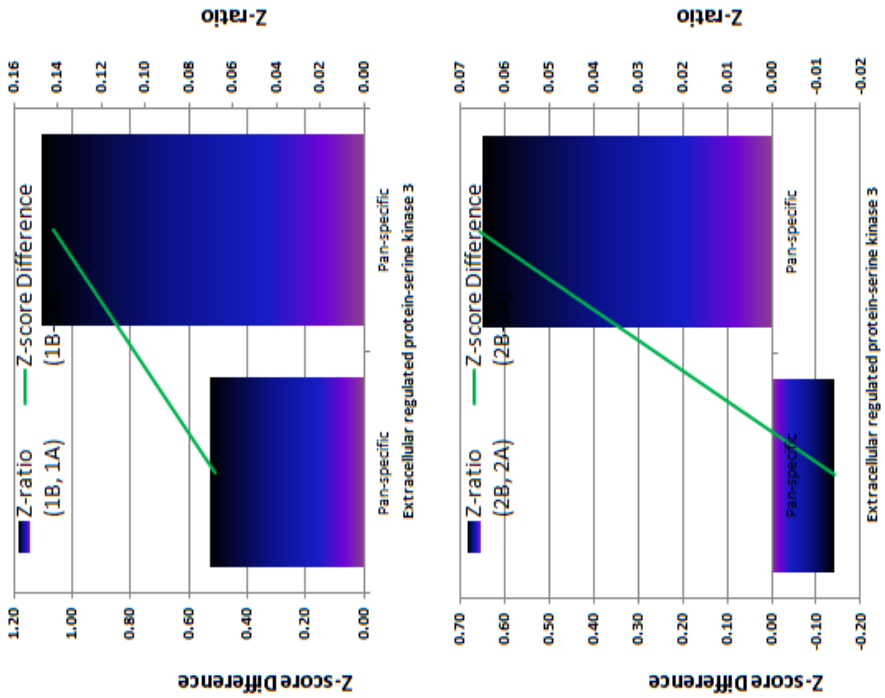

Figure-5.19 WISP-2 and ERK3 interaction in gastric tissues. The difference between cancer and normal tissues. Vertical bars are the Z-Ratio and greens are the Z-Score Difference between normal and tumour tissues. Top: patient ID1; Bottom: patient ID2.

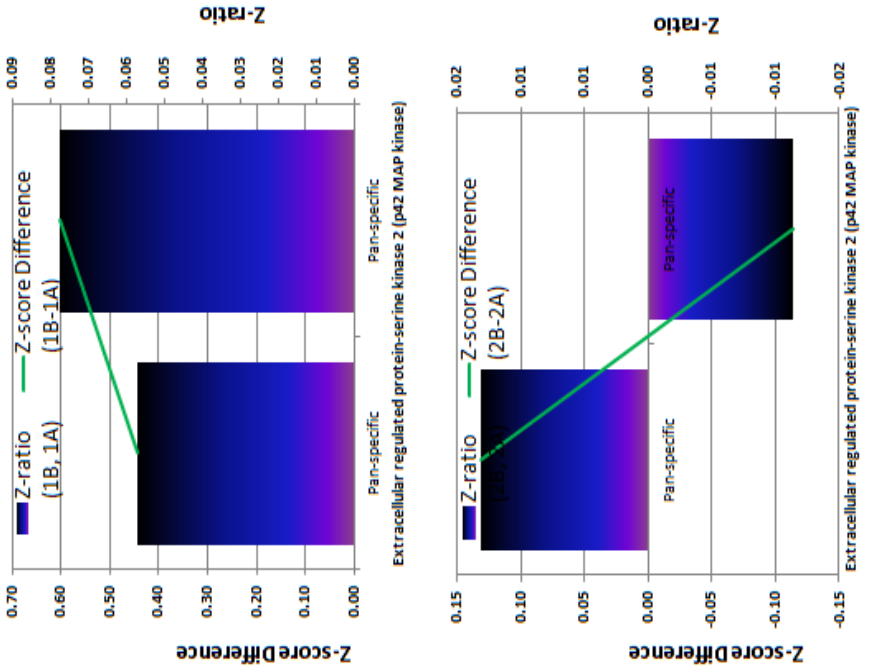

Figure 5.18 WISP-2 and ERK2 interaction in gastric tissues. The difference between cancer and normal tissues. Vertical bars are the Z-Ratio and greens are the Z-Score Difference between normal and tumour tissues. Top: patient ID1; Bottom: patient ID2. gastric cancer tissues.

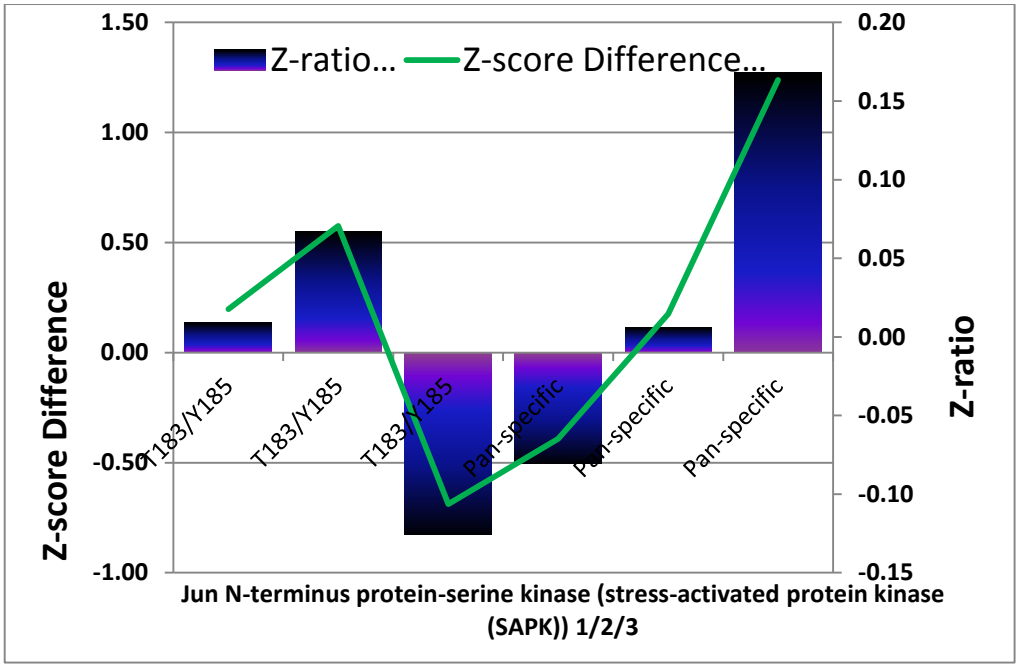

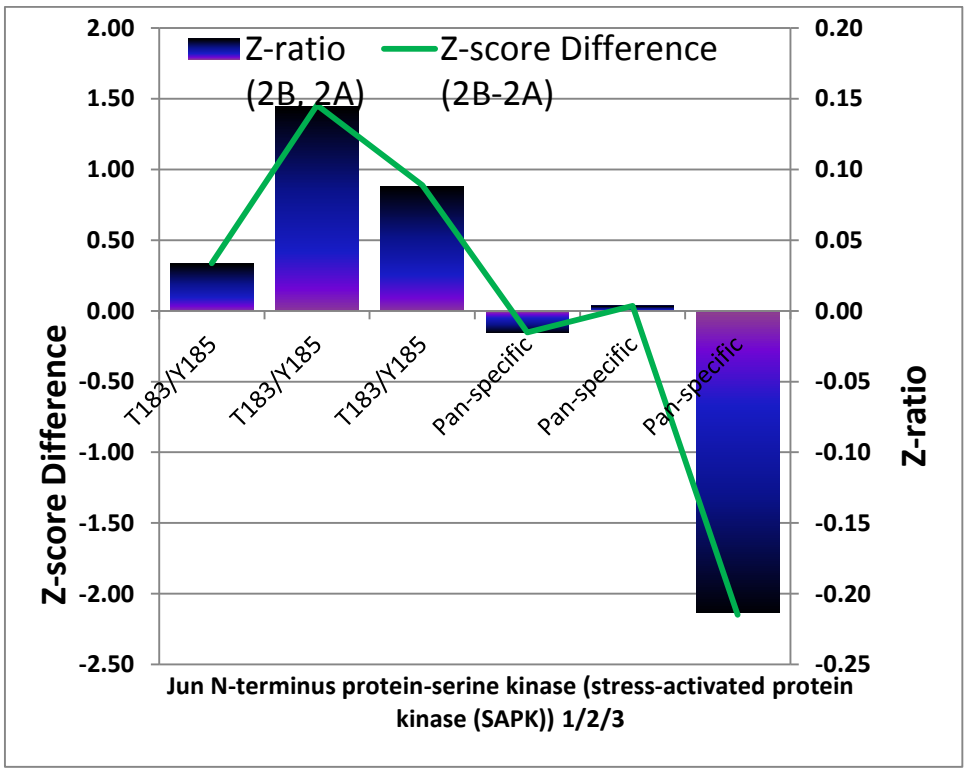

Figure 5.20 WISP-2 and JNK1/2/3 interaction in gastric tissues. The difference between cancer and normal tissues. Vertical bars are the Z-Ratio and greens are the Z-Score Difference between normal and tumour tissues. Top: patient ID1; Bottom: patient ID2.

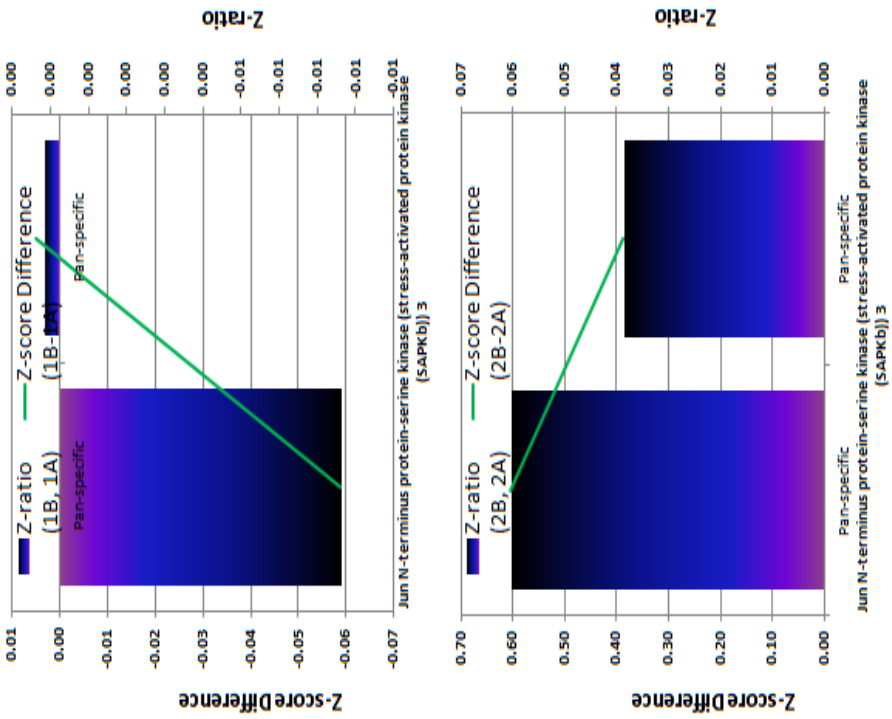

Figure 5.22 WISP-2 and JNK3 interaction in gastric tissues. The difference between cancer and normal tissues. Vertical bars are the Z-Ratio and greens are the Z-Score Difference between normal and tumour tissues. Top: patient ID1; Bottom: patient ID2.

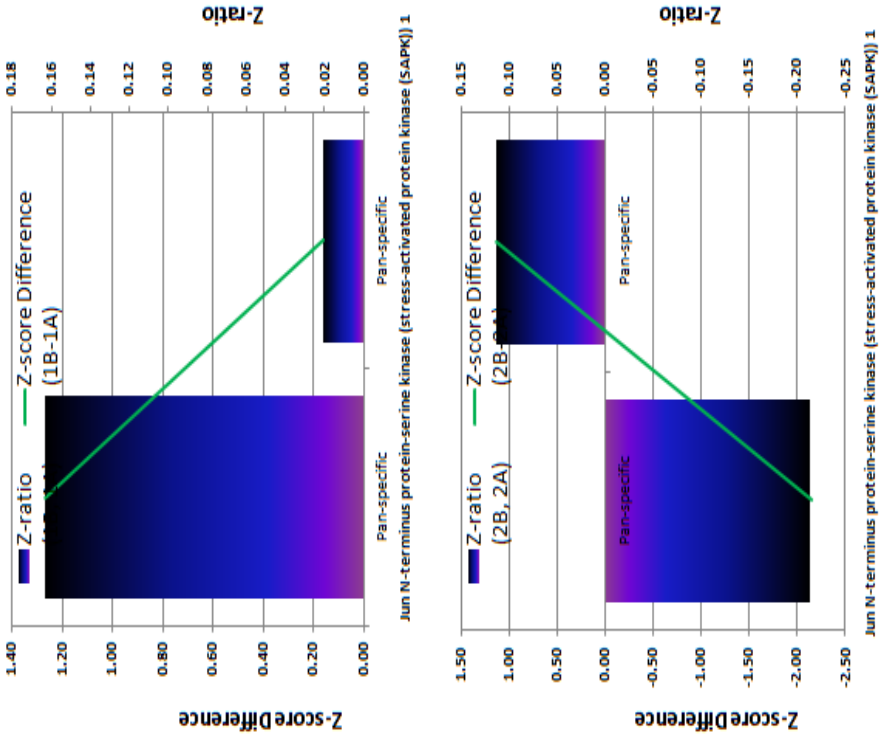

Figure 5.21 WISP-2 and JNK2 interaction in gastric tissues. The difference between cancer and normal tissues. Vertical bars are the Z-Ratio and greens are the Z-Score Difference between normal and tumour tissues. Top: patient ID1; Bottom: patient ID2.

5.3.4 Interaction of WISP-2 with AKT proteins

Previously, AKT1 has been shown to either response to WISP-2 challenge or be a potential downstream event of WISP-2 activation. Here, we analysed the potential interaction between WISP-2 and AKT protein in the paired normal and tumour gastric tissues.

WISP-2 interacted strongly with AKT1, in a similar fashion in normal and tumour tissues (Figure-5.23 and Figure-5.24). This was particularly so when pan-antibodies were used. Of the phospho-specific antibodies, WISP-2 seemed to interacted well with AKT1 phosphorylated on Y236 residue. The difference in comparing the interaction between the paired tissues proved inconclusive (Figure-5.25).

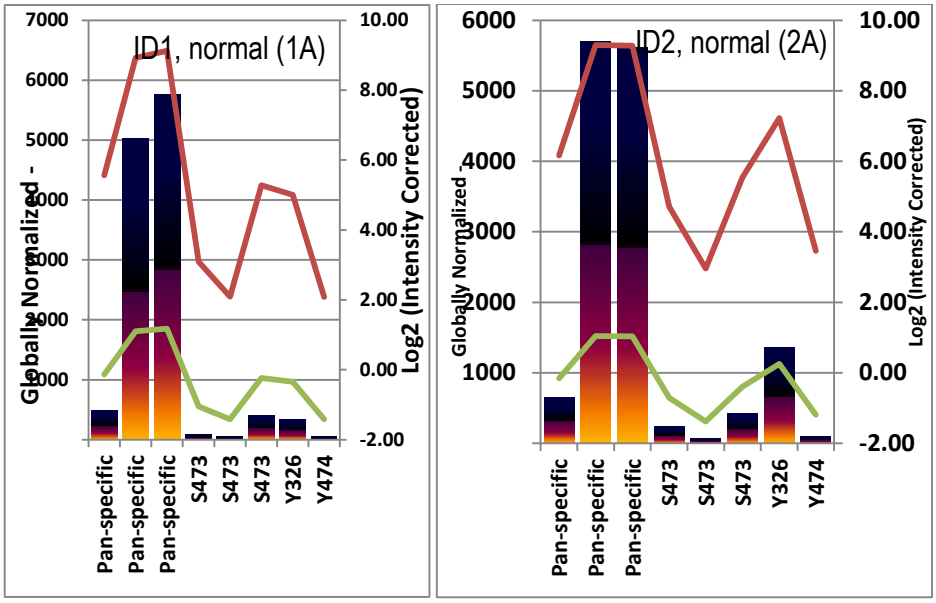

Figure 5.23 WISP-2 and AKT1 in normal tissues. The vertical bars show the levels of the AKT1 protein precipitated by anti-WISP-2 antibody after normalisation. The red line shows the levels of the signal in Log2 transformation and the green line shows the transformation that corrects data internally within a single sample. Left: first sample (1A); Right: the second sample (2A).

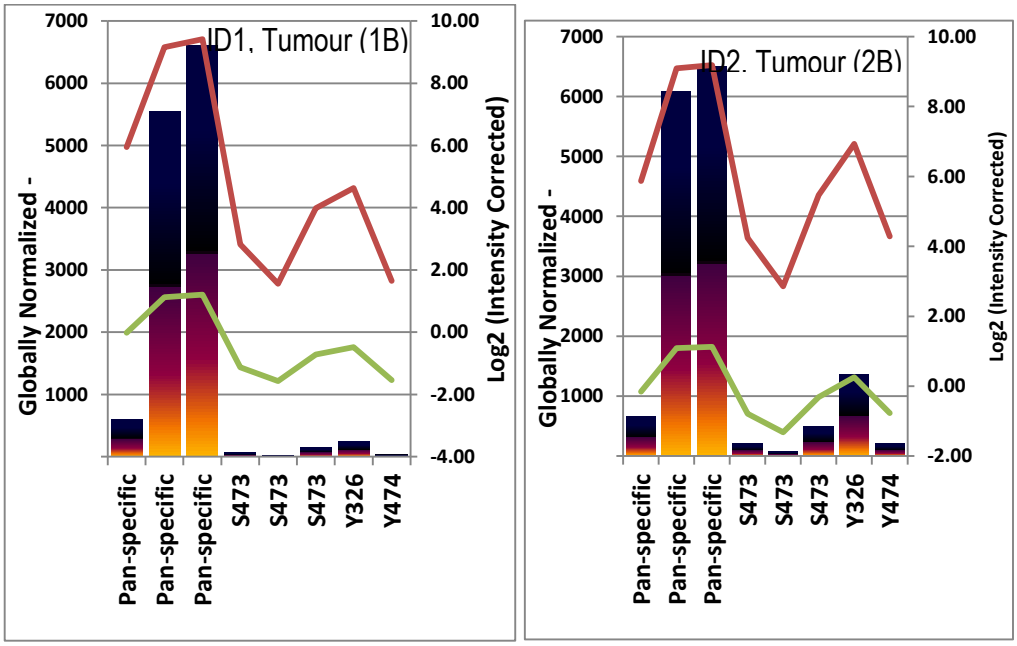

Figure 5.24 WISP-2 and AKT1 interaction in gastric tumour tissues. The layout is the same as Figure-5.23. Left: first sample (1B); Right: the second sample (2B).

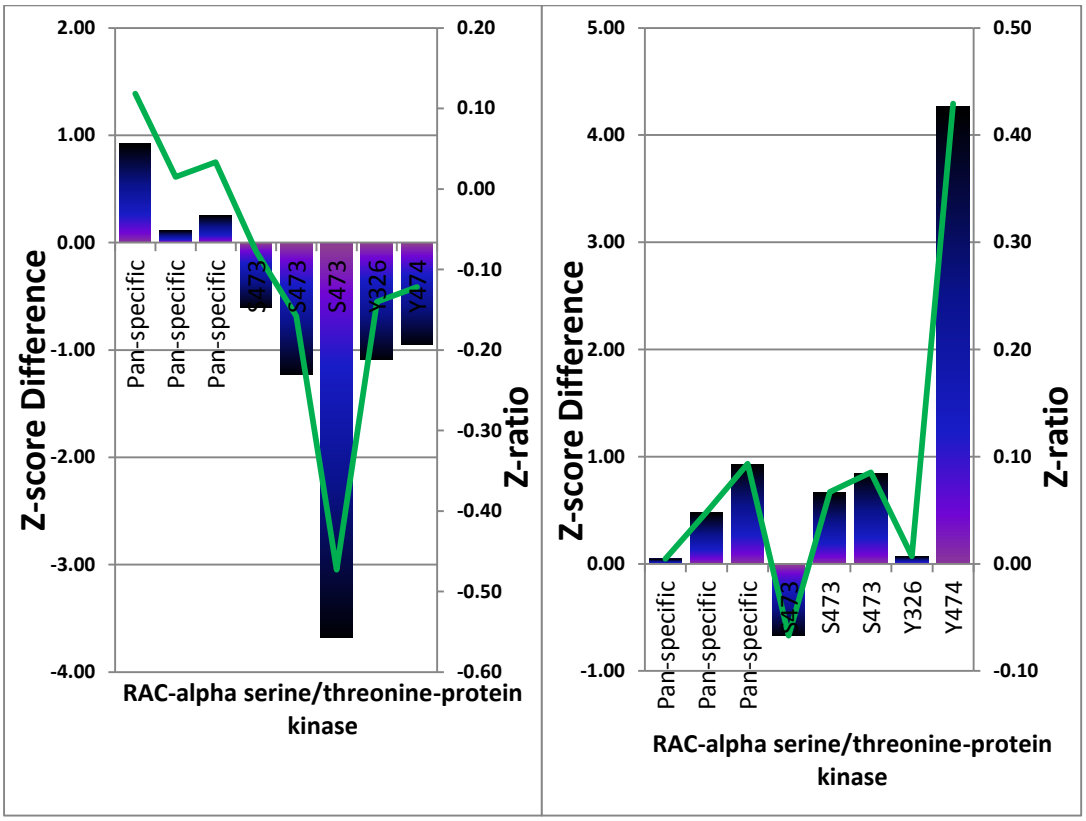

Figure 5.25 WISP-2 and AKT1 interaction in gastric tissues. The difference between cancer and normal tissues. Vertical bars are the Z-Ratio and greens are the Z-Score Difference between normal and tumour tissues. Left: patient ID1; Right: patient ID2.

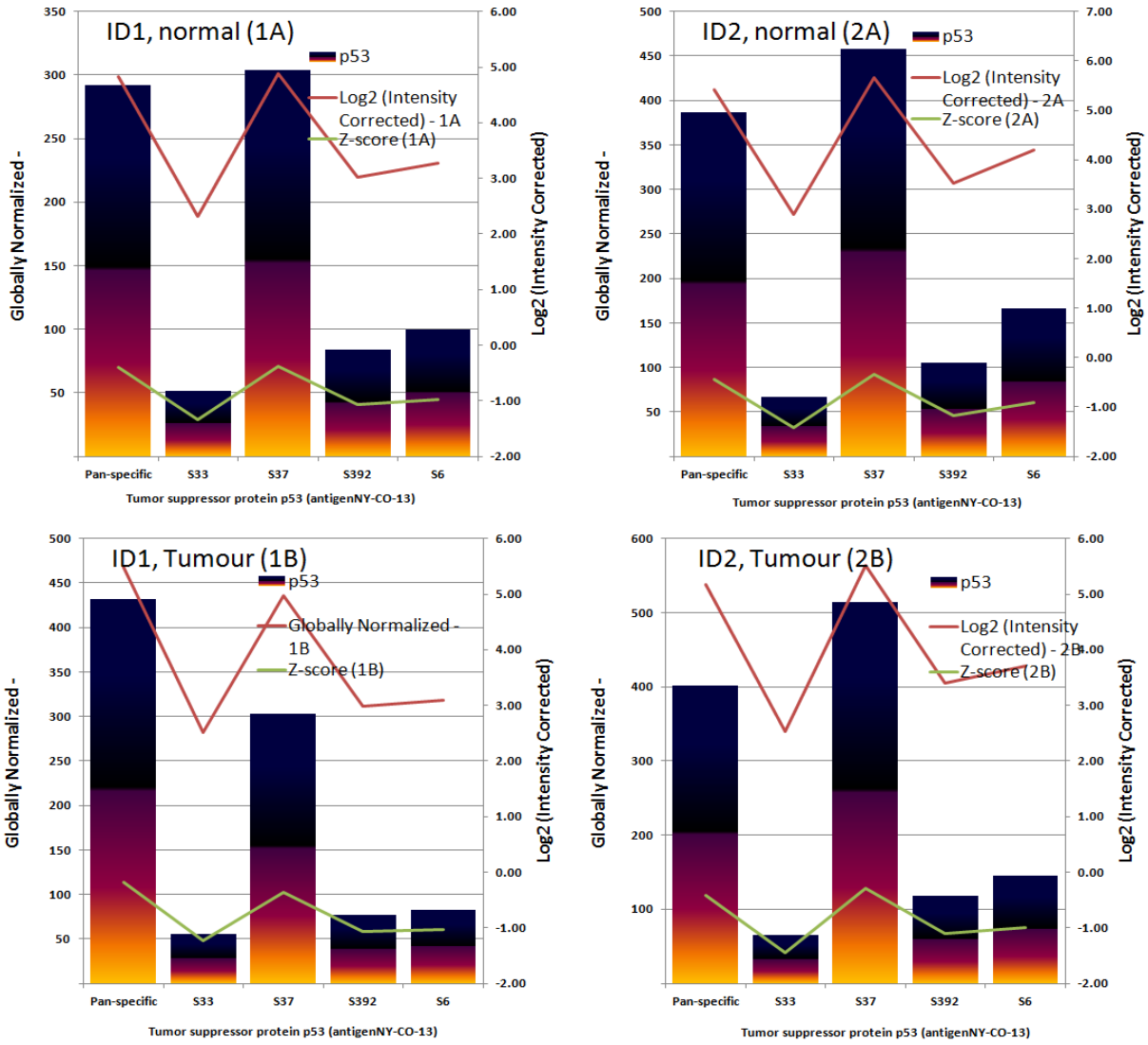

Figure 5.26 Possible interaction between WISP-2 and the p53 protein in gastric tissues. Results from phospho-specific antibodies and pan-specific antibodies recognised the total p53 protein (phosphorylated and non-phosphorylated) were plotted. The vertical bars show the levels of the p53 protein precipiated by anti-WISP-2 antibody after normalisation. The red line shows the levels of the signal in Log2 transformation and the green line shows the transformation that corrects data internally within a single sample. Top: Normal stomach mucosa; Bottom: gastric cancer tissues from both patients.

5.3.5 WISP-2 had little interaction with p53 protein

P53 is a well-established tumour suppressive protein. We also analysed the potential interaction between WISP-2 and p53. As shown in Figure-5.26, WISP-2 had very little interactions with p53, with the strength of the signal virtually below detection limit and Z-Score below zero.

5.3.6 Changes of key signalling event after WISP-2 knock down from gastric cancer cells

From the earlier section, we have identified some key proteins and phospho-specific proteins that potentially interacted with WISP-2 protein. In order to further explore if the signalling events associated with WISP-2 protein in a living cancer cells, we have used the cell models created in the early chapters, namely a WISP-2 knockdown model from gastric cancer cell lines. Here, we employed the AGS cell model, in which WISP-2 was knocked down by way of anti-WISP-2 transgene (Chapter-4). Using the protein microarray, we compared the difference in these key signalling molecules between the control cells and WISP-2 knockdown cells (Figure-5.27).

Change of ERK1 after WISP-2 knockdown. As shown in Figure-5.28 and Figure-5.29, knocking down WISP-2 resulted in a reduction in the total amount of ERK1 and indeed ERK1 phosphorylated on T202/Y204.

Change of ERK5 after WISP-2 knockdown. Different from ERK1, the difference in ERK5 levels between control and WISP-2 knockdown cells were not markedly different (Figure 5.30 and Figure 5.31).

Change of JNK1 after WISP-2 knockdown. Although knocking down WISP-2 had not changed the total levels of JNK1, it is however interesting to note that WISP-2 knockdown resulted in a marked increase in phosphorylation of JNK1 on T183/Y185 (Figure 5.32 and Figure 5.33).

Change of p53 after WISP-2 knockdown. It is interesting to observe that AGS cells had a good level of p53 protein (Figure 5.34). Knocking down WISP-2 from the cells resulted in a rise of p53 phosphorylation on the S37 as S6 sites (Figure 5.34 and Figure 5.35).

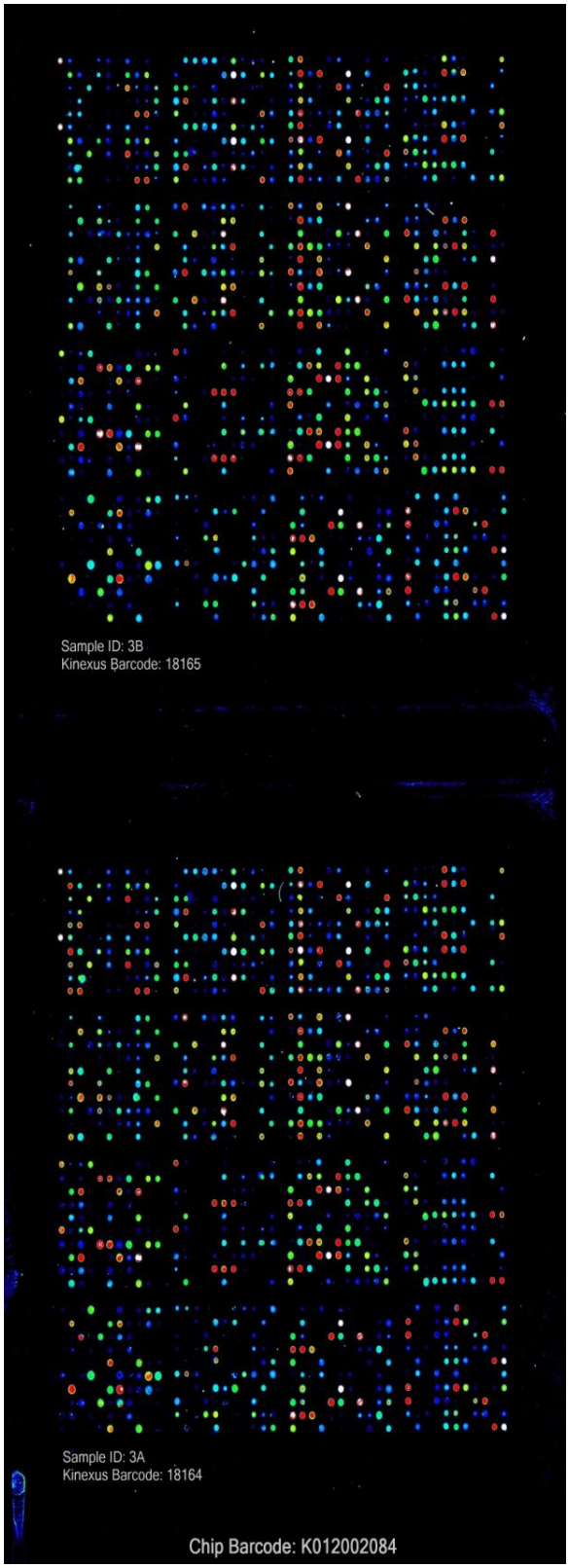

Figure 5.27 Images of the antibody microarray for AGS cell line (3A-Control cell; 3B- WISP-2 knock down cells).

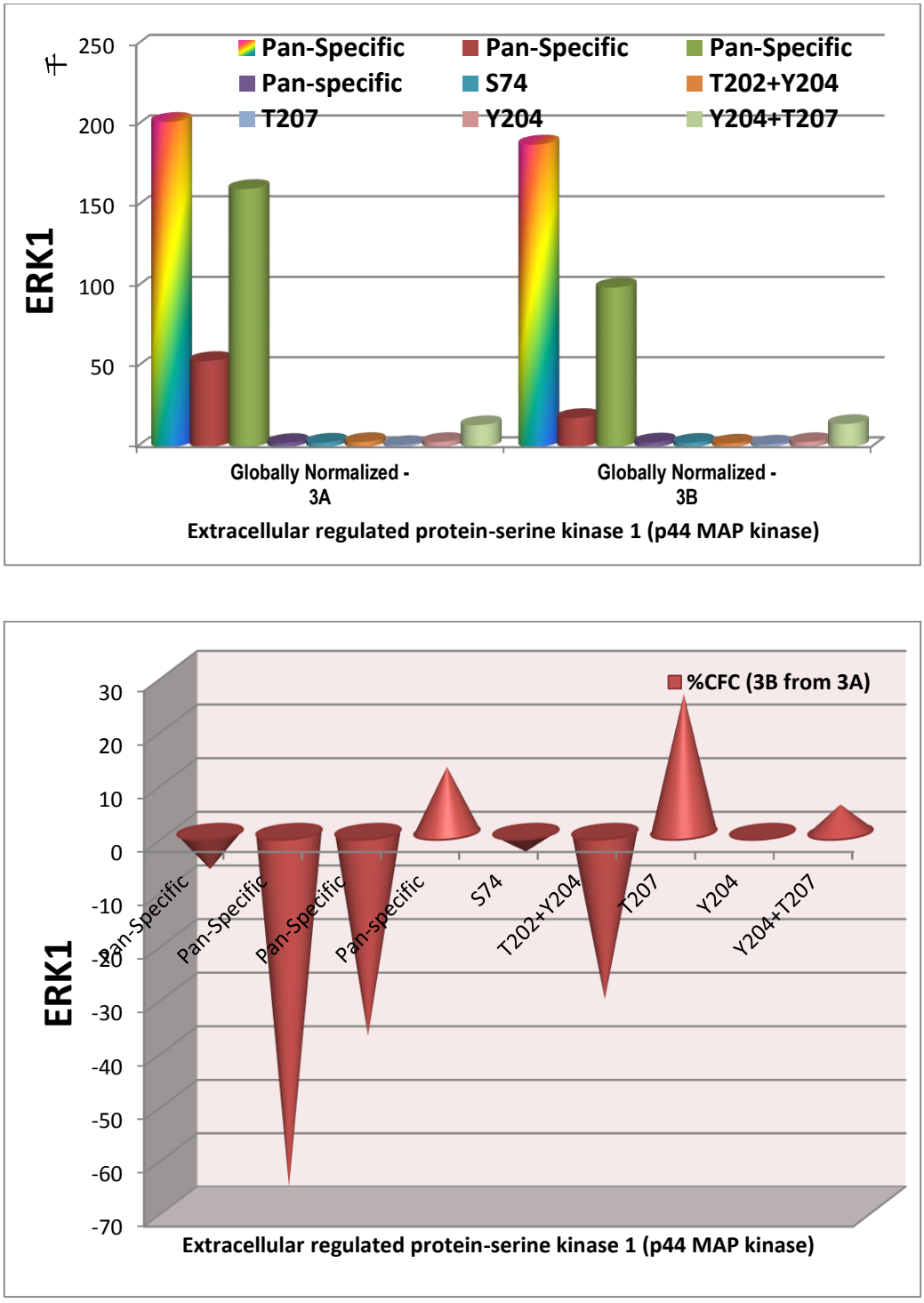

Figure 5.28 Levels of the ERK1 protein detected by KAM850 protein microarray in AGS human gastric cancer cells. AGS cells after WISP-2 knockdown (3B) and control transfected cells (3A) were compared. Top: Globally normalised signals of both cells detected by a panel of antibodies. Bottom: the difference between the two cells as defined as %CFC. Both cells had good levels of ERK1, although the total levels of ERK1 were reduced after the WISP-2 knockdown (bottom).

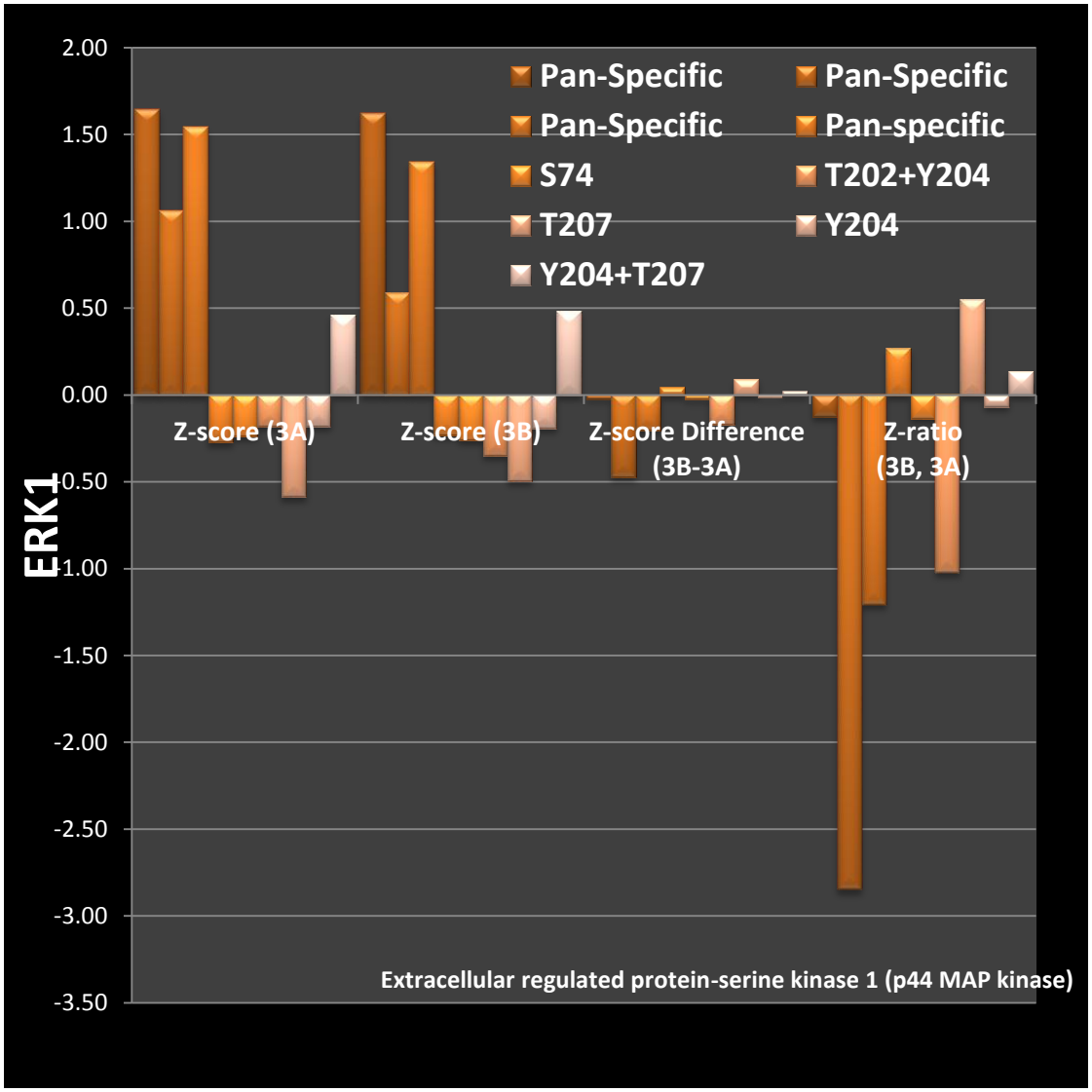

Figure 5.29 Change of levels of the ERK1 protein after WISP-2 knockdown. Z-Ratio has indicated that knocking down WISP-2 resulted in reduction of ERK1 and indeed ERK1 phosphorylated on T202/Y204 sites.

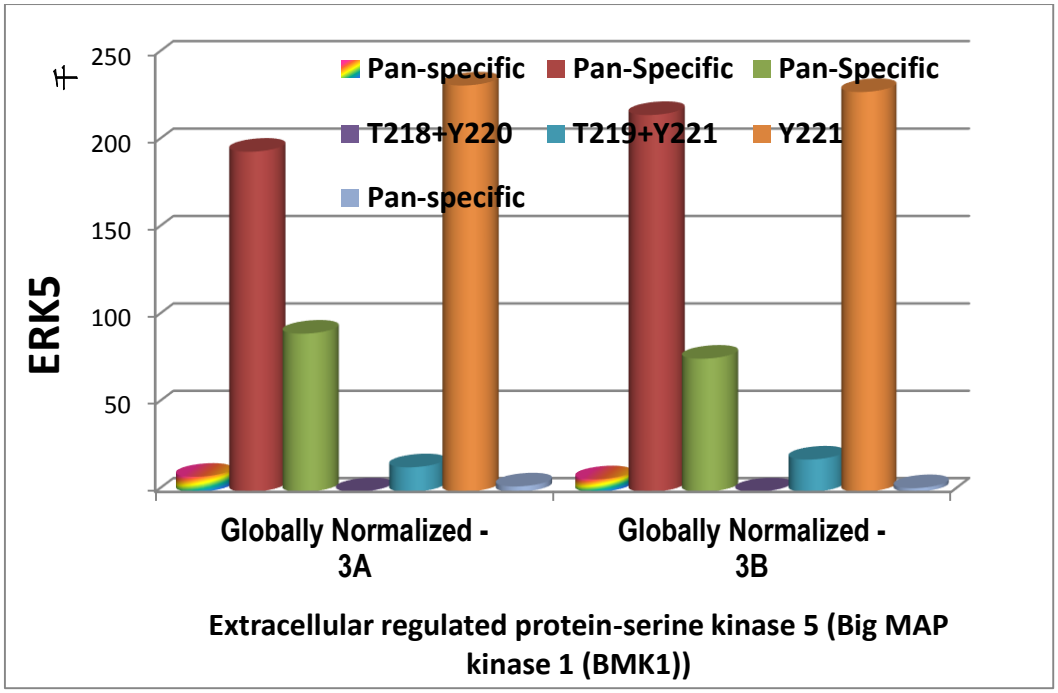

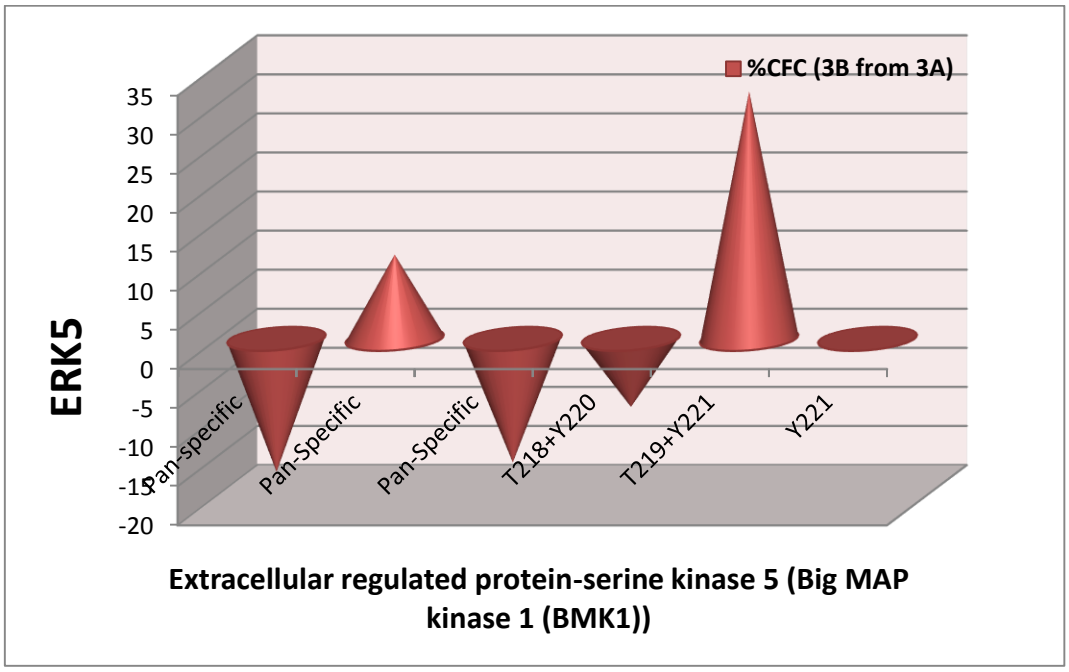

Figure 5.30 Levels of the ERK5 protein detected by KAM850 protein microarray in AGS human gastric cancer cells. AGS cells after WISP-2 knockdown (3B) and control transfected cells (3A) were compared. Top: Globally normalised signals of both cells detected by a panel of antibodies. Bottom: the difference between the two cells as defined as %CFC.

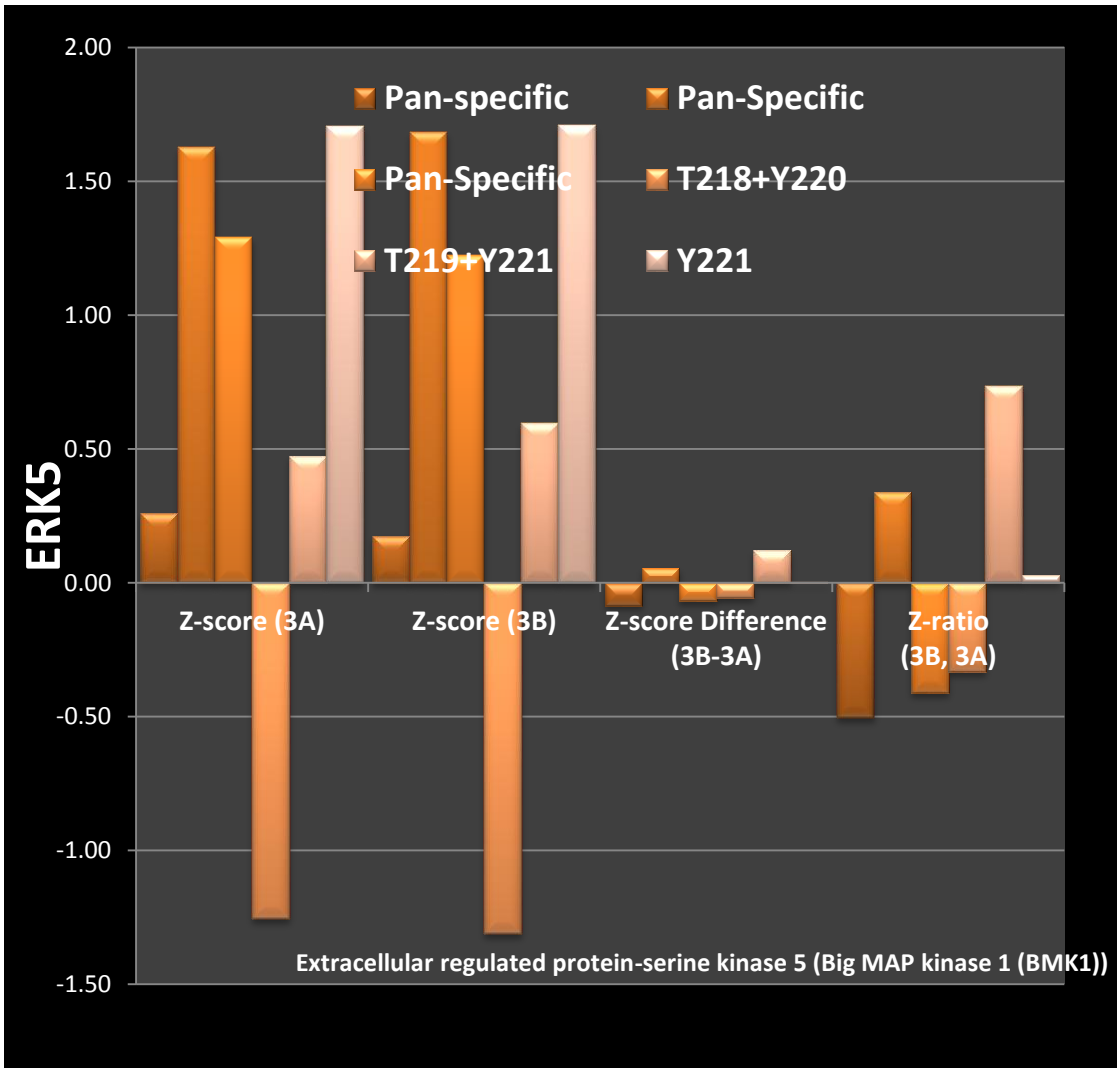

Figure 5.31 Change of levels of the ERK5 protein after WISP-2 knockdown, as shown by the Z-Ratio.

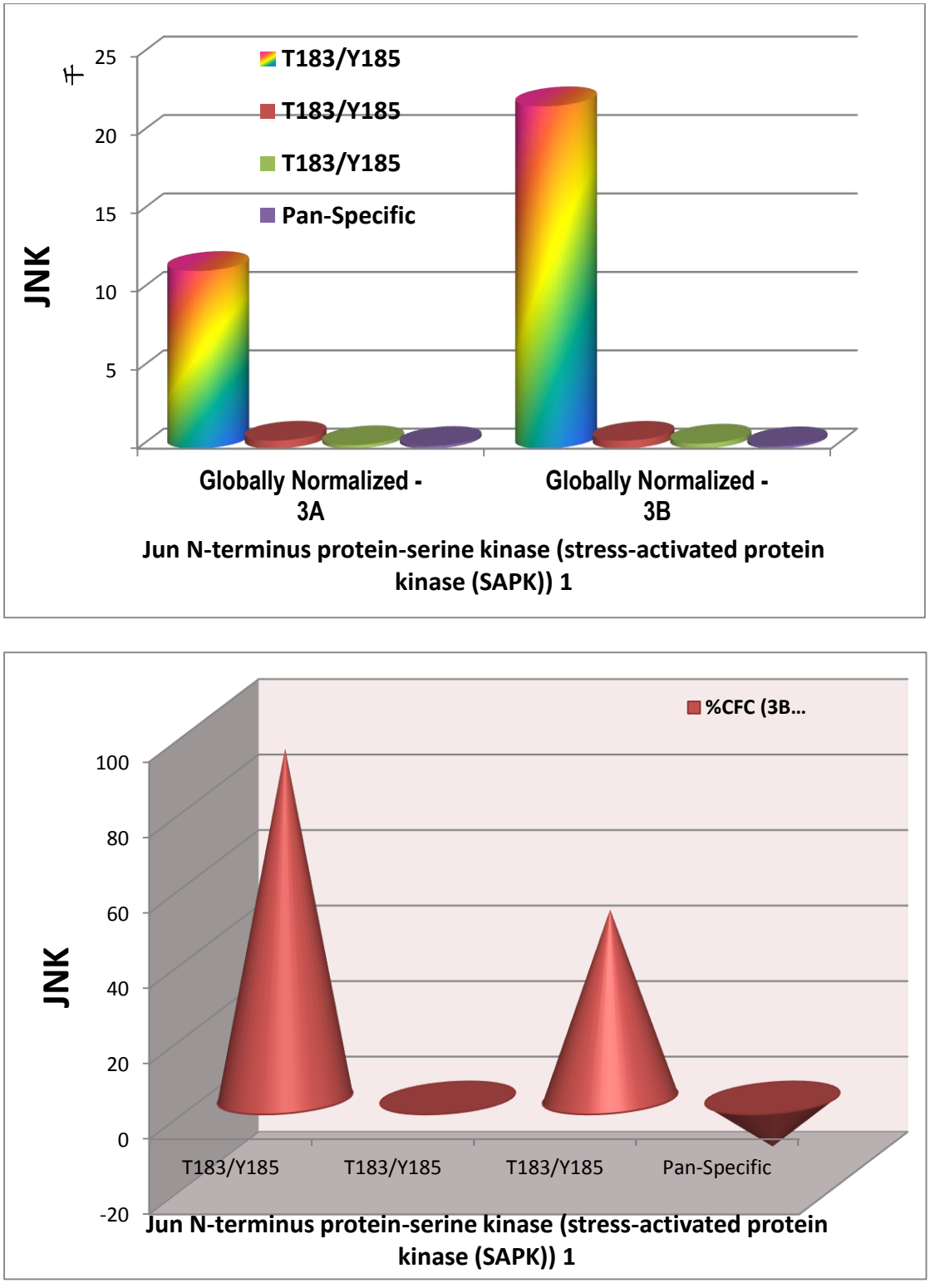

Figure 5.32 Levels of the JNK1 protein detected by KAM850 protein microarray in AGS human gastric cancer cells. AGS cells after WISP-2 knockdown (3B) and control transfected cells (3A) were compared. Top: Globally normalised signals of both cells detected by a panel of antibodies. Bottom: the difference between the two cells as defined as %CFC.

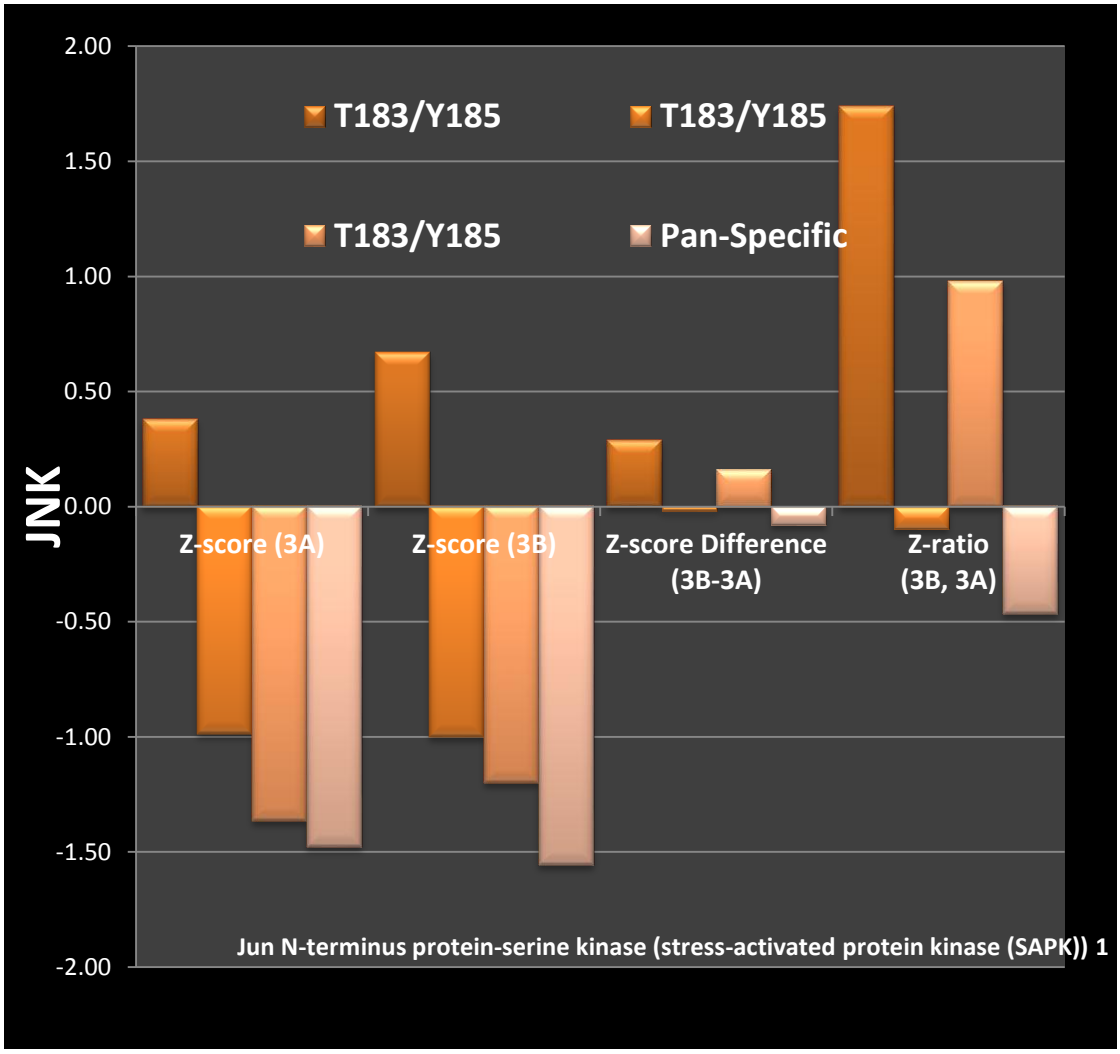

Figure 5.33 Change of levels of the JNK1 protein after WISP-2 knockdown, as shown by the Z-Ratio.

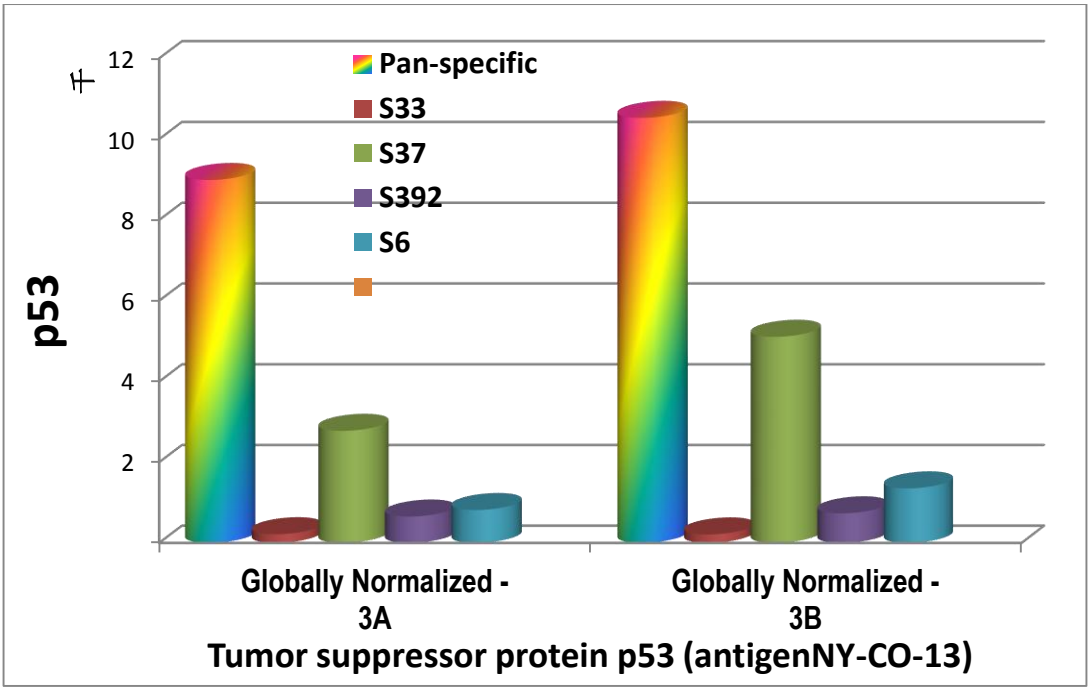

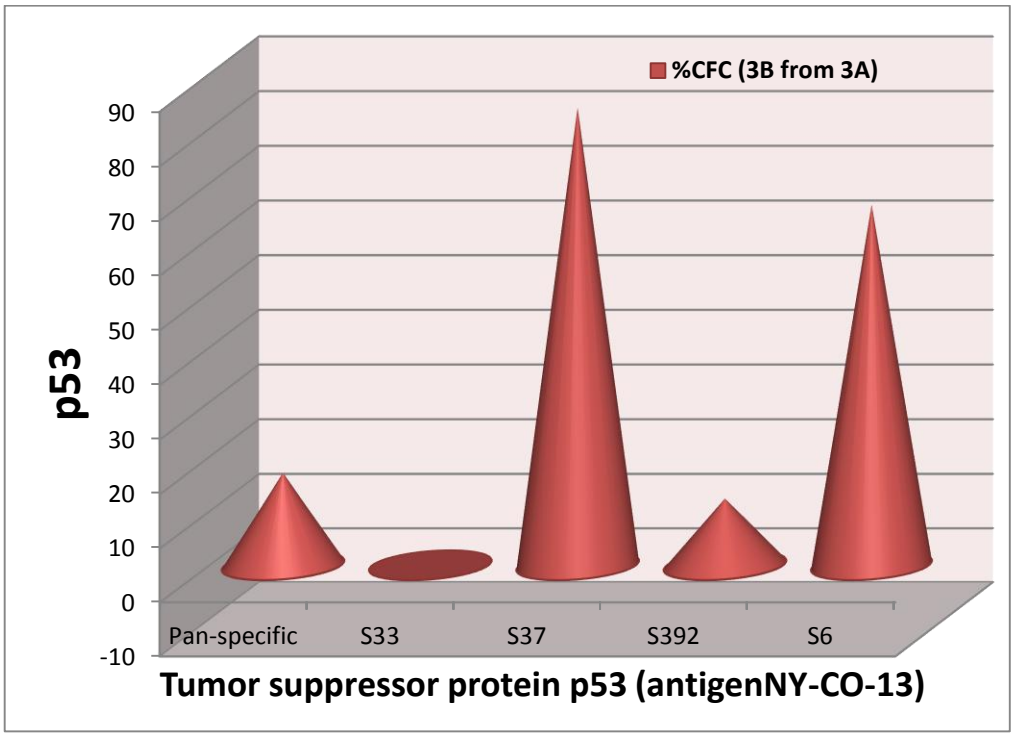

Figure 5.34 Levels of the p53 protein detected by KAM850 protein microarray in AGS human gastric cancer cells. AGS cells after WISP-2 knockdown (3B) and control transfected cells (3A) were compared. Top: Globally normalised signals of both cells detected by a panel of antibodies. Bottom: the difference between the two cells as defined as %CFC.

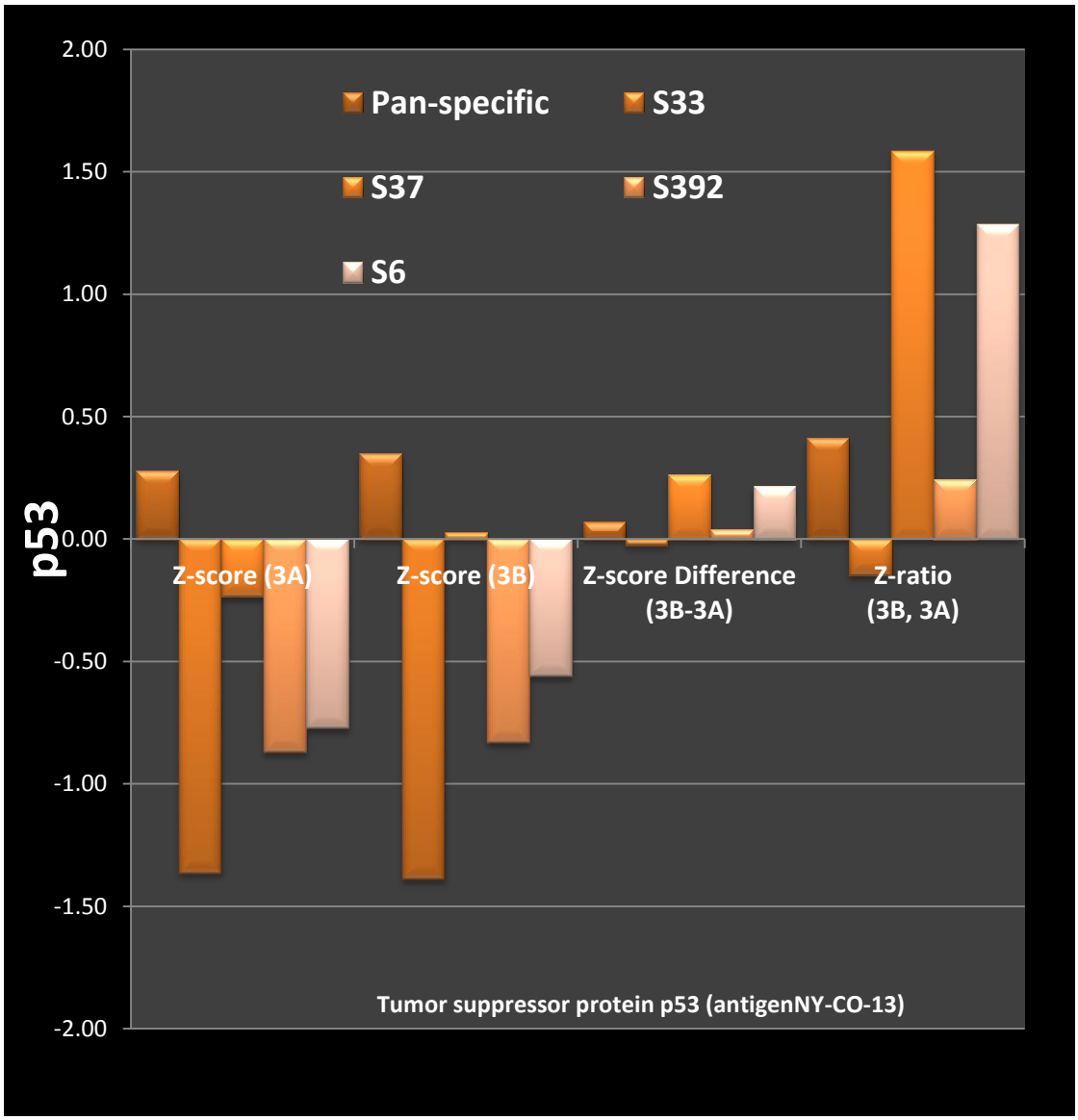

Figure 5.35 Change of levels of the p53 protein after WISP-2 knockdown, as shown by the Z-Ratio.

5.3.7 WISP-2 knockdown (kd) affected migration of HGC27 cell treated with JNK and FAK inhibitors

From the data obtained in the KAM850 antibody protein microarray assay, it was clear that first, WISP-2 interacted with the JNK protein in the protein preparations from human gastric cancer tissues and second, knockdown WISP-2 from human gastric cancer cell lines had a marked effect on JNK pathway. On this observation, here we further evaluated cell's response to JNK inhibitor in control and WISP-2 knockdown cancer cells.

After small inhibitor JNK Ⅱ (1.5μM) was added into the cells, the motility of HGC27 WISP-2 kd decreased obviously than the control cells (P <0.05) (Figure 5.36).

The protein microarray demonstrated that WISP-2 did not interact with WISP-2, or at least not at a high level and that WISP-2 knockdown from AGS cells did not result in significant change with FAK. As a negative control, FAK small inhibitor (1.5μM) was also tested. As shown in Figure 5.37, there was no effect on both cells (P>0.05).

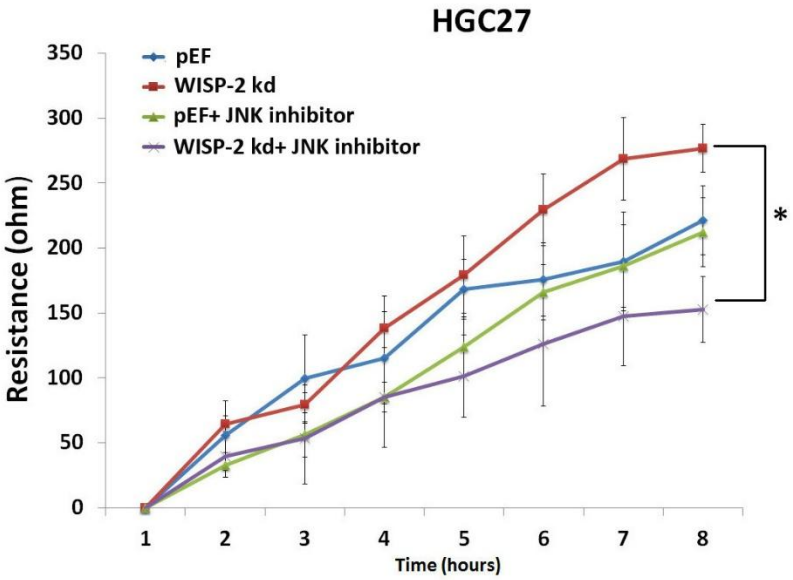

Figure 5.36 The knockdown of WISP-2 in HGC27 cells resulted in increased cell motility via JNK pathways (1.5 μM JNK inhibitor). Overall changes of resistance on the sixth hour with statistical analysis. *, $p < 0.05$.

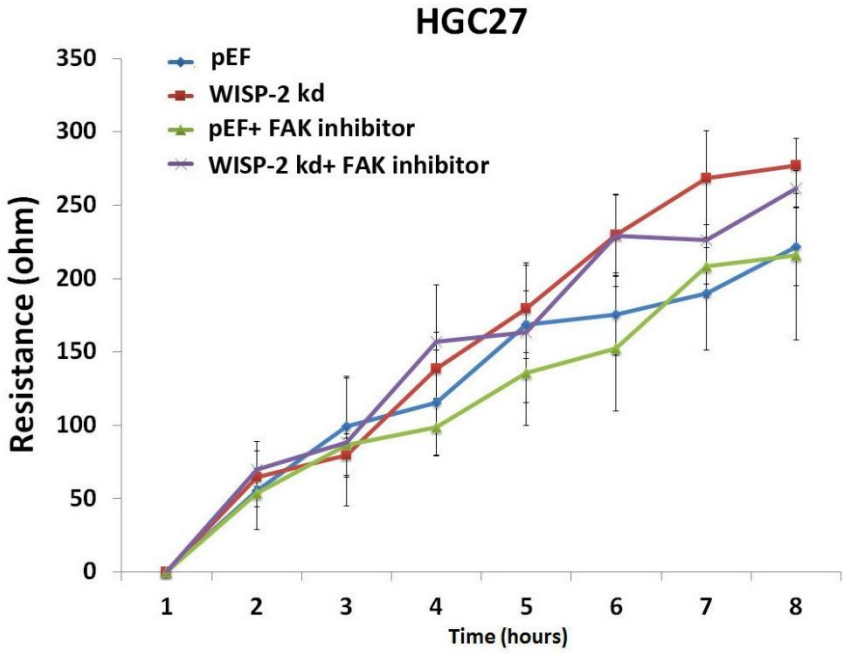

Figure 5.37 The knockdown of WISP-2 in HGC27 cells had no effect on cell motility via FAK pathways.

5.4 Discussion

Following the findings from the earlier chapters that WISP-2 has a significant link to the disease stage, patients survival and, in particular to the cells functions in gastric cancer, one of the key questions arising was how WISP-2 participated in the regulations of the cellular functions, which in turn contributed to the clinical links.

WISP-2 is protein present both intracellularly and extracellularly. As discussed in Chapter-1, the protein has a IGF binding domain, a cystine knot-like domain, a von Willebrand factor type C and a thrombospondin domain. The protein has been implicated in the regulation of cell growth, cell migration and cell adhesion, as indeed shown in the study presented in Chapter-4. Here, we attempted to explore the proteins and siganalling molecules that are potentially associated with WISP-2, by way of an antibody based protein microarray, namely KAM850. KAM850 is a recently developed protein microarray with over 850 antibodies spotted on the slides.

We have first used an immunoprecipitation method, with a specific antibody to human WISP-2, to pull out the proteins from gastric tissues that are interacted with WISP-2. From the data available on the array, we have focused on the potential pathways/proteins that are associated with the key cell functions, shown to be altered by WISP-2, namely cell growth, adhesion and migration as presented in Chapter-4. We found the levels of the ERK protein family, namely ERK1 and ERK5, and JNK1 protein are highly associated with WISP-2, as demonstrated by the level of fluorescence signal on these proteins. Furthermore, the other protein known to be associated with WISP-2, namely AKT1 has also been found to be highly associated with WISP-2. Thus, the ERK pathway, the JNK pathway and AKT pathway appear to be key to the function of WISP-2 in gastric cancer. This is indeed confirmed in the cell based study, in which after

knocking down WISP-2 in AGS cells, the levels of these proteins have changed in a similar fashion. The link between WISP-2, ERK or JNK proteins has been further strengthened by the observation that the changes of the protein interactions are also seen with the changes in the interaction with phosphorylated proteins.

ERK, JNK and AKT pathways are essential pathways in cells. Within the cells, they coordinate a complex framework of intracellular pathways, which participate a rather wide range of cell functions. Shown in Figures-5.38-5.41 are examples plotted based on the current data set at the Kinexus Phosphonet website (www.phosphonet.ca). These pathways would warrant further investigation. WISP-2 has multiple phosphorylation sites at shown in Figure 4.42. With which sites of WISP-2 protein that the newly identified proteins remain to be further investigated.

We also attempted to compare if the interaction between WISP-2 and the partner proteins differs in normal and tumour gastric tissues. In general, the interaction pattern does not vary very much in normal and tumour gastric tissues. This is interesting, as one would argue that the changed protein expression profile in tumour tissues may cause a difference in the interaction. This has not been proven to be a firm case, which may be due to the possibility that this has no difference in reality, that expression level in WISP-2 protein differs in normal and tumour (as shown in Chapter 3), and/or that that the study would require a substantially larger cohort to test this possibility. Limited by the time and resource on this expensive technique, it is not possible to clearly answer this question. We have a follow on study planned for the immediate future.

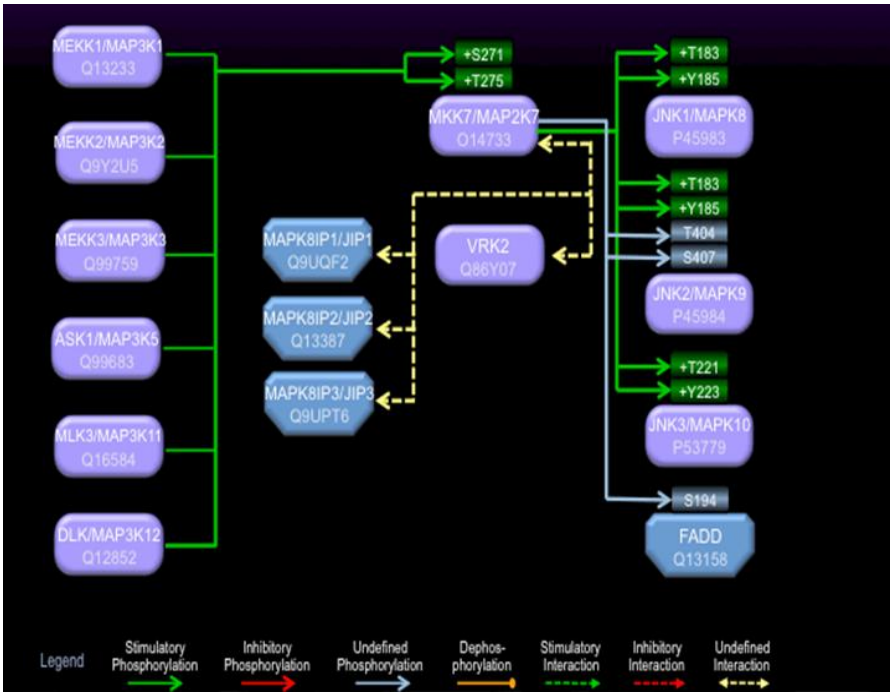

Figure 5.38 The potential interaction between phospho-JNK proteins with other signalling proteins, namely MAKP8/JIP and MKK7. Figure generated by Kinexus^{TM}, based on the KAM850 phosphoprotein array (www.phosphonet.ca).

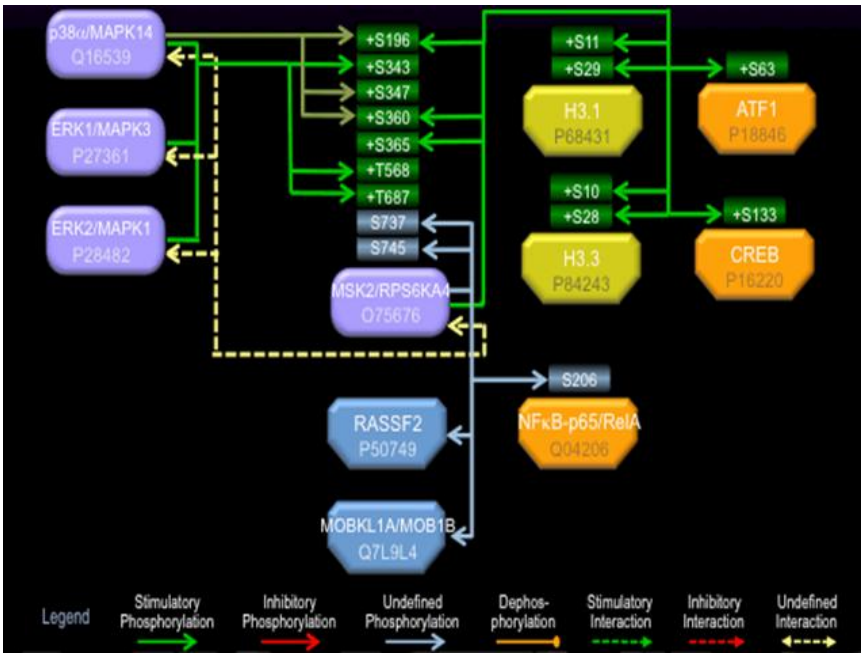

Figure 5.39 The potential interaction between phospho-ERK proteins with other signalling proteins, namely, MSK2, ATF and Creb, a group of transcription factors. Figure generated by Kinexus^{TM}, based on the KAM850 phosphoprotein array (www.phosphonet.ca).

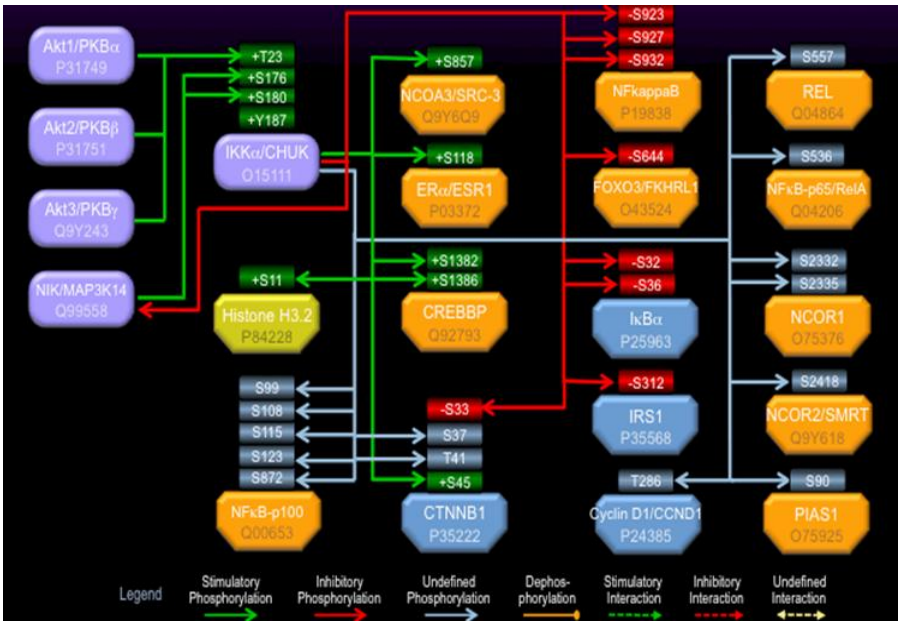

Figure 5.40 The potential interaction between phospho-AKT proteins with other signalling proteins, namely IKK and other signalling proteins. Figure generated by Kinexus^{TM}, based on the KAM850 phosphoprotein array (www.phosphonet.ca).

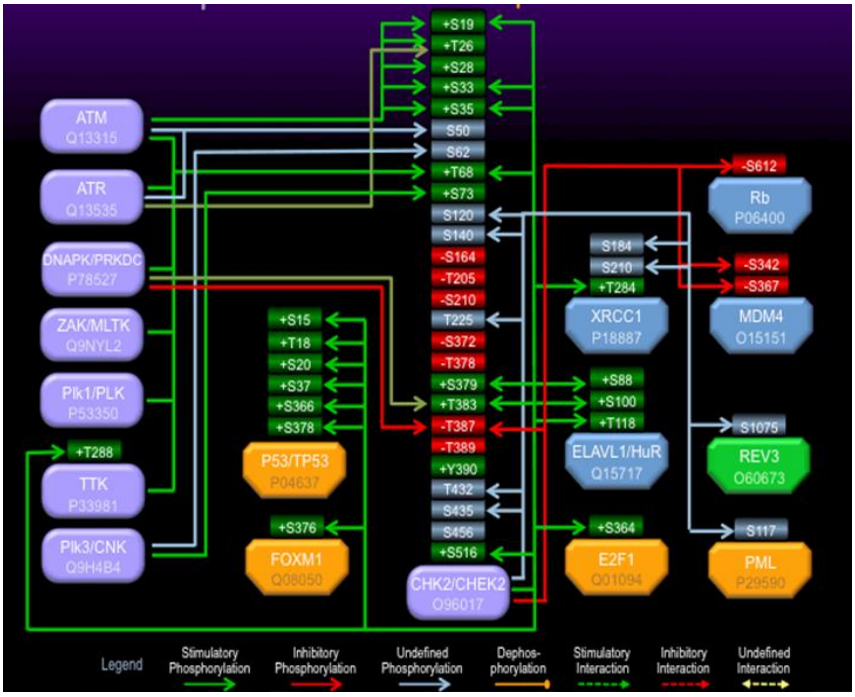

Figure 5.41 The potential interaction between phospho-p53 proteins with other signalling proteins. Figure generated by Kinexus^{TM}, based on the KAM850 phosphoprotein array (www.phosphonet.ca).

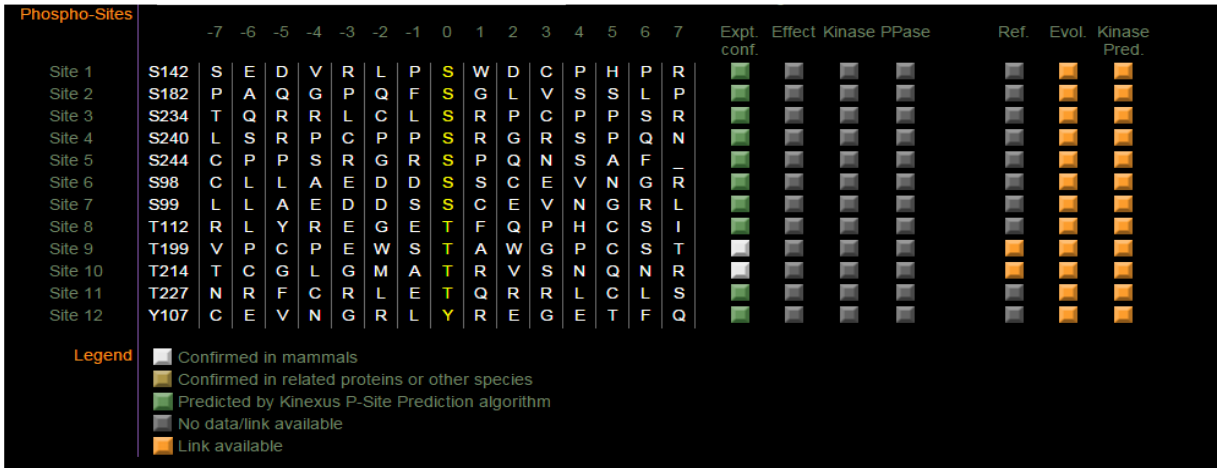

Figure 5.42 The potential phosphorylation sites of WISP-2, generated from (www.phosphonet.ca).

WISP-2 modification has an influence on cell growth. We have analysed another available set of information on p53, a tumour suppressor protein and known to widely regulate cell growth and death. To our surprise, the level of p53 interacted with WISP-2 was very low, about one hundredth of that seen with ERK, JNK and AKT. This could suggest that there is no direct or indirect interaction between WISP-2 and p53.

It is interesting to note that WISP-2 did not have significant interaction with FAK. Modification of expression of WISP-2 in gastric cancer cells clearly resulted in changes in cell migration and cell adhesion as demonstrated in chapter-4. Both cellular migration and matrix adhesion require the participation of integrins, a group of transmembrane proteins that mediate the interaction between cells and extracellular matrix. Central to the regulation of integrin mediated cell-matrix adhesion and migration is FAK, a protein kinase mediating the extracellular and intracellular events within the cells. Upon the interaction between matrix proteins and integrins, FAK is activated by way of phosphorylation. Via the interaction with the downstream signalling molecules, it regulates the cytoskeletal and cytoskeletal associated proteins which in turn mediate the adhesion and migration of the cells. The data presented here suggests that the

WISP-2 influence on adhesion and migration either are not involved in FAK or may be involved in the downstream of FAK. For example, both AKT and JNK pathways are downstream of FAK and both interact with WISP-2 and is markedly affected after WISP-2 knockdown. It is plausible therefore that the impact of WISP-2 on cell adhesion and migration are via the pathways downstream of FAK.

From the foregoing, this part of the investigation has revealed that WISP-2 strongly interacts with JNK pathway. We tried to detect the difference of cell migration between the HGC27 cells treated with JNK inhibitor and the cells without treatment. Through the analysis of ECIS assays, we focused on the investigation of the involvement of the JNK, ERK and FAK on cell migration. As shown in Figures 4.17 and 4.18, the WISP-2 knockdown cells treated with JNK inhibitor showed a significant decrease of migration ability compared with the control groups. It validated again the previous conclusion of the inhibitory effect of WISP-2 on the migration ability of gastric cancer cells using wounding assays. What is more, it pointed out the inhibitory influence of WISP-2 on cell migration via the JNK pathway. Furthermore, there was not any significant difference between the cells treated with FAK inhibitor and the control cells.

Given that there has been previous report on the role of AKT in the action of WISP-2, we decided to focus on the next stage study on the ERK and JNK pathway in gastric cancer cells, in the context of WISP-2. The results are presented in the next two Chapters. The nature and implications of these two pathways are also to be discussed in the following two chapters.

Chapter 6

Knockdown of WISP-2 increased the expression and activity of MMPs via JNK and ERK pathways

6.1 Introduction

Metastasis is the most life-threatening complication of solid tumours [276]. The multistep process of tumour development involves the cell acquiring new phenotypic traits, including overriding growth controls, induction of angiogenesis, evasion from host anti-tumour responses, extravasation and growth at metastatic sites etc. under the influences of successive genetic alterations and environmental impact. In patients with solid tumours, the main cause of death is not the primary neoplasm, but its metastasis in vital organs [263]. The overall growth behaviour of a developing neoplasm is a net result of the combined kinetic interactions among of the heterogenous tumour cells. Intriguingly, the dominating influence of migration on tumour growth is dependent on the balance between tumour cell proliferation and death [264]. During metastasis, a number of process occurs, including EMT, migration and invasion, anoikis resistance, extravasation and organ colonisation. Therefore, a clear understanding of tumour metastasis and the role played by metastasis suppressor genes in regulating this cascade are important [277]. WISP proteins (WNT1-inducible signalling pathway proteins) are a subfamily of the CCN super family [189]. As a subset of the extracellular matrix (ECM), WISP proteins modulate various cellular activities, such as cell growth, differentiation, invasion, migration [265]. WISP-2 has been related to tumorigenesis and malignant transformation, especially in breast cancer [211, 222], colorectal cancer [212] and heptocarcinoma [227]. However, it appears that the WISP-2 functions are tissue-specific and influenced by the tumour microenvironment. Furthermore, it has been speculated that WISP-2 is acting as a dominant negative regulator of other CCN family members, due to its structural difference with other WISP members. However, the mechanism of the metastasis suppressor function of WISP-2 remains unknown. Sengupta *et al* [215] found that the upregulation of WISP-2 by phorbol ester is mediated through a complex PKCα-MAPK/ERK and MAPK/JNK signaling pathway, which leads to growth stimulation of MCF-7 breast tumour cell.

In Chapter-4, it was shown that there was a significant effect of WISP-2 knockdown on the migration and invasion of gastric cancer cells. Chapter-5 demonstrated an intimate link between WISP-2 protein and the JNK, ERK and AKT pathways. In the light of previous study, the current chapter investigated if WISP-2 had an impact on MMP-9 and MMP-2, known as the most important protease related with the invasion and cellular migration of cancer cells and JNK/ERK pathway [278], and explored how JNK and ERK signaling pathway played a role in the regulation of MMP expression.

6.2 Materials and methods

6.2.1 Cell lines

AGS and HGC27 cell lines were routinely cultured in DMEM-F12 medium as described in Chapter 2.

6.2.2 Chemicals

Anti-GAPHD antibody was from Santa Cruz Biotechnologies Inc. A PLC-γ specific inhibitor STK-870702, also known as3-amino-N-(3-chlorophenyl)-5-oxo-5,6,7,8-tetrahydrothieno[2,3-b]quinoline-2-carboxamide was purchased from Vitas-M Laboratory, Ltd (Cat number: STK870702) (Leung *et al* 2014) and a generic PLC inhibitor, U73122 was from Tocris (Bristol, UK); The FAK inhibitor (PF573228, Cat Number: 3239) was from Tocris Bioscience; JNKII inhibitor (SP600125, Cat Number: 420119) was from Merck; N-WASP inhibitor (Wiskostatin, Cat Number: 681525) was from Calbiochem. The MMP-9 inhibitor (Marimastat, Cat number: 2631) and MMP-2 inhibitor (ARP100, Cat number: 2621) were both from Tocris Bioscience; Matrigel was from BD Bio-Science (Cat Number: 354234, BD Bio-Science, Oxford, UK).

6.2.3 Generation of WISP-2 ribozyme transgenes

Hammerhead ribozymes targeting WISP-2 were designed on basis of the secondary structure of WISP-2 mRNA and synthesized following the method described in Chapter 2.

6.2.4 Generation of WISP-2 knockdown in gastric cancer cell lines

The plasmids were transfected into gastric cells through by the electroporation at 310V. Subsequently, the cells were placed into 5 μg/ml blasticidin selection for a sufficient period to kill cells which did not contain the plasmid. Empty plasmid vectors were used to transfect the cells as control. The verification of WISP-2 in the transfected cells was done using RT-PCR, Q-PCR and Western blotting as described in Chapter 4.

6.2.5 Gelatin zymography assay

To test the activity of type IV collagenases MMP-2 and MMP-9, which are of the most important type of MMPs, $1x10^6$ Cells were seeded into a 25 cm^2 culture flask and incubated overnight. Following incubation, cells were washed once with sterile 1x BSS followed by a wash with serum-free DMEM and then either incubated in serum-free DMEM control or treated medium for 6 hours. In this study, we treated cells with 200nM of JNKII or ERKII small inhibitors respectively. After 6 hours, the conditional medium was collected and samples were prepared in non-reducing sample buffer and separated using SDS-PAGE gels containing 1% gelatine (Sigma-Aldrich Inc, USA). After renatured for 1 hour at room temperature in washing buffer containing 2.5% Triton X-100 and 0.02% NaN_3, the gels were then incubated

at 37℃ in incubation buffer for 36 hours. Following incubation, the gels were stained with Coomassie blue for 1 hour and washed in destained buffer for another 1 hour. The gels were analysed using densitometry.

6.3 Results

6.3.1 The expression of MMPs in HGC cells

RT-PCR showed the expression of MMP1, 2, 3 and 9 were increased in HGC27 WISP-2 kd cells and there was no obvious difference of MMP7 compared with controls. Expression of MMP7 was downregulated in AGS WISP-2 kd cells, MMP1, 2, 3 and 9 were upregulated, however, there was no obvious expression of MMP-2 in AGS WISP-2 kd cells compared with controls (Figure 6.1).

6.3.2 WISP-2 knockdown resulted in increased enzymatic activity of MMPs via JNK and/or ERK pathways

MMPs (matrix metalloproteinases) are key proteins implicated in ECM remodelling and degradation by metastatic cells [279]. WISP-2 Knockdown resulted in an up-regulation of MMP-9 in AGS WISP-2 kd cells, and MMP-9 and MMP-2 in HGC27 WISP-2 kd cells, which were consistent with increased invasiveness in both cells. We further treated both cells with 200 nM JNKII and ERKII small inhibitor, respectively. The elevated MMP-9 activity in AGS WISP-2 kd cells was reduced after treatment with ERK and JNK inhibitors. However, the elevated MMP-9 and MMP-2 activity in HGC27 WISP-2 kd cells was reduced only by JNK inhibitor, but not ERK inhibitor (Figure 6.2 and 6.3).

6.3.3 WISP-2 knockdown (kd) affected invasion of AGS cell treated with MMPs inhibitors

WISP-2 knockdown influenced invasiveness of AGS cells treated with MMPs inhibitors. Figure 6.4 shows AGS cells with WISP-2 knockdown after treatment with MMP-9 inhibitor (Marimastat) significantly decreased in invasiveness (p= 0.025) compared with AGS WISP-2 knockdown cells with no treatment. While the group treated with ARP100 did not demonstrate a significant change on cell invasion compare with the control group (p> 0.05).

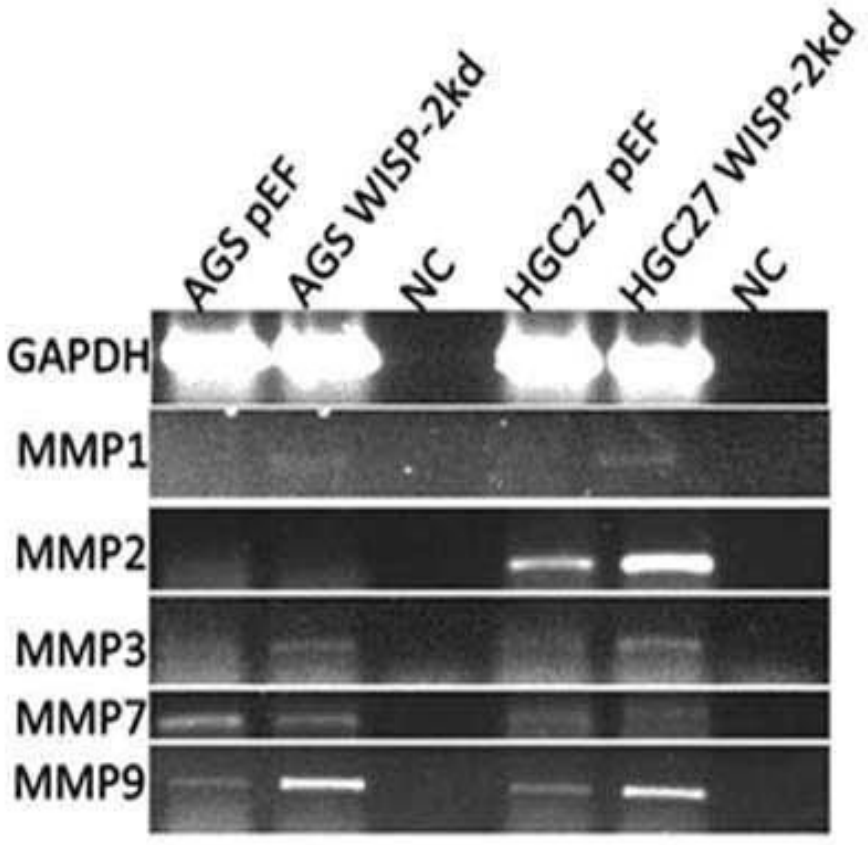

Figure 6.1 The increased transcript expression of MMP1, 2, 3 and 9 in HGC27 WISP-2 kd cells compared with controls.

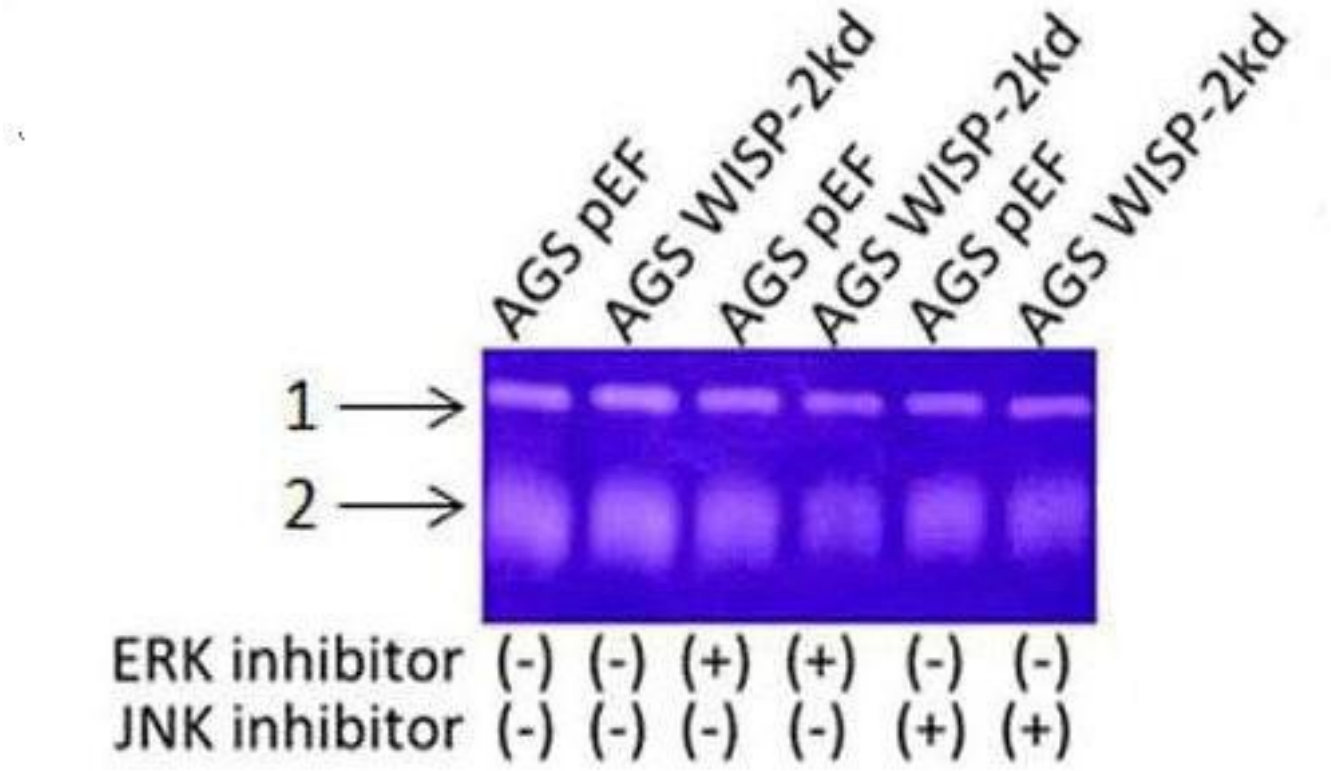

Figure 6.2 The enzyme activity of MMP-9 in AGS pEF and WISP-2 knockdown cells, with or without treatment of ERK inhibitor and JNK inhibitor. Gelatin zymography indicated the reduced enzyme activity of MMP-9 in AGS WISP-2 kd cells treated with ERK and JNK inhibitors and reduced MMP-9 in HGC27 WISP-2 kd cells treated with JNK inhibitors. 1: pro-MMP-9, 2: MMP-9.

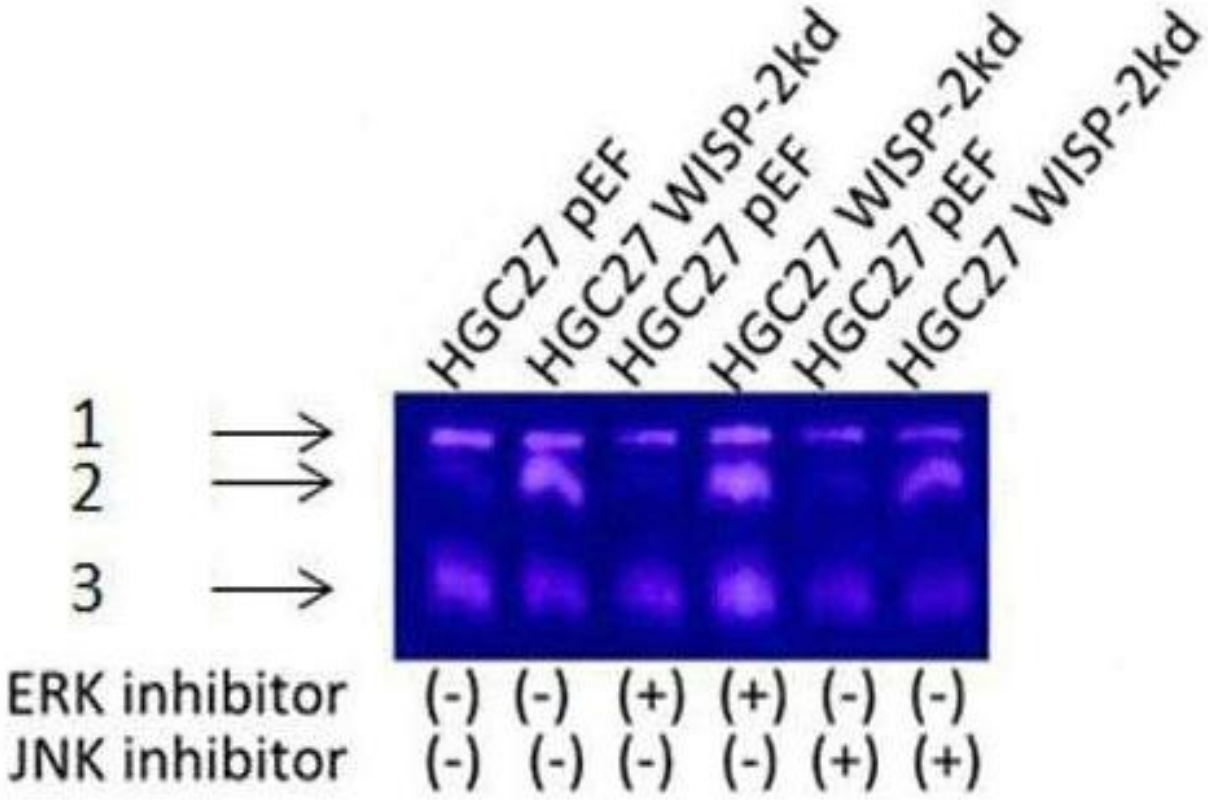

Figure 6.3 The enzyme activity of MMP-9 and MMP-2 in HGC27 pEF and WISP-2 knockdown cells, following treatment with ERK inhibitor and JNK inhibitor. Gelatin zymography indicated the reduced emzyme activity of MMP-9/2 in HGC27 WISP-2 kd cells treated with JNK inhibitors. 1: pro-MMP-9, 2: MMP-9, and 3: MMP-2.

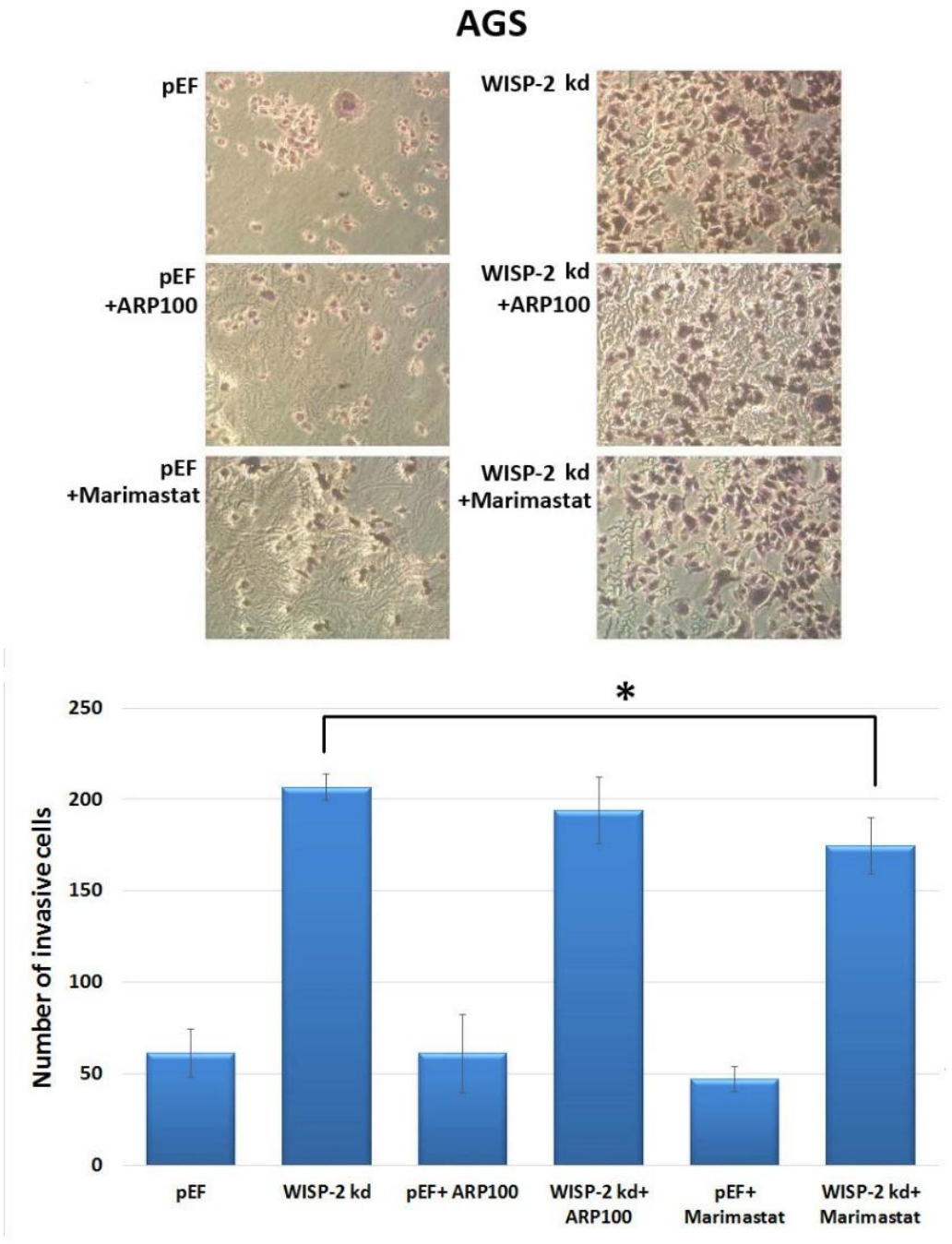

Figure 6.4 AGS cells with WISP-2 knockdown after the treatment with MMP-9 inhibitor (Marimastat) significantly decreased in invasiveness (p= 0.025, compared with AGS WISP-2 knockdown cells with no treatment). While the group treated with MMP-2 inhibitor (ARP100) did not demonstrate a significant change on cell invasion when compared with the control group (Asterisk represents for p> 0.05).

6.4 Discussion

Suppression of WISP-2 expression leads to the upregulation of the matrix metalloproteinases, MMP-2 and MMP-9, which are often found to be highly expressed in the invasive breast cancer phenotype [218]. The expression of MMP-1, MMP-2, MMP-9, and MMP-13 have been shown to be linked to the aggressiveness of tumours and their expressions are mediated by p38 in various tissues including prostate, breast, bladder, liver, and skin keratinocyte cell lines. Recently, several reports have shown that MMP-9 was up-regulated via the ERK signalling pathway in different human cells [280]. However, the mechanism by which WISP-2 deficiency enhances the invasiveness of cancer cells has not been elucidated and remains poorly understood [281].

In the present study, we have discovered that WISP-2 may suppress the expression of MMPs as well as activities of MMP-2 and MMP-9 in gastric cancer cells. Our study further demonstrates a role for JNK and ERK in this regulation，partly owing to the observation that treatment with JNKII and ERKII small inhibitors blocked the effects seen by knocking down WISP-2. This indicates that JNK pathway is one pathway that is suppressed by WISP-2. Our results echoes a recent report in which Twist has been linked to the expression of MMP1 [282]. It is thus argued therefore that loss of WISP-2 result in activation process for MMPs in cancer cells.

Based on the inhibitory effect of WISP-2 on MMPs, we further went back to compare the cell invasion of cells treated with MMPs inhibitor with that of control cells. WISP-2 knockdown influeced invasiveness of AGS cells treated with MMPs inhibitors. Figure 4C shows AGS cells with WISP-2 knockdown after the treatment with MMP-9 inhibitor (Marimastat) significantly

decreased in invasiveness (p= 0.025) compare with AGS WISP-2 knockdown cells with no treatment. While the group treated with ARP100 did not demonstrate a significant change on cell invasion compare with the control group (p> 0.05).

Taken together, the experimental evidence has shown that WISP-2 is a negative regulator of MMP expression and protein activities in cancer cells and that the JNK and ERK pathways are pivotal cellular events in this action.

Chapter 7

WISP-2 and Epithelial to Mesenchymal Transition (EMT) in gastric cancer and its clinical application

7.1 Introduction

Gastric cancer is originating from the epithelium [283]. Most patients with gastric cancer are diagnosed with advanced stage [54, 284]. Metastasis from gastric cancer not only represents the progression of the disease, but the key reason for treatment failure or death [285]. Hence, how to suppress cancer metastasis is the direction of research for gastric cancer treatment.

Epithelial-mesenchymal transition (EMT) is a process in which epithelial cells lose their cell-cell adhesion and obtain the properties of migratory and invasion, so that to form a migratory (mesenchymal) phenotype [286]. Interestingly, the expression of mesenchymal markers, namely N-cadherin and vimentin, are upregulated, while the expression of epithelial marker proteins, such as E-cadherin and keratin, are downregulated during the process of EMT [287]. Hence, EMT has been widely suggested as an important process during tumour metastasis of solid tumours, including gastric cancer [288]. The suppression of EMT may result in the restraint of the metastasis of gastric cancer, therefore EMT markers could be promising therapeutic targets.

WISP proteins, as a part of the extracellular and intracellular signalling molecules, modulate various cellular activities, namely cell growth, differentiation, invasion, migration and survival as shown here and in the literature [265]. Our study also revealed that WISP-2 has a significantly inhibitory effect on cell invasion and migration of gastric cancer cells (Chapter 4). Furthermore, data presented in Chapter 5 suggested that WISP-2 downregulate cellular motility of gastric cancer cells via JNK/ERK signalling pathway. Several studies suggested that EMT in cancer cell is mediated via JNK pathway [289, 290]. Dhar *et al* reported that a

significant correlation between the degree of differentiation and progression of pancreatic adenocarcinoma and decreased expression of the WISP-2 signalling protein. Pancreatic cancer cell line, MIA-PaCa-2, when treated with recombinant WISP-2 protein downregulated the expression of the mesenchymal cell marker vimentin and altered the morphological appearance of the cells to a cobble stone, epithelial-like phenotype [217]. These results suggest that WISP-2 may have a role in maintaining an epithelial-like phenotype in pancreatic adenocarcinoma cells thereby decreasing their invasive potential. In the present study, we determined the expression of EMT (Twist, N-cadherin, Vimentin, E-cadherin and Slug) markers in gastric tumour tissues and gastric cancer cells (HGC25 and AGS), and attempted to analyse the possible correlation between the EMT markers and WISP-2. The data presented in this chapter will show that loss of WISP-2 signalling is a crucial permissive event for epithelial-mesenchymal-transition (EMT) and extracellular matrix degradation and cell migration in gastric cancer.

7.2 Materials and methods

7.2.1 Human gastric tumour tissues

324 patients (Male: 231 cases, female: 93 cases; mean age, 59.8 years; range: 23-87 years, median survival age: 24 months) with gastric cancer, who were diagnosed and surgically treated in Peking University Cancer Hospital between 2004 and 2007, were enrolled in this study. The study was approved by the local ethics committee (Ethics Number: 2006021) and consents were obtained from patients. Some of the patients had received chemotherapy or radiation therapy preoperatively. The following histopathological information was obtained:

the depth of tumour invasion, histological grade, and status of lymph node metastasis, liver metastasis and vascular invasion. Stage of gastric adenocarcinoma was classified according to 1997 tumour node-metastasis (TNM) classification recommended by the International Union against Carcinoma. All patients were followed up until June 2012.

7.2.2 Quantitative analysis of Epithelial to Mesenchymal Transition (EMT) markers in tissues

The mRNA level of EMT markers (E-cadherin, Slug and Twist) from the above prepared cDNA was determined by real-time quantitative PCR using IcyclerIQ™ (Bio-Rad, Hemel Hempstead, UK), based on the Amplifluor™ technology [291] modified from a previously reported method [292]. Cytokeratin-19 (CK19) was used as a house keeping control for the epithelial/cancer cell content. The reaction was carried out under the following conditions: 94˚C for 5 min, 96 cycles of: 94˚C for 15 sec, 55˚C for 35 sec and 72˚C for 20 sec. The levels of the transcripts were generated using an internal standard that was simultaneously amplified with the samples, and are shown here in two ways: levels of transcripts based on equal amounts of RNA, and as a target/CK19 ratio [212].

7.2.3 Gastric cancer cell lines

The two human gastric cell lines, AGS and HGC27 were acquired from the European Collection of Animal Cell Culture (ECACC, Salisbury, UK). Cells were maintained in DMEM-F12 medium supplemented with 10% foetal bovine serum (FBS) and antibiotics.

7.2.4 Quantitative analysis for Epithelial to Mesenchymal Transition (EMT) markers in cell lines

The levels of mRNA expression of EMT markers, E-cadherin, N-cadherin, Twist, Slug and Vimentin were determined by real-time quantitative PCR and RT-PCR in WISP-2 knockdown and control cells. Here, GAPDH was used as an internal control.

7.2.5 Statistical analysis

Statistical analysis was performed using SPSS18 (SPSS Inc., Chicago, USA). The association of the expression of WISPs and EMT markers was analysed using Spearman Rank Order Correlation analysis. Each assay was performed at least three times. The relationship between EMT markers and clinical parameters was analyzed using Mann-Whitney U rank test or Kruskal-Wallis rank test, where appropriate. P-value < 0.05 was considered statistically significant.

7.3 Results

7.3.1 Expression of EMT markers in gastric tissues and the association with clinicopathological characteristics

In the clinical cohort, Slug and Twist transcripts were lower in normal tissues than in tumour ($P=0.015$ and $P<0.0001$ respectively), by contrast, E-cadherin and N-cadherin expression decreased in the tumour tissues compared with the normal tissues ($P<0.0001$) (Figure 7.1 and Table 7.1). The markers individually did not appear to be significantly correlated with the histological type nor other clinical parameters (Tables 7.2 and 7.3).

However, the trio of the markers, namely, E-cadherin, Slug and Twist were significantly correlated with the incidence free survival (p=0.005) and overall survival (p=0.008), based on the Kaplan-Meier survival model (Figure 7.2). Likewise, patients with the trio EMT marker abnormalities had a lower five-year survival rate.

7.3.2 Correlation between WISP-2 and EMT markers in gastric cancer

Levels of the WISP-2 transcripts significantly and inversely correlated with TWIST and SLUG. The correlation between WISP-2 and E-cadherin and N-Cadherin was not significant (Table-7.4a). WISP-1 did not appear to have significant correlations with the EMT markers. However, WISP-3, similar to WISP-2, had a significant reverse correlation with TWIST (Table 7.4a). It was interesting to note that the expression of all the WISPs was highly correlated with each other (Table 7.4b).

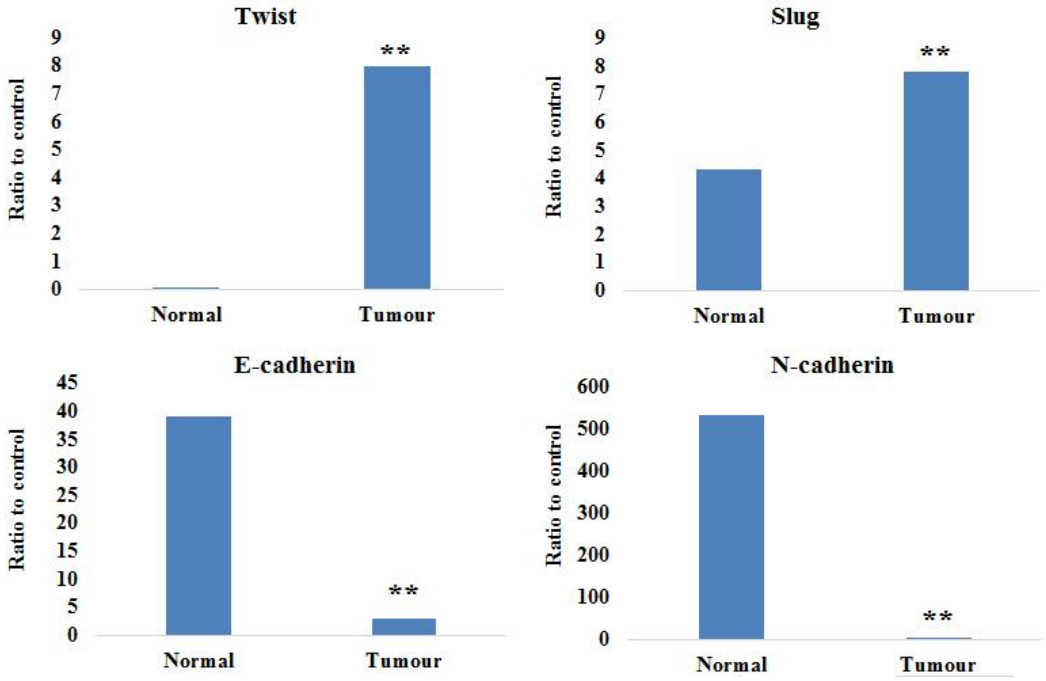

Figure 7.1 Expression of Slug, Twist and E-Cadherin in gastric cancer and paired normal samples. A, Expression of Slug was higher in gastric cancer than in paired normal samples; B, Expression of Twist was higher in gastric cancer than in paired normal samples;
C, Expression of E-Cadherin was much lower in gastric cancer than in paired normal samples. **(****: P<0.01**);** D, Expression of N-Cadherin was significantly lower in gastric cancer than in paired normal samples. **(****: P<0.01)

Table 7.1 Expression of the transcript of EMT markers Twist, Slug and E-cadherin in gastric tissues.

	Twist	Slug	E-cadherin	N-cadherin
Normal tissues[a]	0.056(0.027,0.081)	4.3(0.2,35.3)	39 (3,284)	532 (3,10777)
Tumour tissues[a]	7.98(3.99,32.3)	7.8(1.9,41.5)	3 (0,53)	5 (0,381)
P value[a]	P<0.0001	P=0.0015	P<0.0001	P<0.0001

a: Shown are median (IQR) level of the transcript (copies/ul)
b: by Mann-Whitney U test

Table 7.2 The correlation of the expression of ECAD and NCAD and clinical parameters. Red colouration is used to indicate statistical significance (P< 0.05).

Clinicolpathological Parameters	ECAD					NCAD				
	Case	N$^{\alpha}$	Median (Q1,Q3)	*P*	*P*	Case	N$^{\alpha}$	Median (Q1,Q3)	*P*	*P*
Gender										
Male	207	24	2(0,1)			201	30	10		
Female	80	13	3(0,0)	0.7517		84	9	4	0.0804	
Infiltration depth										
T1	14	2	8.1(0,1.07)			14	2	7		
T2	25	1	1(0,0.01)	0.3959		22	4	0	0.4555	
T3	34	7	5(0,8)	0.1700	0.0009[1]	36	5	10	0.6269	
T4	208	25	2(0,1)	0.8821	0.8456[1]	207	26	9	0.3377	
Nodal status										
N0			5			62	9	1		
N1+2+3			1.7	0.9715		217	30	10	0.2318	
TNM staging										
TNM1	23	2	4.6(0,38.3)			21	4	1		
TNM2+3+4	254	36	3(0,55)	0.9016		257	33	5	0.2666	

Table 7.2 continued on next page...

Table 7.2 continuing from previous page.

Differentiation										
High	1	0	934207			1	0	11970		
High-Medium	6	0	0.5(0,29.9)			6	0	0		
Medium	55	7	5(1,79)	0.1183		52	10	3	0.4287	
Medium-Low	72	10	3(0,54)	0.1990	0.5609[2]	73	9	45	0.2082	
Low	120	18	2(0,55)	0.28	0.20[2]	123	15	4	0.63	0.0067[2]
Clinical outcome										
Alive	117	17	2(0,36)			122	12	4		
Died	164	23	3(0,80)	0.3597		160	27	12	0.2655	
Disease Free	104	15	2(0,37)			109	10	3		
Metastasis	13	2	0.5(0,9.1)	0.1948		13	2	15	0.4477	
Died of GC	164	23	3(0,80)	0.5621		160	27	12	0.1976	

1: Compared with T2 stage; 2: Compared with medium differentiation.

Table 7.3 The correlation of the expression of SLUG and TWIST and clinical parameters. Red colouration is used to indicate statistical significance (P< 0.05).

Clinicolpathological Parameters	SLUG				TWIST				
	Case	N[α]	Median (Q1,Q3)	*P*	Case	N[α]	Median (Q1,Q3)	*P*	*P*
Gender									
Male	229	2	2(2,42)		228	3	13.45		
Female	92	1	3(2.6,40)	0.3244	92	1	18.92	0.1244	
Infiltration depth									
T1	16	0	8.1(4.4, 40.9)		16	0	9.64		
T2	26	0	1(1.2,41.0)	0.3314	26	0	10.412	0.5514	
T3	41	0	5(0.6,39.5)	0.2106	41	0	6.6	0.0610	0.00341
T4	230	3	2(2,42)	0.2479	229	4	8.88	0.6172	0.01412
Nodal status									
N0	70	1	5(2.9,42.3)		68	3	9.38		
N1+2+3	245	2	1.7(2,40)	0.2993	246	1	7.58	0.2199	
TNM staging									
TNM1	25	0	4.6(3.7, 40.5)		25	0	9.70		
TNM2+3+4	287	3	3(1.8,41.3)	0.3710	286	4	7.81	0.1045	

Table 7.3 to be continued on next page....

Table 7.3 continuing from the previous page

Differentiation									
High	1	0	1647.9		1	0	6.0683		
High-Medium	6	0	4.48(1.92,21.41)		6	0	5.78		
Medium	62	0	4.9(1.0,26.7)	0.8882	61	1	8.432	0.3564	
Medium-Low	82	0	8(2,50)	0.4921	82	0	9.07	0.3758	
Low	135	3	8.1(2.1,41.3)	0.5848	135	3	8.08	0.3095	
Clinical outcome									
Alive	134	0	7.2(2.7,41.7)		133	1	9.64		
Died	184	3	8(2,40)	0.3597	184	3	7.24	0.2655	———
Disease Free	119	0	7.9(2.7,43.7)		118	1	9.88		
Metastasis	15	0	6.4(2.6,15.1)	0.1948	15	0	8.85	0.4477	———
Died of GC	184	3	8(2,40)	0.5621	184	3	7.24	0.1976	

1: Compared with T2 stage; 2: Compared with T3 stage.

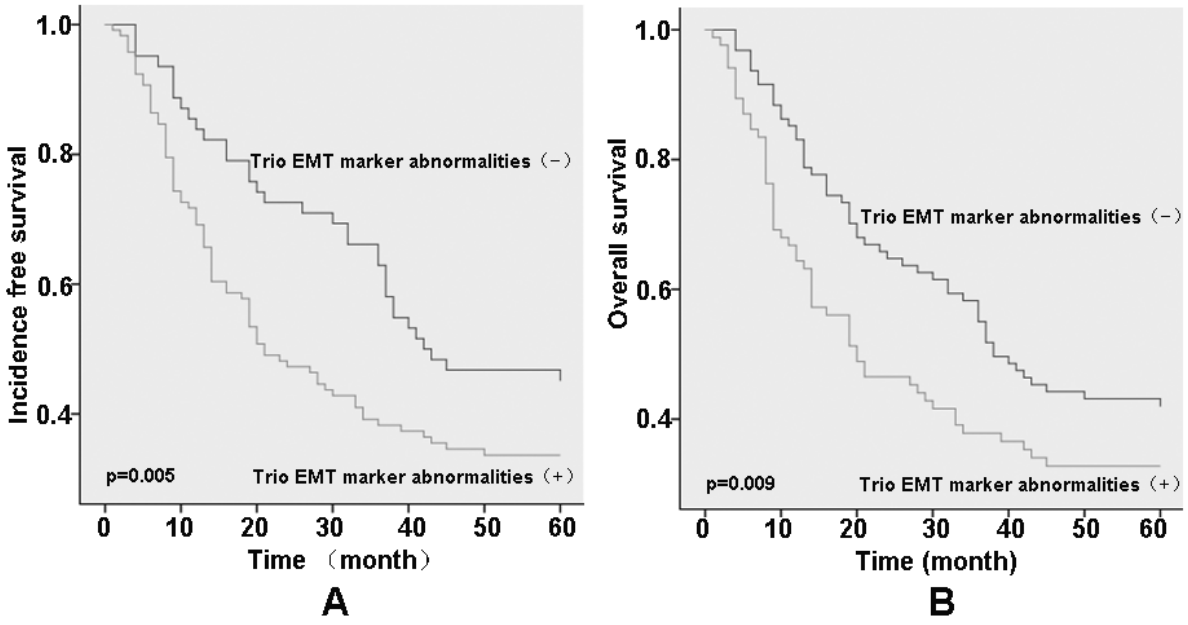

Figure 7.2 The Kaplan-Meier survival model demonstrated the impact of the selective trio of Slug, Twist and E-Cadherin expression in gastric cancer. The trio of Slug, Twist and E-Cadherin were significantly correlated with the disease-free survival (p=0.005) (A) ((-) group, n=82); (+) group, n=118) and overall survival (p=0.009) (B) ((-) group, n=95; (+) group, n=85).

Table 7.4a Correlation between the WISP-2 transcript and that of EMT markers in human gastric cancer tissues.*

		SLUG	**TWIST**	**SNA1**	**N-Cadherin**	**E-cadherin**
WISP-1	*r*=	-0.0305	0.113	0.049	0.0487	0.0398
	p=	0.594	0.0693	0.483	0.46	0.55
WISP-2	*r*=	***-0.231***	***-0.416***	0.102	-0.1	0.0465
	p=	***0.0000355***	***<0.000001***	0.11	0.0935	0.438
WISP-3	*r*=	0.0375	***-0.275***	0.109	-0.122	-0.0478
	p=	0.71	***0.0000296***	0.138	0.0832	0.495

* by Spearman Rank correlation test. Shown in the table are correlation coefficients (r) between WISP-2 and the respective EMT markers and the level of significance (p).

Table7.4b Correlation between the transcript levels of three WISP family memberss in human gastric cancer tissues.*

		WISP-2	WISP-3
WISP-1	r=	0.24	0.409
	p=	0.000107	<0.000001

* by Spearman Rank correlation test. Shown in the table are correlation coefficients (r) between WISP-2 and the respective EMT markers and the level of significance (p).

7.3.3 Expression of EMT markers in cell lines

Based on the interesting correlation between WISP-2 and some of the EMT markers in the clinical cohort, the relationship between WISP-2 and EMT markers was further investigated in gastric cancer cell lines. After WISP-2 knockdown, there was a significant decrease on the expression of E-cadherin ($P<0.05$) and increase on the expression of Twist, N-cadherin and Vimentin ($P<0.01$, $P<0.05$ and $P<0.01$, respectively). Expression of Slug was found of no statistical difference between the two cells. Representative images of Q-RT-PCR and RT-PCR verification of the expression of E-cadherin, N-cadherin, Twist, Slug and Vimentin in cell lines are shown in Figure 7.3 and 7.4.

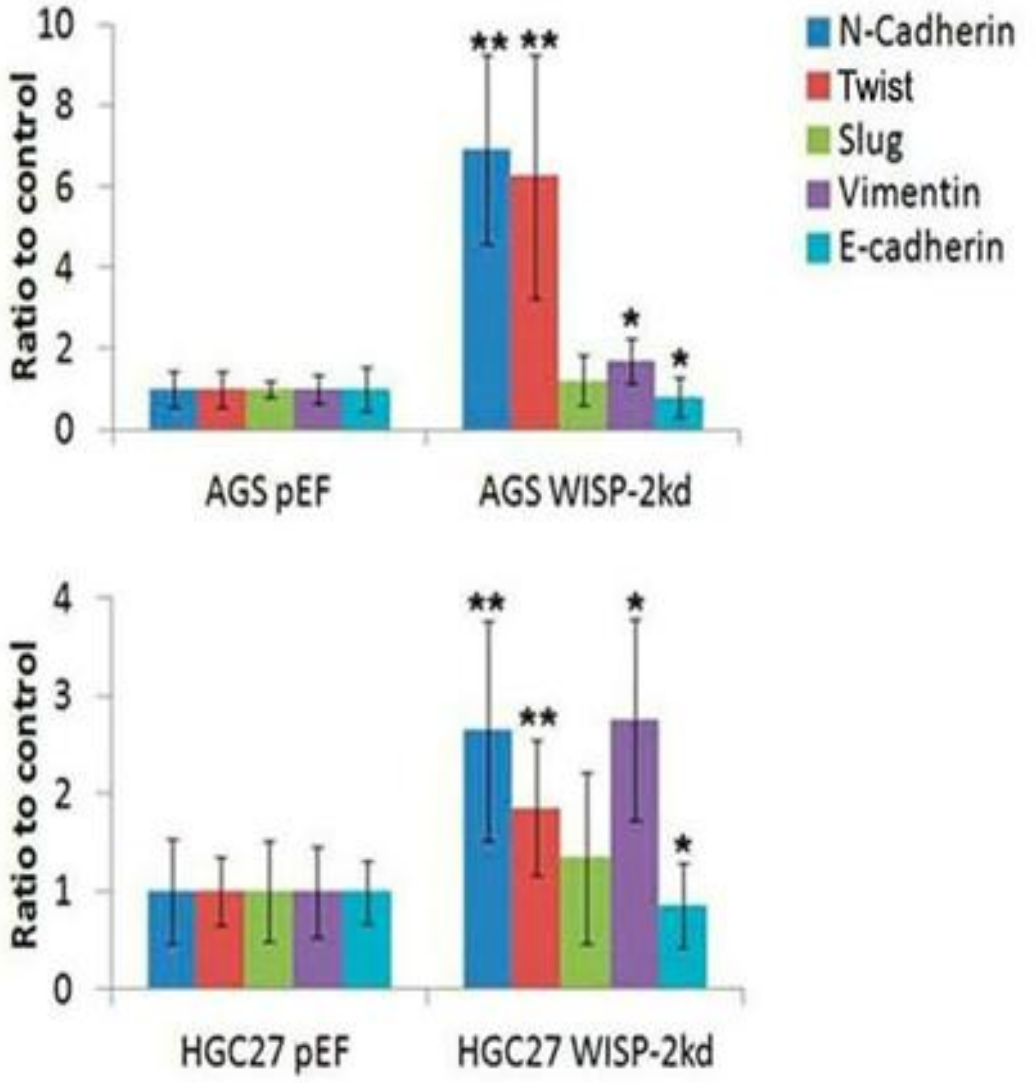

Figure 7.3 Expression of EMT markers (E-cadherin, N-cadherin, Twist, Slug and Vimentin) in AS (top) and HGC27 (bottom) cells by Q-RT-PCR following WISP-2 knockdown (WISP-2kd). EMT markers expression differed after WISP-2 knockdown in AGS and HGC27 cells in that the expression of Twist, N-cadherin and Vimentin were increased and E-cadherin were decreased whereas there was no difference in Slug expression. (*: P< 0.05; **: P< 0.01)

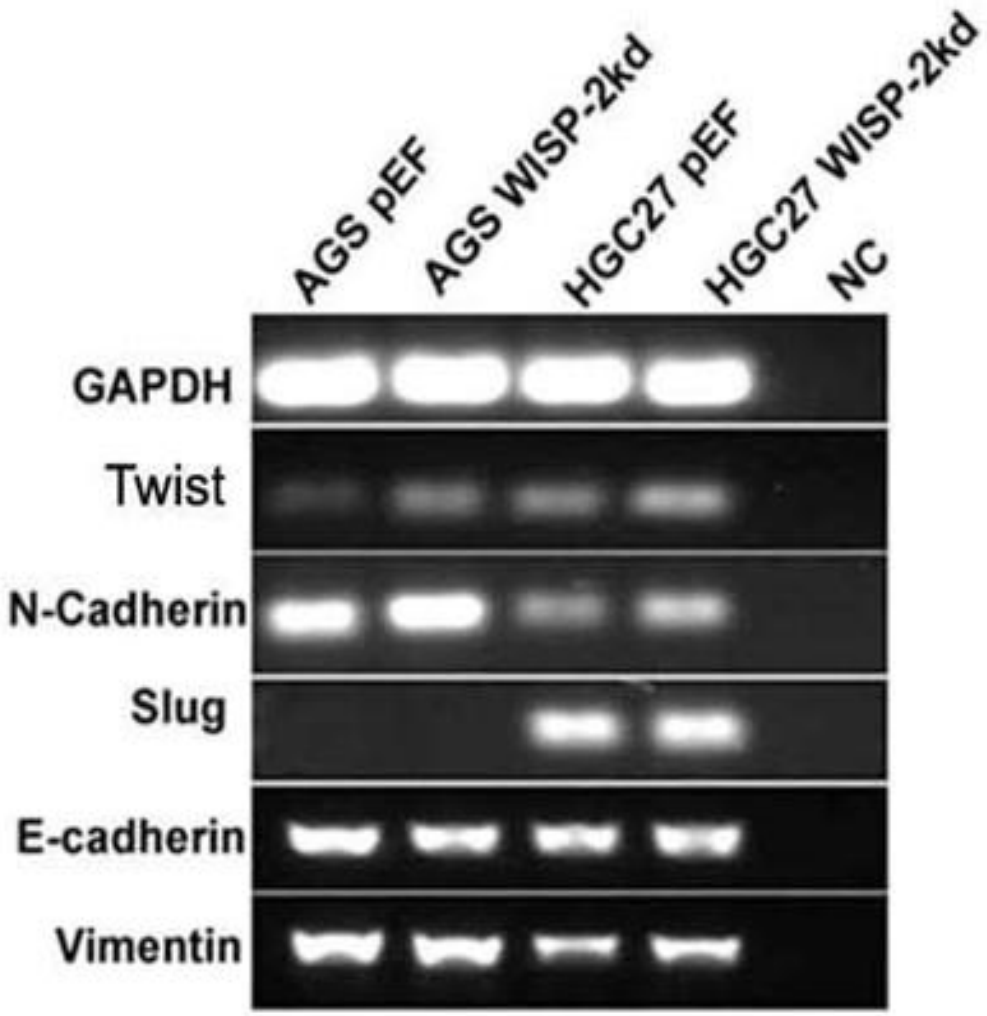

Figure 7.4 Verification of expression of EMT markers (E-cadherin, N-cadherin, Twist, Slug and Vimentin) in AGS and HGC27 cells by RT-PCR. EMT markers expression differences after WISP-2 knockdown in AGS and HGC27 cells. Expression of Twist, N-cadherin and Vimentin were increased and E-cadherin were decreased. And there was no difference in Slug expression.

7.4 Discussion

Twist and Slug are transcription EMT markers, activation of which have been shown to suppress the expression of E-cadherin (Yang *et al* 2004, Lombaets *et al* 2006, Vesuna *et al* 2008). The host laboratory of the present study was the first to report a link between over-expression of Twist and Slug and patients long term survival (Martin *et al* 2005). Slug has been reported to be over-expressed in gastric cancer such as that seen in the present study (Rosivatz *et al* , 2002, Castro-Alves *et al* 2007). The present study has also indicated that a trio of the EMT markers, Twist, Slug and E-cadherin had a significant prediction power of the survival of the patients with gastric cancer.

Previous studies have suggested that WISP-2 is able to reverse the epithelial-mesenchymal transition (EMT) processes [217, 218] as well as recover the function of the mutant p53 [250], which are important in the invasion and metastatic growth of breast cancer cells. The present study has firstly clarified the association of WISP mRNAs and proteins expression with clinicolpathological parameters and outcome in gastric cancer patients as well as the association with those of EMT markers. Here we showed WISP-2, but not WISP-1, was inversely correlated with two of the EMT markers namely Twist and Slug. WISP-3 also significantly correlated, in a reverse order, with Twist.

Thus, the observations on the clinical cohort suggest that low levels of WISP-2 are linked to highly raised Twist and Slug, which in turn lead to a reduction in E-cadherin expression. Further supporting informtion for the WISP-2/EMT link comes from the *in vitro* experiments of our study. At cellular level, knockdown of WISP-2, in both AGS and HGC27 cell lines, led to increased cell proliferation, motility and invasiveness, hallmarks of EMT in cells including cancer cells. At transcription and translation levels, WISP-2 knockdown in gastric cancer cells

triggers an up-regulation of Twist, N-cadherin and Vimentin, markers of mesenchymal genotype (Zeisberg and Neilson, 2009).

Collectively, it is suggested that WISP-2 is an EMT regulator and that WISP-2 expression support an epithelial phenotype. This link has provided a plausible explanation for WISP-2 to be potential suppressor of EMT (or an inducer of MET).

Chapter 8

General discussion

As a complex multistep process, tumour metastasis undergone a series of complex multistep process, which includes impairment of cell-cell adhesion in neoplastic epithelium, invasion of adjacent tissues and dissemination of cancer cells through the lymphatics and via the haematogenous route both leading to distant metastasis [293, 294]. Therefore, one part of this present study was to identify metastasis related genes, which may have the potential to regulate the metastasis process of cancer cells. WISP family members have been shown to play multiple roles in a number of pathophysiological processes, including cell proliferation, adhesion, invasiveness, wound healing, extracellular matrix regulation, and epithelial-mesenchymal-transition (EMT). A number of recent clinical studies have shown that WISP family members are deregulated in a variety of solid tumours and have bearings on the metastases and clinical outcome of the patients [221, 222, 238]. However, the cellular functions of WISPs proteins are not yet fully extablished, which forming the other aim of the study. Previous published work from the host laboratory and others have demonstrated that WISP proteins may have different effects on tumour progression and cell functions, depending on tumour and cell types.

WISP-2 and its clinical significance in human gastric cancer pointing to a putative tumour suppressor role

The present study has demonstrated that WISP proteins are detectable in gastric tissues. However, it is WISP-2 that has the most significant links to clinical and pathological features of the clinical cohort. This study has shown that expression of WISP-2 at mRNA and protein levels are aberrant in gastric cancer. Furthermore, the aberration is inversely correlated with disease progression and survival of the patients. This would support the hypothesis that WISP-2 is a candidate biomarker for disease progression in this cancer type. Indeed, WISP-2 is the most studied of the WISP molecules in different tumour and tiussue types. Higher WISP-2 expression has been detected in less aggressive human breast cancer cells (i.e. MCF-

7 and ZR-75-1). Moderately aggressive breast cancer cell lines (i.e. SKBR-3) express a basal level of WISP-2, whereas WISP-2 expression is not detected in the highly aggressive breast cancer cell line MDA-MB-231 [213, 215]. Growing experimental evidence demonstrates that WISP-2 plays an anti-invasive role in breast carcinogenesis through controlling adhesion and cell motility [218, 245]. Taken together, these observations suggest that WISP-2 is a candidate tumour and metastasis suppressor in solid tumours, particularly in human gastric cancer.

Effect of WISP-2 on the functions (proliferation, adhesion, invasion and migration) of gastric cancer cells and its potential signalling pathway.

The data obtained from our present study suggest that WISP-2 significantly suppresses the growth, invasion and migration of AGS and HGC27 gastric cancer cells, but has no influence on the adhesion of both two gastric cancer cells. Our results are consistent with finding from previous reports in pancreatic adenocarcinoma and colorectal cancer [189, 217]. From the results that downregulation of WISP-2 results in reduction of cellular motility of gastric cancer cells, we hypothesised that this might be linked to the signalling pathways that are central to cell migration. Hence, we screened the proteins and signalling molecules that are potentially related with WISP-2, by way of an antibody based protein microarray, namely KAM850. From the antibodies and data available on the array, we found the high levels of ERK1 and ERK5 proteins, JNK1 protein and AKT protein are significantly associated with WISP-2. This data set is particularly interesting, as it is coherently seen from both human gastric tissues and from gastric cancer cell lines: protein interactions from WISP-2 precipitation using proteins of human gastric tissues and verified by the WISP-2 knockdown of human gastric cancer cell lines. Thus, the JNK, ERK and AKT pathway are considered key to the function of WISP-2 in gastric cancer. The importance of these pathways in the WISP-2 regulated cell functions are

further strengthened by the data when the small inhibitors to these pathways were used: significant suppression of cell migration was observed in HGC27 WISP-2 knockdown cells treated with JNK Ⅱ compared with pEF control cells.

Another interesting finding was that FAK has no interaction with the WISP-2 protein and blocking FAK did not influence the action of WISP-2. FAK is essential to cell-matrix adhesion and cell migration. JNK, ERK and AKT pathways are very important pathways in particular to cell motility of cancer cells, however, these are downstream of FAK. Collectively, WISP-2 plays an important role in the regulation of cellular migration of gastric cancer cells. This role is independent of FAK and is via intracellular events downstream of FAK, primarily involving JNK, ERK and AKT pathways.

WISP-2 and expression of MMPs, a role for the JNK pathway.

WISP-2 has markedly suppressed the invasion and motility of gastric cancer cells. From the data presented here, it is clear that this action is at least partly mediated by regulating the activity of MMPs, namely MMP-2 and MMP-9. WISP-2 expression upregulates the expression and enzymatic activities of MMP-2 and MMP-9, two MMPs frequently found highly expressed in aggressive tumours, for example in invasive breast cancer phenotypes [218]. The expression of MMP-1, MMP-2, MMP-9, and MMP-13 is associated with the aggressiveness of tumours and their expression is mediated by p38 in various tissues including prostate, breast, bladder, liver, and skin keratinocyte cell lines. Several reports have revealed that MMP-9 is up-regulated by the ERK signalling pathway in different human cells [280]. However, the mechanism by which WISP-2 deficiency enhances the invasiveness of cancer cells remains poorly understood [281]. In the present study, we have discovered that WISP-2 suppresses the expression of MMPs as well as activities of MMP-2 and MMP-9 in gastric

cancer cells. Our study also describes a role for JNK and ERK in this regulation, partly owing to the observation that treatment with JNKII and ERKII small inhibitors blocked the effects seen by knocking down WISP-2 and partly owing to the finding that WISP-2 interacts with these signalling proteins. Together, it is suggested that WISP-2 inhibits JNK activation and consequently influences expression and enzymatic activity of MMP-2 and MMP-9.

Expression of WISP-2 and Epithelial to Mesenchymal Transition (EMT) in gastric cancer.

The findings that WISP-2 has a profound impact on the migration and adhesion of gastric cancer cells, hallmarks of EMT, prompted further investigation into if and how WISP-2 may act as an EMT regulator in gastric cancer cells. Indeed, in an early study, Banerjee *et al* reported that WISP-2 was able to reverse some features of the epithelial-mesenchymal transition (EMT) process [218]. The present study first focused on analyzing the association of WISP mRNA and proteins expression with clinicol and pathological parameters and outcome in gastric cancer patients as well as the association with those of EMT markers. WISP-2, but not WISP-1 nor WISP-3, was inversely correlated with two of the EMT markers namely Twist and Slug. Twist and Slug are transcription EMT markers, the activation of which has been shown to suppress the expression of E-cadherin [295, 296]. We were the first to report a link between the over-expression of Twist and Slug and long term survival in patients with breast cancer [297]. Slug has been reported to be over-expressed in gastric cancer similar to that seen in the present study [298, 299]. Thus, the observations on the clinical cohort suggest that low levels of WISP-2 are linked to raised Twist and Slug, which in turn leads to a reduction in E-cadherin expression.

Further supporting information for the WISP-2/EMT link comes from the cell function experiments. At transcription and translation levels, WISP-2 knockdown in gastric cancer cells

triggers an up-regulation of Twist, N-cadherin and Vimentin, markers of mesenchymal genotype [300].

Collectively, these results suggest that WISP-2 is an EMT regulator and that WISP-2 expression supports an epithelial phenotype. This link has provided a plausible explanation for WISP-2 to be potential suppressor of EMT (or an inducer of MET). The suggested link and interaction pathway is summarised in Figure 8.1.

In conclusion, the present thesis, using both in vitro and clinical models of gastric cancer, has presented evidence that WISP-2 is a putative tumour suppressor molecule in human gastric cancer. This is seen by its inhibitory influence on the growth, invasion and migration of gastric cancer cells, on actions achieved by downregulating the enzyme activities of MMP-2 and MMP-9. In the meantime, WISP-2 also activates E-cadherin and reduces Twist and Slug, potentially via its regulation of the ERK/JNK pathway.

Future directions:

The present study has further shown that the pivotal role of WISP-2 in human gastric cancer. However, the study has also raised new directions for future research.

1. The role of WISP-2. Although the present study has demonstrated that WISP-2 regulates the expression and activity of MMP-2 and MMP-9, the exact mechanism of the intermediate processes by which WISP-2 resulted to this regulation remains largely unknown. For example, it will be important to investigate if the interaction between WISP-2 and EMT markers also takes place. It will be useful in the future to investigate

transcriptional regulation and possible post-translation regulation for MMP-2 and MMP-9 in this context.

2. The potential therapeutic implications of WISP-2 in cancer. In most cancer types, WISP-2 has been shown to act as a tumour suppressor. Two areas should be further explored: 1. Mechanism of WISP-2 downregulation: can this be via methylation of the gene transcription? 2. It will be highly useful to investigate if specific activation of WISP-2 may have therapeutic implications.
3. The antibody array has indicated a number of other pathways that would be of potential interest to explore, namely how the JNK/ERK proteins interacts with WISP-2, at what point WISP-2 bypassing the FAK protein in the regulation of cell migration, if and how p53 which interacts with WISP-2 plays a role with WISP-2 in gastric cancer. They will be vital directions to pursue in order to fully understand the biology of WISP-2 in cancer.

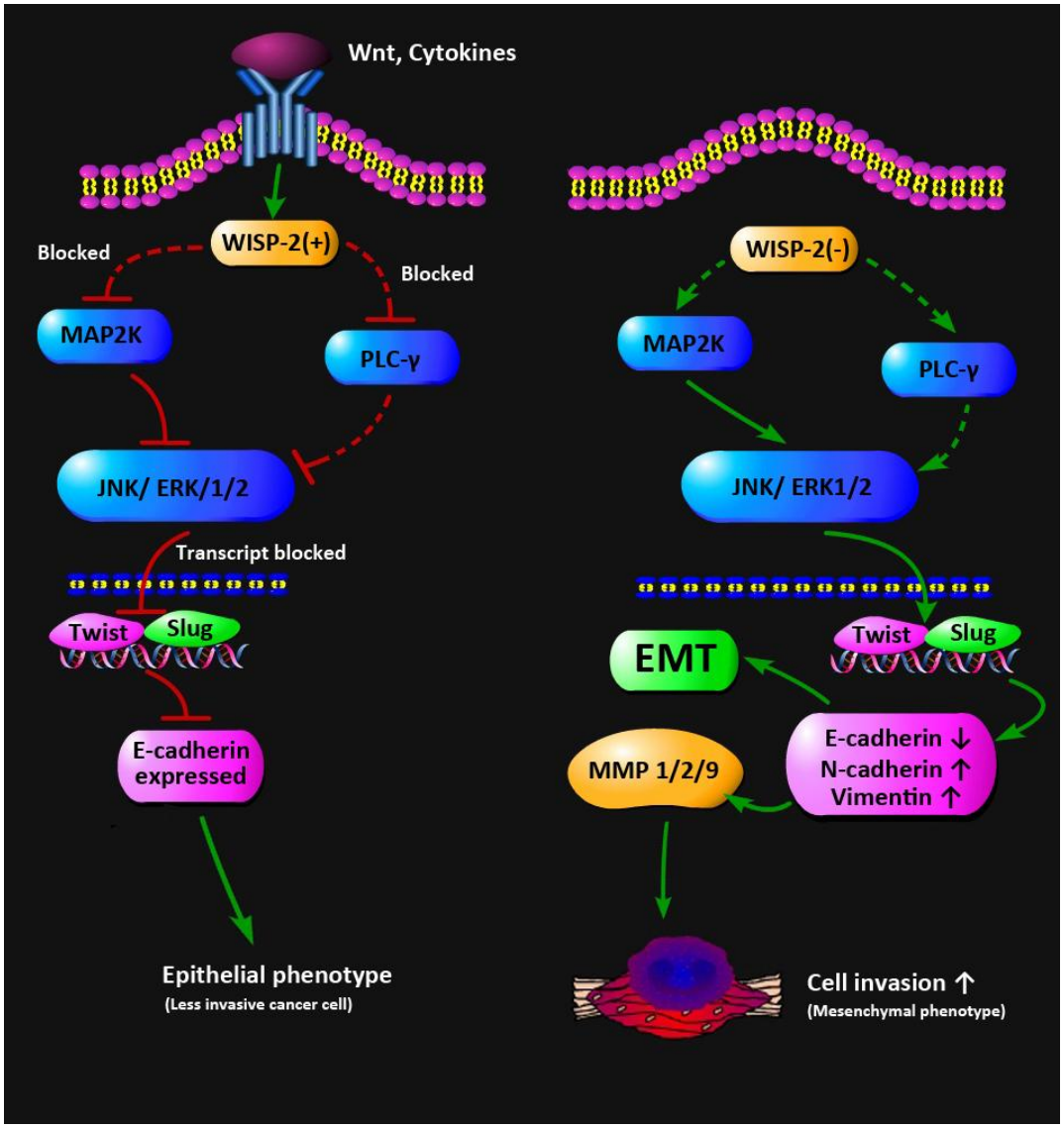

Figure 8.1 Suggested mechanism of action by WISP-2 in gastric cancer cells. In cells in which WISP-2 is well expressed (possibly induced by Wnt proteins), it acts as an inhibitory mechanism to the ERK/JNK pathway and PLC-gamma pathway, thus preventing, to some degree, the activation of transcription event for EMT regulating proteins and MMPs. However, in cells where WISP-2 is reduced/ lost, ERK/JNK pathway is activated, leading to the transcription activation of EMT transcription factors including Twist and Slug. This leads to the reduction of E-cadherin which in turn triggers the EMT process. Similarly, PLC-gamma and JNK activations lead to activation of MMP synthesis. These two pathways collectively contribute to the increase in cellular migration and tissue invasion. Dash lines indicate where gaps exist and require further work.

Reference

1. Shen, L. and Z.H. Lu, *[New perspectives on medical treatment of gastric cancer].* Zhonghua Wei Chang Wai Ke Za Zhi, 2012. **15**(2): p. 103-8.
2. Vannella, L., et al., *Systematic review: gastric cancer incidence in pernicious anaemia.* Aliment Pharmacol Ther, 2013. **37**(4): p. 375-82.
3. Ma, Z., et al., *Effect of statins on gastric cancer incidence: A meta-Analysis of case control studies.* J Cancer Res Ther, 2014. **10**(4): p. 859-65.
4. Bertuccio, P., et al., *Dietary patterns and gastric cancer risk: a systematic review and meta-analysis.* Ann Oncol, 2013. **24**(6): p. 1450-8.
5. Bertuccio, P., et al., *Recent patterns in gastric cancer: a global overview.* Int J Cancer, 2009. **125**(3): p. 666-73.
6. Vogiatzi, P., et al., *Deciphering the underlying genetic and epigenetic events leading to gastric carcinogenesis.* J Cell Physiol, 2007. **211**(2): p. 287-95.
7. Nagini, S., *Carcinoma of the stomach: A review of epidemiology, pathogenesis, molecular genetics and chemoprevention.* World J Gastrointest Oncol, 2012. **4**(7): p. 156-69.
8. Furfaro, M., et al., *[Blood groups of the ABO and Rh (D) system and various diseases].* Arch Sci Med (Torino), 1978. **135**(2): p. 255-68.
9. Correa, P., *Human gastric carcinogenesis: a multistep and multifactorial process--First American Cancer Society Award Lecture on Cancer Epidemiology and Prevention.* Cancer Res, 1992. **52**(24): p. 6735-40.
10. *Guidelines on diet, nutrition, and cancer prevention: reducing the risk of cancer with healthy food choices and physical activity. The American Cancer Society 1996 Advisory Committee on Diet, Nutrition, and Cancer Prevention.* CA Cancer J Clin, 1996. **46**(6): p. 325-41.
11. Botterweck, A.A., P.A. van den Brandt, and R.A. Goldbohm, *Vitamins, carotenoids, dietary fiber, and the risk of gastric carcinoma: results from a prospective study after 6.3 years of follow-up.* Cancer, 2000. **88**(4): p. 737-48.
12. Soybel, D.I., *Anatomy and physiology of the stomach.* Surg Clin North Am, 2005. **85**(5): p. 875-94, v.
13. Rohr, S., *[Anatomy and physiology of the normal stomach].* Soins Chir, 1986(70-71): p. 4-8.
14. Henrich, M., *[Clinical anatomy of the pyloric region].* Zentralbl Chir, 1986. **111**(9): p. 518-25.
15. Ferlay, J., et al., *Cancer incidence and mortality worldwide: sources, methods and major patterns in GLOBOCAN 2012.* Int J Cancer, 2015. **136**(5): p. E359-86.
16. Ferlay, J., et al., *Estimates of worldwide burden of cancer in 2008: GLOBOCAN 2008.* Int J Cancer, 2010. **127**(12): p. 2893-917.
17. Miyamoto, A., et al., *Lower risk of death from gastric cancer among participants of gastric cancer screening in Japan: a population-based cohort study.* Prev Med, 2007. **44**(1): p. 12-9.
18. Parkin, D.M., et al., *Global cancer statistics, 2002.* CA Cancer J Clin, 2005. **55**(2): p. 74-108.
19. Schuz, J., *Cancer Epidemiology: The International Journal of Cancer Epidemiology, Detection and Prevention.* Cancer Epidemiol, 2009. **33**(1): p. 1-2.
20. Parkin, D.M., et al., *Estimating the world cancer burden: Globocan 2000.* Int J Cancer, 2001. **94**(2): p. 153-6.
21. Parkin, D.M., *The global health burden of infection-associated cancers in the year 2002.* Int J Cancer, 2006. **118**(12): p. 3030-44.
22. Danaei, G., et al., *Causes of cancer in the world: comparative risk assessment of nine behavioural and environmental risk factors.* Lancet, 2005. **366**(9499): p. 1784-93.
23. Lee, K.J., et al., *Gastric cancer screening and subsequent risk of gastric cancer: a large-scale population-based cohort study, with a 13-year follow-up in Japan.* Int J Cancer, 2006. **118**(9): p. 2315-21.

24. Naguib, S.F., A.S. Zaghloul, and H. El Marakby, *Gastrointestinal stromal tumors (GIST) of the stomach: retrospective experience with surgical resection at the National Cancer Institute.* J Egypt Natl Canc Inst, 2008. **20**(1): p. 80-9.
25. Yuasa, N. and Y. Nimura, *Survival after surgical treatment of early gastric cancer, surgical techniques, and long-term survival.* Langenbecks Arch Surg, 2005. **390**(4): p. 286-93.
26. Correa, P. and B.G. Schneider, *Etiology of gastric cancer: what is new?* Cancer Epidemiol Biomarkers Prev, 2005. **14**(8): p. 1865-8.
27. Imrie, C., et al., *Is Helicobacter pylori infection in childhood a risk factor for gastric cancer?* Pediatrics, 2001. **107**(2): p. 373-80.
28. Vogelaar, I.P., et al., *Familial gastric cancer: detection of a hereditary cause helps to understand its etiology.* Hered Cancer Clin Pract, 2012. **10**(1): p. 18.
29. Gonzalez, C.A., N. Sala, and G. Capella, *Genetic susceptibility and gastric cancer risk.* Int J Cancer, 2002. **100**(3): p. 249-60.
30. Falchetti, M., et al., *Gastric cancer with high-level microsatellite instability: target gene mutations, clinicopathologic features, and long-term survival.* Hum Pathol, 2008. **39**(6): p. 925-32.
31. Bacani, J., et al., *Tumor microsatellite instability in early onset gastric cancer.* J Mol Diagn, 2005. **7**(4): p. 465-77.
32. Machado, J.C., et al., *A proinflammatory genetic profile increases the risk for chronic atrophic gastritis and gastric carcinoma.* Gastroenterology, 2003. **125**(2): p. 364-71.
33. Nardone, G. and A. Morgner, *Helicobacter pylori and gastric malignancies.* Helicobacter, 2003. **8 Suppl 1**: p. 44-52.
34. Lan, J., et al., *Helicobacter pylori infection generated gastric cancer through p53-Rb tumor-suppressor system mutation and telomerase reactivation.* World J Gastroenterol, 2003. **9**(1): p. 54-8.
35. Morgan, C., et al., *Detection of p53 mutations in precancerous gastric tissue.* Br J Cancer, 2003. **89**(7): p. 1314-9.
36. La Vecchia, C., et al., *Family history and the risk of stomach and colorectal cancer.* Cancer, 1992. **70**(1): p. 50-5.
37. Wang, X.Q., et al., *Interaction between dietary factors and Helicobacter pylori infection in noncardia gastric cancer: a population-based case-control study in China.* J Am Coll Nutr, 2012. **31**(5): p. 375-84.
38. Wu, Y., et al., *Analysis of risk factors associated with precancerous lesion of gastric cancer in patients from eastern China: a comparative study.* J Cancer Res Ther, 2013. **9**(2): p. 205-9.
39. You, W.C., et al., *Gastric dysplasia and gastric cancer: Helicobacter pylori, serum vitamin C, and other risk factors.* J Natl Cancer Inst, 2000. **92**(19): p. 1607-12.
40. You, W.C., et al., *Diet and high risk of stomach cancer in Shandong, China.* Cancer Res, 1988. **48**(12): p. 3518-23.
41. Burr, M.L., et al., *Atrophic gastritis and vitamin C status in two towns with different stomach cancer death-rates.* Br J Cancer, 1987. **56**(2): p. 163-7.
42. Dabrowska-Ufniarz, E., et al., *Vitamin C concentration in gastric juice in patients with precancerous lesions of the stomach and gastric cancer.* Med Sci Monit, 2002. **8**(2): p. CR96-103.
43. Yu, Y., et al., *The Anti-tumor Activity of Vitamin C via the Increase of Fas (CD95) and MHC I Expression on Human Stomach Cancer Cell Line, SNU1.* Immune Netw, 2011. **11**(4): p. 210-5.
44. Sobala, G.M., et al., *Effect of eradication of Helicobacter pylori on gastric juice ascorbic acid concentrations.* Gut, 1993. **34**(8): p. 1038-41.
45. Fuchs, C.S. and R.J. Mayer, *Gastric carcinoma.* N Engl J Med, 1995. **333**(1): p. 32-41.
46. Appelman, H.D., *A cohort study of stomach cancer in a high-risk American population.* Cancer, 1992. **69**(11): p. 2867-8.

47. Nomura, A., et al., *A prospective study of stomach cancer and its relation to diet, cigarettes, and alcohol consumption.* Cancer Res, 1990. **50**(3): p. 627-31.
48. Tong, G.X., et al., *Association of risk of gastric cancer and consumption of tobacco, alcohol and tea in the Chinese population.* Asian Pac J Cancer Prev, 2014. **15**(20): p. 8765-74.
49. Liu, J., et al., *Serum Helicobacter pylori NapA antibody as a potential biomarker for gastric cancer.* Sci Rep, 2014. **4**: p. 4143.
50. *Schistosomes, liver flukes and Helicobacter pylori. IARC Working Group on the Evaluation of Carcinogenic Risks to Humans. Lyon, 7-14 June 1994.* IARC Monogr Eval Carcinog Risks Hum, 1994. **61**: p. 1-241.
51. Maev, I.V., et al., *[Eradication therapy for Helicobacter pylori infection: review of world trends].* Ter Arkh, 2014. **86**(3): p. 94-9.
52. Polinkevych, B.S. and P.B. Pikas, *[The role of Helicobacter pylori in occurrence of the digestive system pathologic processes].* Klin Khir, 2014(6): p. 66-9.
53. Lee, K.E., et al., *Helicobacter pylori and interleukin-8 in gastric cancer.* World J Gastroenterol, 2013. **19**(45): p. 8192-202.
54. Conteduca, V., et al., *H. pylori infection and gastric cancer: state of the art (review).* Int J Oncol, 2013. **42**(1): p. 5-18.
55. Goldgar, D.E., et al., *Systematic population-based assessment of cancer risk in first-degree relatives of cancer probands.* J Natl Cancer Inst, 1994. **86**(21): p. 1600-8.
56. Stone, J., et al., *Low frequency of germline E-cadherin mutations in familial and nonfamilial gastric cancer.* Br J Cancer, 1999. **79**(11-12): p. 1935-7.
57. Kaurah, P., et al., *Founder and recurrent CDH1 mutations in families with hereditary diffuse gastric cancer.* JAMA, 2007. **297**(21): p. 2360-72.
58. Oliveira, C., et al., *Germline CDH1 deletions in hereditary diffuse gastric cancer families.* Hum Mol Genet, 2009. **18**(9): p. 1545-55.
59. Arid I, Bentall HH, and J. Robert, *A relationship between cancer of the stomach and the ABO blood groups.* Br Med J, 1953. **i**: p. 799-801.
60. Cohen, A.M., L.L. Gunderson, and C.E. Welch, *Radiation therapy of rectal cancer.* World J Surg, 1982. **6**(5): p. 560-8.
61. Wang, Z., et al., *ABO blood group system and gastric cancer: a case-control study and meta-analysis.* Int J Mol Sci, 2012. **13**(10): p. 13308-21.
62. You, W.C., et al., *Blood type and family cancer history in relation to precancerous gastric lesions.* Int J Epidemiol, 2000. **29**(3): p. 405-7.
63. Wang, Z., et al., *ABO Blood Group System and Gastric Cancer: A Case-Control Study and Meta-Analysis.* Int J Mol Sci, 2012. **13**(10): p. 13308-21.
64. Ruddell, W.S., et al., *Pathogenesis of gastric cancer in pernicious anaemia.* Lancet, 1978. **1**(8063): p. 521-3.
65. Elsborg, L. and J. Mosbech, *Pernicious anaemia as a risk factor in gastric cancer.* Acta Med Scand, 1979. **206**(4): p. 315-8.
66. Association., J.G.C., *Japanese Classification of Gastric Carcinoma - 2nd English Edition.* Gastric Cancer, 1998. **1**: p. 10-24.
67. Katai, H. and T. Sano, *Early gastric cancer: concepts, diagnosis, and management.* Int J Clin Oncol, 2005. **10**(6): p. 375-83.
68. Bu, Z. and J. Ji, *Controversies in the diagnosis and management of early gastric cancer.* Chin J Cancer Res, 2013. **25**(3): p. 263-6.
69. Park, Y.M., et al., *The effectiveness and safety of endoscopic submucosal dissection compared with endoscopic mucosal resection for early gastric cancer: a systematic review and metaanalysis.* Surg Endosc, 2011. **25**(8): p. 2666-77.
70. Kim, H.H., et al., *Morbidity and mortality of laparoscopic gastrectomy versus open gastrectomy for gastric cancer: an interim report--a phase III multicenter, prospective, randomized Trial (KLASS Trial).* Ann Surg, 2010. **251**(3): p. 417-20.

71. Curtis, J.L., et al., *Primary gastric tumors of infancy and childhood: 54-year experience at a single institution.* J Pediatr Surg, 2008. **43**(8): p. 1487-93.
72. Moschovi, M., et al., *Primary gastric Burkitt lymphoma in childhood: associated with Helicobacter pylori?* Med Pediatr Oncol, 2003. **41**(5): p. 444-7.
73. Mahour, G.H., H. Isaacs, Jr., and L. Chang, *Primary malignant tumors of the stomach in children.* J Pediatr Surg, 1980. **15**(5): p. 603-8.
74. Skinner, M.A., et al., *Gastrointestinal tumors in children: an analysis of 39 cases.* Ann Surg Oncol, 1994. **1**(4): p. 283-9.
75. Harting, M.T., et al., *Treatment issues in pediatric gastric adenocarcinoma.* J Pediatr Surg, 2004. **39**(8): p. e8-10.
76. Schwartz, M.G. and N.A. Sgaglione, *Gastric carcinoma in the young: overview of the literature.* Mt Sinai J Med, 1984. **51**(6): p. 720-3.
77. Goto, S., et al., *Carcinoma of the stomach in a 7-year-old boy--a case report and a review of the literature on children under 10 years of age.* Z Kinderchir, 1984. **39**(2): p. 137-40.
78. Lack, E.E., *Leiomyosarcomas in childhood: a clinical and pathologic study of 10 cases.* Pediatr Pathol, 1986. **6**(2-3): p. 181-97.
79. Ogami, H., et al., *Gastric teratoma in infancy and childhood: report of three cases and review of literature.* Jpn J Surg, 1973. **3**(4): p. 218-28.
80. Ferrari, A., et al., *Childhood liposarcoma: a single-institutional twenty-year experience.* Pediatr Hematol Oncol, 1999. **16**(5): p. 415-21.
81. Arslan, N.C., et al., *Gastric metastasis of breast cancer mimicking primary gastric cancer: a case report.* Turk J Gastroenterol, 2012. **23**(6): p. 808-9.
82. Caruso, R.A., *The histogenesis of mucinous adenocarcinoma of the stomach from observations in early gastric cancer.* Ann Diagn Pathol, 1999. **3**(3): p. 160-4.
83. Sun, D.Z., et al., *Tumor interstitial fluid and gastric cancer metastasis: an experimental study to verify the hypothesis of "tumor-phlegm microenvironment".* Chin J Integr Med, 2012. **18**(5): p. 350-8.
84. *The general rules for The gastric cancer study in surgery.* Jpn J Surg, 1973. **3**(1): p. 61-71.
85. Ming, S.C., *The classification and significance of gastric polyps.* Monogr Pathol, 1977(18): p. 149-75.
86. Ambrosetti, D., et al., *An expansive paranasal sinus tumour-like lesion caused by Bipolaris spicifera in an immunocompetent patient.* Histopathology, 2006. **49**(6): p. 660-2.
87. Bearzi, I. and R. Ranaldi, *Early gastric cancer: a morphologic study of 41 cases.* Tumori, 1982. **68**(3): p. 223-33.
88. Lauren, P., *The Two Histological Main Types of Gastric Carcinoma: Diffuse and So-Called Intestinal-Type Carcinoma. An Attempt at a Histo-Clinical Classification.* Acta Pathol Microbiol Scand, 1965. **64**: p. 31-49.
89. Machado, J.C., et al., *E-cadherin gene mutations provide a genetic basis for the phenotypic divergence of mixed gastric carcinomas.* Lab Invest, 1999. **79**(4): p. 459-65.
90. Hulscher, J.B., et al., *Laparoscopy and laparoscopic ultrasonography in staging carcinoma of the gastric cardia.* Eur J Surg, 2000. **166**(11): p. 862-5.
91. Edge, S.B. and C.C. Compton, *The American Joint Committee on Cancer: the 7th edition of the AJCC cancer staging manual and the future of TNM.* Ann Surg Oncol, 2010. **17**(6): p. 1471-4.
92. Smith, D.D., R.R. Schwarz, and R.E. Schwarz, *Impact of total lymph node count on staging and survival after gastrectomy for gastric cancer: data from a large US-population database.* J Clin Oncol, 2005. **23**(28): p. 7114-24.
93. Ichikura, T., et al., *Evaluation of the New American Joint Committee on Cancer/International Union against cancer classification of lymph node metastasis from gastric carcinoma in comparison with the Japanese classification.* Cancer, 1999. **86**(4): p. 553-8.
94. Japanese Gastric Cancer, A., *Japanese Classification of Gastric Carcinoma - 2nd English Edition.* Gastric Cancer, 1998. **1**(1): p. 10-24.

95. Sun, Z., et al., *Log odds of positive lymph nodes: a novel prognostic indicator superior to the number-based and the ratio-based N category for gastric cancer patients with R0 resection.* Cancer, 2010. **116**(11): p. 2571-80.
96. Aiko, T. and M. Sasako, *The new Japanese Classification of Gastric Carcinoma: Points to be revised.* Gastric Cancer, 1998. **1**(1): p. 25-30.
97. Aikou, T., S. Hokita, and S. Natsugoe, *[Japanese Classification of Gastric Carcinoma (the 13th edition, June 1999): points to be revised].* Nihon Rinsho, 2001. **59 Suppl 4**: p. 159-65.
98. Wanebo, H.J., et al., *Cancer of the stomach. A patient care study by the American College of Surgeons.* Ann Surg, 1993. **218**(5): p. 583-92.
99. Maconi, G., G. Manes, and G.B. Porro, *Role of symptoms in diagnosis and outcome of gastric cancer.* World J Gastroenterol, 2008. **14**(8): p. 1149-55.
100. Kong, S.H., et al., *Clinicopathologic features of asymptomatic gastric adenocarcinoma patients in Korea.* Jpn J Clin Oncol, 2004. **34**(1): p. 1-7.
101. Dewys, W.D., et al., *Prognostic effect of weight loss prior to chemotherapy in cancer patients. Eastern Cooperative Oncology Group.* Am J Med, 1980. **69**(4): p. 491-7.
102. Graham, D.Y. and M. Asaka, *Eradication of gastric cancer and more efficient gastric cancer surveillance in Japan: two peas in a pod.* J Gastroenterol, 2010. **45**(1): p. 1-8.
103. Murakami, R., et al., *Estimation of validity of mass screening program for gastric cancer in Osaka, Japan.* Cancer, 1990. **65**(5): p. 1255-60.
104. Rugge, M., et al., *OLGA gastritis staging in young adults and country-specific gastric cancer risk.* Int J Surg Pathol, 2008. **16**(2): p. 150-4.
105. Ohata, H., et al., *Progression of chronic atrophic gastritis associated with Helicobacter pylori infection increases risk of gastric cancer.* Int J Cancer, 2004. **109**(1): p. 138-43.
106. Shimada, H., et al., *Clinical significance of serum tumor markers for gastric cancer: a systematic review of literature by the Task Force of the Japanese Gastric Cancer Association.* Gastric Cancer, 2013.
107. Zeng, Z., et al., *The diagnostic value of monoclonal gastric cancer 7 antigen: a systematic review with meta-analysis.* Clin Exp Med, 2013.
108. Chuang, J.Y., et al., *Apoptosis Signal-Regulating Kinase 1 Is Involved in WISP-1-Promoted Cell Motility in Human Oral Squamous Cell Carcinoma Cells.* PLoS One, 2013. **8**(10): p. e78022.
109. Silberman, H., *Perioperative adjunctive treatment in the management of operable gastric cancer.* J Surg Oncol, 2005. **90**(3): p. 174-86; discussion 186-7.
110. Ott, K., et al., *Chromosomal instability rather than p53 mutation is associated with response to neoadjuvant cisplatin-based chemotherapy in gastric carcinoma.* Clin Cancer Res, 2003. **9**(6): p. 2307-15.
111. Lenz, H.J., et al., *Thymidylate synthase mRNA level in adenocarcinoma of the stomach: a predictor for primary tumor response and overall survival.* J Clin Oncol, 1996. **14**(1): p. 176-82.
112. Metzger, R., et al., *ERCC1 mRNA levels complement thymidylate synthase mRNA levels in predicting response and survival for gastric cancer patients receiving combination cisplatin and fluorouracil chemotherapy.* J Clin Oncol, 1998. **16**(1): p. 309-16.
113. Kasprzyk, P.G., et al., *Therapy of an animal model of human gastric cancer using a combination of anti-erbB-2 monoclonal antibodies.* Cancer Res, 1992. **52**(10): p. 2771-6.
114. Sipponen, P. and B.J. Marshall, *Gastritis and gastric cancer. Western countries.* Gastroenterol Clin North Am, 2000. **29**(3): p. 579-92, v-vi.
115. Axon, A., *Symptoms and diagnosis of gastric cancer at early curable stage.* Best Pract Res Clin Gastroenterol, 2006. **20**(4): p. 697-708.
116. Cho, A., et al., *Acceptance of repeat esophagogastroduodenoscopy to detect gastric cancer in a Chinese immigrant cohort.* J Clin Gastroenterol, 2006. **40**(7): p. 606-11.
117. Nobuta, A., et al., *Helicobacter pylori infection in two areas in Japan with different risks for gastric cancer.* Aliment Pharmacol Ther, 2004. **20 Suppl 1**: p. 1-6.

118. Maruyama, K., et al., *Lymph node metastases of gastric cancer. General pattern in 1931 patients.* Ann Surg, 1989. **210**(5): p. 596-602.
119. Fly, O.A., Jr., J.M. Waugh, and M.B. Dockerty, *Splenic hilar nodal involvement in carcinoma of the distal part of the stomach.* Cancer, 1956. **9**(3): p. 459-62.
120. Gunderson, L.L. and H. Sosin, *Adenocarcinoma of the stomach: areas of failure in a re-operation series (second or symptomatic look) clinicopathologic correlation and implications for adjuvant therapy.* Int J Radiat Oncol Biol Phys, 1982. **8**(1): p. 1-11.
121. Douglass, H.O., Jr., *Adjuvant therapy of gastric cancer: have we made any progress?* Ann Oncol, 1994. **5 Suppl 3**: p. 49-57.
122. Yonemura, Y., et al., *Effective therapy for peritoneal dissemination in gastric cancer.* Surg Oncol Clin N Am, 2003. **12**(3): p. 635-48.
123. Xu, D.Z., et al., *Meta-analysis of intraperitoneal chemotherapy for gastric cancer.* World J Gastroenterol, 2004. **10**(18): p. 2727-30.
124. Sugarbaker, P.H., W. Yu, and Y. Yonemura, *Gastrectomy, peritonectomy, and perioperative intraperitoneal chemotherapy: the evolution of treatment strategies for advanced gastric cancer.* Semin Surg Oncol, 2003. **21**(4): p. 233-48.
125. Hartley, L.C., E. Evans, and C.J. Windsor, *Factors influencing prognosis in gastric cancer.* Aust N Z J Surg, 1987. **57**(1): p. 5-9.
126. Kennedy, B.J., *T N M classification for stomach cancer.* Cancer, 1970. **26**(5): p. 971-83.
127. Douglass, H.O., Jr. and H.R. Nava, *Gastric adenocarcinoma--management of the primary disease.* Semin Oncol, 1985. **12**(1): p. 32-45.
128. Nagatomo, T., E. Murakami, and K. Kondo, *Histologic criteria of serosal rupture and prognosis in gastric carcinoma.* Cancer, 1972. **29**(1): p. 180-90.
129. Gunderson, L.L., *Gastric cancer--patterns of relapse after surgical resection.* Semin Radiat Oncol, 2002. **12**(2): p. 150-61.
130. Chau, I., et al., *Multivariate prognostic factor analysis in locally advanced and metastatic esophago-gastric cancer--pooled analysis from three multicenter, randomized, controlled trials using individual patient data.* J Clin Oncol, 2004. **22**(12): p. 2395-403.
131. Byfield, S.A., et al., *Treatment and outcomes of gastric cancer among United States-born and foreign-born Asians and Pacific Islanders.* Cancer, 2009. **115**(19): p. 4595-605.
132. Baba, H., et al., *Prognostic factors in gastric cancer with serosal invasion. Univariate and multivariate analyses.* Arch Surg, 1989. **124**(9): p. 1061-4.
133. Korenaga, D., et al., *DNA ploidy is closely linked to tumor invasion, lymph node metastasis, and prognosis in clinical gastric cancer.* Cancer, 1988. **62**(2): p. 309-13.
134. Nanus, D.M., et al., *Flow cytometry as a predictive indicator in patients with operable gastric cancer.* J Clin Oncol, 1989. **7**(8): p. 1105-12.
135. Asakawa, H., et al., *Combination therapy of gastric carcinoma with radiation and chemotherapy.* Tohoku J Exp Med, 1982. **137**(4): p. 445-52.
136. Asakawa, H. and T. Takeda, *High energy x-ray therapy of gastric carcinoma.* Nihon Gan Chiryo Gakkai Shi, 1973. **8**(4): p. 362-71.
137. Tsukiyama, I., et al., *Radiation therapy for advanced gastric cancer.* Int J Radiat Oncol Biol Phys, 1988. **15**(1): p. 123-7.
138. Dockerty, M.B., *Pathologic aspects of carcinoma of the stomach.* Mo Med, 1952. **49**(8): p. 653-8.
139. Lynch, H.T., et al., *Genetics, natural history, tumor spectrum, and pathology of hereditary nonpolyposis colorectal cancer: an updated review.* Gastroenterology, 1993. **104**(5): p. 1535-49.
140. Kokudo, N., et al., *Effect of 70% hepatectomy on DNA synthesis in rat hepatocyte isograft into the spleen.* Transplant Proc, 1994. **26**(6): p. 3464-5.

141. Kitadai, Y., et al., *GC factor represses transcription of several growth factor/receptor genes and causes growth inhibition of human gastric carcinoma cell lines.* Cell Growth Differ, 1993. **4**(4): p. 291-6.
142. Blank, S., et al., *Angiogenic and growth factors in gastric cancer.* J Surg Res, 2014.
143. Hilton, D.A. and K.P. West, *An evaluation of the prognostic significance of HLA-DR expression in gastric carcinoma.* Cancer, 1990. **66**(6): p. 1154-7.
144. Wu, A. and J. Ji, *Adjuvant chemotherapy for gastric cancer or not: a dilemma?* J Natl Cancer Inst, 2008. **100**(6): p. 376-7.
145. Kitano, S., K. Yasuda, and N. Shiraishi, *Laparoscopic surgical resection for early gastric cancer.* Eur J Gastroenterol Hepatol, 2006. **18**(8): p. 855-61.
146. Kitano, S., et al., *A multicenter study on oncologic outcome of laparoscopic gastrectomy for early cancer in Japan.* Ann Surg, 2007. **245**(1): p. 68-72.
147. Huscher, C.G., et al., *Laparoscopic versus open subtotal gastrectomy for distal gastric cancer: five-year results of a randomized prospective trial.* Ann Surg, 2005. **241**(2): p. 232-7.
148. Kim, Y.W., et al., *Improved quality of life outcomes after laparoscopy-assisted distal gastrectomy for early gastric cancer: results of a prospective randomized clinical trial.* Ann Surg, 2008. **248**(5): p. 721-7.
149. Kramling, H.J., et al., *Early results of IORT in the treatment of gastric cancer.* Front Radiat Ther Oncol, 1997. **31**: p. 157-60.
150. Sindelar, W.F., et al., *Randomized trial of intraoperative radiotherapy in carcinoma of the stomach.* Am J Surg, 1993. **165**(1): p. 178-86; discussion 186-7.
151. Diaz-Gonzalez, J.A., et al., *Patterns of response after preoperative treatment in gastric cancer.* Int J Radiat Oncol Biol Phys, 2011. **80**(3): p. 698-704.
152. Cunningham, D., et al., *Perioperative chemotherapy versus surgery alone for resectable gastroesophageal cancer.* N Engl J Med, 2006. **355**(1): p. 11-20.
153. Macdonald, J.S., et al., *Chemoradiotherapy after surgery compared with surgery alone for adenocarcinoma of the stomach or gastroesophageal junction.* N Engl J Med, 2001. **345**(10): p. 725-30.
154. Tanaka, Y., T. Yamamura, and T. Kanda, *[Molecular targeted therapy].* Brain Nerve, 2014. **66**(10): p. 1137- 47.
155. Ohtsu, A., *Chemotherapy for metastatic gastric cancer: past, present, and future.* J Gastroenterol, 2008. **43**(4): p. 256-64.
156. Fornaro, L., et al., *Anti-HER agents in gastric cancer: from bench to bedside.* Nat Rev Gastroenterol Hepatol, 2011. **8**(7): p. 369-83.
157. Bang, Y.J., et al., *Trastuzumab in combination with chemotherapy versus chemotherapy alone for treatment of HER2-positive advanced gastric or gastro-oesophageal junction cancer (ToGA): a phase 3, open-label, randomised controlled trial.* Lancet, 2010. **376**(9742): p. 687-97.
158. Koh, Y.W., et al., *Dual-color silver-enhanced in situ hybridization for assessing HER2 gene amplification in breast cancer.* Mod Pathol, 2011. **24**(6): p. 794-800.
159. Bao, B., et al., *Over-expression of FoxM1 leads to epithelial-mesenchymal transition and cancer stem cell phenotype in pancreatic cancer cells.* J Cell Biochem, 2011. **112**(9): p. 2296-306.
160. Thiery, J.P., *Epithelial-mesenchymal transitions in tumour progression.* Nat Rev Cancer, 2002. **2**(6): p. 442-54.
161. Trelstad, R.L., E.D. Hay, and J.D. Revel, *Cell contact during early morphogenesis in the chick embryo.* Dev Biol, 1967. **16**(1): p. 78-106.
162. Greenburg, G. and E.D. Hay, *Epithelia suspended in collagen gels can lose polarity and express characteristics of migrating mesenchymal cells.* J Cell Biol, 1982. **95**(1): p. 333-9.
163. Stoker, M. and M. Perryman, *An epithelial scatter factor released by embryo fibroblasts.* J Cell Sci, 1985. **77**: p. 209-23.

164. Nakamura, T., et al., *Molecular cloning and expression of human hepatocyte growth factor.* Nature, 1989. **342**(6248): p. 440-3.
165. Naldini, L., et al., *Scatter factor and hepatocyte growth factor are indistinguishable ligands for the MET receptor.* EMBO J, 1991. **10**(10): p. 2867-78.
166. Weidner, K.M., et al., *Molecular characteristics of HGF-SF and its role in cell motility and invasion.* EXS, 1993. **65**: p. 311-28.
167. Torenbeek, R., et al., *Analysis by comparative genomic hybridization of epithelial and spindle cell components in sarcomatoid carcinoma and carcinosarcoma: histogenetic aspects.* J Pathol, 1999. **189**(3): p. 338-43.
168. Wick, M.R. and P.E. Swanson, *Carcinosarcomas: current perspectives and an historical review of nosological concepts.* Semin Diagn Pathol, 1993. **10**(2): p. 118-27.
169. Thompson, L., B. Chang, and S.H. Barsky, *Monoclonal origins of malignant mixed tumors (carcinosarcomas). Evidence for a divergent histogenesis.* Am J Surg Pathol, 1996. **20**(3): p. 277-85.
170. Kalluri, R. and R.A. Weinberg, *The basics of epithelial-mesenchymal transition.* J Clin Invest, 2009. **119**(6): p. 1420-8.
171. Scheel, C. and R.A. Weinberg, *Phenotypic plasticity and epithelial-mesenchymal transitions in cancer and normal stem cells?* Int J Cancer, 2011. **129**(10): p. 2310-4.
172. Giampieri, S., et al., *Localized and reversible TGFbeta signalling switches breast cancer cells from cohesive to single cell motility.* Nat Cell Biol, 2009. **11**(11): p. 1287-96.
173. Xue, C., et al., *The gatekeeper effect of epithelial-mesenchymal transition regulates the frequency of breast cancer metastasis.* Cancer Res, 2003. **63**(12): p. 3386-94.
174. Trimboli, A.J., et al., *Direct evidence for epithelial-mesenchymal transitions in breast cancer.* Cancer Res, 2008. **68**(3): p. 937-45.
175. Rhim, A.D., et al., *EMT and dissemination precede pancreatic tumor formation.* Cell, 2012. **148**(1-2): p. 349-61.
176. Tarin, D., E.W. Thompson, and D.F. Newgreen, *The fallacy of epithelial mesenchymal transition in neoplasia.* Cancer Res, 2005. **65**(14): p. 5996-6000; discussion 6000-1.
177. Thompson, E.W., D.F. Newgreen, and D. Tarin, *Carcinoma invasion and metastasis: a role for epithelial-mesenchymal transition?* Cancer Res, 2005. **65**(14): p. 5991-5; discussion 5995.
178. Yates, C., *Prostate tumor cell plasticity: a consequence of the microenvironment.* Adv Exp Med Biol, 2011. **720**: p. 81-90.
179. Gao, D., et al., *Myeloid progenitor cells in the premetastatic lung promote metastases by inducing mesenchymal to epithelial transition.* Cancer Res, 2012. **72**(6): p. 1384-94.
180. Gregory, P.A., et al., *The miR-200 family and miR-205 regulate epithelial to mesenchymal transition by targeting ZEB1 and SIP1.* Nat Cell Biol, 2008. **10**(5): p. 593-601.
181. Korpal, M., et al., *Direct targeting of Sec23a by miR-200s influences cancer cell secretome and promotes metastatic colonization.* Nat Med, 2011. **17**(9): p. 1101-8.
182. Navin, N., et al., *Tumour evolution inferred by single-cell sequencing.* Nature, 2011. **472**(7341): p. 90-4.
183. Liu, W., et al., *Copy number analysis indicates monoclonal origin of lethal metastatic prostate cancer.* Nat Med, 2009. **15**(5): p. 559-65.
184. Turajlic, S., et al., *Whole genome sequencing of matched primary and metastatic acral melanomas.* Genome Res, 2012. **22**(2): p. 196-207.
185. Katoh, M., *Epithelial-mesenchymal transition in gastric cancer (Review).* Int J Oncol, 2005. **27**(6): p. 1677-83.
186. Rodrigo, I., A.C. Cato, and A. Cano, *Regulation of E-cadherin gene expression during tumor progression: the role of a new Ets-binding site and the E-pal element.* Exp Cell Res, 1999. **248**(2): p. 358-71.
187. Cano, A., et al., *The transcription factor snail controls epithelial-mesenchymal transitions by repressing E-cadherin expression.* Nat Cell Biol, 2000. **2**(2): p. 76-83.

188. Perez-Moreno, M.A., et al., *A new role for E12/E47 in the repression of E-cadherin expression and epithelial-mesenchymal transitions.* J Biol Chem, 2001. **276**(29): p. 27424-31.
189. Pennica, D., et al., *WISP genes are members of the connective tissue growth factor family that are up-regulated in wnt-1-transformed cells and aberrantly expressed in human colon tumors.* Proc Natl Acad Sci U S A, 1998. **95**(25): p. 14717-22.
190. Zhong, N., R.P. Gersch, and M. Hadjiargyrou, *Wnt signaling activation during bone regeneration and the role of Dishevelled in chondrocyte proliferation and differentiation.* Bone, 2006. **39**(1): p. 5-16.
191. O'Brien, T.P., et al., *Expression of cyr61, a growth factor-inducible immediate-early gene.* Mol Cell Biol, 1990. **10**(7): p. 3569-77.
192. Bradham, D.M., et al., *Connective tissue growth factor: a cysteine-rich mitogen secreted by human vascular endothelial cells is related to the SRC-induced immediate early gene product CEF-10.* J Cell Biol, 1991. **114**(6): p. 1285-94.
193. Joliot, V., et al., *Proviral rearrangements and overexpression of a new cellular gene (nov) in myeloblastosis-associated virus type 1-induced nephroblastomas.* Mol Cell Biol, 1992. **12**(1): p. 10-21.
194. Brigstock, D.R., *The CCN family: a new stimulus package.* J Endocrinol, 2003. **178**(2): p. 169-75.
195. Perbal, B., D.R. Brigstock, and L.F. Lau, *Report on the second international workshop on the CCN family of genes.* Mol Pathol, 2003. **56**(2): p. 80-5.
196. Leask, A. and D.J. Abraham, *All in the CCN family: essential matricellular signaling modulators emerge from the bunker.* J Cell Sci, 2006. **119**(Pt 23): p. 4803-10.
197. Zhang, R., et al., *Identification of rCop-1, a new member of the CCN protein family, as a negative regulator for cell transformation.* Mol Cell Biol, 1998. **18**(10): p. 6131-41.
198. Kumar, S., et al., *Identification and cloning of a connective tissue growth factor-like cDNA from human osteoblasts encoding a novel regulator of osteoblast functions.* J Biol Chem, 1999. **274**(24): p. 17123-31.
199. Nessling, M., et al., *Candidate genes in breast cancer revealed by microarray-based comparative genomic hybridization of archived tissue.* Cancer Res, 2005. **65**(2): p. 439-47.
200. Chappell, S.A., et al., *Loss of heterozygosity at the mannose 6-phosphate insulin-like growth factor 2 receptor gene correlates with poor differentiation in early breast carcinomas.* Br J Cancer, 1997. **76**(12): p. 1558-61.
201. Mancuso, D.J., et al., *Structure of the gene for human von Willebrand factor.* J Biol Chem, 1989. **264**(33): p. 19514-27.
202. Hashimoto, G., et al., *Matrix metalloproteinases cleave connective tissue growth factor and reactivate angiogenic activity of vascular endothelial growth factor 165.* J Biol Chem, 2002. **277**(39): p. 36288-95.
203. de Winter, P., P. Leoni, and D. Abraham, *Connective tissue growth factor: structure-function relationships of a mosaic, multifunctional protein.* Growth Factors, 2008. **26**(2): p. 80-91.
204. Holt, G.D., M.K. Pangburn, and V. Ginsburg, *Properdin binds to sulfatide [Gal(3-SO4)beta 1-1 Cer] and has a sequence homology with other proteins that bind sulfated glycoconjugates.* J Biol Chem, 1990. **265**(5): p. 2852-5.
205. Karagiannis, E.D. and A.S. Popel, *Peptides derived from type I thrombospondin repeat-containing proteins of the CCN family inhibit proliferation and migration of endothelial cells.* Int J Biochem Cell Biol, 2007. **39**(12): p. 2314-23.
206. Bork, P., *The modular architecture of a new family of growth regulators related to connective tissue growth factor.* FEBS Lett, 1993. **327**(2): p. 125-30.
207. Voorberg, J., et al., *Assembly and routing of von Willebrand factor variants: the requirements for disulfide-linked dimerization reside within the carboxy-terminal 151 amino acids.* J Cell Biol, 1991. **113**(1): p. 195-205.

208. Brigstock, D.R., et al., *Purification and characterization of novel heparin-binding growth factors in uterine secretory fluids. Identification as heparin-regulated Mr 10,000 forms of connective tissue growth factor.* J Biol Chem, 1997. **272**(32): p. 20275-82.
209. Holbourn, K.P., B. Perbal, and K. Ravi Acharya, *Proteins on the catwalk: modelling the structural domains of the CCN family of proteins.* J Cell Commun Signal, 2009. **3**(1): p. 25-41.
210. Kubota, S. and M. Takigawa, *CCN family proteins and angiogenesis: from embryo to adulthood.* Angiogenesis, 2007. **10**(1): p. 1-11.
211. Davies, S.R., et al., *Differential expression and prognostic implications of the CCN family members WISP-1, WISP-2, and WISP-3 in human breast cancer.* Ann Surg Oncol, 2007. **14**(6): p. 1909-18.
212. Davies, S.R., et al., *Differential expression of the CCN family member WISP-1, WISP-2 and WISP-3 in human colorectal cancer and the prognostic implications.* Int J Oncol, 2010. **36**(5): p. 1129-36.
213. Banerjee, S., et al., *Epidermal growth factor induces WISP-2/CCN5 expression in estrogen receptor-alpha-positive breast tumor cells through multiple molecular cross-talks.* Mol Cancer Res, 2005. **3**(3): p. 151-62.
214. Dhar, K., et al., *Insulin-like growth factor-1 (IGF-1) induces WISP-2/CCN5 via multiple molecular cross-talks and is essential for mitogenic switch by IGF-1 axis in estrogen receptor-positive breast tumor cells.* Cancer Res, 2007. **67**(4): p. 1520-6.
215. Sengupta, K., et al., *WISP-2/CCN5 is involved as a novel signaling intermediate in phorbol ester-protein kinase Calpha-mediated breast tumor cell proliferation.* Biochemistry, 2006. **45**(35): p. 10698-709.
216. Lake, A.C., et al., *CCN5 is a growth arrest-specific gene that regulates smooth muscle cell proliferation and motility.* Am J Pathol, 2003. **162**(1): p. 219-31.
217. Dhar, G., et al., *Loss of WISP-2/CCN5 signaling in human pancreatic cancer: a potential mechanism for epithelial-mesenchymal-transition.* Cancer Lett, 2007. **254**(1): p. 63-70.
218. Banerjee, S., et al., *CCN5/WISP-2 expression in breast adenocarcinoma is associated with less frequent progression of the disease and suppresses the invasive phenotypes of tumor cells.* Cancer Res, 2008. **68**(18): p. 7606-12.
219. Inadera, H., et al., *WISP-2 as a novel estrogen-responsive gene in human breast cancer cells.* Biochem Biophys Res Commun, 2000. **275**(1): p. 108-14.
220. Inadera, H., H.Y. Dong, and K. Matsushima, *WISP-2 is a secreted protein and can be a marker of estrogen exposure in MCF-7 cells.* Biochem Biophys Res Commun, 2002. **294**(3): p. 602-8.
221. Banerjee, S., et al., *WISP-2 gene in human breast cancer: estrogen and progesterone inducible expression and regulation of tumor cell proliferation.* Neoplasia, 2003. **5**(1): p. 63-73.
222. Zoubine, M.N., et al., *WISP-2: a serum-inducible gene differentially expressed in human normal breast epithelial cells and in MCF-7 breast tumor cells.* Biochem Biophys Res Commun, 2001. **282**(2): p. 421-5.
223. Ray, G., et al., *Stimulation of MCF-7 tumor progression in athymic nude mice by 17beta-estradiol induces WISP-2/CCN5 expression in xenografts: a novel signaling molecule in hormonal carcinogenesis.* Oncol Rep, 2005. **13**(3): p. 445-8.
224. Saxena, N., et al., *Differential expression of WISP-1 and WISP-2 genes in normal and transformed human breast cell lines.* Mol Cell Biochem, 2001. **228**(1-2): p. 99-104.
225. Tanner, M.M., et al., *Increased copy number at 20q13 in breast cancer: defining the critical region and exclusion of candidate genes.* Cancer Res, 1994. **54**(16): p. 4257-60.
226. Bischoff, J.R., et al., *A homologue of Drosophila aurora kinase is oncogenic and amplified in human colorectal cancers.* EMBO J, 1998. **17**(11): p. 3052-65.
227. Cervello, M., et al., *Expression of WISPs and of their novel alternative variants in human hepatocellular carcinoma cells.* Ann N Y Acad Sci, 2004. **1028**: p. 432-9.
228. Fukutomi, T., et al., *Hepatitis C virus core protein stimulates hepatocyte growth: correlation with upregulation of wnt-1 expression.* Hepatology, 2005. **41**(5): p. 1096-105.

229. Tomimaru, Y., et al., *Upregulation of T-cell factor-4 isoform-responsive target genes in hepatocellular carcinoma.* Liver Int, 2013.
230. Quan, T., et al., *Expression of CCN family of genes in human skin in vivo and alterations by solar-simulated ultraviolet irradiation.* J Cell Commun Signal, 2009. **3**(1): p. 19-23.
231. Colli, L.M., et al., *Components of the canonical and non-canonical Wnt pathways are not mis-expressed in pituitary tumors.* PLoS One, 2013. **8**(4): p. e62424.
232. Tian, C., et al., *Overexpression of connective tissue growth factor WISP-1 in Chinese primary rectal cancer patients.* World J Gastroenterol, 2007. **13**(28): p. 3878-82.
233. Fang, F., et al., *Silencing of WISP3 suppresses gastric cancer cell proliferation and metastasis and inhibits Wnt/beta-catenin signaling.* Int J Clin Exp Pathol, 2014. **7**(10): p. 6447-61.
234. Soon, L.L., et al., *Overexpression of WISP-1 down-regulated motility and invasion of lung cancer cells through inhibition of Rac activation.* J Biol Chem, 2003. **278**(13): p. 11465-70.
235. Chen, P.P., et al., *Expression of Cyr61, CTGF, and WISP-1 correlates with clinical features of lung cancer.* PLoS One, 2007. **2**(6): p. e534.
236. Xu, L., et al., *WISP-1 is a Wnt-1- and beta-catenin-responsive oncogene.* Genes Dev, 2000. **14**(5): p. 585-95.
237. Tanaka, I., et al., *Expression and regulation of WISP2 in rheumatoid arthritic synovium.* Biochem Biophys Res Commun, 2005. **334**(4): p. 973-8.
238. Russo, J.W. and J.J. Castellot, *CCN5: biology and pathophysiology.* J Cell Commun Signal, 2010. **4**(3): p. 119-30.
239. Bejsovec, A., *Wnt pathway activation: new relations and locations.* Cell, 2005. **120**(1): p. 11-4.
240. De, A., *Wnt/Ca2+ signaling pathway: a brief overview.* Acta Biochim Biophys Sin (Shanghai), 2011. **43**(10): p. 745-56.
241. Inadera, H., *Estrogen-induced genes, WISP-2 and pS2, respond divergently to protein kinase pathway.* Biochem Biophys Res Commun, 2003. **309**(2): p. 272-8.
242. Wierer, M., et al., *PLK1 Signaling in Breast Cancer Cells Cooperates with Estrogen Receptor-Dependent Gene Transcription.* Cell Rep, 2013. **3**(6): p. 2021-32.
243. Ferrand, N., et al., *Glucocorticoids induce CCN5/WISP-2 expression and attenuate invasion in oestrogen receptor-negative human breast cancer cells.* Biochem J, 2012. **447**(1): p. 71-9.
244. Stiehl, D.P., et al., *Non-canonical HIF-2alpha function drives autonomous breast cancer cell growth via an AREG-EGFR/ErbB4 autocrine loop.* Oncogene, 2012. **31**(18): p. 2283-97.
245. Fritah, A., et al., *Role of WISP-2/CCN5 in the maintenance of a differentiated and noninvasive phenotype in human breast cancer cells.* Mol Cell Biol, 2008. **28**(3): p. 1114-23.
246. Delmolino, L.M., N.A. Stearns, and J.J. Castellot, Jr., *COP-1, a member of the CCN family, is a heparin-induced growth arrest specific gene in vascular smooth muscle cells.* J Cell Physiol, 2001. **188**(1): p. 45-55.
247. Ulrich, C., et al., *Low osteogenic differentiation potential of placenta-derived mesenchymal stromal cells correlates with low expression of the transcription factors Runx2 and Twist2.* Stem Cells Dev, 2013.
248. Bourdeau, I., et al., *Gene array analysis of macronodular adrenal hyperplasia confirms clinical heterogeneity and identifies several candidate genes as molecular mediators.* Oncogene, 2004. **23**(8): p. 1575-85.
249. Wang, J., G.Y. Zhang, and X.H. Li, *Effect of indomethacin on Bfl-1, WISP-1 and proliferating cell nuclear antigen in colon cancer cell line HCT116 cells.* Chin J Dig Dis, 2006. **7**(4): p. 219-24.
250. Dhar, G., et al., *Gain of oncogenic function of p53 mutants induces invasive phenotypes in human breast cancer cells by silencing CCN5/WISP-2.* Cancer Res, 2008. **68**(12): p. 4580-7.
251. Jiafu Ji, S.J., Wen G Jiang *WISP2 is an independent prognosis indicator of gastric cancer patients and regulates the biological function of gastric cancer cells via the JNK pathway.* European Cancer Congress 2013, 2013.
252. Hugo, H., et al., *Epithelial--mesenchymal and mesenchymal--epithelial transitions in carcinoma progression.* J Cell Physiol, 2007. **213**(2): p. 374-83.

253. Thiery, J.P., et al., *Epithelial-mesenchymal transitions in development and disease.* Cell, 2009. **139**(5): p. 871-90.
254. Ouelaa-Benslama, R., et al., *Identification of a GalphaGbetagamma, AKT and PKCalpha signalome associated with invasive growth in two genetic models of human breast cancer cell epithelial-to-mesenchymal transition.* Int J Oncol, 2012. **41**(1): p. 189-200.
255. Sabbah, M., et al., *CCN5, a novel transcriptional repressor of the transforming growth factor beta signaling pathway.* Mol Cell Biol, 2011. **31**(7): p. 1459-69.
256. Akagi, T. and T. Kimoto, *Human cell line (HGC-27) derived from the metastatic lymph node of gastric cancer.* Acta Medica Okayama, 1976. **30**(3): p. 215-217.
257. Haseloff, J. and W.L. Gerlach, *Simple RNA enzymes with new and highly specific endoribonuclease activities.* Nature, 1988. **334**(6183): p. 585-91.
258. Uhlenbeck, O.C., *A small catalytic oligoribonucleotide.* Nature, 1987. **328**(6131): p. 596-600.
259. Zuker, M., *Mfold web server for nucleic acid folding and hybridization prediction.* Nucleic Acids Res, 2003. **31**(13): p. 3406-15.
260. Jiang, W.G., et al., *Targeting matrilysin and its impact on tumor growth in vivo: the potential implications in breast cancer therapy.* Clin Cancer Res, 2005. **11**(16): p. 6012-9.
261. Jiang, W.G., et al., *Regulation of motility and invasion of cancer cells by human monocytic cells.* Anticancer Res, 1995. **15**(4): p. 1303-10.
262. Keese, C.R., et al., *Electrical wound-healing assay for cells in vitro.* Proc Natl Acad Sci U S A, 2004. **101**(6): p. 1554-9.
263. Leber, M.F. and T. Efferth, *Molecular principles of cancer invasion and metastasis (review).* Int J Oncol, 2009. **34**(4): p. 881-95.
264. Enderling, H., L. Hlatky, and P. Hahnfeldt, *Migration rules: tumours are conglomerates of self-metastases.* Br J Cancer, 2009. **100**(12): p. 1917-25.
265. Chen, C.C. and L.F. Lau, *Functions and mechanisms of action of CCN matricellular proteins.* Int J Biochem Cell Biol, 2009. **41**(4): p. 771-83.
266. Calvisi, D.F., et al., *Activation of the canonical Wnt/beta-catenin pathway confers growth advantages in c-Myc/E2F1 transgenic mouse model of liver cancer.* J Hepatol, 2005. **42**(6): p. 842-9.
267. Xie, D., et al., *Elevated levels of connective tissue growth factor, WISP-1, and CYR61 in primary breast cancers associated with more advanced features.* Cancer Res, 2001. **61**(24): p. 8917-23.
268. Lorenzatti, G., et al., *CCN6 (WISP3) decreases ZEB1-mediated EMT and invasion by attenuation of IGF-1 receptor signaling in breast cancer.* J Cell Sci, 2011. **124**(Pt 10): p. 1752-8.
269. Banerjee, S.K. and S. Banerjee, *CCN5/WISP-2: A micromanager of breast cancer progression.* J Cell Commun Signal, 2012. **6**(2): p. 63-71.
270. Jiang, W.G., et al., *Inhibition of hepatocyte growth factor-induced motility and in vitro invasion of human colon cancer cells by gamma-linolenic acid.* Br J Cancer, 1995. **71**(4): p. 744-52.
271. Chowdhury, S., et al., *IGF-I stimulates CCN5/WISP2 gene expression in pancreatic beta-cells, which promotes cell proliferation and survival against streptozotocin.* Endocrinology, 2014. **155**(5): p. 1629-42.
272. Faouzi, M., et al., *Down-regulation of Orai3 arrests cell-cycle progression and induces apoptosis in breast cancer cells but not in normal breast epithelial cells.* J Cell Physiol, 2011. **226**(2): p. 542-51.
273. Ferrand, N., et al., *Loss of WISP2/CCN5 in estrogen-dependent MCF7 human breast cancer cells promotes a stem-like cell phenotype.* PLoS One, 2014. **9**(2): p. e87878.
274. Hammarstedt, A., et al., *WISP2 regulates preadipocyte commitment and PPARgamma activation by BMP4.* Proc Natl Acad Sci U S A, 2013. **110**(7): p. 2563-8.
275. Ohkawa, Y., et al., *Wisp2/CCN5 up-regulated in the central nervous system of GM3-only mice facilitates neurite formation in Neuro2a cells via integrin-Akt signaling.* Biochem Biophys Res Commun, 2011. **411**(3): p. 483-9.

276. Harms, J.F., D.R. Welch, and M.E. Miele, *KISS1 metastasis suppression and emergent pathways.* Clin Exp Metastasis, 2003. **20**(1): p. 11-8.
277. Bailly, M., N. Zebda, and J.F. Dore, *Human melanoma metastasis related to specific adhesion with lung cells rather than direct growth stimulation.* Anticancer Res, 1994. **14**(5A): p. 1791-9.
278. Lee, K.H. and J.R. Kim, *Kiss-1 suppresses MMP-9 expression by activating p38 MAP kinase in human stomach cancer.* Oncol Res, 2009. **18**(2-3): p. 107-16.
279. Coussens, L.M., B. Fingleton, and L.M. Matrisian, *Matrix metalloproteinase inhibitors and cancer: trials and tribulations.* Science, 2002. **295**(5564): p. 2387-92.
280. Li, S.P., et al., *p38 Mitogen-activated protein kinase pathway suppresses cell survival by inducing dephosphorylation of mitogen-activated protein/extracellular signal-regulated kinase kinase1,2.* Cancer Res, 2003. **63**(13): p. 3473-7.
281. Vandooren, J., et al., *Zymography methods for visualizing hydrolytic enzymes.* Nat Methods, 2013. **10**(3): p. 211-20.
282. Weiss, M.B., et al., *TWIST1 is an ERK1/2 effector that promotes invasion and regulates MMP-1 expression in human melanoma cells.* Cancer Res, 2012. **72**(24): p. 6382-92.
283. Rahman, R., A.W. Asombang, and J.A. Ibdah, *Characteristics of gastric cancer in Asia.* World J Gastroenterol, 2014. **20**(16): p. 4483-90.
284. Choi, I.J., *[Gastric cancer screening and diagnosis].* Korean J Gastroenterol, 2009. **54**(2): p. 67-76.
285. Zhang, Z.Y. and H.Y. Ge, *Micrometastasis in gastric cancer.* Cancer Lett, 2013. **336**(1): p. 34-45.
286. Gao, D., et al., *Microenvironmental regulation of epithelial-mesenchymal transitions in cancer.* Cancer Res, 2012. **72**(19): p. 4883-9.
287. Tsai, J.H. and J. Yang, *Epithelial-mesenchymal plasticity in carcinoma metastasis.* Genes Dev, 2013. **27**(20): p. 2192-206.
288. Watanabe, T., et al., *Epithelial-mesenchymal transition in human gastric cancer cell lines induced by TNF-alpha-inducing protein of Helicobacter pylori.* Int J Cancer, 2014. **134**(10): p. 2373-82.
289. Santibanez, J.F., *JNK mediates TGF-beta1-induced epithelial mesenchymal transdifferentiation of mouse transformed keratinocytes.* FEBS Lett, 2006. **580**(22): p. 5385-91.
290. Epstein Shochet, G., et al., *Placenta-breast cancer cell interactions promote cancer cell epithelial mesenchymal transition via TGFbeta/JNK pathway.* Clin Exp Metastasis, 2014. **31**(8): p. 961-75.
291. Nazarenko., I.A., S.K. Bhatnagar., and R.J. Hohman., *A closed tube format for amplification and detection of DNA based on energy transfer.* Nucleic Acid Res, 1997. **25**: p. 2516-2521.
292. Jiang, W.G., et al., *Prognostic value of rho GTPases and rho guanine nucleotide dissociation inhibitors in human breast cancers.* Clin Cancer Res, 2003. **9**(17): p. 6432-40.
293. Sourla, A., et al., *Plasminogen activator inhibitor 1 messenger RNA expression and molecular evidence for del(7)(q22) in uterine leiomyomas.* Cancer Res, 1996. **56**(13): p. 3123-8.
294. Koutsilieris, M., et al., *The assessment of disease aggressivity in stage D2 prostate cancer patients (review).* Anticancer Res, 1990. **10**(2A): p. 333-6.
295. Yang, J., et al., *Twist, a master regulator of morphogenesis, plays an essential role in tumor metastasis.* Cell, 2004. **117**(7): p. 927-39.
296. Glunde, K., et al., *Hypoxia regulates choline kinase expression through hypoxia-inducible factor-1 alpha signaling in a human prostate cancer model.* Cancer Res, 2008. **68**(1): p. 172-80.
297. Martin, T.A., et al., *Expression of the transcription factors snail, slug, and twist and their clinical significance in human breast cancer.* Ann Surg Oncol, 2005. **12**(6): p. 488-96.
298. Rosivatz, E., et al., *Differential expression of the epithelial-mesenchymal transition regulators snail, SIP1, and twist in gastric cancer.* Am J Pathol, 2002. **161**(5): p. 1881-91.
299. Castro Alves, C., et al., *Slug is overexpressed in gastric carcinomas and may act synergistically with SIP1 and Snail in the down-regulation of E-cadherin.* J Pathol, 2007. **211**(5): p. 507-15.

300. Zeisberg, M. and E.G. Neilson, *Biomarkers for epithelial-mesenchymal transitions.* J Clin Invest, 2009. **119**(6): p. 1429-37.